Contractor Report ARAED-CR-88017

TEST PLAN DEVELOPMENT FOR PLASTIC AMMUNITION CONTAINERS, VOLUME I

J. E. Brzuskiewicz
DSET Laboratories, Inc.
Box 1850, Black Canyon Stage I
Phoenix, AZ 85027

Carlton Morrison
ARDEC
Project Engineer

March 1989

US ARMY ARMAMENT MUNITIONS & CHEMICAL COMMAND ARMAMENT RDE CENTER

U.S. ARMY ARMAMENT RESEARCH, DEVELOPMENT AND ENGINEERING CENTER

Armement Engineering Directorate

Picatinny Arsenal, New Jersey

The views, opinions, and/or findings contained in this report are those of the author(s) and should not be construed as an official Department of the Army position, policy, or decision, unless so designated by other documentation.

The citation in this report of the names of commercial firms or commercially available products or services does not consitute official endorsement by or approval of the U.S. Government.

Destroy this report when no longer needed by any method that will prevent disclosure of contents or reconstruction of the document. Do not return to the originator.

REPORT DOCUMENTATION PAGE

1a REPORT SECURITY CLASSIFICATION Unclassified	1b. RESTRICTIVE MARKINGS
2a. SECURITY CLASSIFICATION AUTHORITY	3 DISTRIBUTION / AVAILABILITY OF REPORT Approved for public release; distribution unlimited
2b DECLASSIFICATION / DOWNGRADING SCHEDULE	
4 PERFORMING ORGANIZATION REPORT NUMBER(S) DSET Report No. R2970-23 (Final Report)	5. MONITORING ORGANIZATION REPORT NUMBER(S) ARAED CR-88017
6a. NAME OF PERFORMING ORGANIZATION DSET LABORATORIES, INC. 6b OFFICE SYMBOL (If applicable)	7a. NAME OF MONITORING ORGANIZATION ARDEC, AED
6c. ADDRESS (City, State, and ZIP Code) Box 1850 Black Canyon Stage I Phoenix, Arizona 85027	7b. ADDRESS (City, State, and ZIP Code) Packaging division (SMCAR-AEP) Picatinny Arsenal, New Jersey 07806-5000
8a. NAME OF FUNDING / SPONSORING ORGANIZATION ARDEC, IMD STINFO BR 8b. OFFICE SYMBOL (If applicable) SMCAR-IMI-I	9. PROCUREMENT INSTRUMENT IDENTIFICATION NUMBER DAAA-21-86-C-0275
8c. ADDRESS (City, State, and ZIP Code) Picatinny Arsenal, New Jersey 07806-5000	10 SOURCE OF FUNDING NUMBERS PROGRAM ELEMENT NO. / PROJECT NO. / TASK NO. / WORK UNIT ACCESSION NO.

11. TITLE (Include Security Classification)

TEST PLAN DEVELOPMENT FOR PLASTIC AMMUNITION CONTAINERS - VOLUME I

12. PERSONAL AUTHOR(S)
J.E. Brzuskiewicz, DSET LABORATORIES, INC. and Carlton Morrison, ARDEC Project Engineer

13a. TYPE OF REPORT	13b. TIME COVERED	14. DATE OF REPORT (Year, Month, Day)	15. PAGE COUNT
Final	FROM 08-19-86 TO 11-30-88	89-03-15	232

16. SUPPLEMENTARY NOTATION

17. COSATI CODES			18. SUBJECT TERMS (Continue on reverse if necessary and identify by block number)
FIELD	GROUP	SUB-GROUP	Ammunition containers, packaging, plastics, logistics, lifetime prediction models, accelerated testing, Arrhenius relationships test development. (725)

19. ABSTRACT (Continue on reverse if necessary and identify by block number)

The replacement of wood and metal by plastic materials in ammunition packaging container applications offers the potential for substantial weight and cost reduction. Although plastic packaging has been common in the commercial sector for a considerable number of years, no long-term performance data is available. This is perhaps due to the short design life of commercial packaging. The use of plastic packaging, and polymeric materials in general, for military purposes requires consideration of environmental factors that are not encountered by commercial packaging. Military requirements dictate that ammunition items be offered protection for up to thirty years in a variety of transit and storage conditions. The evaluation and ultimately the qualification of plastic packaging materials and plastic ammunition container designs must be based on test procedures that will allow the accurate prediction of performance.

(continued)

20 DISTRIBUTION / AVAILABILITY OF ABSTRACT ☐ UNCLASSIFIED/UNLIMITED ☒ SAME AS RPT ☐ DTIC USERS	21. ABSTRACT SECURITY CLASSIFICATION Unclassified
22a. NAME OF RESPONSIBLE INDIVIDUAL I. Hazendari	22b. TELEPHONE (Include Area Code) (201) 724-3316 22c. OFFICE SYMBOL SMCAR-IMI-I

DD FORM 1473, 84 MAR 83 APR edition may be used until exhausted. All other editions are obsolete.

Two plastic ammunition containers and their materials were tested using a combination of environmental exposure tests in order to provide the basis for a viable test plan which can be used for a variety of container items, materials and designs. The test plan developed reflects the testing philosophy required to determine the long-term acceptability of plastic materials and plastic container design. The test data obtained also provides a basis for a continued test effort required to produce accurate lifetime prediction and moisture vapor transmission rate models for the two container items tested.

It was demonstrated that the typical accelerated environmental test procedures, generally followed to evaluate the materials used in military items and to determine the acceptability of items, in fact accelerate effects only to the extent that material degradation and time dependent material's properties allow. The material and full-scale item test data used to prepare the lifetime prediction models developed over the nine month period in which the tests were conducted therefore, do not provide the reliability required to make judgements concerning the acceptability of the two container items tested or for the use of plastic materials in general.

FOREWARD

This is Report No. R2970-23 (Final Report) of DSET Project No. R2970 entitled, "Test Plan for Plastic Containers." Report No. R2970-23 is entitled, "Test Plan Development for Plastic Ammunition Containers" and covers the work conducted to develop accelerated test procedures for predicting the effective lifetime of plastic ammunition packaging containers. The report is presented in two separate volumes. Volume I contains the Final Technical Report and includes the analysis of environmental test data, the characterization of ammunition container logistic chains and container item lifetime prediction analyses. Volume II contains the Final Test Plan prepared on the basis of actual tests conducted on the 155mm Propelling Charge Container and the M2A1 Small Ammo Container.

The project work effort was conducted from August 1986 through September 1988 at DSET Laboratories, Inc. under the technical direction of the Packaging Division of the U.S. Army Armament Research, Development and Engineering Center. Mr. Jasper C. Griggs and Mr. D. E. Jones served as technical consultants to the project during the Phase I effort and assisted DSET in the logistics and literature studies, respectively. The Texas Research Institute, Inc. conducted thermal analysis measurements on container materials during the Phase II effort.

The project was funded under Contract No. DAAA-21-86-C-0275. Volume I of this report fulfills CDRL Item No. A008. The Volume II Test Plan fulfills CDRL Item No. A009.

Data are recorded in DSET Logbook No.'s 171, 174 and 200.

(THIS PAGE LEFT BLANK)

CONTENTS

CONTENTS (cont)

(THIS PAGE LEFT BLANK)

TABLES

(THIS PAGE LEFT BLANK)

FIGURES

FIGURES (cont)

TEST PLAN DEVELOPMENT FOR PLASTIC AMMUNITION CONTAINERS - VOLUME I

1.0 INTRODUCTION

The purpose of this project was to establish a database and demonstrate testing procedures that will predict the long-term reliability of plastic ammunition containers. The project was divided into two phases. The first phase determined the logistic chain of several ammunition containers, identified the environmental extremes of their logistic chains, and attempted to identify technical literature pertinent to the long-term performance properties of plastic materials. The second phase of the project initiated the testing suggested by the Phase I effort. This testing included conducting real-time and accelerated exposure test procedures on container materials and full-scale items. Plastic container materials subjected to these environmental tests, were evaluated using optical, physical and thermal measurement techniques in order to determine changes that might affect their function in packaging applications. Full-scale items were used to determine the moisture vapor transmission rate of two container items and the ability of the containers to remain sealed. The two containers tested during the project were the 155mm Propelling Charge Container and the M2A1 Small Ammo Container.

The test data obtained from the Phase II effort was used to illustrate the preparation of performance prediction models for the container materials and the moisture vapor transmission rate of the two container items tested. Volume II of this report describes the test plan that is required to produce the data needed for the preparation of accurate models. The approach taken to develop the test plan attempted to relate the change in container materials properties to the functional integrity of the container in preventing moisture from entering the container. The details of the specific approach used during the project were dictated primarily by the short time period allowed for actual testing and the lack of appropriate test sample materials. Ideally, the environmental testing conducted on container materials would have resulted in engineering property data as a function of environmental exposure, which could then be used to predict the ability of the container to resist impact and the effects of creep and compression set due to palletization loads. However, no engineering test samples were available for testing during the course of the project. The only recourse therefore, was to use test specimens from actual container items. Thermal analysis was the only technique that could be used to evaluate these samples and produced data that are related to changes in engineering properties by identifying changes in the structure of the polymer. The data obtained using these measurement techniques can be related quantitatively to engineering properties only when engineering property tests are concurrently conducted.

At the start, the project had the ambitious goal of identifying and proving that specific accelerated test procedures could be used to produce lifetime prediction models, all within a 49-week project, of which only 26 weeks were allowed for actual testing. The Phase II effort was therefore intentionally extended over an 11-month period in order to maximize the availability of actual test data on which to base and test the models developed. The outcome of the project effort has resulted in a test and

modelling scheme which, if the Volume II test plan is implemented, will ultimately produce the lifetime prediction models required to judge the efficacy of particular plastics and plastic container items. The actual test data and relationships described in the Volume I technical report lack the precision for accurate performance prediction models. The materials tests were too short in duration to precisely identify the end of the induction stage of degradation or fully characterize the time and temperature conditions that could be used to accelerate the end of the induction stage. The full-scale item tests were also not statistically extensive enough to draw firm conclusions concerning the moisture vapor transmission rate of the container items tested.

Volume I of this report describes the approach, procedures, results and conclusions of the development and testing aspects of the project. Volume II of this report describes the test plan recommended for the characterization and evaluation of plastic materials and plastic ammunition container items. The format of the plan attempts to provide a test specification within the constraints of the overall project.

2.0 PHASES I and II- APPROACH

2.1 Background

The Phase I approach involved identifying the features of the logistic chain of a number of ammunition items and the technical literature available concerning the long-term performance of a number of plastic materials considered for ammunition packaging applications. The approach taken to understand the features of the logistic chain which are most important to the development of a lifetime prediction model required that the items be studied from the "cradle to the grave." The information on the container items was obtained by contacting the appropriate ammunition item managers and characterized using the following criteria:

- The items were studied from the load plant to the firing point
- The geographical locations with the highest concentration of each type of item were considered as the typical use environments
- Maintenance, war reserve rotation, loading and unloading during training operations, return to load plant and refurbishment logistics were to be considered as having a minimal impact on the lifetime of ammunition
- An estimate of the time and conditions the items were in transit from the load plant and in depot storage was used to characterize and define typical environmental histories for each item.

The literature search was limited to public information and unclassified Defense Technical Information Center (DTIC) databases. The

databases used were searched using a strategy based on key words describing the materials to be studied, the dependence of material properties on environmental parameters and lifetime modelling. The Phase I effort also involved identifying appropriate accelerated test equipment, test procedures, test instrumentation and the design of the test approach to be used during Phase II of the project. Instruments, tests and measurements were selected for use on the basis of their ability to detect materials degradation for sample tests and the determination of moisture vapor transmission and pressure changes inside the container test items during full-scale item tests.

The Phase II work effort implemented test procedures identified during Phase I. A combination of outdoor and laboratory exposure tests were conducted on ammunition container sample materials and full-scale container items. These tests were conducted to provide material degradation data and container performance data. Real-time, outdoor exposure tests were conducted to identify failure modes which are likely to occur as a result of natural degradation processes. The laboratory exposure tests were conducted in order to accelerate the degradation process. The full-scale item laboratory testing also included the determination of the moisture vapor transmission characteristics of the container items.

Although the Phase I effort identified general materials property information on which the Phase II test program was based, the Phase II effort was hampered by the shortness of the initial Phase II schedule, the lack of specific materials property information and the lack of suitable materials test specimens. The lack of engineering test specimens for the project dictated the measurement approach taken during the Phase II effort. The measurements used, although necessary to a thorough understanding of the material degradation process, could not be used to quantify the changes in engineering properties needed to quantify changes in container functional properties that might occur over the container life cycle.

The initial Phase II schedule also required that a time based exposure test schedule be used, rather than a schedule based on dose. This approach provided the flexibility needed to maximize exposure durations and doses while minimizing project schedule and cost. Exposure test projects are more typically based on the basis of dose, for example total ultraviolet below 385nm wavelength in terms of MJ/m^2. This approach allows more precise control of environmental test parameters but generally requires specific time of year start dates and undefined end dates for testing.

Materials degradation data were obtained using optical property measurements to evaluate appearance changes related to surface degradation and thermal analysis measurements to evaluate changes in the polymer structure and composition of the container materials. The thermal analysis measurement data are related to engineering property data qualitatively in that they can suggest changes in properties such as tensile strength, elongation, creep, and impact resistance by measuring changes in properties such as modulus, crystallinity, and oxidative stability.

The logistics chain environmental characterization was applied to the full-scale item testing for moisture vapor transmission by considering

the vapor pressure differential occurring during the container life cycle. This approach allows the test data to be used in determining both the rate of moisture ingress or egress over time and to evaluate the moisture permeability characteristics of a given container item.

2.2 Literature Survey

The objective of the literature survey was to establish a database pertinent to developing specific test procedures that would demonstrate and predict the long-term reliability of ammunition containers constructed of plastic materials. The literature survey had the following goals:

- Obtain information detailing the environmental conditions and their effect on plastic components and materials after more than five years of exposure.
- Identify specific information on accelerated test programs on plastics and the results.
- Obtain information on related areas where plastics were exposed to extreme conditions such as excessive heat, cold, solar radiation, humidity, etc.
- Obtain degradation mechanism information pertinent to a better understanding of long-term ageing and weathering effects on plastic containers.
- Obtain information on the Water Vapor Transmission Rate (WVTR) of polymeric materials and detailed information on testing practices used to determine the WVTR.
- Obtain information on the physical characteristics of polymeric materials.

A key word list using elements of the noted objectives and general principles of polymeric materials performance was developed to search scientific and technical literature. The final key word list used is shown in Table 1. The key words were incorporated into appropriate syntax forms and uploaded into five major computerized databases. The five databases listed in Table 2 were searched to obtain titles, identifying terms, descriptors and key words. The initial list was reviewed and culled for appropriate citations. Abstracts and source information for these citations were obtained. The procedure followed is summarized in Figure 1.

The information obtained was organized into nine categories shown in Table 3. Specific citations within each category were then arranged into a single standard citation format. The format grouped the information into the four sections in Table 4. In addition to the survey performed with the databases listed in Table 2, a survey of the Defense Technical Information Center (DTIC) database was also conducted.

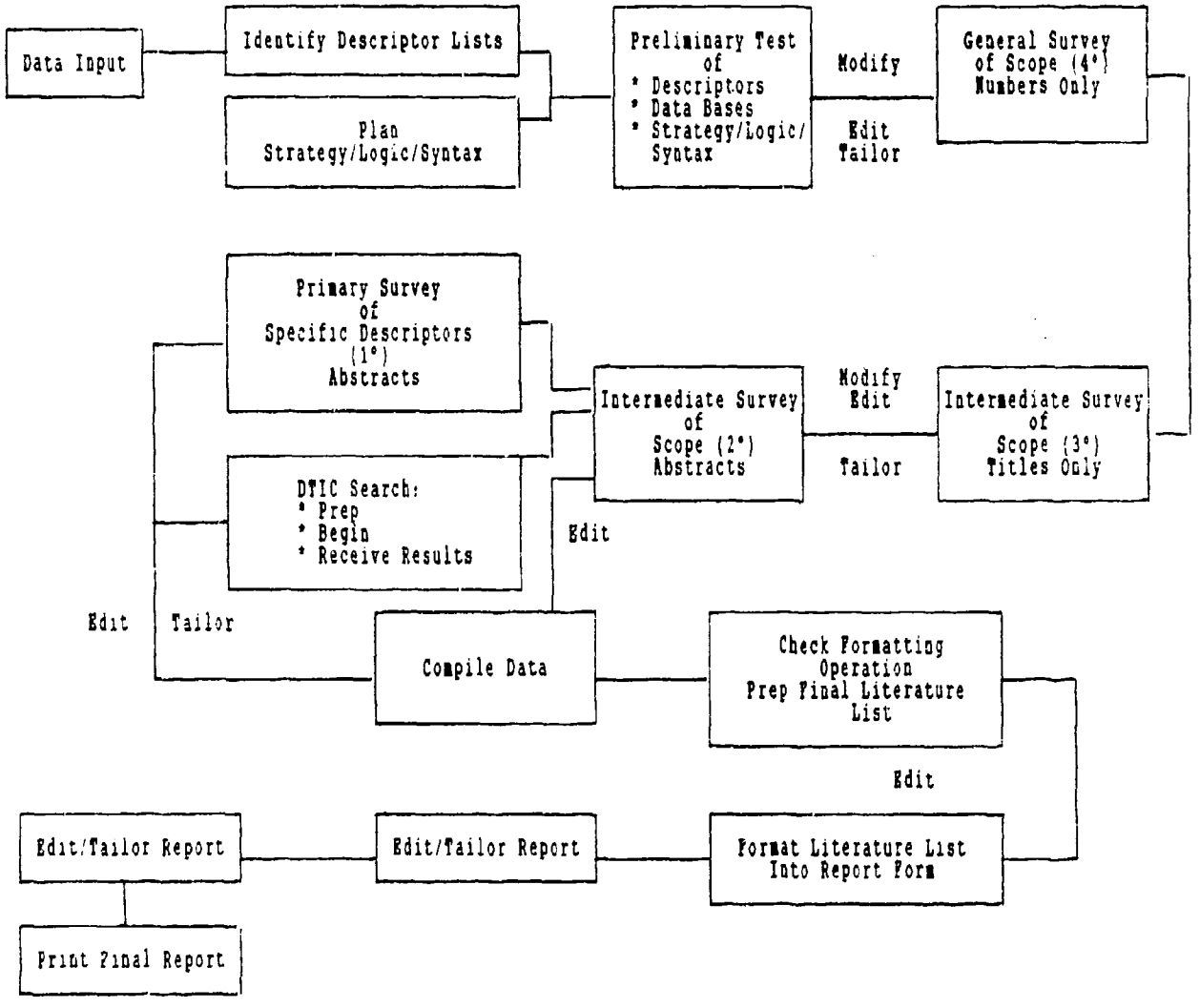

Figure 1: Flow Chart Indicating Literature Survey Procedure

TABLE 1: Key Word List

PLASTICS/MATERIALS	PHYSICAL CHARACTERISTICS (PROPERTIES)	TEST PROGRAMS	EXTREME CONDITIONS
Acrylonitrile Butadiene Styrene (ABS)	Density	Thermogravimetric Analysis	Heat
High Density Polyethylene	Water Vapor Transmission Rate	Water Vapor Transmission Rate (WVTR) Test	Cold
Polyester	Moisture Vapor Transmission Rate	Moisture Vapor Transmission Rate	Temperature
Fiber Reinforced Polyester	Tensile Strength	Termomechanical Analysis	Humidity
Polycarbonate	Modulus (of elasticity)	Glass Transition	Ageing
Acetal	Impact Strength	Coefficient of Expansion	Low Temperature (cold)
Polypropylene	Elongation	Coefficient of Contraction	Thermal
Polyurethane	Yield Strength	Fatigue	Ultraviolet Radiation
Reinforced Polyester Composite	Compression Strength	Creep	Solar
Acetal Homopolymer	Compression Set	Dynamic Mechanical Analysis	Radiation
Acetal Copolymer	Hardness	Differential Scanning Calorimetry	Vibration
	Structural Strength	Thermal Cycling	Pressure
	Structural Stability	Humidity Cycling	Shock
	Dimensional Stability	Tropical Exposure	Abrasion
	Thermomechanical (properties)	Arid Exposure	Oxidation
	Glass Transition	Solar Exposure	Environmental Condition Effects
	Coefficient of Expansion	Weatherometer Tests	
	Coefficient of Contraction	Weathering Tests	
	Fatigue	Exposure Tests	
	Creep	Vibration Testing	
	Craze Resistance	Long-term (ageing)	
	Crack Resistance	Accelerated Testing	
	Abrasion Resistance	Tensile Testing	
	Viscoelasticity	Arctic Exposure	
	Calorimetry Properties	Desert Exposure	
	Stress Crazing	Environmental Tests	
	Solvent Resistance	Predict Ageing	
	Thermal Degradation (resistance)	Predict Weathering	
	Heat Distortion (resistance)	Test Practice	
	Oxidation (resistance)		
	Thermal-Photo		
	Endurance		
	Hydration		
	Moisture (water)		
	Permeability		
	Absorbtion		
	Diffusion		
	Test Method		

TABLE 2: Databases Searched

DATABASE : Aerospace Database

Coverage : 1962 to the present
File Size: 1,500,000 records
Updates : Twice a month
Provider : American Institute of Aeronautics and Astronautics/Technical Information Service (AIAA/TIS), New York, NY

The Aerospace Database provides references, abstracts and controlled vocabulary-indexing of key scientific and technical documents, as well as books, reports and conferences, covering aerospace research and development in over 40 countries including Japan and Communist-bloc nations. This database supports basic and applied research in aeronautics, astronautics and space sciences, as well as technology development and applications in complementary and supporting fields such as chemistry, geosciences, physics, communications and electronics.

DATABASE : CA Search

Coverage : 1967 to the present
File Size: 7,100,000 records
Updates : Monthly
Provider : Chemical Abstracts Service, Columbus, OH

The CA Search database includes citations to the literature of chemistry and its applications. CA Search is an expanded database which contains the basic bibliographic information appearing in the printed Chemical Abstracts.

DATABASE : Compendex©

Coverage : 1970 to the present
File Size: 1,485,000 records
Updates : Monthly
Provider : Engineering Information, Inc., New York, NY

The Compendex© database is the machine-readable version of the Engineering Index (monthly/annual), which provides abstracted information from the world's significant engineering and technological literature. The Compendex database provides worldwide coverage of approximately 4,500 journals and selected government reports and books. Subjects covered include: civil, energy, environmental, geological and biological engineering; electrical electronics and control engineering; chemical, mining, metals and fuel engineering; mechanical, automotive, nuclear and aerospace engineering; and computers, robotics and industrial robots.

DATABASE : Inspec

Coverage : 1977 to the present
File Size: 2,629,000 records (for 1969 to present)
Updates : Monthly
Provider : The Institution of Electrical Engineers, London, England

The on-line Inspec file covers the printed Physics Abstracts, Electrical and Electronics Abstracts, and IT Focus. Non-English language source materials are also covered but abstracted and indexed in English. The principal subject areas are: Atomic and molecular physics; computer programming and applications; computer systems and equipment; and elementary particle physics. Journal papers, conference proceedings, technical reports, books, patents and university theses. The total number of journals in the database is approximately 3,000; over 200 of these are abstracted completely.

DATABASE : NTIS

Coverage : 1964 to the present
File Size: 1,164,000 records
Updates : Bi-weekly
Provider : National Technical Information Service (NTIS), U.S. Department of Commerce, Springfield, VA

The NTIS database consists of government-sponsored research, development and engineering and analyses prepared by federal agencies, their contractors, or grantees. It is the means through which unclassified, publicly available, unlimited distribution reports are made available for sale from agencies such as NASA, DDC, DOE, HUD, DOT, Department of Commerce and some 240 other agencies. In addition, some state and local government agencies now contribute their reports to the database.

This database subjects include: administration and management, agriculture and food, behavior and society, building, business and economics, chemistry, civil engineering, energy, health planning, library and information science, materials science, medicine and biology military science, transportation, etc.

TABLE 3: Description of Categories

Category	Description of Content
1	Accelerated weathering programs on plastic materials and associated information.
2	Natural weathering and ageing test programs on plastic materials and associated information, e.g., tropical exposure tests, arid exposure tests.
3	Extreme conditions (other than accelerated or natural weathering and ageing) on plastic materials and associated information, e.g., exposure to high relative humidity environments, chemical environments.
4	Water vapor transmission, absorbtion and permeability of plastic materials and associated information which engineers may use to better understand transmission phenomenon, e.g., diffusion rates, absorbtion characteristics.
5	Other information useful in predicting long-term ageing characteristics of plastic materials under a variety of environmental conditions, e.g., effects of shock and effects of vibration.
6	Physical characteristics of plastic materials, e.g., tensile characteristics, modulus characteristics.
7	Theoretical or accepted models of physical changes occurring in plastic materials under various conditions including ideas which may be used to explain weathering phenomena, e.g., mechanisms of degradation, crack growth propagation models.
8	Procedures used to enhance weatherability or desired physical characteristics of plastic materials.
9	Miscellaneous information deemed useful for the overall goal of the project which did not fit into categories 1-8.

2.3 Logistics Chain Study

The logistics of six ammunition items were studied by contacting the appropriate item managers. The study started at the item load plant and traced the items from the load plant to their permanent storage areas. The items studied were:

- 105mm Tank Round
- 81mm Mortar Round
- 155mm Propelling Charge
- 2.75 inch Rocket
- 5.56mm Small Arms Ammunition
- 7.62mm Small Arms Ammunition

The flow chart in Figure 2 shows the investigative path followed to characterize the logistics of each item. The logistics of all the items are similar in that they are all transported from the load plant by rail, truck and ship prior to CONUS and OCONUS storage. It was learned that no specified conditions of temperature and humidity were used at the load plant and that information on an allowable limit of moisture inside the container items was unavailable when loaded or at the end of the design life. The items sometimes spend up to one year in temporary storage at the load plant before deployment to the permanent storage area. The majority of production at the present time is for OCONUS and uses primarily the same ports of embarkation. Times in transit after leaving the load plant were also reported as being similar for all items. The items generally were transported to the port of embarkation using milvan or breakbulk. The items are transported by ship in a dry ship hold environment with sealed hatches. Ship transport of the ammunition items typically occurs over a period of approximately twenty days and spend approximately one week in the port of debarkation before transportation to the permanent storage area by rail or truck.

The similarity in logistics between the different items studied ends at the permanent storage area. Each item is stored, rotated from war reserve and tested on schedules which depend on the availability of the item and the policy of the Defense Ammunition Director and AMCCOM. The containers undergo care and preservation by ammunition maintenance personnel after inspection in accordance with SB 742-1. The ammunition containers studied are generally discarded after the contents were removed. However, reuse of the container items might be desired under some circumstances of supply, logistics and war. The details of the logistics of each item are described in Appendix A.

2.3.1 Physical Considerations for Plastic Container Logistics

Ammunition containers are subject to many physical rigors during transportation and at the permanent storage area which could detrimentally affect the rate at which the container material ages and the rate at

which the container gains moisture. The most typical to occur during transportation include vibration, varying atmospheric pressure if moved by air transport and impact during loading and unloading. Container items undergo maintenance procedures, such as painting and depainting, and are moved by fork lift, hand truck and conveyor. Palletization during storage also presents a rigorous physical environment since items located on the bottom of the pallet could experience considerable loads. Container handles, latches and seals could undergo stresses caused by short term use and during maintenance procedures which could result in permanent deformation. Detrimental effects of these seemingly minor abuses may not manifest themselves for years after they occur.

Testing for all of the possible effects of the physical environment on the design life of a plastic container item is virtually impossible because of the infinite number of situations that could occur over a thirty-year period. However, the effects of the physical environment can be anticipated by considering the physio-chemical state of the container material at the end of its design life. Accelerated environmental exposure procedures could be conducted on the containers and container materials in order to subsequently subject the container materials and container items to the most likely physical environmental features while they are in a condition representative of the end of the design life. The results of this testing could be used to implement container design changes such as thickness, handle and latch geometry, fasteners and other container features which are found to affect performance.

The 155mm Propelling Charge container and the M2A1 Small Ammo container emphasized during the Phase II test effort present significantly different material and design features on which to base a testing philosophy. The first and most obvious difference is size and weight. These differences dictate different handling procedures and thus potentially different physical environments. The high density polyethylene (HDPE) used for the 155mm Propelling Charge container is unlikely to ever be painted since HDPE is unpaintable. On the other hand the HDPE could have hot stamped identification labels which might localize surface stresses which could reduce impact resistance after long periods of storage or outdoor exposure. The M2A1 container could conceivable be painted at some point during its lifetime since the polyester molding compound is paintable and since the polyester material is susceptible to fading. The painting and depainting process could also cause stress cracking due to the solvents that might be used. This would also decrease the impact resistance of the container.

HDPE is known to be susceptible to deformation by creep and thermal mechanisms. Therefore, the long-[illegible] effects of palletization loads in warm climates should be a concern for the 155mm Propelling Charge container. The fiber reinforcement used in polyester M2A1 container could be particularly sensitive to moisture absorption and desorption effects over long periods of time. Approximately 11,000 daily temperature and humidity cycles will occur over a thirty-year period. These cycles are of major concern to the performance of both container materials since the cycles could produce significant stresses from the temperature induced dimension changes.

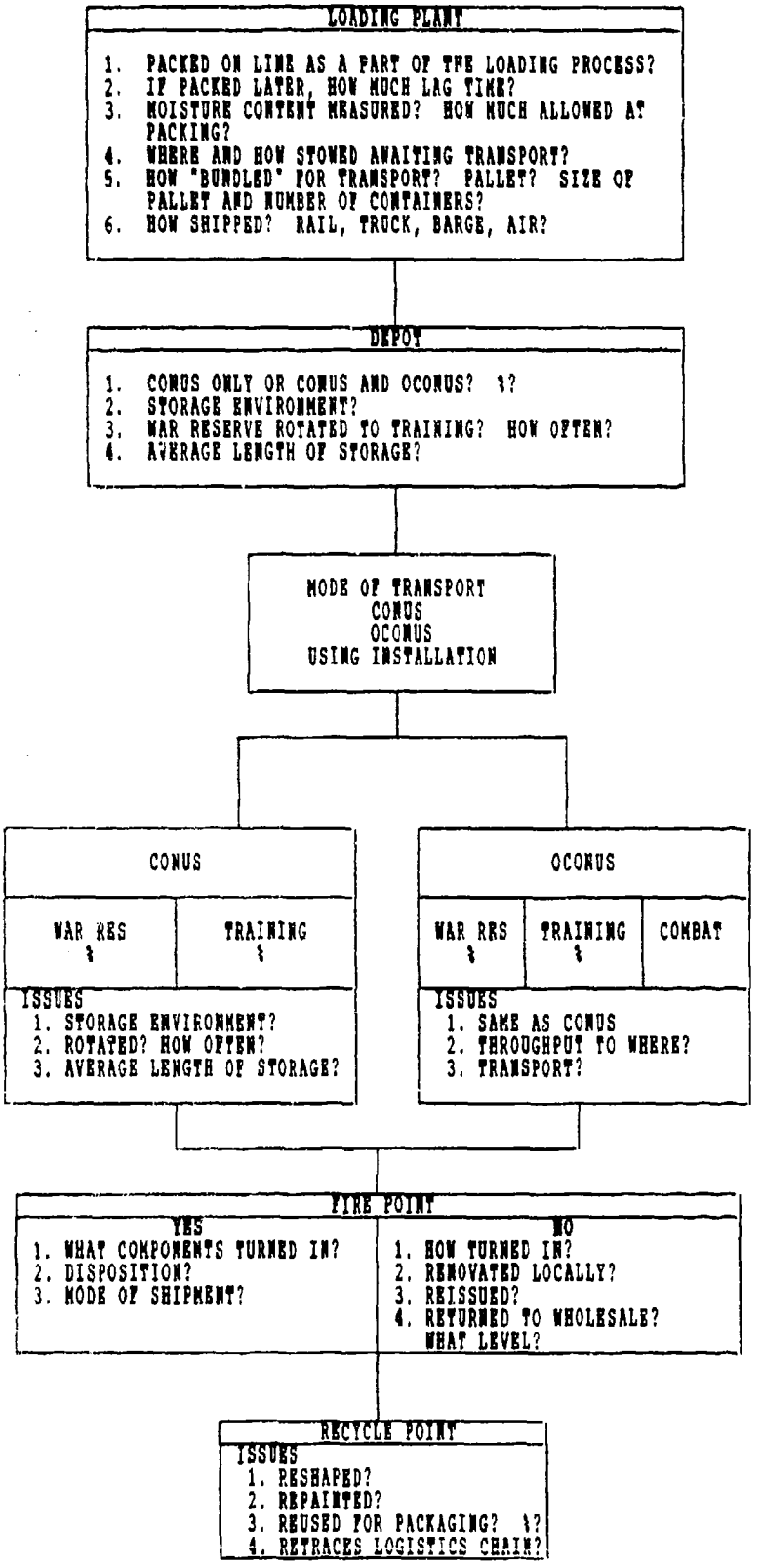

Figure 2: Logistics Chain Study

The approach needed to characterize the physical environment and the long-term effects of the physical environment will initially require that physical property tests be conducted on container materials and container items as a function of accelerated environmental testing. Plastics have been used in military items for a considerable number of years and although the particular formulations for the plastics used may no longer be available, the plastic military items that have been in use could provide the information necessary to establish specific test criteria. The approach to using plastic items with a reasonably well known history, outlined in the Volume II Test Plan will involve evaluation of failure if it occurred, and the determination of structural changes in the polymer which could be related to engineering property changes such as tensile strength or impact resistance.

2.3.2 Definition of the Environment

As noted in the logistic chain descriptions in Appendix A, the environmental considerations early in a container's life cycle are limited to the geographic locations between and including the load plant and permanent storage areas. The ammunition items are further deployed from the areas noted in the logistic chain descriptions to storage areas surrounding the main storage areas. The general vicinity and typical environmental features of these storage areas are described in Appendix B. Comparison of the specific sites shows a considerable variation in altitude, temperature, humidity and sunlight. An important consideration in understanding the effects of long-term storage is the knowledge that environmental conditions can be quite different, and thus different effects may result, for ammunition items stored at locations separated by only a few miles.

The climates in the vicinity of specific storage sites were characterized by obtaining and evaluating average temperature, humidity, rainfall and solar radiation data. The data was obtained from References 1 through 8. The average data was typically based on measurements made over more than five years, the exception being the solar radiation data for Korea which represents only two years of measurements. Comparison of the data in Appendix B indicates that the environments characterized in Mil-Std-210 can be used over the container item logistics chain environments and can be typified into four climate types in accordance with U.S. Army Regulation No. 70-38 to choose specific test conditions (References 9 and 10). These are:

1. Hot climates
2. Basic climates
3. Cold climates
4. Severe cold climates

AR 70-38 further classifies each of the climates into daily weather cycles, operational, storage and transit conditions. The following sections summarize the major features of the climatic conditions that were to be considered during the course of this project.

2.3.2.1 Hot Climates

Hot climatic conditions are of primary concern in low latitude deserts. In addition to high air temperatures, and low relative humidities, intense solar radiation also plays a part in the degradation of material performance. Two daily cycles have been used to characterize the operational conditions of this type of environment: hot and dry, in which the daily temperature could range between 32°C and 49°C with a maximum relative humidity of 8%; hot and humid, in which the daily temperature could range between 31°C and 40°C with relative humidity ranging between 59% and 88%.

The performance of polymeric materials is sensitive to both the thermal degradation and photodegradation effects of sunlight. Both factors must be considered by any test program designed to predict performance. The specific mechanisms for thermal and photodegradation may differ for different materials and have different resulting effects on the bulk properties of the material. Humidity may also change the mechanism by which a material degrades. In order to fully understand the degradation of a polymeric material over a long period of time each environmental factor must be studied separately and in combination.

2.3.2.2 Basic Climates

Climates classified as basic are generally found in the humid tropics and mid-latitudes and are characterized by more moderate temperature extremes than found in the other climatic types. Four daily cycles are recognized as being characteristic for this climate type:

1. Constant high humidity
2. Variable high humidity
3. Basic hot
4. Basic cold

The outstanding features of the operational, storage, and transit conditions of each type are: constant temperature and greater than 95% relative humidity, for the constant high humidity condition, variable temperature and humidity between 26°C and 63°C with humidity ranging between 5% and 44%, for the basic hot conditions, and temperature between -33°C and -21°C with close to 0% relative humidity for the basic cold environment.

The same considerations for solar radiation noted in paragraph 2.3.2.1 apply to the basic climatic types. The most notable difference between the two environments discussed thus far is the low temperature extreme in the latter. The effects of low temperature on polymeric materials offer additional complication for the understanding of degradation mechanisms and therefore make the development of a lifetime prediction model more difficult.

2.3.2.3 Cold Climates and Severe Cold Climates

The cold climatic type is generally found towards the extremes of both northern and southern hemispheres and in some areas at high altitudes. Air temperatures, with relative humidity levels tending towards saturation, range between -37°C and -47°C. Solar radiation is negligible. The severe cold climate is found in the very extreme areas of the northern and southern hemispheres. The design minimum temperature condition for this type of climate is -51°C.

2.3.2.4 Transportation Environments

Transportation of military items throughout the world can rapidly, and drastically change the environment and, therefore, the potential degradation mechanisms to which a polymeric material, used in a military application, might be subjected. The act of transport itself offers a potential for degrading the performance of a material and a fabricated part by introducing physical forces to the item by impact or vibration.

The effects of vibration on an unrestrained polymeric material are for all practical purposes, nil. However, if the polymer material is solidly attached as a component to an assembly, so that the vibrational forces can be directly translated into tensile or compressive stress on the material, the material could however degrade as a result of fatigue, creep, or fracture. The effects of vibration on seals, joints, or adhesive bonds can directly degrade the function of an assembly. The same is true for impact-induced degradation, but obviously in a much shorter time.

2.4 Development of the Approach to Phase II Testing

The successful development of an accelerated environmental exposure test procedure which can be used to predict the lifetime of plastic ammunition container items requires the knowledge of the dependance of plastic materials properties degradation on environmental parameters in a quantitative sense. Further, the dependance of the container's functional properties on the material properties must also be known. The test approach used in the Phase II therefore pursued both design, or functional testing of actual container items, and materials tests to evaluate the stability of the specific polymers used in the containers. The extent to which this knowledge can ultimately be used in a lifetime prediction model is highly dependent upon the nature of the mechanisms by which a given material degrades and the extent to which these mechanisms can be controlled during the accelerated testing procedures. In order to develop an accurate lifetime prediction model using the test samples made available during the project and in the time frame allowed for testing, it was necessary to identify instrumentation capable of detecting the structural properties degradation of container materials on a molecular scale. A combination of thermal analysis and optical properties measurement techniques was chosen to study materials degradation. Ideally these measurements would have been conducted in concert

with engineering property testing, such as tensile strength and impact resistance, to provide a defined link between material structure and material properties. Such a link could then be used to directly predict container performance as a function of environmental history.

The lack of suitable engineering property test specimens for the 155mm Propelling Charge Container and the M2A1 container items suggested that the engineering properties of another material be studied for purposes of illustrating the use of properties, such as tensile strength and elongation, for the development of a lifetime prediction model. A crosslinkable HDPE was selected on the basis of the availability of environmental performance data for comparison. The material, tested in an unpigmented and unstabilized form, is not comparable to the blow molding grade of HDPE used for the 155mm Propelling Charge Container, however it provides an excellent contrast to the container material by identifying material property changes directly related to environmental effects on the chemical aspects of the material in a short period of time.

Phillips Marlex CL-100 was chosen for study during the Phase II test effort. This material is a rotational molding compound and is typically used in outdoor applications and when properly compounded and processed, has been found to have good retention of physical properties for long periods of time. The 155mm Propelling Charge Container Material was a high density polyethylene compound comprised of Phillips HXM-50100 HDPE and a proprietary mixture of green pigment and stabilizers, the M2A1 container was made from a sheet molding compound comprised of Silmar polyester resin, approximately 45% glass fiber and approximately 25% filler. The filler contained a green pigment and calcium carbonate.

Full-scale item functional testing had the objective of determining the moisture vapor transmission rate (MVTR) and the ability of the container to remain sealed. The logistics chain of ammunition generally includes a two-year uncontrolled outdoor exposure. A desired aspect of the testing conducted was to predict the performance of the container items during a two-year outdoor exposure. This outdoor exposure period could occur at any time after the manufacture of the ammunition container. However, the test items used for the full-scale testing were newly manufactured and not subjected to pretest conditioning or preageing before testing. Thus, the extent to which MVTR is dependent on the container material's age could not be investigated during the project.

2.4.1 Materials Testing Approach

Optical, thermal and physical properties tests were selected to characterize the degradation of the container materials and the Marlex CL-100 HDPE. The specific measurement techniques selected have been used successfully in a number of materials study programs to quantify and model materials degradation due to environmental exposure (References 11 through 18).

Reflectance measurements, made between 350nm and 2400nm, and colorimetric measurements were used to quantify surface degradation. Spectral reflectance measurements were chosen to show changes in absorption coefficients and to identify spectral changes which might be related to pigment and polymer matrix degradation. Colorimetric measurements, using CIE chromaticity coordinates, were used to quantify visual changes in color and could be related to camouflage requirements.

Physical properties measurements included tensile and elongation testing of the Marlex CL-100. Thermal analysis measurements were used to determine structural changes in the polymeric container item materials. Container item materials were studied using thermogravimetric analysis (TGA), thermomechanical (TMA), differential scanning calorimetry (DSC) and dynamic mechanical analysis (DMA). The use of thermal analysis techniques to study ageing effects on polymeric materials had the advantages of providing information on viscoelastic properties in the case of DMA, the glass transition temperatures (Tg) in the case of TGA and DSC, the heat of fusion in the case of DSC and decomposition temperatures in the case of TGA and DSC.

Broadly interpreted, the glass transition temperature of a polymer is the temperature at which no further molecular rearrangement occurs. Below this critical temperature, molecular movement is a result of thermal vibration. That is, as a polymer approaches its glass transition temperature, it undergoes temperature dependent dimensional changes caused by the rearrangement of the polymer structure. The glass transition temperature is dependent primarily on chemical structure, the most important aspect being polymer chain stiffness. Processing and environmental conditions also influence glass transition temperature and therefore can play a great role in the degradation mechanisms which affect performance not only at a given temperature but over a given temperature range. A change in glass transition temperature due to some aspect of a material's environmental history could then be used to indicate changes in performance characteristics. The thermomechanical properties of plastics for use as ammunition packaging materials in this sense is important since the items are rarely intended to serve solely in a single environment.

Most accelerated test programs subject materials to abnormal conditions in order to induce failures in short periods of time. The objectives of testing a material in this manner are the evaluation and prediction of a material's long-term performance with a short term test. The current state-of-the-art methods to evaluate and predict materials' performance characteristics involve the concurrent study of chemical structure/property relationships and mechanical property changes. The environmental test procedures followed are classified by their use to predict outdoor performance in the presence of solar radiation and thermal tests which are conducted in the absence of solar radiation. The design and use of accelerated testing must be based on the failure of a specific property. The failure of many commercial items is judged on the basis of appearance which, as a surface effect, may occur long before there is a measurable change in mechanical properties. In applications where plastics are used for their

structural properties, changes in the appearance of the item may be acceptable. However, the use of plastics for ammunition containers requires that both physical and optical properties remain stable and constant throughout the container lifetime in order to protect the ammunition until it is fired, to reduce maintenance costs and to meet camouflage color requirements.

The use of thermal analysis techniques offers a practical and accurate method for determining the useful lifetime of many plastic materials. The data obtained from thermal analysis measurements are also well suited to modelling because the data are closely related to the chemical and thermal processes that occur as a result of specific materials property degradation mechanisms. These mechanisms, once related to the polymer structure dependent properties, can be used to predict changes in basic engineering properties. The various thermal analysis techniques available offer the advantages of several different dynamic combinations of time, temperature and stress in a single test. The use of appropriate test samples and appropriate test sample preparation techniques cannot be overstated in evaluating the suitability of thermal analysis for lifetime prediction modelling since these factors are critical to obtaining reliable and reproducible data. Further, if engineering property tests are not conducted concurrently with the initial material characterization tests, it is difficult to quantitatively relate thermal analysis data to engineering properties. A thorough review of thermal analysis principles and instrumentation may be found in Reference 19.

The use of DMA was evaluated for the fiber reinforced polyester used for the M2A1 container. Specifically, it was attempted to use storage and loss moduli and the loss tangent to evaluate the integrity of the adhesion between the polymer and fiber reinforcement. These properties are also related to the crystallinity of the material. DMA as a viscoelastic property measurement technique can be used to study other properties, such as creep, by applying the measurement data to time/temperature superposition principles and the Boltzmann superposition principle (References 17,20). Time/temperature superpositioning principles are derived from the W-L-F and Arrhenius equations which are used to determine the degree of horizontal shift, or rather the time, that a given set of data can be used with respect to temperature. The underlying principle for these mathematical relationships is the dependency of polymer structural properties on time and temperature. This is because the rate at which molecular relaxations and rearrangements occur increase with increasing temperature due to the fact that all polymers exhibit viscoelastic behavior. The storage of mechanical energy and release of heat by the "viscous liquid" and "elastic solid" phases of the polymer is thus time and temperature dependent.

Engineering plastics are known to have typically higher modulus at room temperature than at elevated temperatures while the modulus of elastomers is higher at low temperatures than at room temperatures. This phenomenon is related to Tg. The time dependency of viscoelastic properties is illustrated by the generalization that a polymer subjected to a constant load, will result in a decrease in the elastic modulus over time. Further, polymers deformed at high frequencies at a given temperature will show a high

modulus whereas the same polymer deformed at the same temperature with low frequency will exhibit lower modulus. Therefore, the time that these processes take to occur is reduced at higher temperature.

Experimental determination of the factors allowing time/ temperature superposition of viscoelastic properties in using DMA offers a technique for determining the functional lifetime of plastic packaging since these properties are affected by ageing. Thermo- and photo- oxidation effects could be quantified with a relatively few measurements by comparing shift factor curves and master curves developed for the materials before, during and after various environmental exposure tests. The successful development of the property relationships needed to make lifetime predictions from DMA data however, is complicated both by the degree of crystallinity of the material and geometrical factors associated with the test sample. The former problem relates primarily to the deviation of many real materials from the superpositioning principles due to property differences in the amorphous and crystalline phases. Although these differences can be determined and applied to modifications of basic viscoelastic principles, the process of developing the relationships is tedious and costly. The latter problem relates to the reproducibility of the measurement data. The combination of these two problem areas and the potential impact on project schedule and cost, limited the use of DMA to the M2A1 container material and was only pursued to the extent of attempting to evaluate the fiber and polymer matrix integrity.

A second example of the use of thermal analysis to predict lifetime is the use of TGA to study decomposition kinetics as described in Reference 21. This technique assumes first order kinetics and uses extrapolation to estimate the long lifetimes encountered at normal use temperature. Further, the technique assumes that the limit of acceptability, or lifetime, of the material is dependent on the thermal stability of a polymer or the presence of a stabilizer, or a combination of the two. In light of the preceding discussion on viscoelastic properties, the functional lifetime of the ammunition container materials studied, could possibly exceed lifetimes predicted by TGA data since there was no defined relationship between a failure point and thermal decomposition. The thermal decomposition of the materials is related to the presence of stabilizers and various additives in addition to the stability of the polymer. TGA is useful in studying various stages of thermal degradation and the compositional changes that occur during the ageing process. However, the TGA data must be associated with a functional property in order to predict useful lifetimes.

As an example, the HDPE used for the 155mm Propelling Charge container could be terribly cracked after 30 years but, because it was fabricated with a sufficient wall thickness, it could still provide adequate protection to the contents. Similarly, the M2A1 container could appear white, due to the blooming of the glass fiber reinforcement, and yet afford the contents of the container adequate protection because the composite retained sufficient strength. Therefore, the use of TGA determined "lifetime

prediction" data must be related to critical engineering properties. TGA only provides structural property data to the extent that properties are dependent on the chemical makeup of the material.

A detailed decomposition kinetics study of the 155mm Propelling Charge container material using TGA was considered during the project work effort. However, the project schedule did not allow enough time and no information was available for container materials regarding an acceptable limit of property degradation. Therefore, the acceptable level of decomposition had to be determined empirically. TGA was used to study both the 155mm Propelling Charge container material and the M2A1 container material by attempting to associate decomposition temperatures, mass loss and composition changes with the various exposure conditions.

DSC was used to follow thermodynamic changes in container materials by measuring the heat flow into and out of test samples. Physical transitions such as Tg, melting temperature and crystallization and; chemical transitions such as decomposition were monitored to study both physical and chemical processes. The degree of crystallinity, as related to the heat of fusion has a fundamental effect on material physical properties such as modulus, permeability, density and melting point. The decomposition temperature obtained from DSC relates to the oxidizable groups present in the material. Lower onset of decomposition temperatures indicate that fewer oxidizable groups are present in the material or the material has been preoxidized. The onset of decomposition temperature is not a quantitative value in respect to specific physical properties in the sense that it only represents the temperature at which the material decomposes after passing through the melt phase. The stability of the polymer, and thus the stability of properties which are dependent on the oxidation state of the polymer, is related to the decomposition temperature. Therefore, as a temperature value it can be used to indicate the oxidative stability of the polymer. The heat flow value associated with the onset of decomposition temperature is the area under the decomposition curve. It represents the energy required to decompose the sample and is dependent on the molecular weight, mass, and surface area of the sample in addition to the thermal properties of the material.

TMA was used to determine dimensional changes in the container materials as a function of temperature. This measurement technique provides information on the thermal expansion, Tg and the softening point.

The Marlex CL-100, crosslinkable HDPE was studied using tensile and elongation testing. Changes in tensile strength and elongation are used to indicate ageing effects and are dependent on both the thermodynamic and viscoelastic properties discussed in the preceding paragraphs. Marlex CL-100 was compression molded into plaques and subsequently cut into ASTM D638 Type IV tensile test specimens. These test specimens were tested in accordance with ASTM D638. The materials testing procedures and materials properties studied are summarized in Table 4.

Table 4
Summary of Material Tests

Material	Properties Measured	Measurement Technique
155mm Prop Charge Charge Container HDPE	Spectral Reflectance	ASTM E903
	CIE Color	ASTM D2244
	Thermal Decomposition	TGA
	Heat of Fusion, Heat Flow and Degree of Crystallinity	DSC
	Coefficient of Thermal Expansion	TMA
M2A1 Container Glass Reinforced Polyester	Spectral Reflectance	ASTM E903
	CIE Color	ASTM D2244
	Thermal Decomposition and Composition Changes	TGA
	Storage and Loss Modulus, and Damping	DMA
	Coefficient of Thermal Expansion	TMA
Marlex CL-100 Crosslinkable HDPE	Tensile Strength and Elongation	ASTM D638

2.4.2 Full-Scale Item Test Considerations

The development and use of accelerated test procedures for estimating the useful life of a product must consider the mechanisms by which the polymer degrades and the influence that product design can have on the stability of the polymer. Materials tests are used to show the stability of the polymer for a particular end use but do not show how the material will perform as a component of a final product. An example of this is the rapid failure of stabilized polymers in contact with an active metal which could catalyze the oxidation of the stabilizer used in the polymer material. Similarly, effects of environmental exposure on the functionality of the container assembly could occur that would not otherwise be predicted by short term testing of the container assembly alone since the rate of many of the failure mechanisms associated with materials and product design are controlled by diffusion processes which may not have the same synergistic effect even when above ambient conditions are used. The mechanisms by which container items could gain moisture in the seal area presents a good example of this possibility.

By design, the performance of the seal area is dependent on the performance of the elastomeric seal and the containe material. Plasticizers and lubricants are often used to enhance the ductility of elastomeric seal. The evolution of these materials from the seal is time and temperature dependent as is the absorption of these materials by the container material. Mil-Std environmental testing typically subjects test items to a combination of environmental conditions. Temperature and humidity cycle testing is very often used to judge the acceptability and durability of military items. Under cyclic testing of this sort, the component materials are not subjected to the time at temperature and temperature change rates, both of which are critical to a diffusion rate controlled process, which are experienced under use conditions. The rapid temperature change rates and short cycle times used for many tests also do not produce the same strains in the material that would occur in real use. Therefore, the resulting effect on the container materials after the test could be entirely different than would result in the use environment.

Moisture gain and moisture gain rate are also to a great extent diffusion rate controlled processes. The categorization of moisture gain into high and low vapor pressure regimes can be used to determine the severity of test conditions relative to real environmental conditions. However, the extent to which test conditions can be used to increase moisture vapor transmission rate and thus accelerate effects of moisture damage may be dependent entirely on the material's inherent moisture permeation coefficients. Therefore, the use of an acceleration or a test severity factor based entirely on the ratio of test conditions to real environmental conditions to predict results must be judicious. An example of determining a test severity factor is given in Reference 22 where normal vapor pressures are about 43 dynes/cm^2 for the worst tropical conditions, while the test conditions had vapor pressures in the range of 340 dynes/cm^2. The ratio of the vapor pressures would suggest an acceleration factor of 7.9. However, more appropriate is the determination of test severity on the basis of a

ratio of transmitted moisture at different vapor pressure conditions. In this example 0.6mg of transmitted moisture was measured at constant conditions of 40°C with a vapor pressure of 65 dynes/cm^2 while 0.012mg where measured at constant conditions of 25°C with a vapor pressure of approximately 30 dynes/cm^2. In this example the acceleration factor based on transmitted moisture is 0.6/0.012 or 50, while an acceleration factor based on the test condition is 65/30 or 2.2.

The application of this model to the case of an ammunition container must account for the changes in vapor pressure differential which occur as the container gains moisture. Thus, as the container gains moisture, the moisture vapor transmission rate would tend to decrease. That is, as the vapor pressure differential between the environment outside the container and the inside of the container approaches zero, the moisture vapor transmission rate also approaches zero. Since the containers could be deployed to hot and dry and cold and dry environments, the containers could also lose moisture over long periods of time.

The approach taken to determine the moisture vapor transmission characteristics of the container items pursued the relationship of moisture gain in terms of grams per hour as a function of vapor pressure differential for the test conditions used. In order to accomplish this, the dew point was measured inside the container using a chilled mirror type hygrometer. Dew point measurements were related to vapor pressure and the moisture inside the container volume using the relationships in Reference 23.

2.4.3 Environmental Exposure Testing

A variety of environmental exposure test procedures were followed to subject test specimens taken from actual ammunition containers and ASTM D638 Type IV tensile test specimens made from Marlex CL-100 HDPE to a wide range of environmental conditions. These tests covered the range of typical environmental exposure tests and included those shown in Table 5. The conditions used allowed the determination of the sensitivity of the materials to particular aspects of the environment (i.e., solar radiation, humidity, etc.). Test specimens were placed on exposure in numbers sufficiently large to allow individual pieces to be removed on a predetermined schedule for properties measurements. Samples were not returned to their respective exposures after completion of the measurements.

Accelerated outdoor (EMMAQUA®) exposure testing was conducted in accordance with ASTM G90. Sample temperature was monitored periodically during the exposure in order to determine the high, low and typical temperature extremes occurring during the course of the test. Sample temperatures were determined using a thermocouple attached to a control sample of 155mm Propelling Charge Container material. Temperature measurements were recorded around solar noon.

Table 5
Summary of Environmental Exposure Tests
Conducted on Sample Materials

Exposure Tests	Environmental Conditions	Related Test Standard
Temperature/Humidity Chamber	Constant elevated temperature and high humidity	MIL-STD 810D Method 507.2 (tailored)
DSET Solar Simulator	Constant elevated temperature and high humidity with simulated solar radiation	MIL-STD 810D Method 505.2 (tailored)
Suntest	Xenon arc lamp exposure with ambient conditions	-
Oven	Constant elevated temperature with ambient humidity	ASTM D3045
Real-time Outdoor	Natural outdoor Arizona, at-latitude exposure angle	ASTM D1435
EMMAQUA®	Intensified natural solar radiation with ambient outdoor conditions	ASTM G-90

Real-time exposure tests were conducted in Arizona on both full-scale items and test specimens. Test items were mounted on a south facing rack at a 34° angle. As noted for the accelerated outdoor testing, sample temperatures were monitored around solar noon during the test. The effects of elevated temperature with ambient laboratory humidity conditions were evaluated using a mechanical convection oven. The test was conducted with a constant 71°C temperature. Test specimens and the cap-seal portion of a 155mm Propelling Charge container were subjected to these conditions.

Elevated temperature/humidity exposure testing was conducted at 60°C/90%RH in a 1812 liter Envirotronics environmental chamber. The chamber is capable of producing various conditions over a temperature range of -73°C to +176°C with relative humidity control capability covering a range between 20% and 95%. The effects of solar radiation with elevated temperature and humidity was also studied using this environmental chamber in combination with a solar simulator array. The solar simulator array was 122cm x 122cm and comprised of compact source iodide metal halide and UVA-340 fluorescent lamps.

The array was positioned and operated to produce approximately 95 $MJ/m^2 \cdot day$ total radiation between 300nm and 2500nm with approximately 3.8 $MJ/m^2 \cdot day$ ultraviolet radiation occurring below 385nm. The test articles were located in a 76.2 cm x 96.5 cm target area behind an ultraviolet absorbing acrylic panel. The spectral energy distribution at the target plane is shown in Figure 3.

Test specimens were also exposure tested in a Xenon arc ultraviolet exposure cabinet using ambient temperature and humidity conditions. The samples were exposed to simulated solar radiation using a Heraeus Original Hanau Suntest Accelerated Exposure Machine. A filter eliminating ultraviolet below 290nm was used over a 1.1kw Xenon light source to approximate the global radiation of natural sunlight in the 300nm to 800nm wavelength region. The irradiance of the filtered light is approximately 185 mW/cm^2, with approximately 8.4 mW/cm^2 below 400nm. The test samples were located approximately 9 inches from the light source. Ambient air is circulated in the exposure chamber to maintain the samples at close to ambient temperature. Black panel temperature in the chamber was maintained at about 45°C. The spectral distribution of the light source used in the chamber is compared to natural sunlight in Figure 4.

2.5 Correlation of Data and Lifetime Prediction Models

2.5.1 Mathematical Modelling of Durability

The approach taken to mathematically correlate durability characteristics obtained from accelerated tests to real time tests was to attempt to kinetically relate a material's exposure-induced properties to the level of stress (e.g., exposure) taking into account structure-property relationships. This requires information on rate constants as a function of structure and temperature-related changes in those rate constants. The development of complete expressions that predict performance apriori of the actual exposure tests is essentially impossible. This is due primarily to a lack of information on well-defined structure-property and stress-property relationships for the same properties. However, the degradation rates of certain important properties of plastics may be described by S-shaped curves in which the property, or retention of property, is plotted as the dependent variable as a function of the environmental stress. Plotted as change in property, the relationship takes the form shown in Figure 5 where the independent variable acts as the driving force which is a combination of solar radiation, temperature, oxygen and moisture in this treatment of the ageing process. The successful application of this modelling approach depends on the availability of property data in the linear region of the curves in Figures 5 and 6 and the identification of the limit of acceptability.

Examination of the concepts of induction, rate-controlled, and saturation processes is a prerequisite to a thorough understanding of the ageing process. The term <u>induction</u> is represented by region I of Figure 6; it is a convenient descriptor for the value "i" that

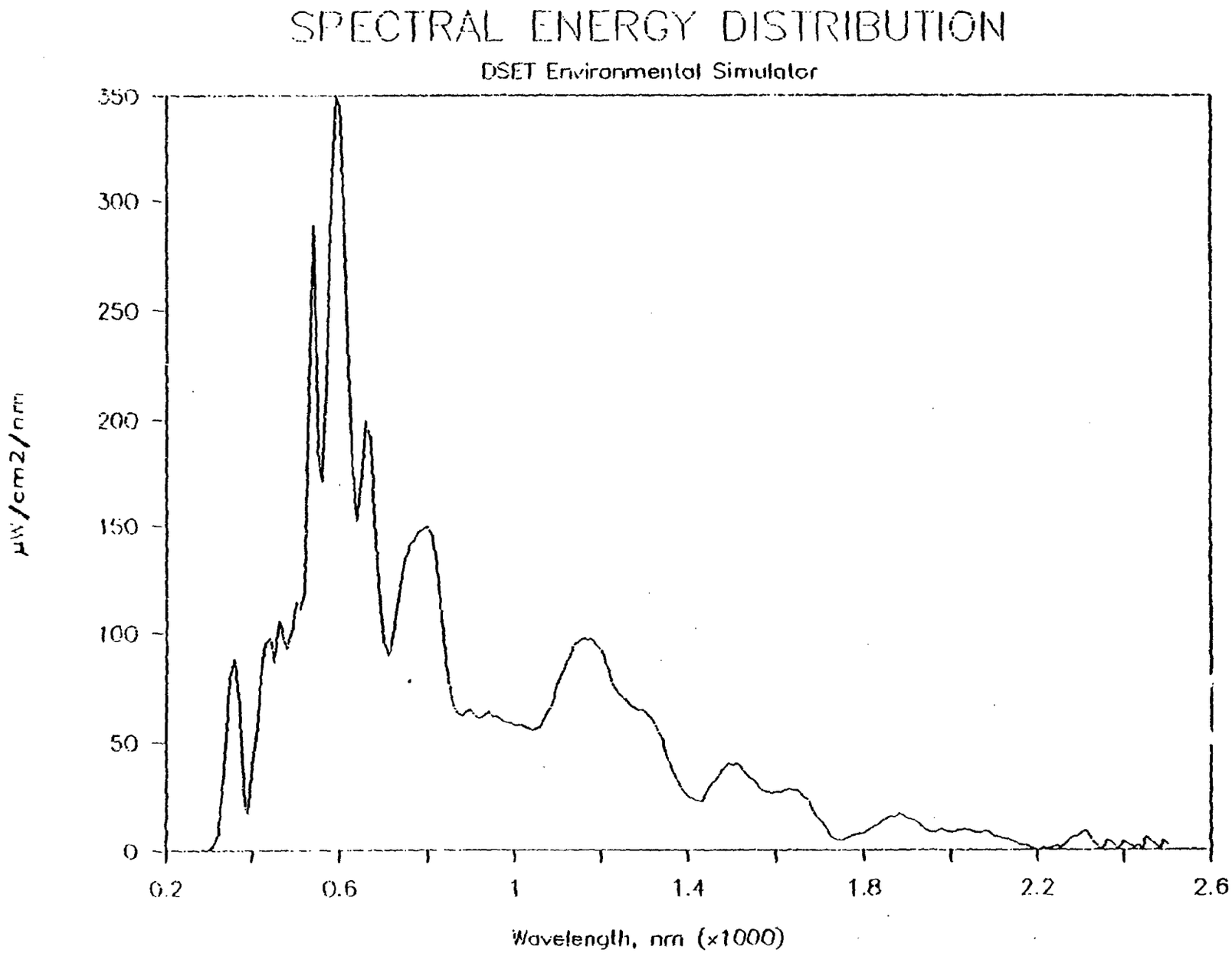

Figure 3: Spectral Distribution of DSET Solar Simulator

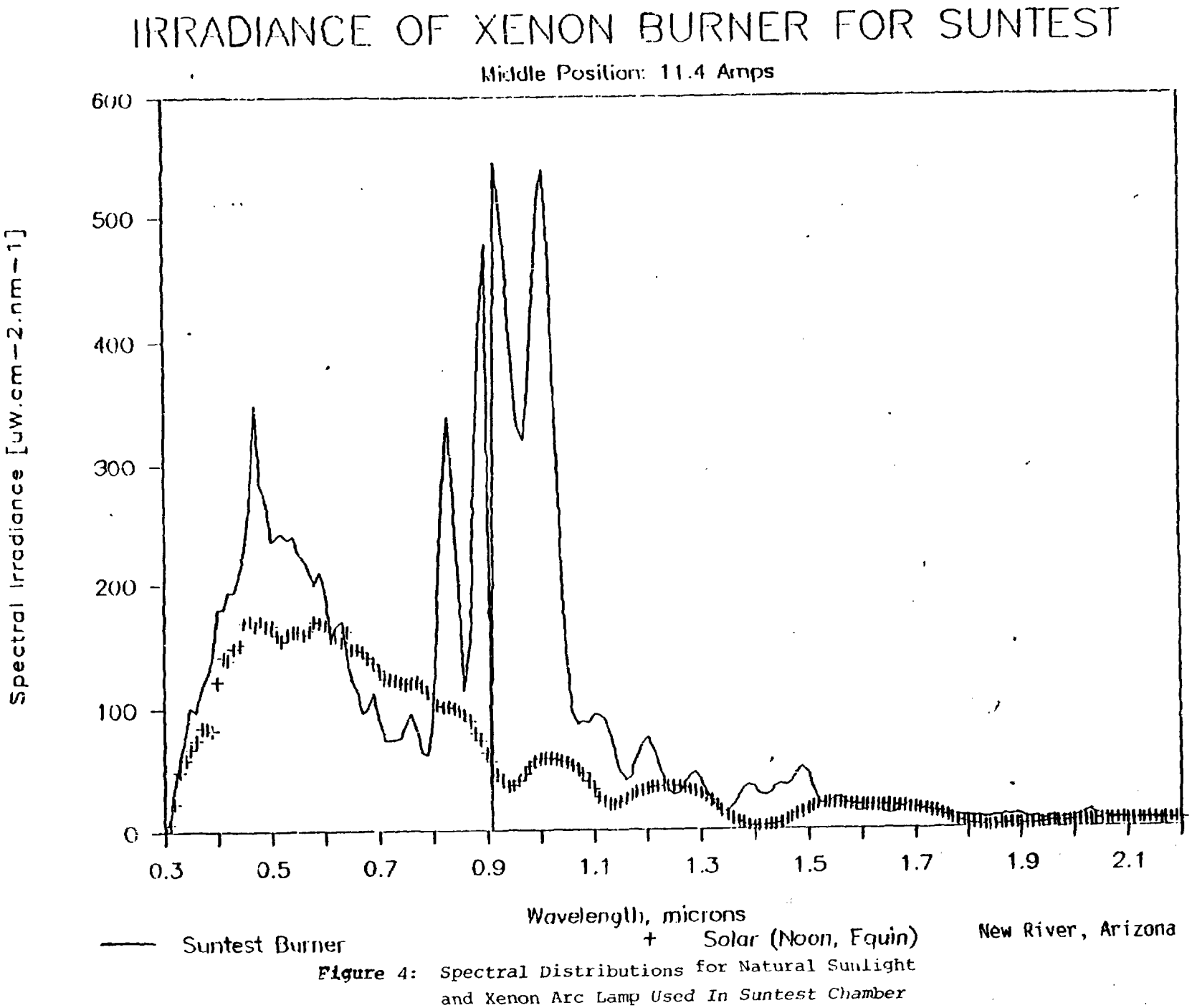

Figure 4: Spectral Distributions for Natural Sunlight and Xenon Arc Lamp Used In Suntest Chamber

represents quantitatively the magnitude of the independent variable necessary to initiate the rate-controlled property change. More fundamentally, induction describes both the reaction rates specific to initiation and the quantity of stress required for the production of a sufficient number of defects, or "observable events," that are necessary in order to be measurable by whatever diagnostic tools are employed to assess the dependent variable. Region II of Figure 6 is known as the rate-controlling step and is that portion of the reaction, or ageing process, that is represented by a single linear rate equation. More fundamentally, it is that time period of stress application after initiation where the concentration of reactive sites available for reaction obeys a well defined depletion rate. When this does not occur, either region II cannot be mathematically represented as a linear relationship or the saturation phase has been reached. Obviously, saturation is a descriptor that is employed to describe the material condition in which most, if not all, reactive sites, or critical events, have been depleted during the application of stress.

The linear portion of Figure 6 can be described by writing a slope intercept equation, $y = mx + b$, where $\Delta P = mE + b$, m is the slope and b is the intercept. Solving for E, we obtain

$$E = 1/m \{\Delta P - b\} \quad (1)$$

where $-b/m = i$, the intercept on the abscissa that is the induction measured in terms of the independent variable as exposure. Equation 1 can be written in terms of loss of property as a function of exposure, giving

$$\Delta P = m\{E - i\} \quad (2)$$

permitting prediction of durability of that property in the rate controlling step in terms of the exposure. It is important to note that few materials plot as a normal linear relationship defined by equation 2 and that generally a log-normal and sometimes a log-log plot is required to achieve a linear relationship. This is particularly true for systems with exponential or logarithmic decay in the availability of reactive sites, or where the stress such as ultraviolet radiation, exhibits such a decay as it penetrates into the material's matrix. In this case equation 2 becomes

$$\Delta P = m\{\log E - \log i\}, \text{ or } \log \Delta P = m\{E - i\} \quad (3)$$

Correlation of accelerated and real-time exposures should seldom, if ever, be performed on exposed, or stressed, materials in only the induction or the saturation phase since these expressions only explain linear portions of the ageing process. We do use these regions in combination to define the entire exposure process; however, acceptance decisions should never be made when either the real-time or the accelerated exposure level is representative of one of these regions -- especially in the induction phase. Nonetheless, a number of researchers have undertaken studies to mathematically describe both the induction and saturation portions of rate equations. These range from purely empirical to highly theoretical analyses.

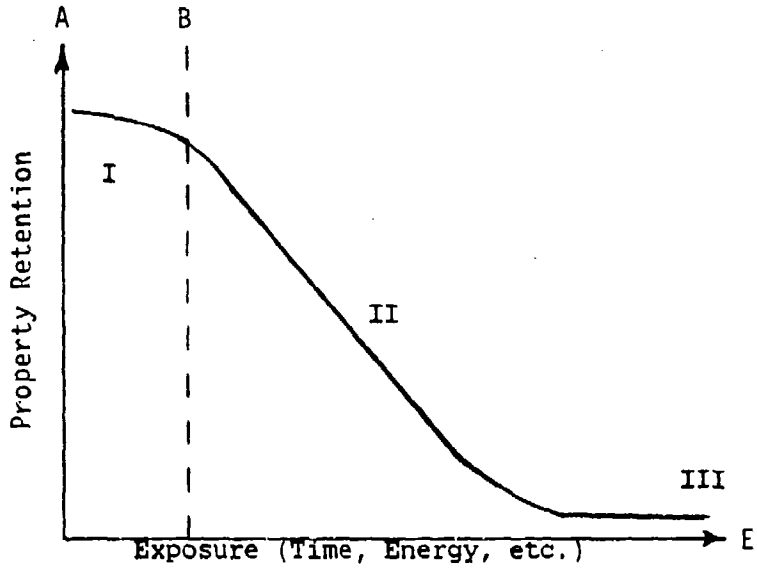

Figure 5: Plot of Property Retention Versus Exposure for Two Different Processes

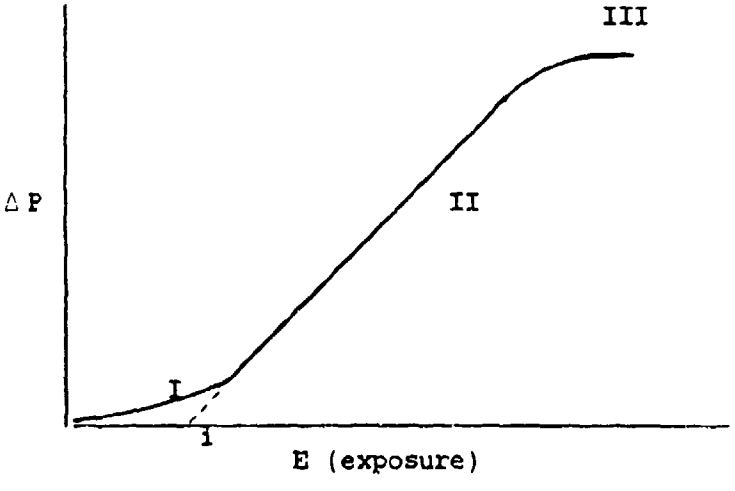

Figure 6: Property Loss Representative of Induced Property Change

2.5.2 Kinetic Expressions of Ageing Processes

The instantaneous rates at which the concentration of reactive molecular sites change with time (both the creation of new and the depletion of existing species) in photochemical, oxidative, or photo-oxidative reactions may be represented by the derivative dC/dt -- which states a reaction velocity. In zero order reactions, we simply set the derivative equal to the proportionality factor "k", the value of which depends on the temperature as well as the order. In first, second and higher order reactions which may be also opposing, or back reactions, or secondary reactions of different order, these expressions become complicated by the mathematical description of the instantaneous concentrations of unreacted species, new species, etc. Nonetheless, it is instructive to examine the simple first order reaction [mM + nN = products] where by definition the rate depends only on the concentration of, for example, M.

$$dM/dt = -kM \tag{4}$$

which, on integrating, becomes

$$\ln M = -kM + b \tag{5}$$

which is similar to equation 3.

The influence of temperature on these relationships is shown by a consideration of the Van't Hoff and Arrhenius equation. Arrhenius developed the relationship

$$d\ln(k)/dT = E/RT \tag{6}$$

from the Van't Hoff equation for the temperature coefficient of the equilibrium constant, where k is the specific rate constant, E is the material specific activation energy for the reaction and R and T are the gas constant and the absolute temperature, respectively. Integration of equation 6 yields the expression

$$\ln(k) = - E/RT + \ln(A) \tag{7}$$

where A is a constant of integration known as the Arrhenius factor. Equation 7 is useful for plotting exposure data to develop activation energies. If we consider that the reaction rate "k" can be described by the relationship dP/dt as the change of property with time and if we consider the expression dt to be represented by an incremental exposure then we can, as an example, expose a plastic for a specific ultraviolet exposure (in kJ/m^2) at several different temperatures and employ equation 7 to determine its activation energy. This can be done by plotting dP/dEuv versus 1/T and computing the activation energy from the relationship tan α = E/R from

$$dP/dE_{uv} = E/R\ (1/T) - \ln(A) \tag{8}$$

Placing equation 7 in exponential form, as presented in equation 8, a thermal reaction coefficient S for exposure of this plastic at temperature T can be developed as shown in equation 9.

$$S = dP/dE_{uv} = A\ e\{-E/RT\} \quad (9)$$

A thermal velocity coefficient V can be computed from the ratio of two thermal reaction coefficients S and S' normalized to an arbitrarily selected reference temperature T' such that

$$V = S/S' = e\{-E/RT\}/e\{-E/RT'\} \quad (10)$$

and since this velocity coefficient applies to the independent variable, or ultraviolet exposure in this example, we may now thermally adjust the measured ultraviolet exposure data used to expose a plastic whose activation energy we either know or have determined. Using this thermally adjusted ultraviolet irradiance data, we may now plot the change in property (or log of the change in property) versus the thermally adjusted ultraviolet exposure E_{tuv} (or log of exposure) to give. for example,

$$\Delta P = m\ (\log E_{tuv} - \log i), \text{ or} \quad (11)$$

$$\log \Delta P = m\ (E_{tuv} - i) \quad (12)$$

These equations may be considered as representing a "unified exposure theory" that will permit the normalization of both irradiance data (ultraviolet) and exposure temperature in exposure tests. This, in turn, means that differences in exposure results can then be interpreted in terms of differences in environmental constituents such as humidity/ moisture/dew formation and localized environmental constituents (ozone, smog, acid rain, etc.).

Although this approach emphasized ultraviolet effects for outdoor exposure, the analysis technique is applicable to the thermal effects that occur as a result of indoor exposure. The extent to which this modelling approach could be applied to the container materials investigated, as will be discussed further in subsequent paragraphs, was limited by the performance of the materials during the exposure tests and the short duration of the exposure testing. That is the HDPE was found to exhibit a failure very close to the end of the induction phase while neither of the materials were exposure tested long enough to characterize the rate controlling step.

3.0 PHASE I - DISCUSSION OF RESULTS

3.1 Literature Survey Results

The results of the literature survey were reported on in DSET Report No. R2970-5 (Reference 24). The procedural objectives of the effort, as discussed in paragraph 2.2, were met. The survey showed that little

public information exists on the quantitative performance of plastic materials beyond five year test programs. The fact that plastic materials, and polymers in general, are in use well beyond a five-year period suggests the potential for plastic products with greater than five year lifetimes. Unfortunately, the literature survey clearly proved that little engineering information exists on which to base the design life of products manufactured with plastic materials, especially in long-term applications where performance is critical.

The results of the literature survey proved valuable to the overall understanding of the performance of plastic materials since it studied the eleven materials listed in Table 1, and specifically addressed the development of test procedures for the HDPE and polyester materials used for the test items studied in Phase II. The survey identified information on the degradation mechanisms, and thus the environmental sensitivities, of the materials. This information allowed the development of the Phase II environmental testing approach and the materials properties measurement approach. The degradation of the materials studied, the sensitivities of the materials investigated and how the results of the literature survey were used are discussed in the following paragraphs.

3.1.1 Example of the Use of Literature Survey Results

The use of the technical literature survey to identify the chemical basis for the degradation of generically classified plastic materials, is exemplified by the following discussion concerning one of the literature citations identified during the survey and highlights the limited usefulness of using reported data to judge the acceptability and qualification of any specific materials. The information contained in Figure 7 alludes to the durability of plastic materials, in this case fiber reinforced polyester which is generically related to the sheet molding compound of interest to the M2A1 container, being acceptable for 10 to 12 years. Even if the articles reported on in literature were fabricated from the same material intended for the M2A1 container, the usefulness of the information to the prediction of the M2A1 container's functional lifetime would be limited by the probability that the specific materials, additives and processes used after 10 to 12 years would be changed. The significance of the information to the project resides simply in the logic that a specific fiber reinforced material, exhibiting an acceptable degree of durability for up to 12 years of outdoor exposure, suggests that a like material subjected to primarily indoor exposure conditions would have potential to exhibit an acceptable degree of durability in excess of 12 years.

STUDY OF THE AGEING RESISTANCE UNDER NATURAL CLIMATIC CONDITIONS OF POLYMETHACRYLATE, POLYCARBONATE AND POLYESTER PLATES AND SELECTED COATINGS AND FACINGS; Journal Article

Goliszek, Anna; Pol.; Pr. Inst. Tech. Budow., 10(3), 54-61; 1981; Polish;

The weathering resistance was reported for 16 plastic panels, coatings and facings exposed to natural weathering in Warsaw for up to 13 years. The investigated materials included glass fiber-reinforced polyester panels, fire-resistant glass fiber-reinforced polyester panels, chlorinated rubber of acrylic coatings, etc. For example, decorative durability of glass fiber-reinforced polyester panels was 6 yr., whereas their durability with respect to mechanical properties was 10-12 yr.

Descriptors: *Weathering resistance; *Glass reinforced polyester; *Weathering resistance; *Polycarbonate weathering resistance; *Fire resistant polyester weathering resistance; *Acrylic weathering resistance; *Natural weathering; *Rubber chlorinated coating weathering resistance;

Figure 7: Literature Survey Citation - Excerpt From Reference 24

The major conclusion to be made from this example is that the test plan resulting from this project must provide for concurrent real-time and accelerated exposure testing of the component materials used in container items. This will be made obvious in subsequent paragraphs by the performance of the containers in real-time exposure tests. Other literature identified the chemical mechanisms by which the plastic materials studied degrade and thus suggested the environmental parameters which could be used to accelerate the effects of long-term ageing. The degradation mechanisms for several of the plastics studied are summarized in the following paragraphs:

3.1.2 Material Degradation Mechanisms

3.1.2.1 Polycarbonate

Polycarbonate is available in number of grades which offer exceptional impact resistance. It is based on dihydric or polyhydric phenols which are linked through carbonate groups. Its structural properties are adversely affected by ultraviolet exposure but when appropriately stabilized or filled it is used in wide variety of applications. Until the work of Clark and Munro in 1982 (Reference 25),

solid state polycarbonate was thought to degrade by the Photo-Fries rearrangement shown in equation 13 both at the surface and in the bulk (Reference 26). Their findings indicate that the surface of polycarbonate actually degrades by photoxidation shown in equation 14. Their work further showed that, at equilibrium, surface degradation and the mechanism of degradation depends greatly on the wavelength of irradiation and flux rate. The significance of these findings is in the low probability of forming ultraviolet absorbing phenyl salicylates at the surface of polycarbonate during natural outdoor exposure.

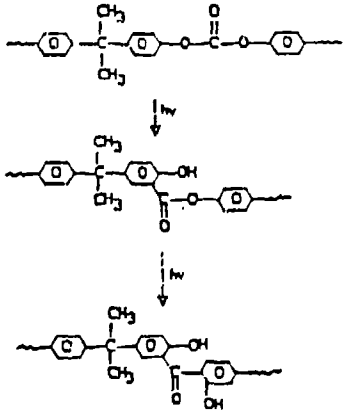

(13)

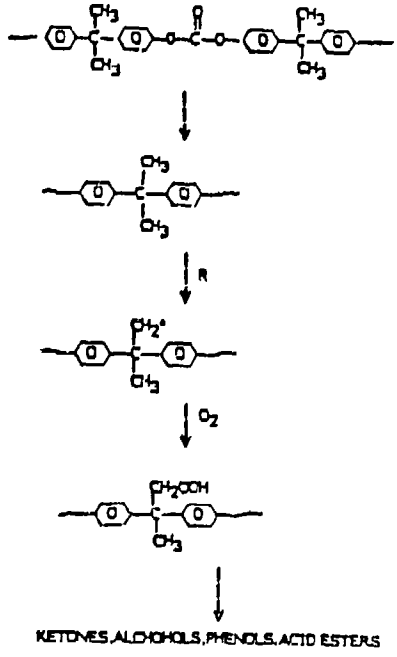

(14)

The effect of water on the photochemistry of polycarbonate is made obvious by the study of stoichiometry and kinetics (Reference 25). The detrimental effects of hydrolysis is increased when polycarbonate is initially irradiated under dry conditions. Surface degradation effects due to short wavelength irradiation (formation of phenyl salicylates) are generally water leachable or removable. The products formed during irradiation under dry conditions although not affected by water, cause chain breaks and form polar groups which favor the penetration of water and the liberation of bisphenol A monomers which photooxidize faster than the polymer (Reference 27).

The strength, impact resistance and craze resistance of polycarbonate are closely related to thermal conditions during processing. As noted in Reference 28, the annealing conditions used to treat polycarbonate are closely related to impact resistance. Cyclic temperature excursions are particularly detrimental when polycarbonate materials contain a relatively high percentage of moisture. Water resides in microvoids which cause the material to craze with temperature changes.

The mechanism by which unfilled polycarbonate degrades is sensitive to the synergistic effects of the wavelength distribution of incident solar radiation, temperature and moisture. It is unlikely that the use of polycarbonate as military item packaging material would use unfilled or unpigmented polycarbonate. Intuitively, degradation due to solar radiation exposure would therefore be limited to the surface of packaging items. This surface degradation is important to impact resistance however. Logistic chain information suggests that direct exposure to solar radiation (i.e., the two-year uncontrolled exposure) would be minimal early in the life cycle of any of the containers studied in this project and therefore suggests that the effects of solar exposure would be greater at the end of the life cycle.

3.1.2.2 Acrylonitrile, Butadiene, Styrene Polymers (ABS)

The performance of ABS is dependent upon the contribution of each of the monomers from which it is comprised. Acrylonitrile offers the property presence of butadiene while the styrene monomer contributes rigidity. The mechanism by which ABS degrades includes the oxidation of the rubber component. The rubber component, under normal circumstances, allows the formation of microcracks which serve to relieve intrinsic stress. The embrittlement of the rubber component by oxidation, prevents the formation of microcracks and leads to major fracture. The oxidative process begins at the surface and as a result of this, oxygen is allowed to penetrate to an increasing depth within the bulk material. The net result of the oxidative mechanism is a drastic loss of impact resistance which will occur as soon as the surface is attacked.

The rubber portion of ABS polymers is susceptible to photooxidation initiated by ultraviolet irradiation. The butadiene units are photooxidized by molecular oxygen through free radical oxidation mechanisms

or by singlet oxygen -ene type oxygen mechanisms (Reference 29). Ghaemy and Scott, in Reference 12, state that the loss of impact strength due to photooxidation is paralleled by a decrease in the concentration of 1, 2-dialkylethylene groups in the polybutadiene component. They also found that the degradation of impact strength was closely related to irradiation time.

The necessity for considering the synergistic effects of environmental conditions when designing an accelerated test are shown for ABS in References 30 and 31 where the effects of processing and thermal history were found to influence tensile and elongation properties in addition to the rate of change of tensile strength due to ultraviolet exposure. The work reported by Geuskens and Bastin also showed that a phenolic antioxidant used to stabilize the ABS had a detrimental effect on the tensile properties, in addition to the negative effect that a hindered amine ultraviolet light stabilizer had on the antioxidant.

The effects of processing conditions (160°C) in air were found to be related to the occurrence of acetophenone groups (significant to a decrease in average molecular weight) and therefore a decrease in tensile strength. Samples prepared using increasing periods of time at temperature, subsequently irradiated with ultraviolet light from 280nm to 360nm, with peak wavelength at 310nm, where found to have increased concentrations of acetophenone groups.

The significance of the work reported in the study of ABS polymers is that drastic changes in the surface chemistry resulting from ultraviolet and/or thermal exposures can occur in a matter of minutes. However, the rate of property change generally reaches a plateau after several hundred hours of exposure only because the chemistry of the surface layer provides a barrier to further degradation.

The mechanism by which unprotected ABS degrades is particularly sensitive to the effects of solar radiation after even very short term exposures. The volume of literature describing the poor environmental performance of uncoated ABS suggests that unprotected ABS is not suited for long-term packaging applications. The use of surface coatings to protect ABS would considerably complicate the determination of realistic accelerated test conditions because the test conditions must also consider the performance and effects of the coating on the ABS. Degradation of ABS is greatly dependent upon the rate of oxidation occurring within the bulk of the polymer. Solar exposure would accelerate this rate. However, stable surface coatings could be used to prevent the degradation due to solar radiation exposure until the surface coating itself failed. The structural property degradation of the coated ABS item would under these circumstances depend primarily on thermal and humidity environmental parameters.

3.1.2.3 Polyethylene

Polyethylene is a partially crystalline thermoplastic, although inherently unstable, it is used in a variety of outdoor

service items. This is made possible through the use of stabilizers and antioxidants. High density polyethylene results from a low pressure polymerization reaction which allows the formation of long linear chains with little or no branching (Reference 32). Polyethylene (and polypropylene) undergo photooxidation where the mechanism proceeds through a hydroperoxide stage. The following equations show a degradation mechanism for the general case. Specific morphology and different processing conditions will have modified reaction stages that are essentially specific to each (Reference 33 and 34).

$$RH \xrightarrow{h\nu} R^* + H^* \qquad \text{(Photo)} \qquad (15)$$

$$RH + O_2 \longrightarrow R^* + HO_2^* \qquad \text{(Thermal)} \qquad (16)$$

Propagation

$$R^* + O_2 \longrightarrow ROO^* \qquad \text{(Chain Reaction)} \qquad (17)$$

$$ROO^* + RH \longrightarrow ROOH + R^* \qquad (18)$$

Termination

$$R^* + R'^* \longrightarrow RR' \qquad \text{(non-propagating)} \qquad (19)$$

$$R'^* + ROO^* \longrightarrow R'OOR \qquad (20)$$

$$ROO^* \quad R'OO \longrightarrow ROOOOR' \qquad (21)$$

The study on thermal oxidation reported in Reference 35, at a temperature of 100°C at the surface of low density polyethylene, showed that the rate of thermal oxidation at the surface increases after 150 hours of exposure while the rate of thermal oxidation in the bulk tends toward steady state. This work also showed that hydro-peroxide formation, as a result of photooxidation, reached a maximum after approximately 300 hours of exposure and began to decrease long before carbonyl formation reached a maximum. Although this information cannot be entirely applied to the high density polyethylene materials pertinent to this project because the study was conducted on unfilled and unstabilized low density polyethylene, the degradation trends reported are very significant.

This work showed that, compared to photooxidation, the uptake of oxygen during thermal oxidation is low. Further, the role of hydroperoxides in the thermal degradation mechanisms at the surface is not as important as in the bulk and that the extent of oxygen uptake is greater in the bulk than in the surface. This suggests that the thermally induced oxidative degradation of polyethylene is predominantly a bulk effect. Therefore, in a real system (one containing the appropriate stabilizers and antioxidants) at a given temperature the rate of degradation due to thermal oxidation is primarily dependent on the concentration and stability of additives and that over a defined temperature range thermal oxidation effects cannot be accelerated. This does not say however, that photooxidation or

photooxidation combined with thermal oxidation will not accelerate degradation of surface dependent physical properties and thus cause bulk failures. The report also indicates that the rate of degradation in the bulk due to photooxidation tends to decrease with exposure time which suggests that a barrier layer may be formed due to reaction products, although it also seems likely that the rate of photooxidation depends on the diffusion rate of UV-stabilizer to the surface.

The choice of pigments and fillers also greatly affect the weatherability of polyethylenes. The mechanism by which they contribute to or decrease stability is complex and undoubtedly dependent upon their absorption properties, in the case of ultraviolet induced effects, and their synergism with additives and oxygen, in the case of thermal oxidation induced effects. Degradation due to solar radiation exposure would be limited to the surface of packaging items early in the life cycle. As noted for polycarbonate, logistic chain information suggests that direct exposure to solar radiation (i.e., the two-year uncontrolled exposure) would be minimal early in the life cycle and therefore suggests that thermal oxidative degradation mechanisms will predominate. The literature indicates that thermal oxidation effects cannot be accelerated at a given temperature however, higher temperatures would increase the degradation rate. Therefore, if we assume that the reaction products of thermal degradation are not temperature dependent (for instance over a small increase in temperature above actual use conditions, but below critical transition temperatures) it should be possible to realistically accelerate thermal degradation effects by testing at temperatures slightly above maximum service temperatures.

3.1.2.4 Polypropylene

Commercial polypropylene is primarily crystalline and is more thermally stable than polyethylene. Like polyethylene, the photooxidation of polypropylene involves hydroperoxide and carbonyl formation. The photooxidation mechanism differs from polyethylene in that the concentration of hydroperoxides continues to increase with increasing irradiation time (Reference 36). In a series of articles by Allen and Fatinikun (References 37-39), it is shown that carbonyl groups dominate the rate of photodegradation for highly oxidized polypropylene however, their role in initiating photooxidation is questioned. They also show that in mildly oxidized polypropylene, hydroperoxides control the rate of photo-oxidation.

The authors show evidence for an oxygen-polymer charge transfer mechanism for the initiation of photooxidation. Their data also strongly indicates that the degradation mechanism, in this case the rate controlling mechanism, is dependent on the wavelength distribution of irradiation. The charge transfer mechanism is not important to the determination of an accelerated test procedure because the initial degree of oxidation exhibited in the test article will be dependent on the processing conditions used to fabricate the test article. The influence of the wavelength distribution of the irradiation on the rate of hydroperoxide and

carbonyl formation is most significant. The effect of wavelength distribution on the photooxidation of polypropylene is shown by an increase in the induction period when polypropylene is irradiated with wavelengths greater than 370nm as compared to polypropylene irradiated with a complete spectrum including ultraviolet. Under this circumstance the hydroperoxides are expected to react but not the carbonyls. However, the induction period is also increased, although not to the extent of the former case, when polypropylene is irradiated with wavelengths less than 2000nm. The significance of these findings is in the fact that even though hydroperoxides photolyze to give carbonyl groups, photooxidation will not progress unless the carbonyl groups undergo further reaction.

Accelerating the degradation of polypropylene will depend on producing a high degree of oxidation during the initial portion of the exposure and the production of a complete solar spectrum in the test chamber. The high degree of oxidation required can be produced by high temperature. However, to maximize the wavelength distribution in the test chamber, it would be necessary to minimize humidity at least for some portion of the exposure cycle.

3.1.2.5 Polyester Sheet Molding Compound

The information obtained for polyester sheet molding compounds pertinent to the design of an accelerated test method was minimal as compared to the other materials investigated. This lack of specific, detailed degradation mechanism information may in part be due to the constant change and improvements made in composite materials over the last several years. Our discussion of degradation mechanisms for polyester sheet molding compounds is therefore cursory.

Polyesters for reinforced plastics for military items are generally based on the unsaturated polyesters and the allyl type resins. Unsaturated polyesters are polymerized from a mixture of unsaturated and saturated acids or anhydrides. The unsaturates provide sites for reaction with the monomer, while the saturates control the location of these sites within the polymer molecule. Maleic anhydride and its isomer fumaric acid are the principal unsaturates in polyester synthesis. The common saturates are orthophthalic anhydride and isophthalic acid. The principal dibasic alcohols are propylene, diethylene and ethylene glycols. Monomers for laminating resins include dialkylphthalate, diallylisophthalate, triallylcyanurate, styrene, vinyl toluene, methymethacrylate and dichlorostyrene.

The usual means of initiating the copolymerization of the polyester with the monomer is by the action of peroxide catalysts. The specific catalyst determines the temperature at which curing takes place. Some catalysts are reactive at room temperatures, while others require the application of heat. Common catalysts for laminating formulations are activated in a temperature range between 112°C and 155°C. Characteristic of polyester cure is the fact that once the reaction has been initiated, it

proceeds to completion and cannot be interrupted at an intermediate stage. Completion occurs when 92 to 95% of the unsaturated ester sites have been depleted (Reference 40).

The blooming of glass fibers for unfilled polyester composites is generally preceded by yellowing of the matrix due to solar radiation. The yellowing of these composites is due to photooxidation of unreacted unsaturated sites on the polymer chain. The first sign of the effects of weathering generally associated with filled composites is the exposure of glass fibers at the surface of the material. The exposure of the glass fibers is a result of cracking and erosion of the matrix around the glass fibers. This process is the combination of photolytic processes involving the resin and the physical effects of temperature and humidity fluctuations. The stress fatigue associated with failure of the matrix depends on the coefficient of thermal expansion mismatch between the glass and the matrix and the differential swelling and shrinkage of the resin due to moisture (Reference 41).

The number of accessible hydrolyzable ester groups in polyesters have been found to affect the extent of hydrolysis leaching in hot water. The formation of surface cracks and the debonding of glass fibers are also related to the number of hydrolyzable ester groups. Debonding and surface cracks are generally the first signs of damage in glass reinforced laminates. Pritchard and Taneja report in Reference 42, that although bisphenol polyesters exhibited considerable cracking after 50 days of exposure to 100°C water, vinyl ester resins had no cracking, samples exposed to 80°C water showed no degradation of mechanical properties even after 83 days.

3.2 Logistics Chain Study Results

The logistics chain study resulted in a detailed documentation of the physical movement of ammunition items from the load plant to permanent storage areas and the characterization of the logistics chain environments. The features of the logistics chain, as described in Appendices A and B, are related to a time scale which can change with the need for ammunition items, changes in production schedules, training schedules, test schedules and war. As noted in Appendix A, the expected lifetime of ammunition, and thus the packaging containe: items is at the present time far less than thirty years. The expected lifetime could be changed by an increase in production or the stockpiling of ammunition over time, the use of the items in the event of war or an increase in the frequency of maneuvers. The dynamics of the logistics chain must therefore be considered when designing plastic ammunition containers, the selection of container materials and during the interpretation of plastic packaging qualification and acceptance test results.

As an example, one of the ammunition items studied is currently in short supply. Therefore, a study of the performance of plastic packaging on a statistical basis for this item, similar to that which has typically been conducted for ammunition protected by metal packaging in order to determine

the statistics of accurate delivery to the target, will not provide long-term performance data. The use of ammunition performance to evaluate the performance of packaging in this case therefore cannot be used as a basis for qualification of material or packaging design.

At the present time, packaging containers are apparently produced at a rate similar to the ammunition items. Loaded containers are unlikely to spend more than one year in storage at the load plant before deployment. The initial portion of the lifetime of a plastic ammunition container is dependent on the features of the load plant environment and, at least at the present time, covers a period on the order of one year. The transportation environment occurring after the ammunition is loaded into the container covers a period of months. The deployment of the items to the permanent storage areas is also on the order of months. Containers may be stored indoors or outdoors prior to loading. The environment to be experienced by the containers early in the life cycle will never be worse than the environment presented at the load plant and the environment presented at the ports of embarkation and debarkation. In order to minimize the dependence of lifetime prediction models on statistical testing, the container items should be subjected to the worst possible conditions of the load plant, transportation environment and the port of debarkation, over an equivalent period of time before conducting exposure tests to determine the effects of any environment on the long-term performance of the container items.

The ability of the container items to meet "form, fit, and function" requirements after the first one or two years of their manufacture could be determined using typical Mil-Std 810D test procedures as tailored by the MVTR requirements. However, these test procedures carried through to an arbitrarily chosen set of conditions, cycle time and number of cycles would be inadequate for determining the acceptance and qualification of plastic container items or container item materials for long-term use. The reason for this relates to the time at temperature dependent degradation mechanisms of the specific plastic materials used for the containers. As suggested in the preceding paragraphs, plastics are stabilized for specific environmental uses, additives are used to enhance processing and the manufacturing procedures and manufacturing procedures are continually made more efficient by changes in the manufacturing thermal cycles and processing aids used. Therefore, lot-to-lot variations of plastic items will be a major concern for the qualification of plastics for use in ammunition packaging applications and must be accommodated by acceptance test procedures.

The results of the logistics chain study combined with the knowledge of typical plastic material compounding and manufacturing procedures and processes, clearly suggests that the efficacy of plastic container items can be predicted for up to two years using typical military test procedures. The extension of these lifetime prediction models to the lifetimes expected, after long periods of time under typical use and storage conditions, requires not only tailoring of typical procedures currently used, but close monitoring and testing of container items on a lot-to-lot and batch-to-batch basis. The test plan that is adopted must be based on experience with plastic materials under current consideration the

processing procedures and must also accommodate future improvements and changes in materials and processing techniques ranging over the production life of the item.

3.3 General Features of the Logistics Chain and Considerations for Test Environments

The typical average environment of the 155mm Propelling Charge is described in Table 6. The times and locations listed in Table 6 also apply to the M2A1 container with the exception of the load plant which is located near Independence, MO. The average environment for Independence, MO is similar to the average environment of Charleston, IN. The extreme environment characteristics for the ammunition containers are summarized in Table 7. A comparison of the ultraviolet radiation environments occurring in several United States locations and for the accelerated tests conducted during the project is shown in Table 8. The environmental conditions that occurred during the outdoor Arizona exposure tests are described in Appendix C.

The consideration of the t' ·', moisture, and solar aspects of the logistics chain environment with t container materials degradation characteristics form the basis for the interpretation of the environmental test results. The preceding discussion of materials degradation rate dependencies on environmental factors, such as temperature, humidity, and ultraviolet, suggests that the degree of acceleration can be limited by the characteristics of the plastic material. The chemical processes which occur in the material as a result of environmental exposure follow predictable kinetic paths. These paths, as described by rate equations, relate to material property changes as the chemical structure of the plastic changes. The structural and chemical changes of the plastic material are a function of the time at specific conditions.

Accelerated exposure testing often has the objective of producing materials effects rather than the objective of accelerating the degradation of materials properties by specific mechanisms. Environmental exposure ting, specifically accelerated environmental exposure testing, must p.ovide conditions by which a material can degrade following realistic mechanisms in order to quantify the change in properties with respect to time at condition. As an example, accelerated environmental testing typically includes ultraviolet exposure. Chemical degradation by photo- processes is generally limited to the surface of materials. Thus, material properties which can be degraded by changes in the surface can be "accelerated". However, bulk properties may remain unchanged or degrade by mechanisms which are u 'istic. The use of data obtained from this test approach often results in poor correlation of test data with actual performance. The potential for unpredicted performance is especially great for materials and products with very long expected lifetimes when lifetime predictions are based on short duration tests which do not cause realistic degradation mechanisms through the induction phase at the surface and in the bulk.

The reason this test approach is often used relates to the limit of a material's acceptability being in the induction region of the property degradation curve shown in Figures 5 and The success of the test procedures used to reach the end of th ion period thus depends chiefly on identifying the end of the inductio od rather than the manner by which the degradation of the property was caused. The times needed, by accelerated and real-time environmental testing, to reach the end of the induction period are in a relative sense, close. Therefore, the accuracy of lifetime prediction for materials designed to reach a failure point in the induction period is greater than a material which fails in the rate controlling region of the property degradation curve. The prediction of ammunition container performance over a thirty-year expected lifetime therefore requires that the sensitivity of container material performance be well characterized in the induction phase since a viable container material and container design will likely reach a failure point in the rate controlling region of the curve.

Table 6
155mm Propelling Charge Logistics Environment

	Temperature (°C) Max.	Min.	Avg.	Average % RH	Average Daily Solar Radiation (MJ/m²)
European					
Load Plant Charlestown, IN 90 days	30	-4	13	69	13.8
Port of Embarkation Sunny Point, SC 13 days	32	3	18	75	15.3
Port of Debarkation Nordenham, West Germany 7 days	22	-2	9	79	10.4
Permanent Storage Miesau, West Germany 10-15 years	25	-2	11	74	10.4
Asian					
Load Plant Charlestown, IN 90 days	30	-4	13	69	13.8
Port of Embarkation Concord, CA 19 days	23	6	15	75	17.4
Port of Debarkation Pusan, South Korea 7 days	29	-2	14	66	15.3
Permanent Storage Uijongbu, South Korea 10 to 15 years	31	-9	11	69	11.4

Table 7
Environmental Extremes of Ammunition Logistics Chain

	Temperature (°C) Max.	Min.	Avg.	Average % RH	Average Daily Solar Radiation (MJ/m^2)
Canal Zone, Panama	32	22	27	88	16.2
Yuma, Arizona	42	6	23	37	21.8
Fairbanks, Alaska	22	-30	-3	63	8.7

Table 8
Comparison of Average Yearly Total Ultraviolet Radiation Below 385nm Using Various Exposures

EMMAQUA®	1617.8	MJ/m^2
24° South Florida	308.0	MJ/m^2
34° South Arizona	333.5	MJ/m^2
Los Angeles Basin	211.4	MJ/m^2
Suntest Exposure Cabinet	2453	MJ/m^2*
DSET Solar Simulator	1900	MJ/m^2*

* 24 hours per day, 365 days per year - below 400nm

The manner by which and the chemical mechanisms by which the material degrades through the induction period is important to the container lifetime prediction model since the conditions occurring during the induction phase will affect the time that a material will function acceptably in the rate controlling phase. Unfortunately, modelling performance and properties in the induction phase is complicated by the dependence of plastic materials on additives and processing conditions. This complexity is compounded by the use of more than one material in container designs which offers the potential for adverse effects of material incompatibility. This feature of container testing must especially addressed during full-scale item testing.

The environmental features of the ammunition container logistics chain which are most likely to influence the performance of the container item during the induction phase will most likely cause thermal and moisture

degradation processes to occur. This is due to the minimal probability that the container items will be exposed to the outdoors early in the items' life cycle. The requirement for the accelerated test procedures used being capable of predicting the effects of a two-year, uncontrolled outdoor exposure at anytime during a thirty-year lifetime provides the test guidelines needed to screen candidate container materials and also demands that the material, once selected, be thoroughly characterized in regards to performance after exposure to typical long-term conditions. Container material screening and acceptability testing should logically include the solar radiation environment since a material which degrades to an unacceptable level early in its life cycle after a two-year outdoor exposure would obviously not function in a two-year outdoor exposure late in the life cycle. The use of combined environment testing as the basis for lifetime prediction models for containers manufactured from materials which exhibit acceptable performance during initial testing could be used to identify the worst case, or shortest life cycle.

3.4 Development of Full-Scale Item Test Procedures

The role of full-scale item testing in the development of a lifetime prediction model centers on measuring the functionality of the container items. In light of the preceding discussions on the role of materials properties in a container's life cycle, a full-scale item test must account for the degradation of each container material component in addition to providing functional performance data. The approach to accomplishing this, as a result of the Phase I effort, includes the idea of pre-ageing and conditioning the container items prior to full-scale item testing. As noted in the preceding paragraph for container materials, screening tests can be conducted to determine the acceptability of particular container design features, and combined environment tests can be used to identify worst case performance. However, in order to quantify container performance as a function of material age, the container items must be tested in a known "state of degradation".

The approach taken to determining the moisture vapor transmission in the container and relating the transmitted moisture to a vapor pressure differential with respect to time at constant conditions could be used both as a screening test for container design as well as for predicting long-term performance. As an example of predicting moisture gain or loss, the vapor pressure differential occurring between the container and the load plant environment could be determined by direct measurement of the temperature and humidity at the time of loading, or be based on the average conditions inside the load plant when the containers are filled. The change in the vapor pressure differential after long-term storage in another environment could then be predicted on the basis of the expected rate of change in vapor pressure differential. The vapor pressure differential resulting after a period of time could then be used to determine the amount of moisture in the container. As noted in paragraph 2.4.2, acceleration of the factors resulting in an increase in moisture vapor transmission are not directly related to the test conditions used. However, accurate monitoring of

moisture vapor transmission and the characterization of a particular container design under a variety of test conditions would allow different containers to be compared and judged on a merit basis.

The measurement of pressure inside the container was also considered during the Phase I effort. The pressure retention capability of the container item can be characterized by the breaking pressure of the seal and by the decay in pressure occurring in a pressurized container. Although these features can be used to make judgements on the efficiency of the container seal, the total pressure measured inside the container items however, is dependent on temperature, water vapor pressure and the diffusion of air through the container walls and seal. Therefore, pressure is only related to the long-term functionality of the container to the extent that the container seal remains intact to prevent the physical ingress of water. Fluctuations in total pressure due to temperature changes or altitude can be measured and used to identify a major leak, however the natural decay in pressure level due to diffusion processes cannot be used for performance prediction modelling since total pressure is dependent on the partial pressures of all the gaseous contents of the container. Further, since containers are neither pressurized or evacuated at the load plant, the pressure differential will never exceed much more than several pounds per square inch in pressure or vacuum. The pressure differential would have an effect on moisture vapor transmission rate. Measurement of moisture vapor transmission therefore is a more accurate means for determining the sealability of containers that are well sealed to begin with.

4.0 PHASE II - RESULTS

4.1 Arizona Outdoor Exposure Testing

Container test sample materials, Marlex CL-100 samples and full-scale 155mm Propelling Charge container and M2A1 container items were exposure tested in Arizona. Test items were mounted on a south facing rack oriented at a 34 degree angle. The 34 degree angle is the exposure site at-latitude angle and was chosen to maximize solar radiation. This exposure test was the only real-time test conducted during the project and thus provides the baseline information to which accelerated exposure test results will be compared. The test was conducted between November 13, 1987 and September 12, 1988. Climate data for the exposure period is exhibited in Appendix C. Test samples were removed at several intervals for properties testing. These results will be discussed in a subsequent paragraph.

Test sample temperature was monitored during the exposure about solar noon time. Average maximum sample and air temperature data for the exposure intervals used during the test are shown in Table 9 with the corresponding ultraviolet irradiance data for the time period. The ultraviolet flux during the exposure, based on approximately ten hours of daylight each day, was on the order of 0.1 $MJ/m^2 \cdot hr$. A ten-hour day was also used to represent the typical times at maximum temperature for purposes of the data

analysis conducted to differentiate thermal effects from ultraviolet induced effects. This daylight hour time period was typical for the exposure test and chosen to provide a relative time basis to compare the outdoor exposure tests with laboratory and outdoor accelerated exposure tests. Actual time at temperature and daylight hour measurements could be derived from the test data. However, doing so would not enhance the understanding of the test results since all of the exposure testing conducted during the project used the same relative time frame.

Table 9
Arizona At-Latitude Test Sample Temperature and Radiation Data

Exposure Interval	Cumulative Duration (Days)	Avg. Maximum Air Temperature (°C)	Avg. Max. Sample Temperature (°C)	Ultraviolet Radiation Below 385nm (MJ/m^2)
11-15-87 to 03-28-88	128	26	35	101
03-29-88 to 05-31-88	188	31	50	175
05-31-88 to 09-12-88	290	39	65	295

Just prior to the end of the exposure test, the 155mm Propelling Charge container was noted to have cracked on surfaces that were in at least partial view of the sun during the exposure test. This cracking was noted for the 155mm Propelling Charge container test samples also. The cracks were not noticed the week before when the test items were being photographed. The 155mm Propelling Charge container was noticeably faded in comparison to containers which had been stored in the laboratory. The test items were subjected to the desert environment for a total of 290 days representing some 1160 low-high and high-low temperature excursions due to day and night temperature changes at the time these defects were noted.

The M2A1 container was exposed with the cover and handle facing upward. The container cover and the upper portion of the container sides exhibited a significant degree of fiber bloom at the end of the exposure test. The fiber bloom, with the associated fading of color, was noticed some months before and progressively increased. The container handle was also cracked at the end of the test.

The results of this testing suggest that the functional properties of the container items investigated could be detrimentally affected by short outdoor exposures early in the container items' life cycle. However,

prediction of the functional lifetime of the containers cannot be made from this single test since no functional tests were conducted on the container items after the exposure test and no limits of acceptability were set for the defects observed. Cracking of the HDPE used for the 155mm Propelling Charge container could obviously have a significant influence on the impact resistance of the container but the thickness of the container walls could afford adequate protection. Likewise, the cracked handle and fiber bloom occurring on the M2A1 container obviously decreases the load bearing capability and impact resistance of the container, respectively.

4.2 Accelerated Outdoor Exposure Testing

Container test sample materials and Marlex CL-100 samples were subjected to accelerated outdoor exposure testing following ASTM G90 using the EMMAQUA© test method. The test method uses a parabolic solar concentrating mirror array, which follows the sun throughout the day, and an eight minute purified water spray cycle at hourly intervals of the irradiation. Test items were mounted in the target plane of the mirror array. Samples were maintained near their temperature in ambient air during irradiation by continually blowing air over their surfaces. The sample temperature decreased to ambient air temperature or to just below ambient air temperature before the end of each water spray cycle and rose to its maximum temperature within eight minutes after the end of the water spray cycle. The test was conducted between November 13, 1987 and September 12, 1988. Climate data for the exposure period is exhibited in Appendix C. Test samples were removed at several intervals for properties testing. These results will be discussed in a subsequent paragraph.

Test sample temperature was monitored during the exposure about solar noon time. Average maximum sample and air temperature data for the exposure intervals used during the test are shown in Table 10 with the corresponding ultraviolet irradiance data for the time period. The ultraviolet flux during the exposure, based on approximately ten hours of daylight each day, was on the order of 0.4 $MJ/m^2 \cdot hr$. The same ten hour day noted for the at-latitude testing was also used to represent the typical times at maximum temperature during the EMMAQUA© tests for purposes of the data analysis conducted to differentiate thermal effects from ultraviolet induced effects. This daylight hour time period was typical for the exposure test and chosen to provide a relative time basis to compare the outdoor accelerated exposure tests with the other exposure tests conducted during the project.

Container material test specimens exhibited the same mode of failure noted for the Arizona at-latitude test. Namely, cracking and fading of the HDPE for the 155mm Propelling Charge container material and fading and fiber bloom for the M2A1 container material. The test items were subjected to the test environment for a total of 200 days with the failures described occurring between 60 and 157 days of exposure. After 157 days of exposure the test samples had been subjected to some 1800 temperature excursions from the water spray and day and night cycles. At the time the failures were noted, the samples had a total ultraviolet fluence of 588 MJ/m^2.

Table 10
EMMAQUA® Test Sample Temperature and Radiation Data

Exposure Interval	Cumulative Duration (Days)	Avg. Maximum Air Temperature (°C)	Avg. Max. Sample Temperature (°C)	Ultraviolet Radiation Below 385nm (MJ/m^2)
11-13-87 to 12-13-87	30	22	40	107
12-14-87 to 01-13-88	60	17	37	169
01-14-88 to 04-18-88	157	25	71	588
04-19-88 to 06-02-88	195	29	72	852
02-23-88 to 09-12-88	200	31	65	1154

Using cracking and fiber blooming as the failure criteria, the results of this testing compared to the results of the Arizona at-latitude test suggest that outdoor exposure results are accelerated by small temperature excursion cycles as well as by the ultraviolet flux or the average maximum sample temperature, at least to the extent that the at-latitude failures were noted within the range of ultraviolet fluence and the time at temperature before such failures occurred during the EMMAQUA® test. A possible explanation for this apparent relationship could be derived from the discussion of time-temperature superpositioning, as discussed in paragraph 2.4.1 for DHA, as it relates to the action of the pigment, the ultraviolet and thermal stabilizers in the HDPE and as it would relate to the debonding of fibers from the polyester in the M2A1 container material.

4.3 Elevated Temperature and Elevated Temperature/Humidity Testing

Elevated temperature tests were conducted at 71°C using a mechanical convection oven. Test samples of the container materials, Marlex CL-100 and the cap-seal portion of a 155mm Propelling Charge container were subjected to the elevated temperature conditions for over 5000 hours. No visual changes were noted during the course of the test.

Elevated temperature/humidity tests were conducted at 60°C with 90% RH. As for the other tests discussed, container material test samples and Marlex CL-100 samples were tested using these conditions. The elevated temperature/humidity test was conducted for 3765 hours. No visual changes were noted as a result of the exposure.

4.4 Solar Simulator Exposure Testing

The solar simulator and environmental chamber facility described in paragraph 2.4.3 was used to evaluate the test materials in a combined environment laboratory test. The environmental chamber was operated at 48°C/90% RH during the course of the test. The sample temperature was maintained at 60°C by the chamber temperature and the simulated solar radiation. The test was conducted for a total of 908 hours resulting in a total ultraviolet fluence of 129 MJ/m^2 at a rate of approximately 0.14 $MJ/m^2 \cdot hr$. Although no visual changes were observed for the container material test samples during the exposure, the Marlex CL-100 samples exhibited a light brown color shortly after the start of the irradiation.

4.5 Xenon Arc Exposure Testing

As described in paragraph 2.4.3, an Original Hanau Suntest Accelerated Exposure machine was used to evaluate the effects of Xenon arc lamp exposure on the container materials and Marlex CL-100. Although a complete matrix of test specimens for each material was not tested under these conditions, the few test specimens investigated produced interesting results. The container materials exhibited the same cracking, fading, and fiber blooming features seen as a result of the other exposure tests involving ultraviolet. Sample temperature during the exposure test was 58°C. The noted failures were observed after approximately 2304 hours with a total of 645 MJ/m^2 of ultraviolet for the 155mm Propelling Charge container HDPE and after 2147 hours with a total of 601 MJ/m^2 of ultraviolet for the M2A1 container material. The ultraviolet flux during the Xenon arc exposure was approximately 0.28 $MJ/m^2 \cdot hr$.

4.6 Sample Material Thermal Property Measurements

4.6.1 DSC Measurements on 155mm Propelling Charge Container Material

DSC was used to study changes in the crystallinity and oxidative stability of the 155mm Propelling Charge container HDPE resulting from the various exposure tests. The degree of crystallinity was determined using equation 22 from Reference 43,

$$\% \text{ crystallinity} = \frac{\Delta H_{sample}}{\Delta H_{std}} \times 100\% \qquad (22)$$

where ΔH_{sample} is the measured heat of fusion and ΔH_{std} is the heat of fusion for 100% crystalline material. A ΔH_{std} value of 70 calories/gram, reported in Reference 44 for a polyethylene-hexene copolymer, was used to analyze the effects of the different exposure conditions on the 155mm Propelling Charge container HDPE. The technical product data sheet for the Phillips Marlex HXM-50100 used in the 155mm Propelling Charge container indicated that it was a similar material and as a constant in equation 22, the ΔH_{std} value has no effect on calculating the change in crystallinity occurring as a result of the exposure testing.

The oxidative stability of the HDPE was studied using the onset of decomposition temperature and the decomposition heat flow. This property is related to the quantity of oxidizable groups in the sample. Thus, decreasing decomposition temperature and decomposition heat flow suggests a decrease in molecular weight, a breakdown of the polymer and the presence of stabilizers or additives. As will be discussed subsequently, the decomposition heat flow was also used with the degree of crystallinity to investigate changes in the crystalline and amorphous nature of the HDPE. A typical DSC spectra is shown in Figure 8. DSC measurement data are exhibited in Table 11.

The data in Table 11 shows a downward trend for the onset of decomposition temperature and decomposition heat flow for all exposure tests. The degree of crystallinity is seen to increase, if only slightly, while the melting temperatures remain stable. These trends suggest that while the degree of crystallinity remains stable or increases slightly, the stability of the polymer decreases with environmental exposure, probably due to changes in the amorphous region. The degree of crystallinity compared with the decomposition properties appears to be related to the occurrence of surface cracking. Interestingly, the "Adjusted Heat Flow" values shown in Table 11 and plotted against time at maximum temperature in Figure 9 and ultraviolet radiation in Figure 10, suggests a limiting value for the onset of cracking. The Adjusted Heat Flow used for this analysis is described by equation 23 for the exposure interval. The basis for this calculation is the conjecture that the energy required to decompose the sample above its crystalline melting point is proportional to the degree of crystallinity. The extent to which this conjecture can hold true could only be determined by testing sample materials with longer term exposures.

$$\text{measured heat flow} - (\%\ \text{crystallinity} \times \text{measured heat flow}) = \text{adjusted heat flow} \qquad (23)$$

The percent crystallinity data in Table 11 and Figures 11 and 12 indicate that the polymer undergoes a rapid change in crystallinity during the initial stages of the exposure tests. As noted in Reference 45, thermal oxidation of polyethylene is temperature dependent and peaks within the first several hundred hours of elevated temperature exposure. Thermal oxidative effects also influence the mechanism of photooxidation. Photo-oxidation occurs at the surface in pigmented systems and thus only affects the bulk through diffusion processes. As noted in previous paragraphs, all exposure tests were conducted within a limited temperature range around 60°C.

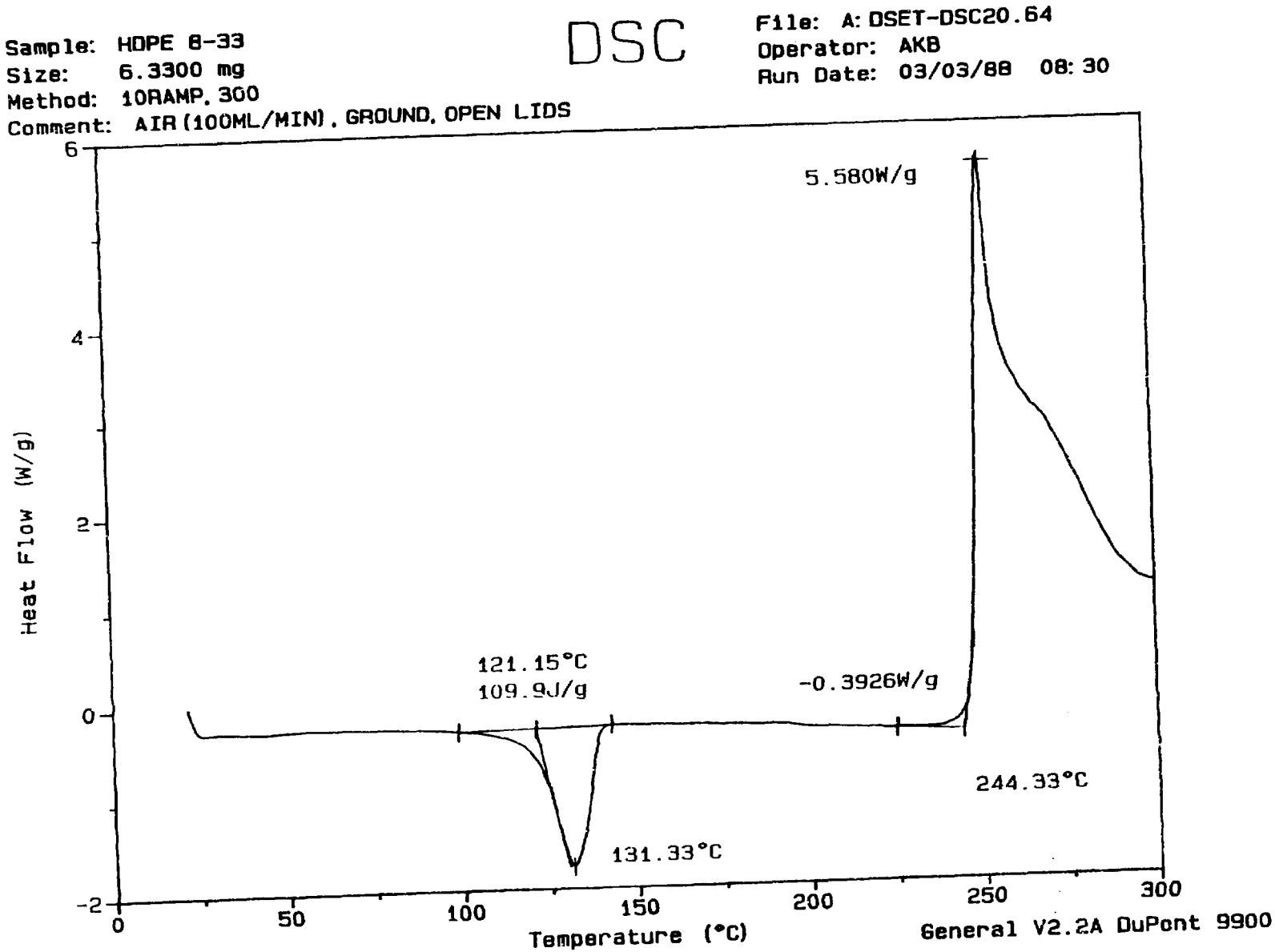

Figure 8: Typical DSC Spectra for 155mm Propelling Charge Container Material

Table 11
155mm Propelling Charge Container DSC Exposure Test Data

Exposure Condition	Ultraviolet (MJ/m2)	Time at Maximum Temperature (hrs.)	Melting Point Onset (C)	Melting Point Peak (C)	Heat of Fusion (J/g)	Crystal-linity (%)	Onset of Decomp. Temperature (C)	Decomp. Heat Flow (W/g)	Adjusted Heat Flow (W/g)	
Humidity Chamber		0	121.6	131.4	110.8	37.8%	246.3	7.32	4.55	
at 60 C		429	121.9	132.1	104.7	35.7%	248.4	7.24	4.65	
with 90% RH		693	122.0	132.1	101.6	34.7%	246.1	6.22	4.06	
		1156	122.0	131.5	110.2	37.6%	246.8	6.61	4.12	
		1757	122.0	131.2	131.1	44.8%	245.1	7.90	4.36	
		3411	122.0	132.1	119.6	40.8%	246.9	6.79	4.02	
		3765	121.4	131.5	111.8	38.2%	244.9	6.46	3.99	
Elevated Temperature		0	121.6	131.4	110.8	37.8%	246.3	7.32	4.55	
at 71 C		720	121.7	131.7	103.2	35.2%	246.0	5.91	3.83	
		1537	121.7	131.7	105.4	36.0%	247.0	6.72	4.30	
		2138	122.4	131.6	119.3	40.7%	247.1	8.42	4.99	
		4000	121.7	131.8	121.8	41.6%	246.1	7.48	4.37	
		4834	124.3	133.4	120.4	41.1%	238.3	6.74	3.97	
EMMAQUA	0	0	121.6	131.4	110.8	37.8%	246.3	7.32	4.55	
	107	300	122.2	132.4	104.5	35.7%	242.8	6.17	3.97	
	169	600	121.6	131.8	113.1	38.6%	243.1	6.30	3.87	
	388	1570	121.4	131.6	112.7	38.5%	235.1	4.64	2.85	*Cracks*
	852	1950	121.6	131.9	114.2	39.0%	234.9	5.06	3.09	*Cracks*
Xenon-Arc	0	0	121.6	131.4	110.8	37.8%	246.3	7.32	4.55	
	645	2304	121.4	131.9	107.2	36.6%	239.4	5.30	3.36	*Cracks*
	883	3152	121.4	131.3	119.1	40.7%	226.5	3.92	2.33	*Cracks*
Arizona	0	0	121.6	131.4	110.8	37.8%	246.3	7.32	4.55	
At-Latitude	101	1280	121.3	131.6	116.3	39.7%	242.3	6.44	3.88	
	175	1750	121.5	131.6	117.4	40.1%	239.1	5.77	3.46	
	295	2900								*Cracks*
Solar	0	0	121.6	131.4	110.8	37.8%	246.3	7.32	4.55	
Simulator	44	307	121.6	131.8	107.3	36.6%	244.8	5.89	3.73	
	67	477	122.6	132.6	104.6	35.7%	243.8	6.48	4.17	
	98	690	122.4	131.8	118.9	40.6%	244.1	8.06	4.79	
	129	908	122.2	131.1	120.9	41.3%	242.1	7.75	4.55	

Therefore, the probable mechanism by which the HDPE changes relates to an initial thermally induced decrease in crystallinity which makes the material more sensitive to photooxidation at the surface, with rapid photooxidation of the amorphous regions. The resulting effect, as seen from the tests with ultraviolet, is surface cracking. The bulk effects, occurring by thermal oxidation, would tend to follow the results of the elevated temperature and elevated temperature/ humidity exposure tests.

The relative effects of ultraviolet radiation on the degradation of the properties studied is clearly seen in the figures. The surface cracks noted in Table 11 are typical for polyethylene material and would have an obvious negative effect on strength and impact resistance. Applying the above discussion of the change in crystallinity and decomposition heat flow to the prediction of the functional lifetime of the 155mm Propelling Charge container using the models suggested in paragraph 2.5 requires additional data points from longer term exposure testing in order to clearly identify the rate controlling portion of the curve. The extrapolation of the data presented in Table 11 to longer exposure times and doses would be dangerous since the curves are not well defined and are clearly not logarithmic. On the other hand, extrapolation of the elevated temperature and elevated temperature/humidity adjusted heat flow data to the level that cracks occurred during the ultraviolet exposure tests suggests a lifetime of considerably less than 20 or 30 years. This is qualified by the 60°C exposure temperatures used presenting a worst case for the logistics chain and the fact that no engineering property test data are available for the container material to relate thickness effects to the function of the material.

The limitation in using the data presented is also seen in the linear regressions presented in Tables 12 and 13 and in Figures 13 and 14 where low R squared values were obtained. The simulated solar exposure test regressions are particularly interesting, although potentially misleading, in that they suggest a different degradation mechanism. However, it is noted that the test was not as long in duration as the other tests, which could account for the strikingly different rates.

4.6.1.1 Surface and Bulk Effects

Considerable effort was devoted to the development of sample preparation techniques which allowed the production of measurement samples with reasonably uniform and reproducible particle size. The preparation procedure followed involved the use of a Spex laboratory cryogenic grinder. This procedure also allowed surface and bulk effects to be investigated by preferentially grinding from the center and front surface of a test sample. Test data for sample material exposed to approximately 635 MJ/m^2 ultraviolet radiation from Xenon arc lamp exposure are shown in Table 14.

The percent crystallinity and oxidative stability values for both regions of the sample are noted to be significantly changed

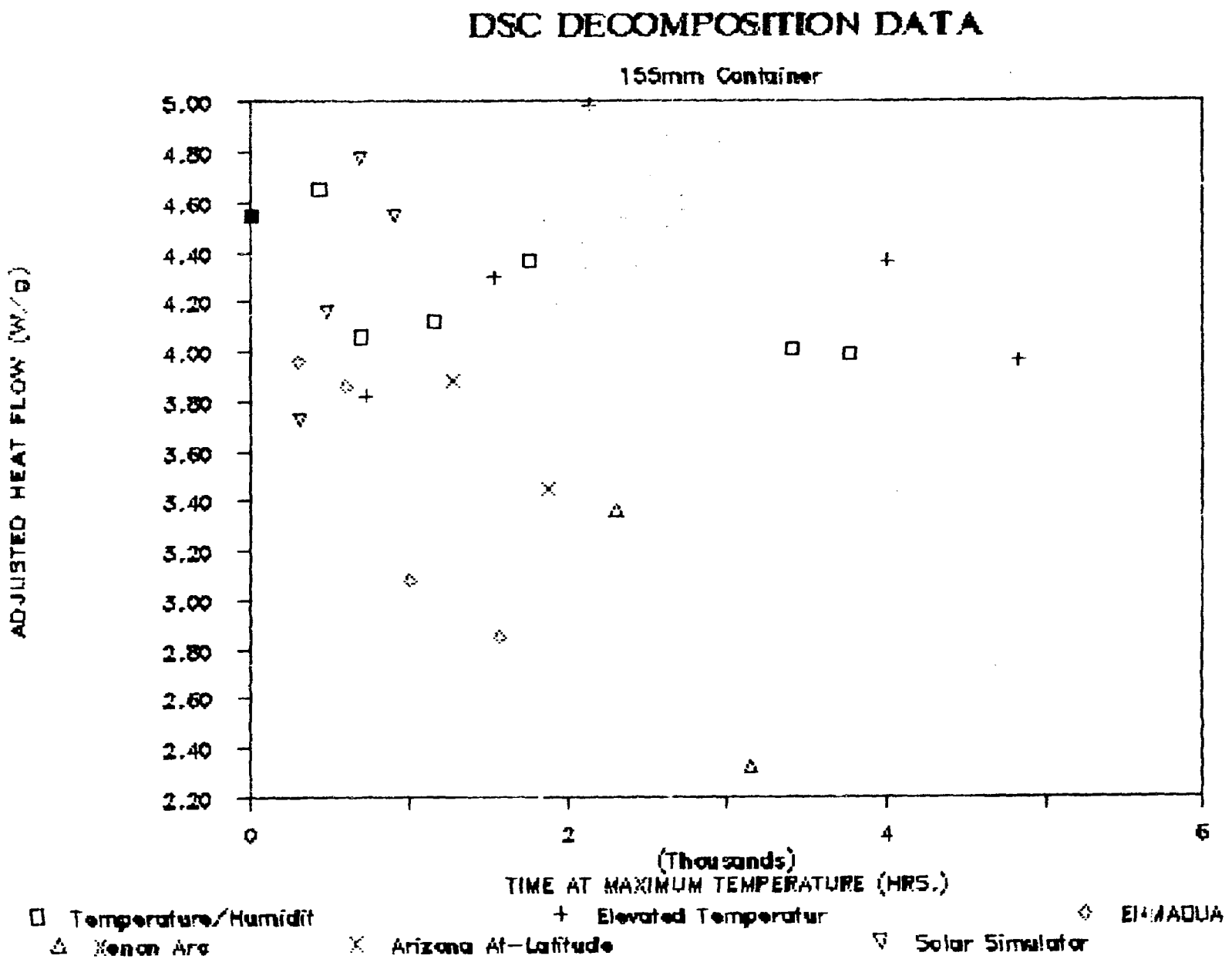

Figure 9: DSC Decomposition Data vs. Time At Maximum Temperature for the 155mm Propelling Charge Container

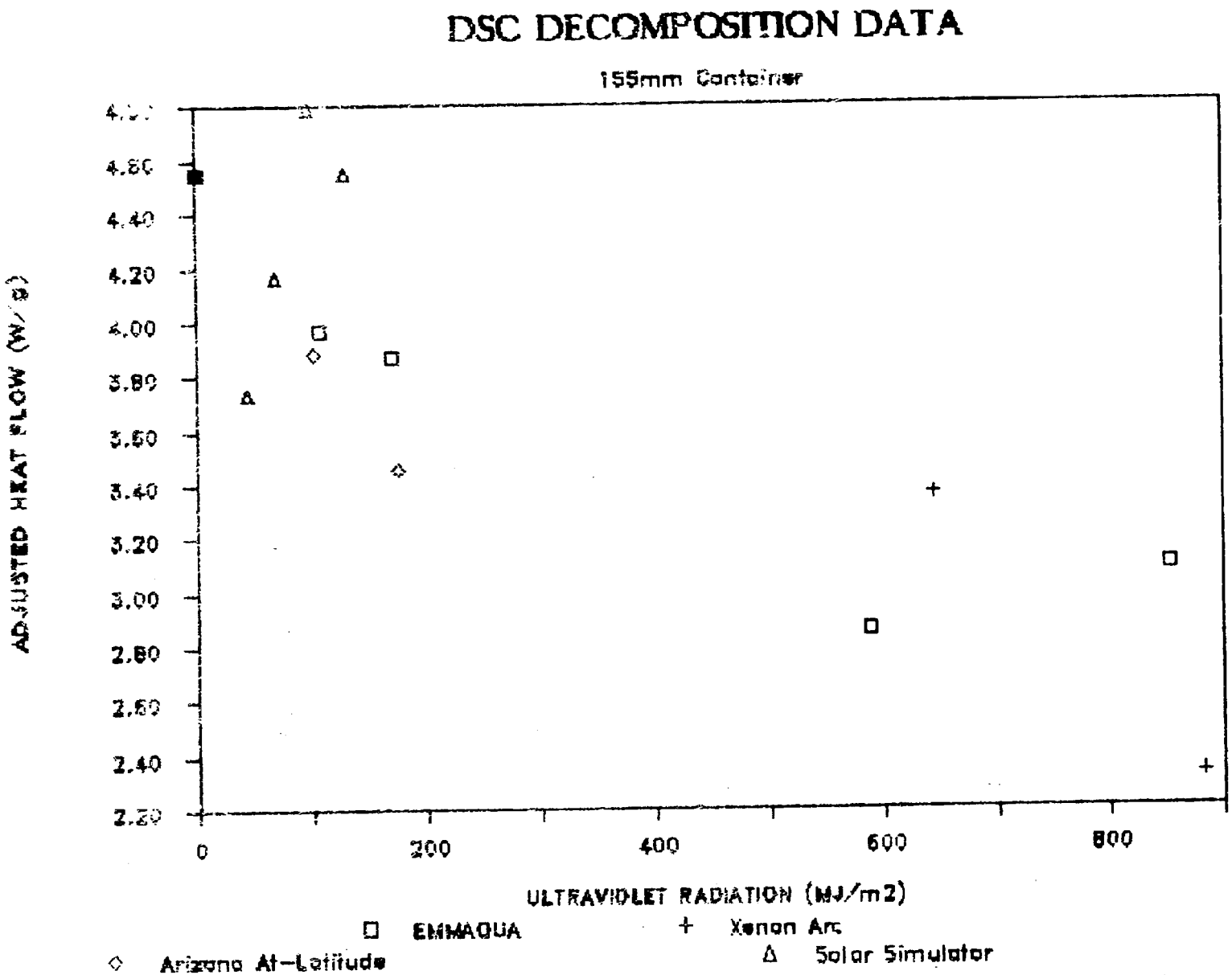

Figure 10: DSC Decomposition Data vs. Ultraviolet Radiation for the 155mm Propelling Charge Container

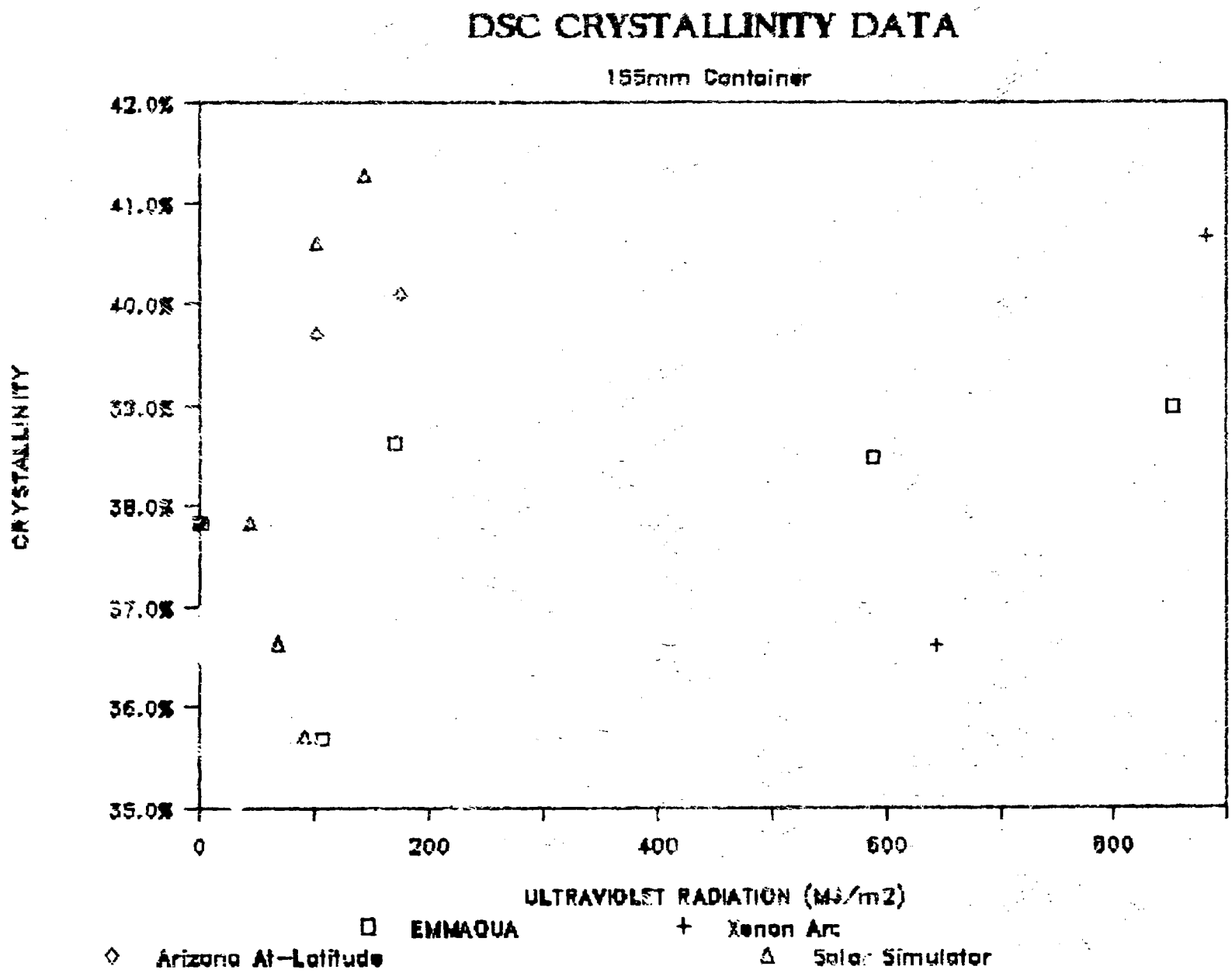

Figure 11: Ultraviolet Effects on Crystallinity

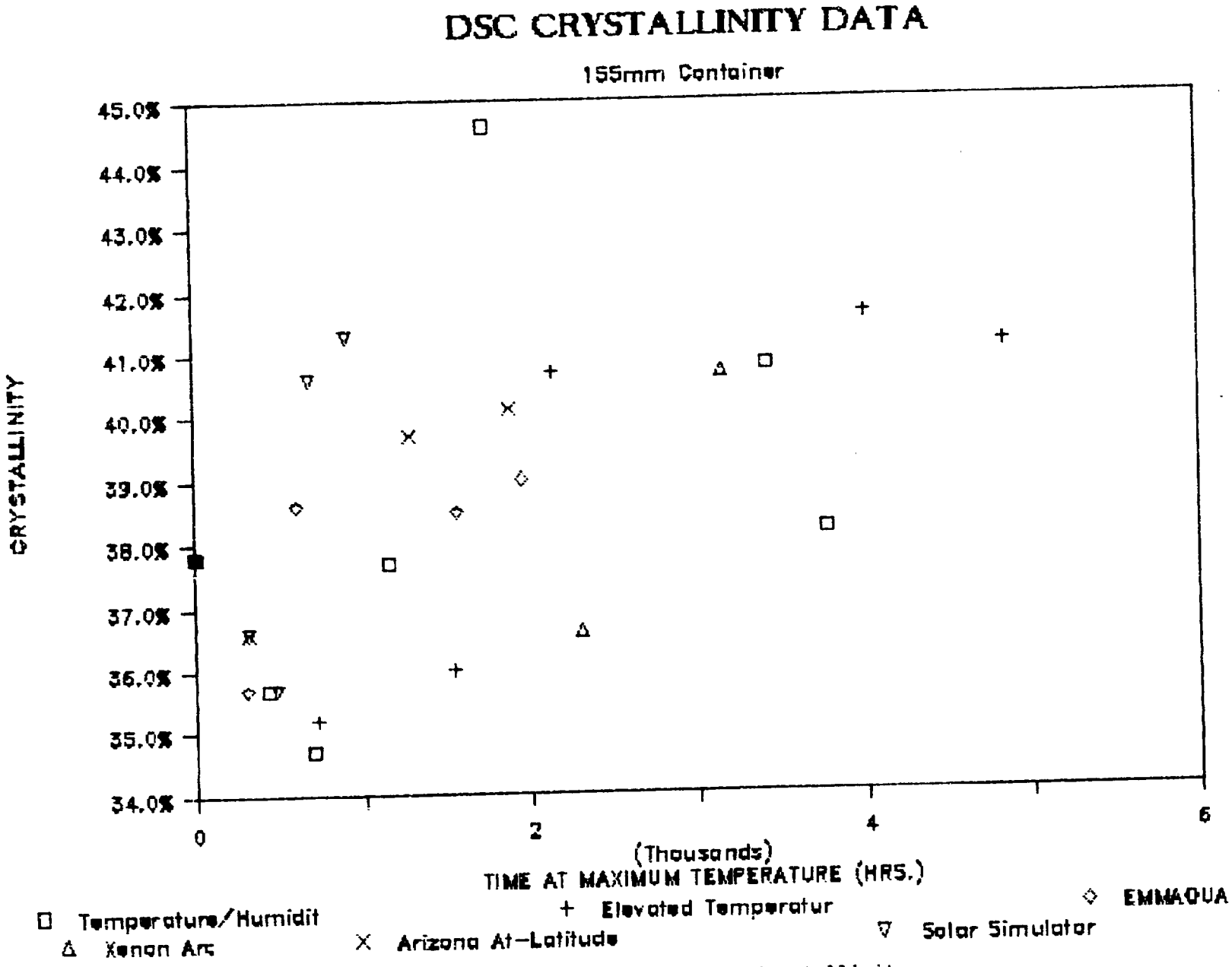

Figure 12: Time At Temperature Effects on Crystallinity

from the pre-exposure values. The surface region exhibits a decrease in crystallinity and a decrease in oxidative stability while the bulk exhibits an increase in crystallinity. Although the sample preparation procedure did not allow for the measurement of depth into the surface, the difference in properties measured from the surface of the sample can be used to account for the cracking phenomenon. The decrease in crystallinity with the decrease in oxidative stability indicates a decrease in strength and ductility at the surface. The increase in crystallinity with the reduction of molecular weight, as indicated by the decrease in oxidative stability, suggests the bulk of the sample became embrittled and possibly weaker.

The Adjusted Heat Flow value noted in Table 14 for the sample surface is significantly lower in magnitude than values determined for the bulk region. The correspondence of surface cracking at this level suggests its use as a failure point. Bulk measurements in this range would indicate that the cross-section of the container has embrittled to an unacceptable level.

4.6.2 TGA Measurements on 155mm Propelling Charge Container Material

The previous paragraph described the use of DSC to measure the heat of fusion, evaluate the oxidative stability and relate these measurements to changes in the crystalline and amorphous regions of the polyethylene to explain the surface cracking which occurred. TGA measurements were also used to evaluate the material's oxidative stability. The results of this testing showed that the thermal decomposition involved a two-step process. The first step was believed to be related to easily oxidizable portions of the polymer, such as branched chains, cross linked polymer or antioxidant additives. The closeness of the onset of decomposition temperature, as measured using DSC, to the onset of decomposition temperature for the first step in the TGA suggests that these temperatures represent the same event. The second step in the process was not reproducible and is probably related to the more stable species in the sample, particle size and sample weight during the measurement. A typical TGA thermal curve is shown in Figure 15. Test data are presented in Table 15 and Figures 16 through 19.

The 5% loss data in Table 15 and Figures 18 and 19 exhibit a trend in oxidative stability similar to that noted for the DSC measurement data. The time line however is longer for the TGA data. Further, a limiting value of the 5% loss temperature is not noted at the points where surface cracking was noted. These observations are attributed to the weight loss kinetics of the 5% loss temperature not being representative of the physical characteristics and thermal history of the surface where cracking was observed. Thus, TGA is more appropriate for the study of bulk changes. As seen by the data, the exposure tests were not conducted for a duration sufficient to allow a lifetime prediction analysis.

Table 12
155mm Propelling Charge Container DSC Regression Data
Ultraviolet Radiation Analysis

Regression for Degree of Crystallinity
EMMAQUA Test
Regression Output:

Constant	0.371841336
Std Err of Y Est	0.012342212
R Squared	0.344612083
No. of Observations	5
Degrees of Freedom	3
X Coefficient(s)	0.000021440
Std Err of Coef.	0.000017070

Regression for Degree of Crystallinity
Xenon Arc Test
Regression Output:

Constant	0.372783
Std Err of Y Est	0.026038
R Squared	0.219216
No. of Observations	3
Degrees of Freedom	1
X Coefficient(s)	0.000021363
Std Err of Coef.	0.000040318

Regression for Degree of Crystallinity
Arizona At-Latitude Test
Regression Output:

Constant	0.379926619
Std Err of Y Est	0.004695213
R Squared	0.924380400
No. of Observations	3
Degrees of Freedom	1
X Coefficient(s)	0.000132137
Std Err of Coef.	0.000037793

Regression for Degree of Crystallinity
Solar Simulator Test
Regression Output:

Constant	0.361773
Std Err of Y Est	0.020828
R Squared	0.452371
No. of Observations	5
Degrees of Freedom	3
X Coefficient(s)	0.000331492
Std Err of Coef.	0.000210575

Regression for Adjusted Heat Flow
Solar Simulator Test
Regression Output:

Constant	4.172191661
Std Err of Y Est	0.452365924
R Squared	0.107478034
No. of Observations	5
Degrees of Freedom	3
X Coefficient(s)	0.002748844
Std Err of Coef.	0.004573400

Regression for Adjusted Heat Flow
Arizona At-Latitude Test
Regression Output:

Constant	4.540454
Std Err of Y Est	0.029956
R Squared	0.998523
No. of Observations	3
Degrees of Freedom	1
X Coefficient(s)	-0.00627086
Std Err of Coef.	0.000241131

Regression for Adjusted Heat Flow
Xenon Arc Test
Regression Output:

Constant	4.623692700
Std Err of Y Est	0.343517338
R Squared	0.952398763
No. of Observations	3
Degrees of Freedom	1
X Coefficient(s)	-0.00237924
Std Err of Coef.	0.000531911

Regression for Adjusted Heat Flow
EMMAQUA Test
Regression Output:

Constant	4.258725
Std Err of Y Est	0.340215
R Squared	0.818056
No. of Observations	5
Degrees of Freedom	3
X Coefficient(s)	-0.00172822
Std Err of Coef.	0.000470561

Table 13
155mm Propelling Charge Container DSC Regression Data
Time at Maximum Temperature Analysis

Regression for Degree of Crystallinity
Temperature/Humidity Test

Regression Output:

Constant	0.369597
Std Err of Y Est	0.033385
R Squared	0.181349
No. of Observations	7.000000
Degrees of Freedom	5.000000
X Coefficient(s)	0.000010
Std Err of Coef.	0.000009

Regression for Degree of Crystallinity
Elevated Temperature Test

Regression Output:

Constant	0.362179
Std Err of Y Est	0.019453
R Squared	0.605484
No. of Observations	6.000000
Degrees of Freedom	4.000000
X Coefficient(s)	0.000011
Std Err of Coef.	0.000005

Regression for Degree of Crystallinity
EMMAQUA Test

Regression Output:

Constant	0.370656634
Std Err of Y Est	0.012039291
R Squared	0.376388323
No. of Observations	5
Degrees of Freedom	3
X Coefficient(s)	0.000009664
Std Err of Coef.	0.000007181

Regression for Degree of Crystallinity
Xenon Arc Test

Regression Output:

Constant	0.372785
Std Err of Y Est	0.026040
R Squared	0.219139
No. of Observations	3.000000
Degrees of Freedom	1.000000
X Coefficient(s)	0.000006
Std Err of Coef.	0.000011

Regression for Degree of Crystallinity
Arizona At-Latitude Test

Regression Output:

Constant	0.378695697
Std Err of Y Est	0.001811443
R Squared	0.988744283
No. of Observations	3
Degrees of Freedom	1
X Coefficient(s)	0.000013255
Std Err of Coef.	0.000001414

Regression for Degree of Crystallinity
Solar Simulator Test

Regression Output:

Constant	0.361835325
Std Err of Y Est	0.020897372
R Squared	0.448745665
No. of Observations	5
Degrees of Freedom	3
X Coefficient(s)	0.0000467
Std Err of Coef.	0.0000299

Table 13
155mm Propelling Charge Container DSC Regression Data
Time at Maximum Temperature Analysis
(continued)

Regression for Adjusted Heat Flow
Solar Simulator Test

Regression Output:	
Constant	4.172666
Std Err of Y Est	0.452574
R Squared	0.106658
No. of Observations	5.000000
Degrees of Freedom	3.000000
X Coefficient(s)	0.000388
Std Err of Coef.	0.000648

Regression for Adjusted Heat Flow
Temperature/Humidity T. &

Regression Output:	
Constant	4.460050420
Std Err of Y Est	0.208384166
R Squared	0.501912858
No. of Observations	7
Degrees of Freedom	5
X Coefficient(s)	-0.000130
Std Err of Coef.	0.0000579

Regression for Adjusted Heat Flow
Elevated Temperature Test

Regression Output:	
Constant	4.415200710
Std Err of Y Est	0.459890938
R Squared	0.027003402
No. of Observations	6
Degrees of Freedom	4
X Coefficient(s)	-0.00003647
Std Err of Coef.	0.000109461

Regression for Adjusted Heat Flow
[illegible] Test

Regression Output:	
Constant	4.354463254
Std Err of Y Est	0.259532254
R Squared	0.894120956
No. of Observations	5
Degrees of Freedom	3
X Coefficient(s)	-0.000779
Std Err of Coef.	0.0001548

Regression for Adjusted Heat Flow
Xenon Arc Test

Regression Output:	
Constant	4.623697843
Std Err of Y Est	0.343660258
R Squared	0.952359146
No. of Observations	3
Degrees of Freedom	1
X Coefficient(s)	-0.00066611
Std Err of Coef.	0.000148983

Regression for Adjusted Heat Flow
Arizona At-Latitude Test

Regression Output:	
Constant	4.572798737
Std Err of Y Est	0.104044075
R Squared	0.982190173
No. of Observations	3
Degrees of Freedom	1
X Coefficient(s)	-0.000603
Std Err of Coef.	0.0000812

Table 14
155mm Propelling Charge Container
DSC Data Showing Surface and Bulk Ultraviolet Effects

Sample	Melting Point Onset (°C)	Melting Point Peak (°C)	Heat of Fusion (J/g)	Crystallinity (%)	Onset of Decomp. Temp. (°C)	Decomp. Heat Flow (W/g)	Adjusted Heat Flow (W/g)
Pre-Exposure	121.6	131.4	110.8	37.8	246.3	7.32	4.55
Surface	123.5	131.3	96.3	32.9	225.8	3.75	2.52
Bulk	121.4	131.5	119.1	40.7	240.1	5.25	3.11

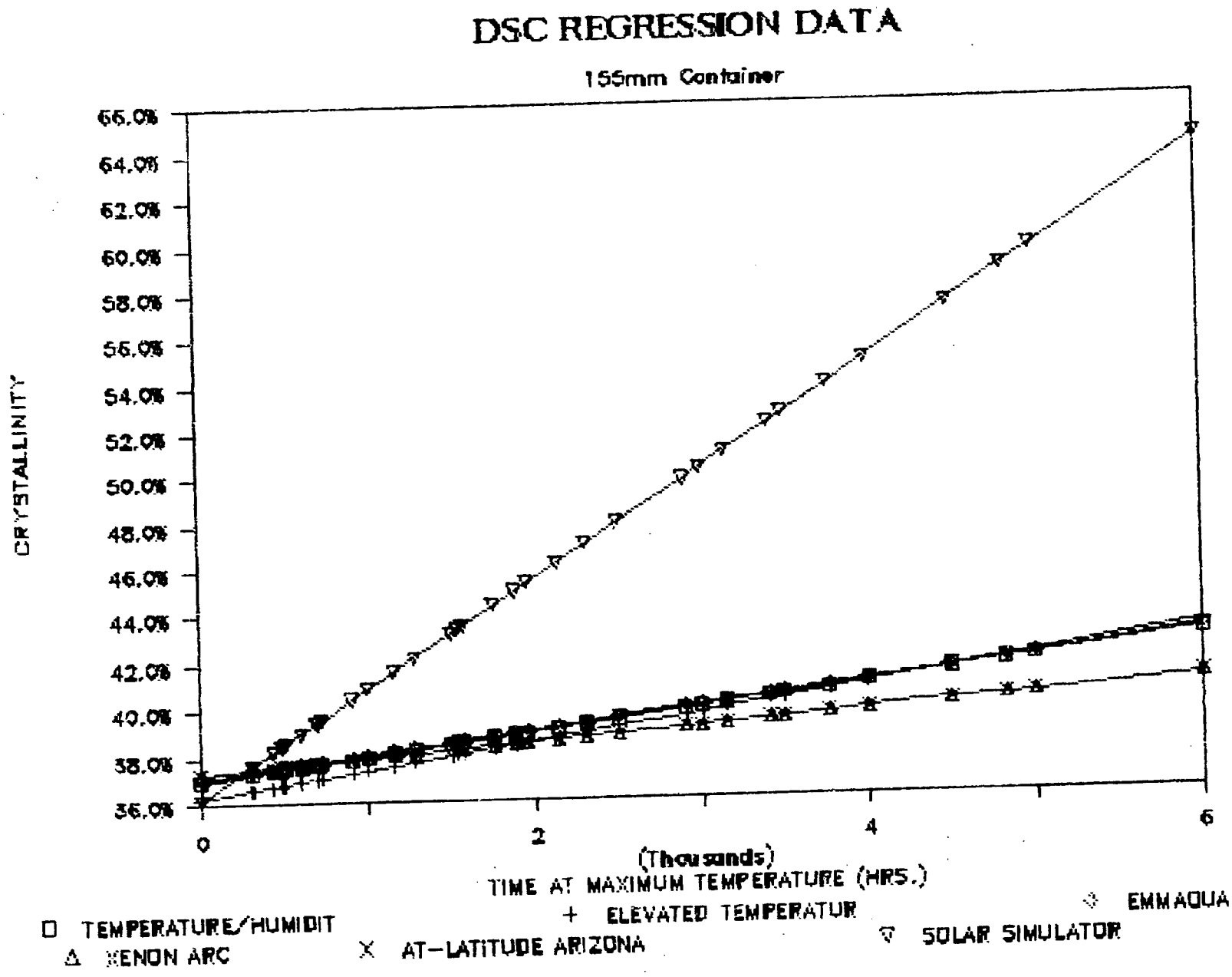

Figure 13: Linear Regressions of DSC Crystallinity Data

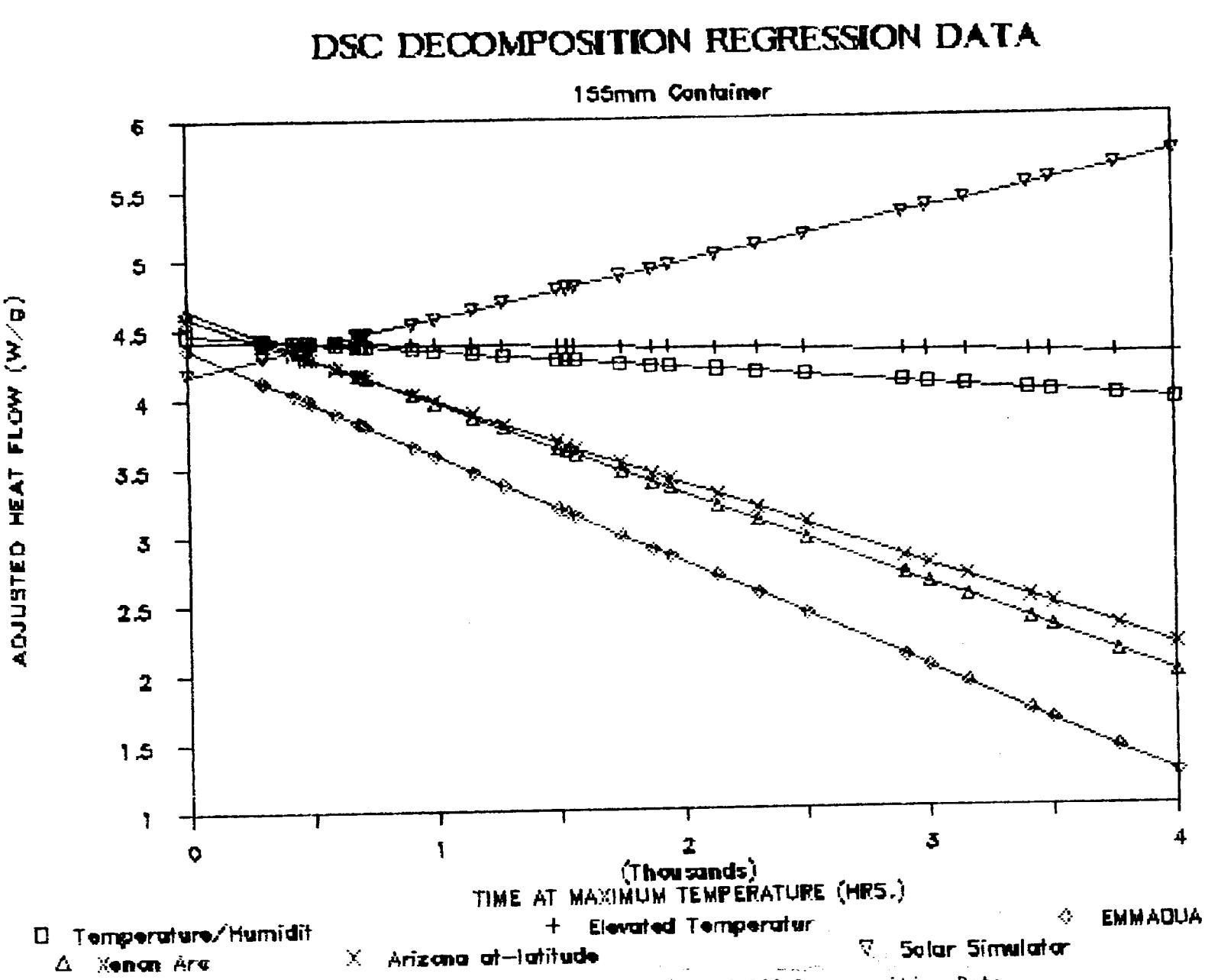

Figure 14: Linear Regressions of DSC Decomposition Data

4.6.3 TGA and DMA Measurements on M2A1 Container Material

Four thermal analysis techniques were used to obtain baseline and characterization data for the M2A1 container material. TGA was used to study decomposition and to determine the relative proportions of the fillers and polymer comprising the material. DSC was used to characterize the crystalline melting point of the polyester resin. TMA measurements attempted to determine the linear coefficient of thermal expansion, the softening point and the glass transition of the resin. DMA was used to measure storage and loss moduli and the loss tangent. These properties are useful for the characterization of crystallinity and the loss of adhesion between resin and filler.

As might be expected due to the randomness of the glass reinforcement, TMA measurements were not reproducible. The DSC results for unexposed material suggested that the resin, comprising only 35% of the composite, might be too low in concentration for accurate measurements to be made. This proved true; however, a crystalline melting point was not detected in the material suggesting that the technique would not be suitable for monitoring changes in the polymer during the course of exposure testing. DMA data shown in Figure 20 and Table 16 indicate that although storage and loss moduli measurements, and the temperatures where the loss modulus and loss tangent reach a maximum could be determined, they could not be measured with enough precision to allow a meaningful data analysis to be conducted. The reason for this problem is thought to be related to the nature of the material and the samples used for the testing. The material is not homogeneous, especially at the surface, and the technique quite sensitive. Therefore, it was postulated that until significant changes occurred in the material, the measurement technique would not be capable of differentiating between sample-to-sample differences from actual material changes.

TGA measurements conducted on unexposed control sample material showed that the decomposition kinetics of the M2A1 container material is complex. The occurrence of the several decomposition reactions shown in the TGA thermal curve in Figure 21 made a kinetic decomposition study impossible during the course of the project. However, a compositional study of exposure test materials was undertaken. Measurements of the relative changes in glass, filler, and resin concentration as a function of the exposure tests were made. These data are shown in Table 17 and Figures 22 through 29.

The data in Table 17 do not indicate a significant change in the material as a result of any of the exposure tests. However, the degradation mode based on visual appearance, includes fading and blooming of the reinforcing fibers. The scatter exhibited by the decomposition data are probably in part due to minor compositional differences in the individual measurement samples which would have a significant effect on the TGA measurement that is compounded by exposure induced changes. The visual evaluation of test samples indicated the probability that the physical properties of the container material were detrimentally affected as a result of the exposure testing. However, the changes determined using TGA are not

Table 15
155mm Propelling Charge Container TGA Data

Exposure Condition		Ultraviolet (MJ/m2)	Time at Maximum Temperature (hrs.)	Onset of Decomp. Temperature (C)	5% Loss Temperature (C)	
Humidity			0.0	278.7	295.0	
Chamber at			429.0	275.4	292.0	
60 C with			693.0	272.6	291.8	
90% RH			1155.5	274.4	296.2	
			1757.0	277.3	296.9	
			3411.0	280.6	299.7	
			3765.0	276.5	301.4	
Elevated Temperature			0.0	278.7	295.0	
at 71 C			720.0	276.8	292.9	
			1537.0	276.3	295.5	
			2138.0	277.3	296.0	
			4000.0	278.7	301.6	
			4834.0	272.1	307.4	
EMMQUA	0	0.0	0.0	278.7	295.0	
	91	107.0	300.0	271.9	292.2	
	144	169.0	600.0	273.8	298.1	
	500	586.0	1537.0	264.8	303.3	*** Test Items Cracked ***
	724	852.0	1950.0	270.7	304.5	*** Test Items Cracked ***
Solar		0.0	0.0	278.7	295.0	
Simulator		43.5	307.0	276.3	298.4	
		67.1	477.0	270.1	295.5	
		97.8	690.0	270.1	292.5	
		120.6	908.0	275.8	295.3	
Arizona		0.0	0.0	278.7	295.0	
At-Latitude		101.0	1280.0	275.0	303.4	
		175.0	1750.0	274.4	307.4	
		295.0				*** Test Items Cracked ***
Xenon Arc		0.0	0.0	278.7	295.0	
		645.0	2304.0	269.1	292.3	*** Test Items Cracked ***
		882.5	3152.0	266.4	305.0	*** Test Items Cracked ***
		1315.0	4696.0	273.6	316.5	*** Test Items Cracked ***

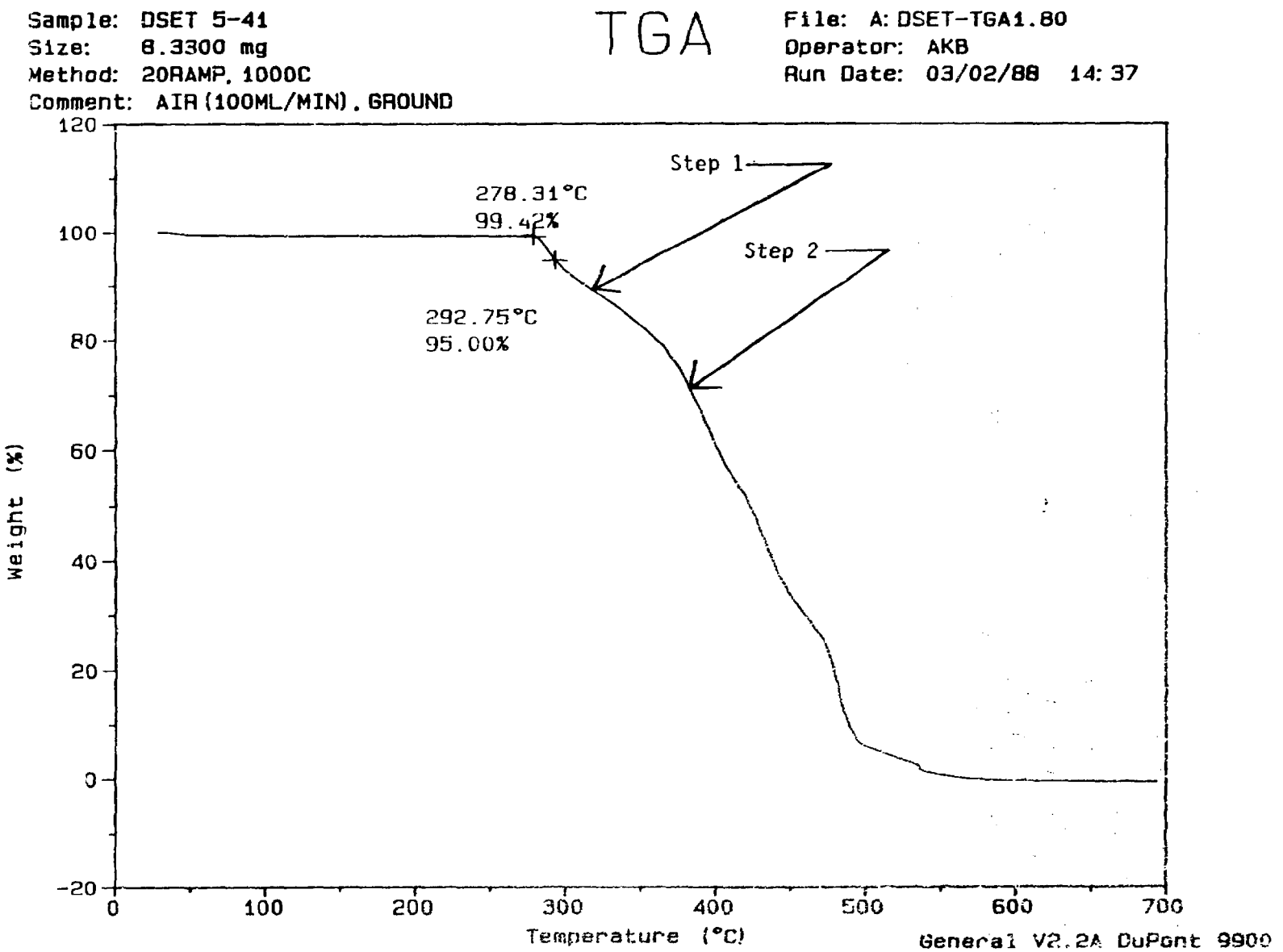

Figure 15: Typical TGA Thermal Curve for 155mm Propelling Charge Container Material

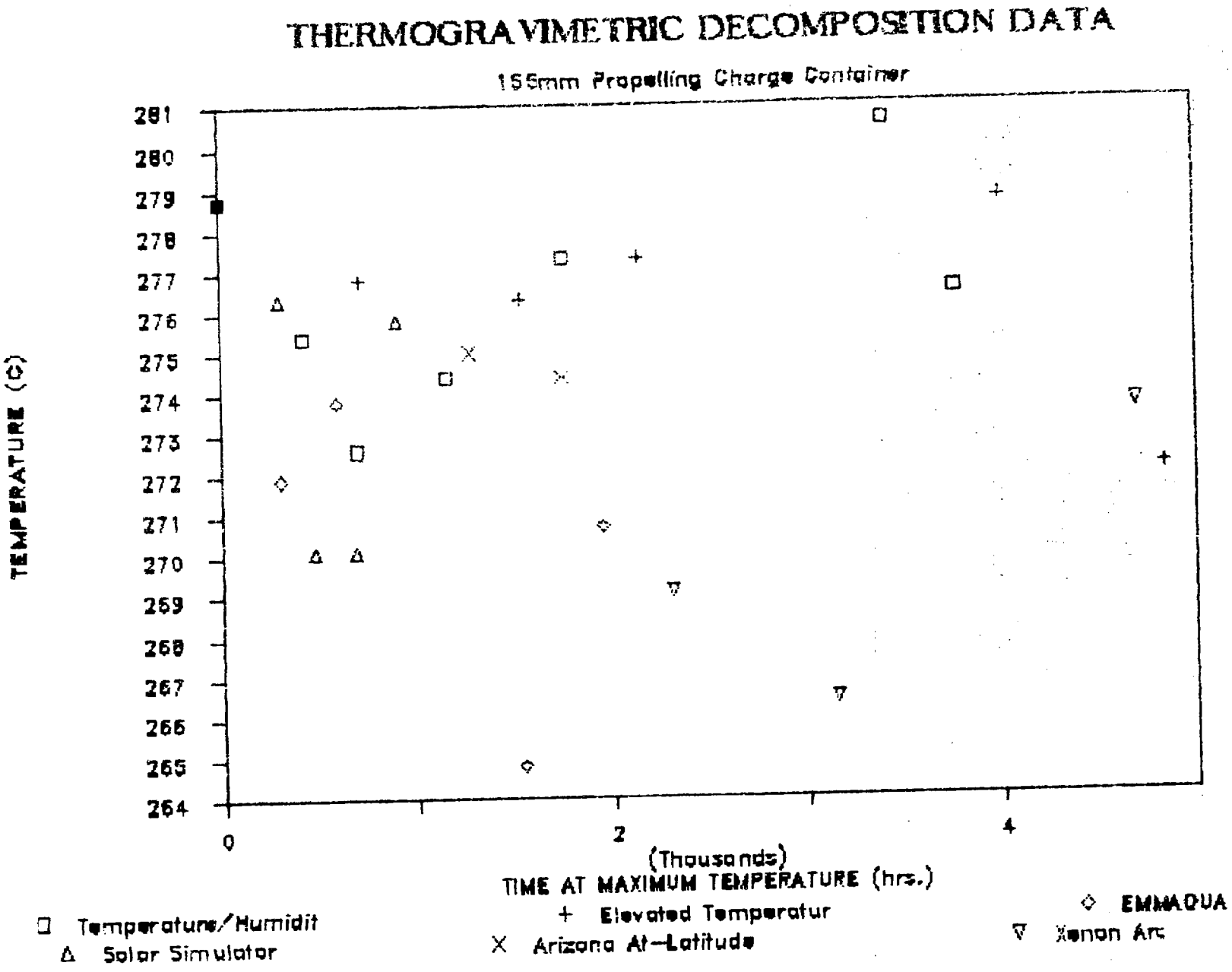

Figure 16: TGA Decomposition Temperature Data vs. Time at Maximum Temperature

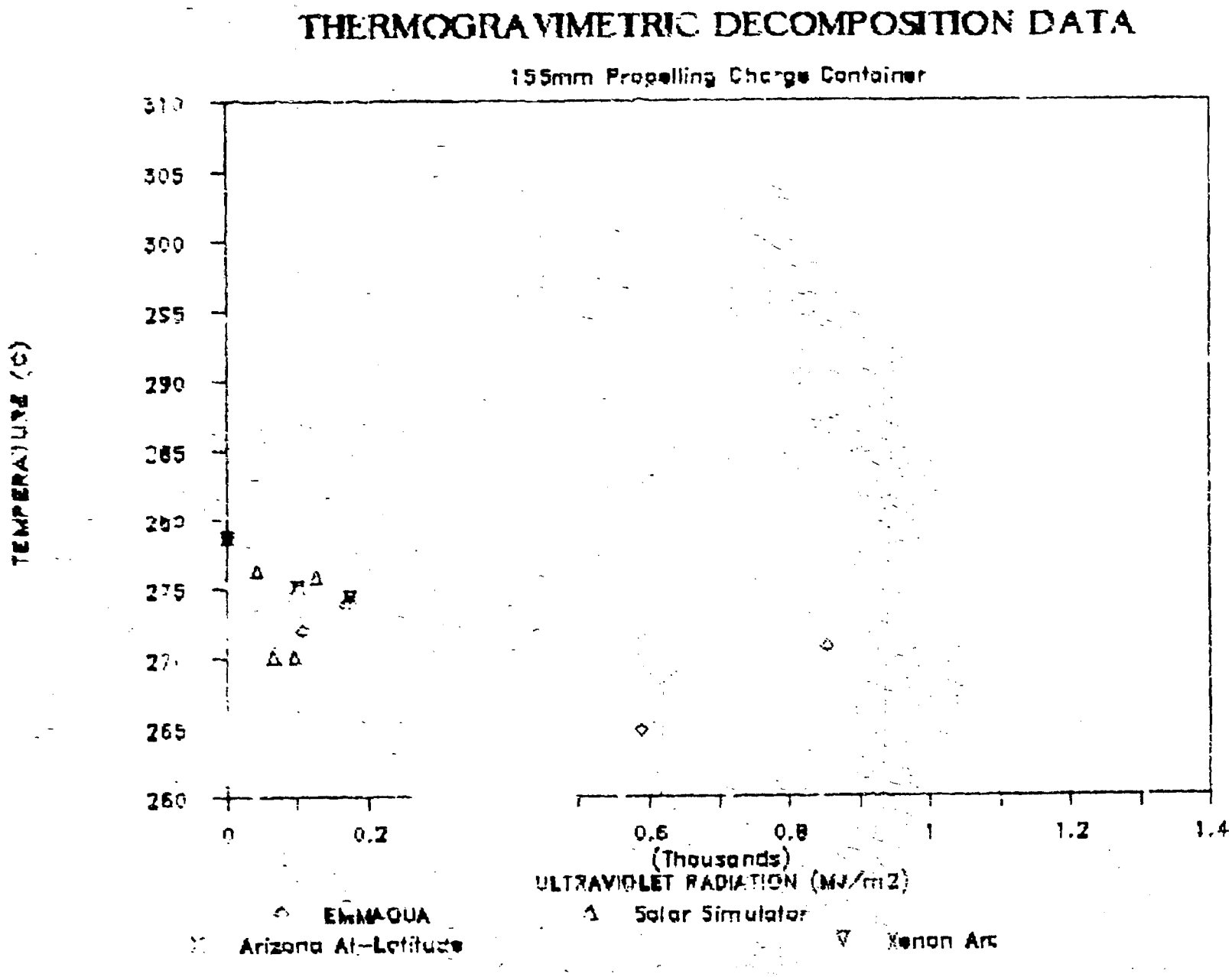

Figure 17. TGA Decomposition Temperature Data vs. Ultraviolet Radiation

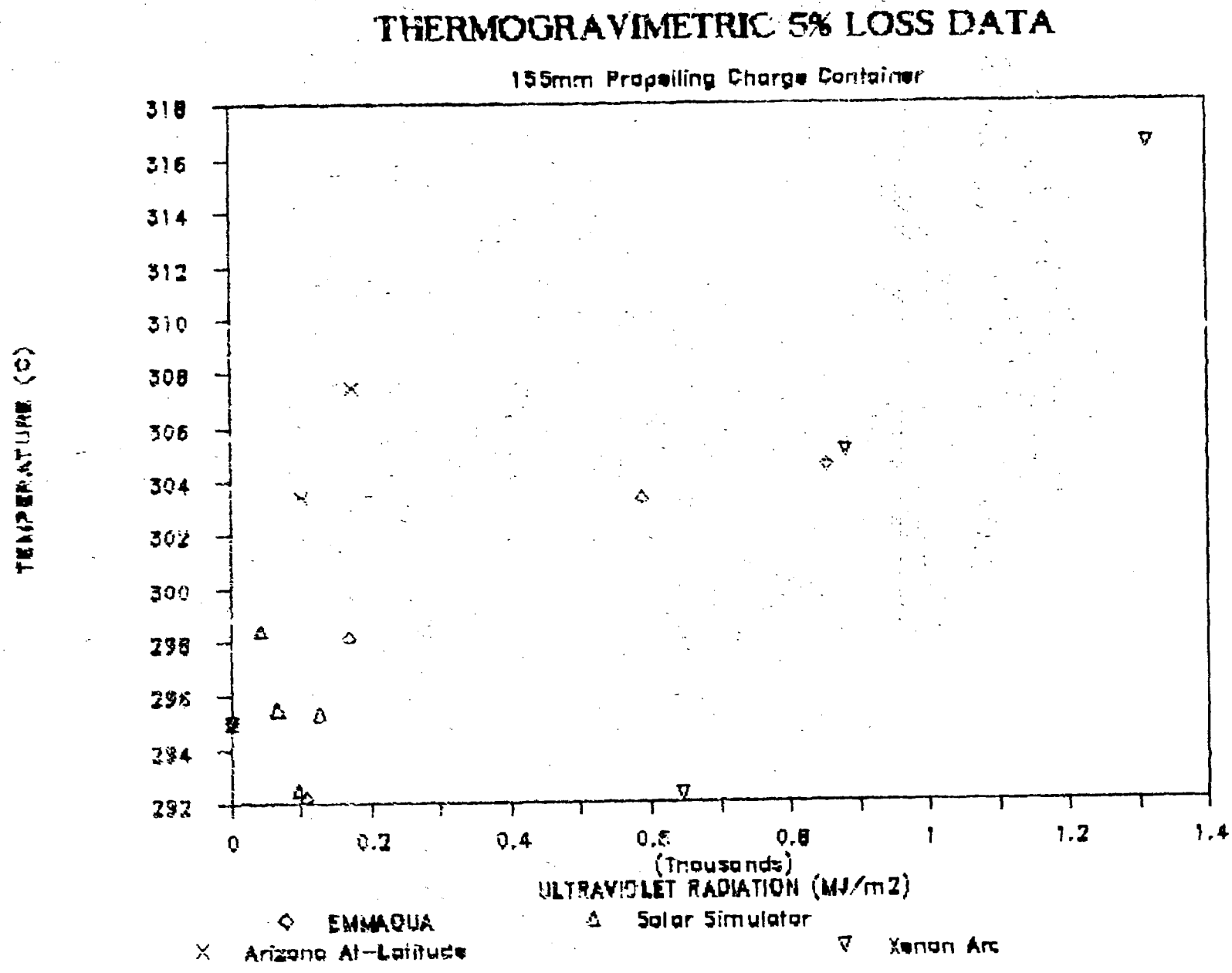

Figure 18: TGA 5% Loss Data vs. Ultraviolet Radiation

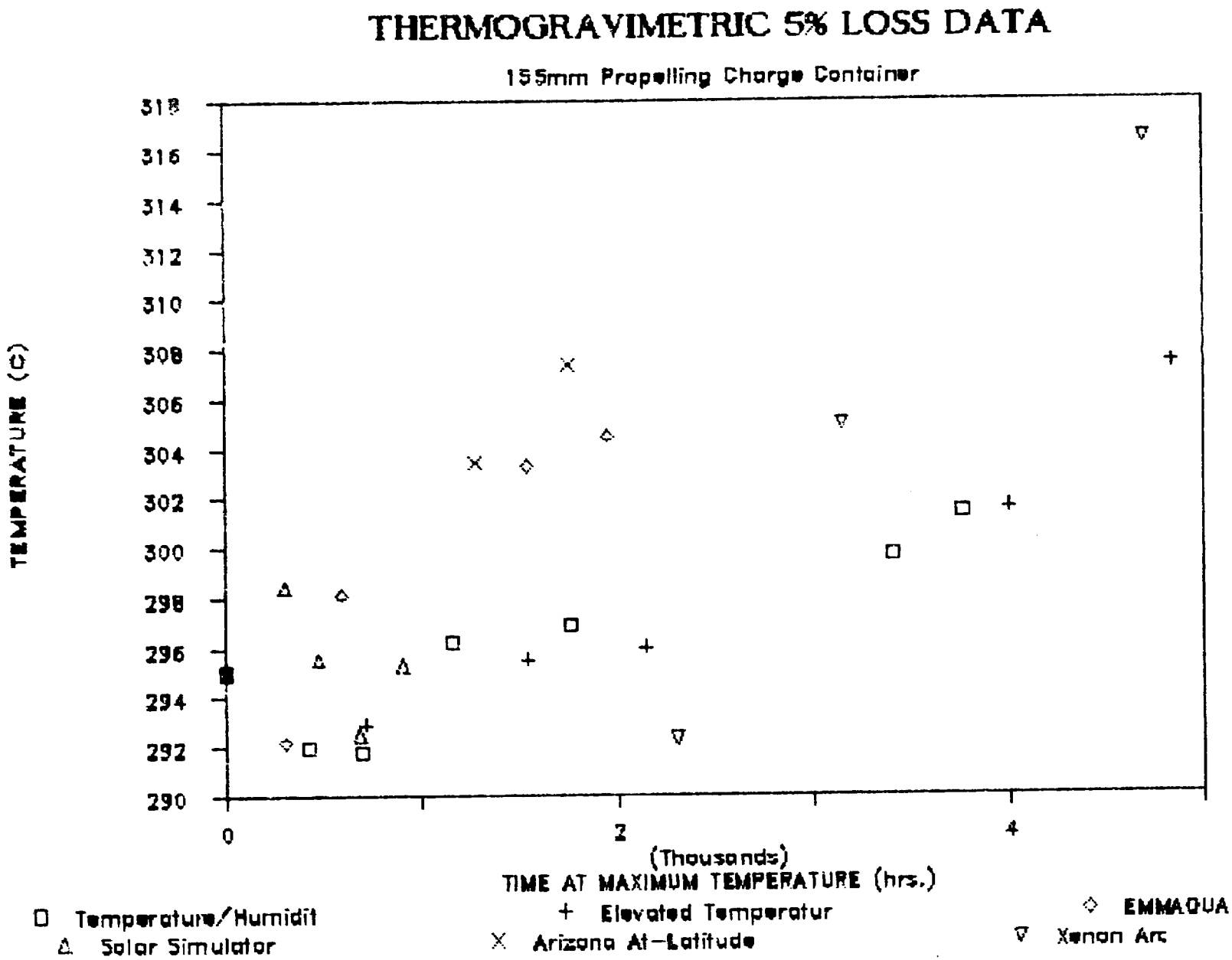

Figure 19: TGA 5% Loss Data vs. Time at Maximum Temperature

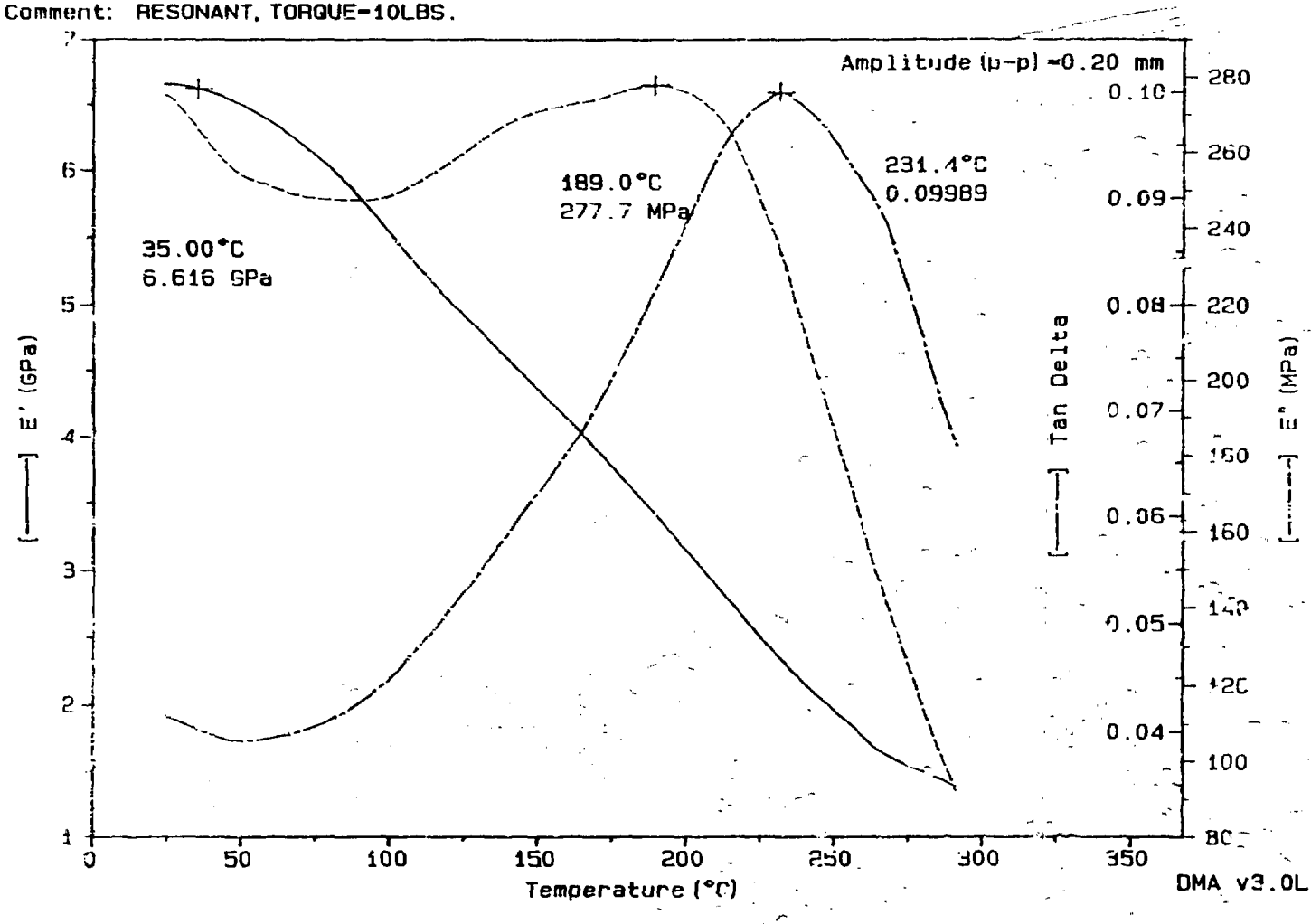

Figure 20: Typical DMA Spectra for M2A1 Container Material

great enough to model or relate to a physical property. The blooming of the reinforcing fibers could provide a protective layer for the 155mm Propelling Charge Container TGA Data bulk of the material during outdoor exposure in desert environments, however the fibers would provide a path for moisture in wet and humid environments which could accelerate the degradation of the material in temperate climates and indoor storage conditions that have typical temperature changes.

Table 16
DMA Data for M2A1 Container Material

Sample No.	Exposure Condition	Duration	E' @ 35°C (GPa)	E'' (MPa)	Peak E'' (°C)	Peak tan δ	Peak tan δ (°C)
16-5	pre-exposure	---	7.85	387	200.5	0.12	227.7
16-6	pre-exposure	---	6.62	277	189.0	0.10	231.4
17-7	pre-exposure	---	4.77	202	197.3	0.10	234.4
17-13	pre-exposure	---	5.35	266	190.6	0.11	232.2
17-14	pre-exposure	---	7.03	304	195.2	0.09	239.1
17-17	pre-exposure	---	6.90	342	199.7	0.11	226.1
		Average	6.3	296	195.4	0.10	231.8
		σ_{n-1}	1.1	64	4.7	0.009	4.7
16-139	Xenon Arc	277 MJ/m²UV	7.02	259.1	209.3	0.09	242.9
	Elevated Temp/Hum	1155 hrs	5.94	236.9	186.4	0.11	223.7
		σ_{n-1}	(.32)	(3.2)	(3.1)	(0.001)	(1.4)
		1757 hrs	6.79	320.3	191.4	.12	223.4
		σ_{n-1}	(.2)	(20)	(3.5)	(0.014)	(0.92)
	Elevated Temperature	1537.5 hrs	7.05	292.1	202.0	0.11	236.8
		σ_{n-1}	(.14)	(25)	(4.8)	(.004)	(3.9)
		2138 hrs	7.49	339.7	206.8	.10	233.5
		σ_{n-1}	(.49)	(33)	(1.8)	(.002)	
	EMMAQUA®	106.7 MJ/m²UV	7.12	313.4	202.0	.11	233.3
		σ_{n-1}	(.36)	(31.3)	(5.3)	(0.007)	(2.9)
	Solar Simulator	43.5 MJ/m²UV	6.23	240.3	201.3	0.10	234.3
		σ_{n-1}	(.32)	(34.8)	(4.8)	(0.005)	(1.9)
		67.6 MJ/m²UV	7.36	348	203.4	0.11	236.2
		σ_{n-1}	(.46)			(0.005)	(5.6)
		97.8 MJ/m²UV	6.69	272.5	203.6	0.10	231.3
		σ_{n-1}	(.26)	29.2	(2.3)	(0.01)	(2.9)

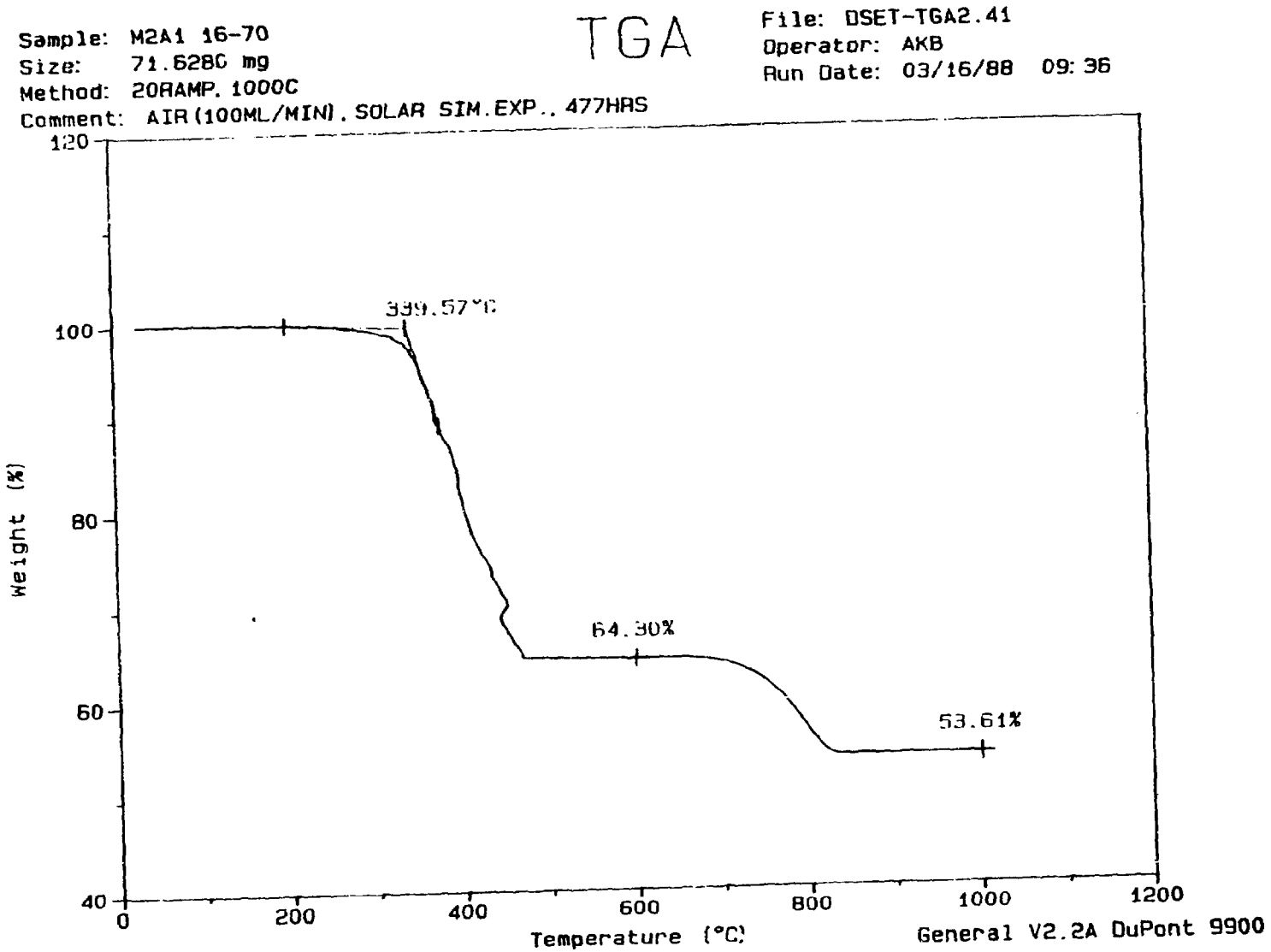

Figure 21: Typical TGA Thermal Curve for M2A1 Container Material

Table 17
TGA Measurement Data for M2A1 Container Material

Exposure Condition	Ultraviolet (MJ/m2)	Time at Maximum Temperature (hrs.)	Onset of Decomp. Temperature (C)	Filler (%)	Glass (%)	Polymer (%)
Xenon Arc	0	0	357.8	25.1	40.1	34.8
	208	743	350.7	22.8	43.5	33.6
	277	989	352.6	22.8	43.4	33.8
	601	2146	363.4	16.3	56.6	27.0
Humidity		0	357.8	25.1	40.1	34.8
Chamber at		429	367.1	23.4	42.3	34.4
60 C with		693	360.0	23.9	41.3	34.8
90% RH		1155	343.3	23.9	41.2	34.9
		1757	353.8	23.6	41.6	34.8
		3411	364.0	26.0	36.0	38.0
		3675	362.8	24.1	40.4	35.4
Elevated Temperature		0	357.8	25.1	40.1	34.8
at 71 C		720	364.8	22.9	43.0	34.1
		1537	358.5	23.2	43.1	33.6
		2138	349.1	24.6	40.1	35.3
EMMAQUA	0	0	357.8	25.1	40.1	34.8
	107	300	363.2	24.5	40.0	35.5
	169	600	347.4	23.6	41.5	34.8
	588	1537	362.3	23.3	42.6	34.1
	852	1950	356.5	22.5	43.7	33.8
Solar	0	0	357.8	25.1	40.1	34.8
Simulator	44	307	362.5	23.0	42.8	34.1
	68	477	345.1	24.0	40.7	35.3
	98	690	345.7	23.4	42.5	34.1
	129	908	347.5	23.1	42.6	34.3
Arizona	0	0	357.8	25.1	40.1	34.8
At-Latitude	101	1280	358.0	23.2	42.3	34.5
	175	1750	358.4	23.3	42.6	34.1

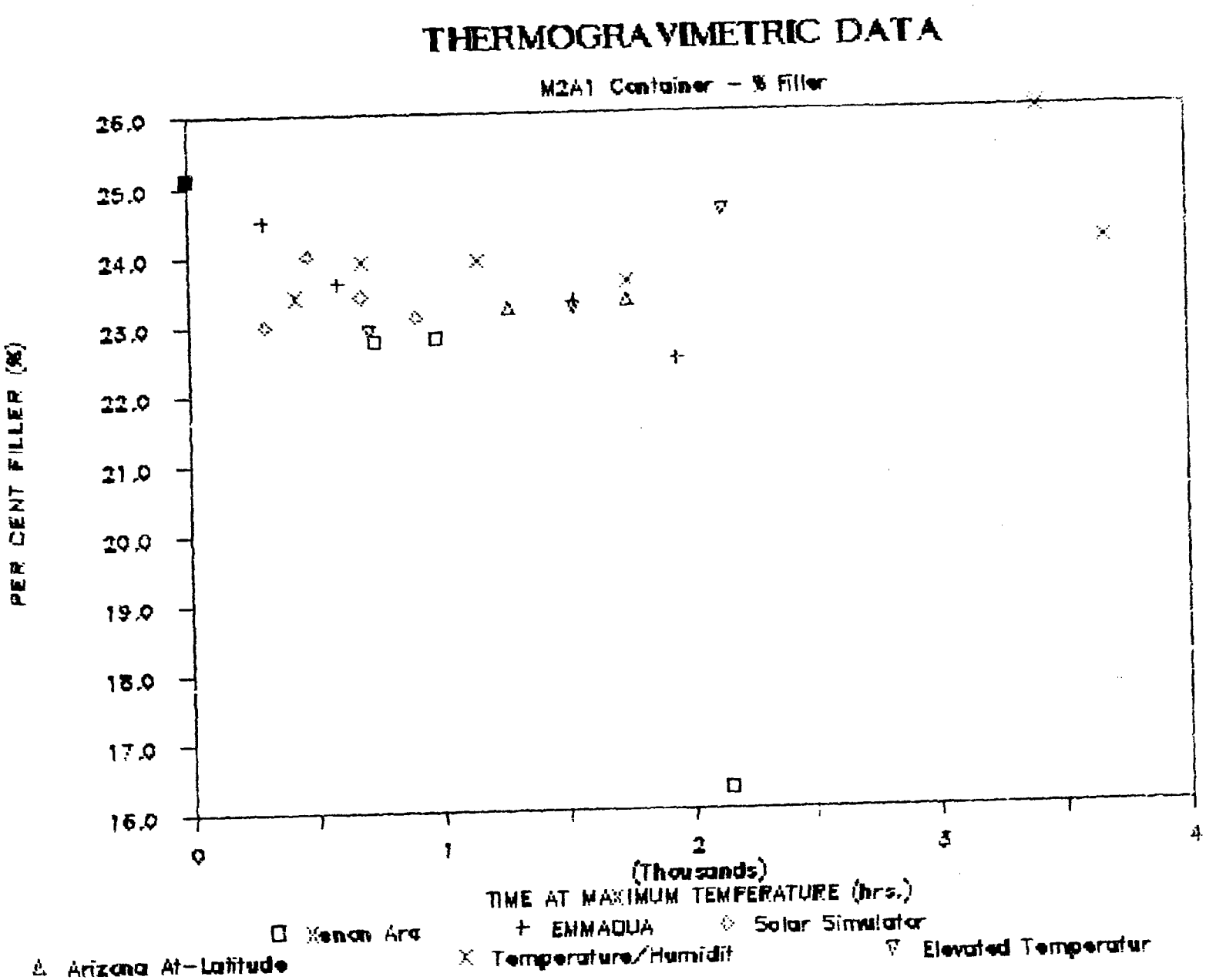

Figure 22: M2A1 Container Filler vs. Time at Temperature

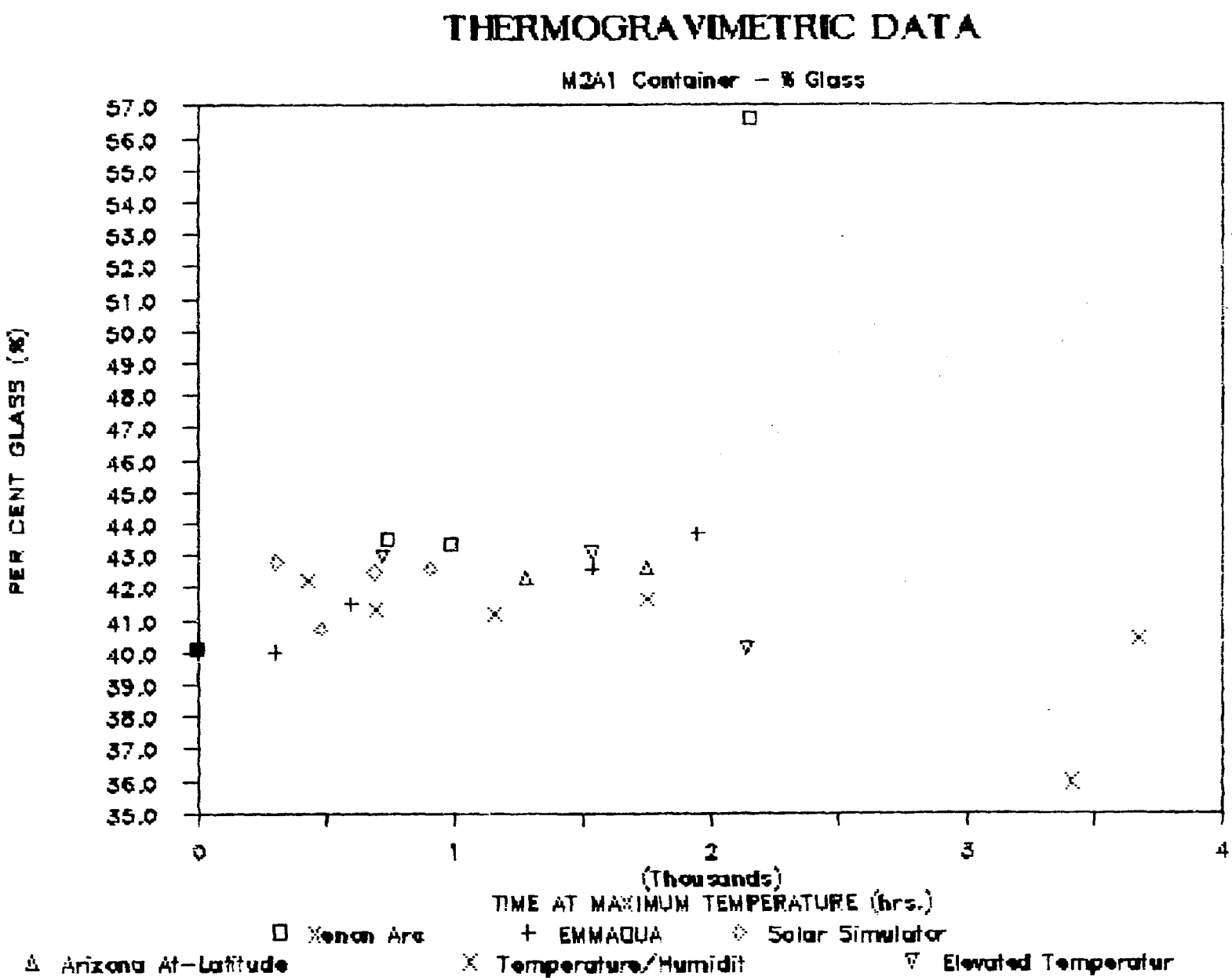

Figure 23: M2A1 Container Glass Reinforcement vs. Time at Temperature

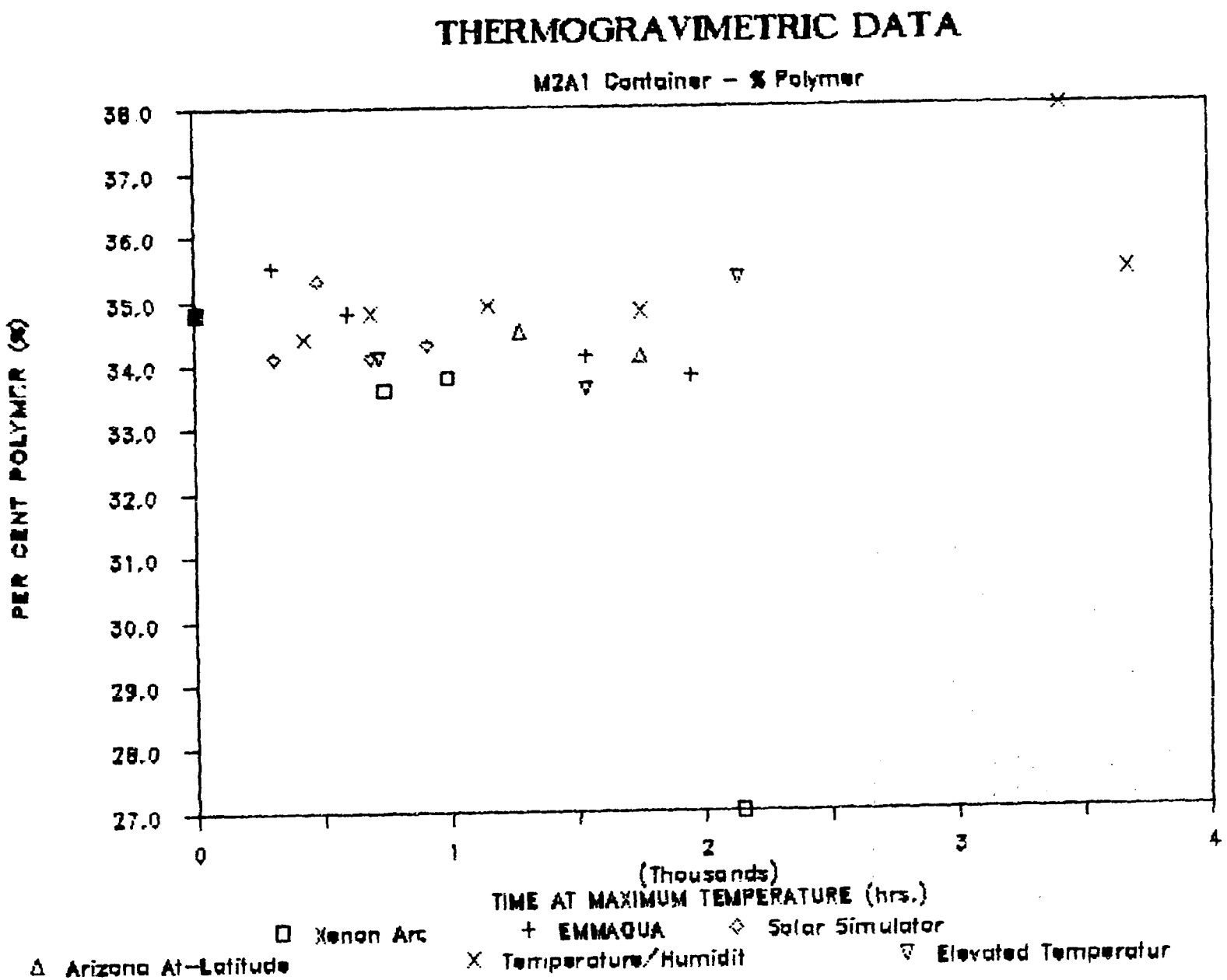

Figure 24: M2A1 Container Resin vs. Time at Temperature

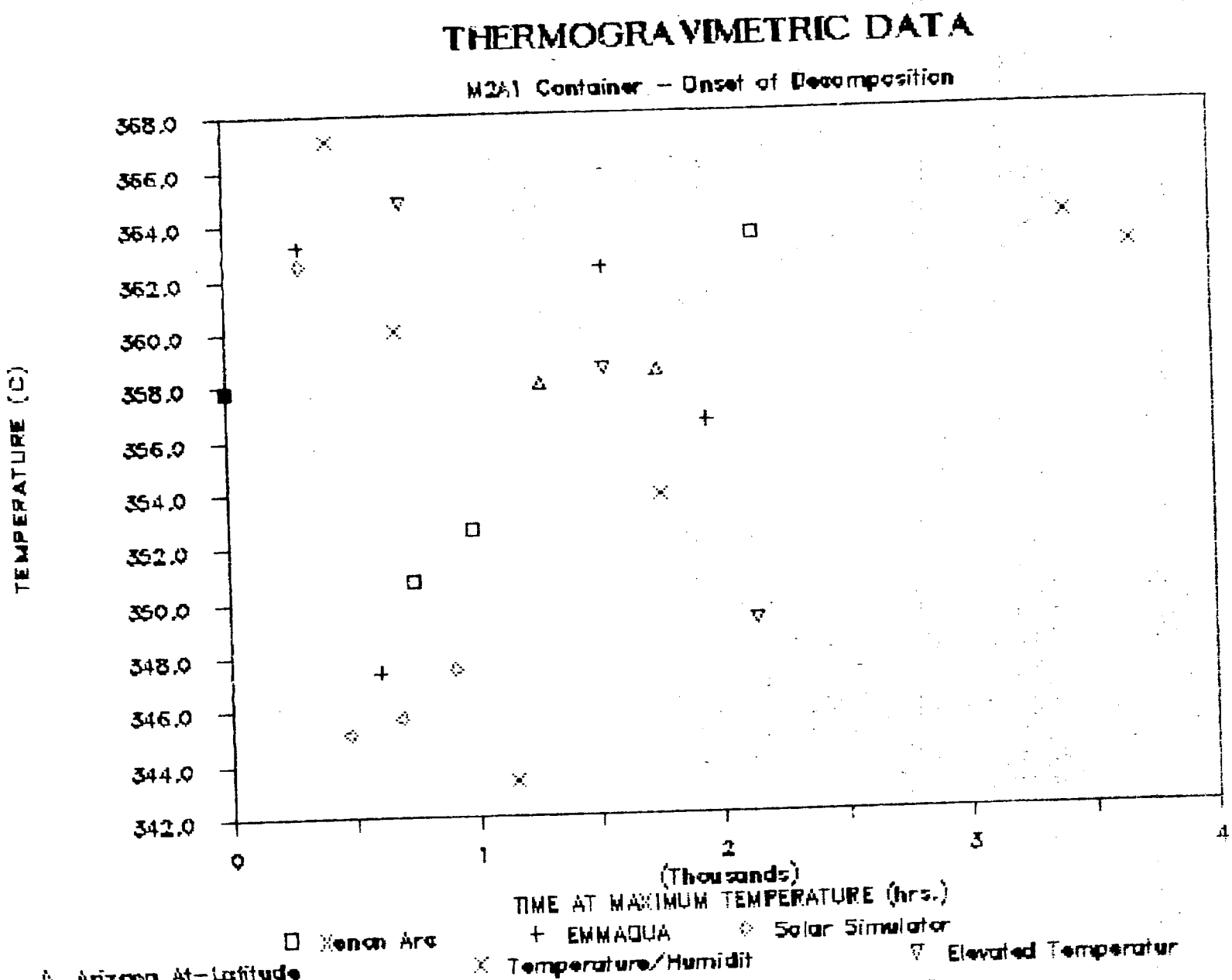

Figure 25: M2A1 Container Decomposition vs. Time Data

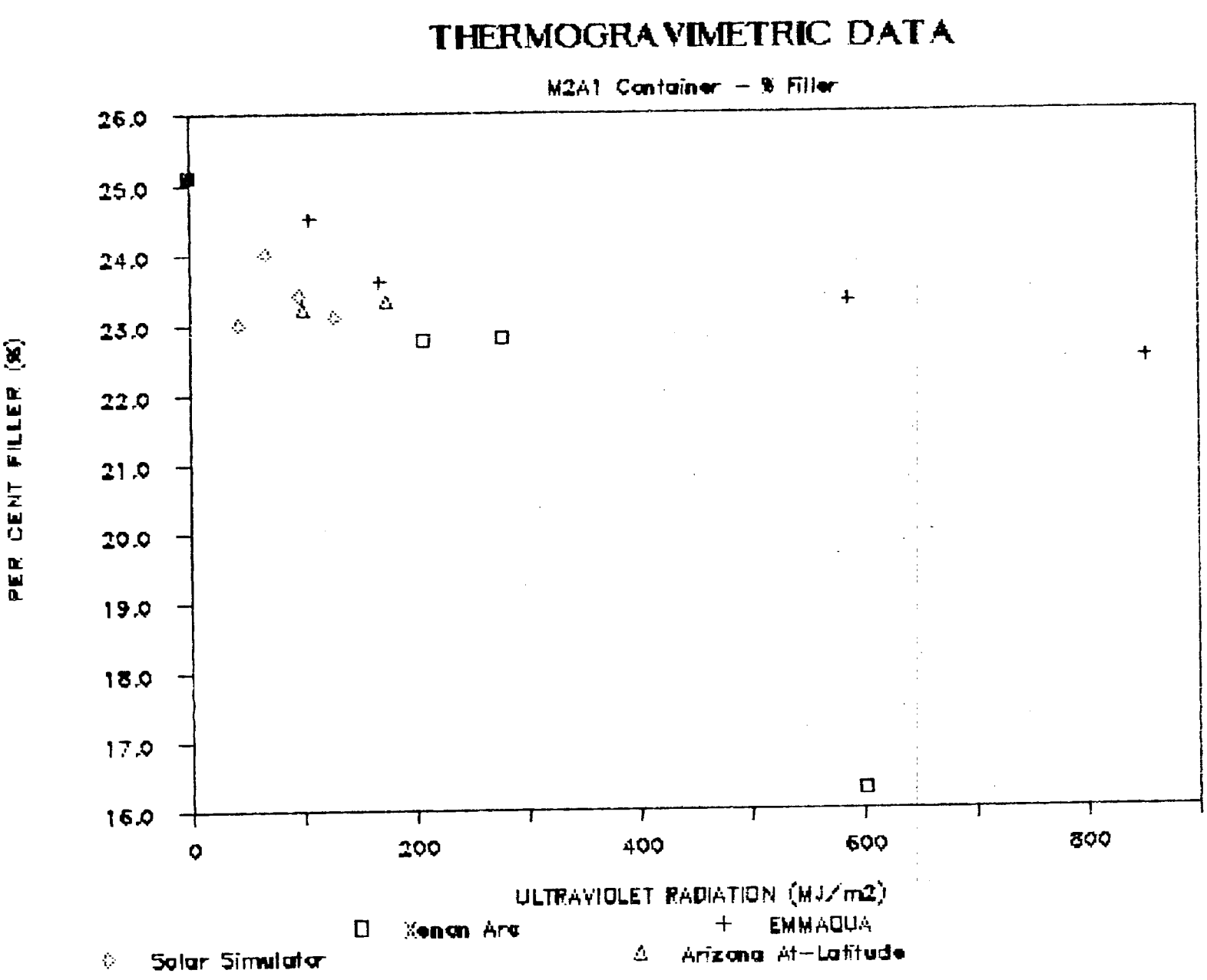

Figure 26: M2A1 Container Filler vs. Ultraviolet Radiation

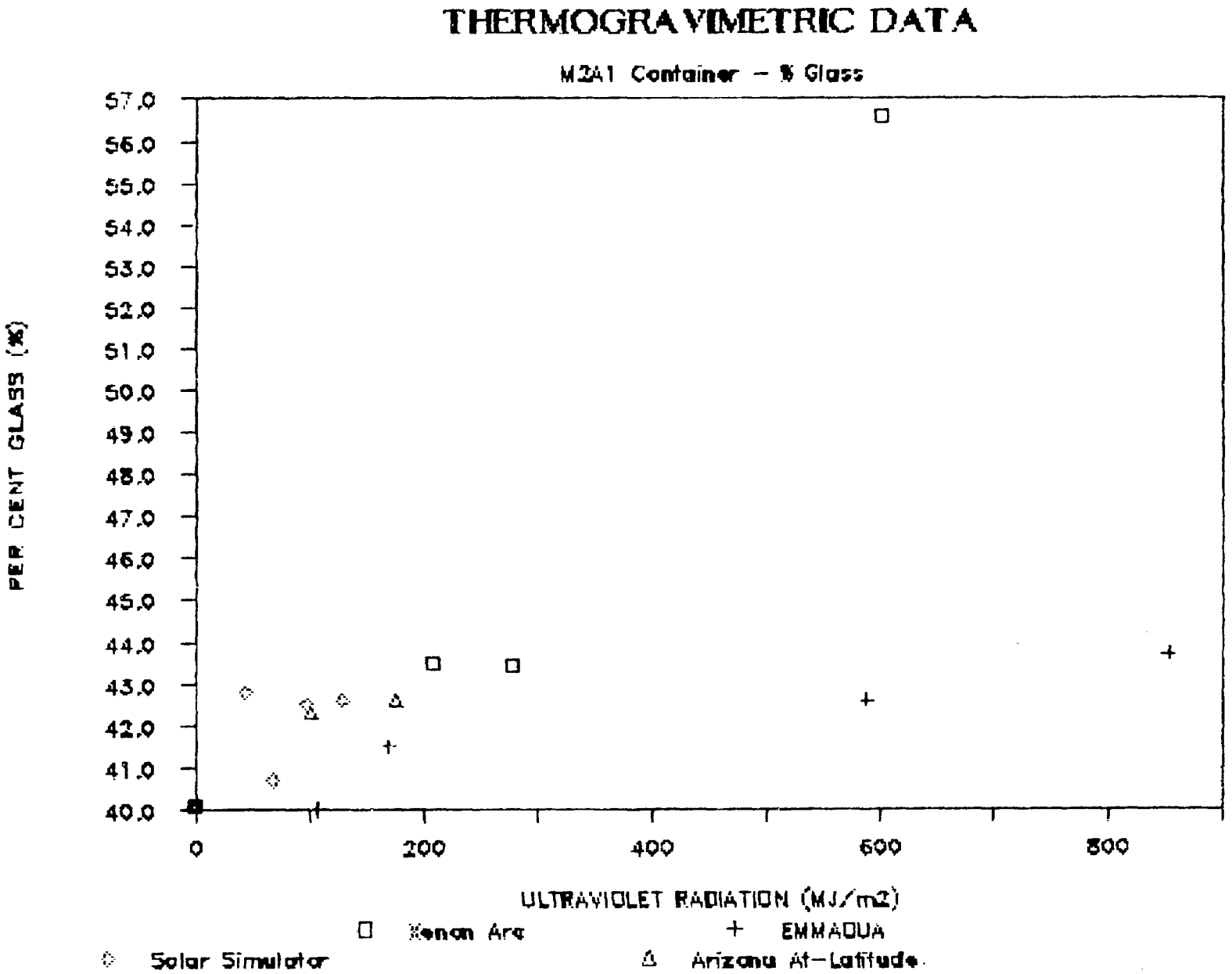

Figure 27: M2A1 Container Glass Reinforcement vs. Ultraviolet Radiation

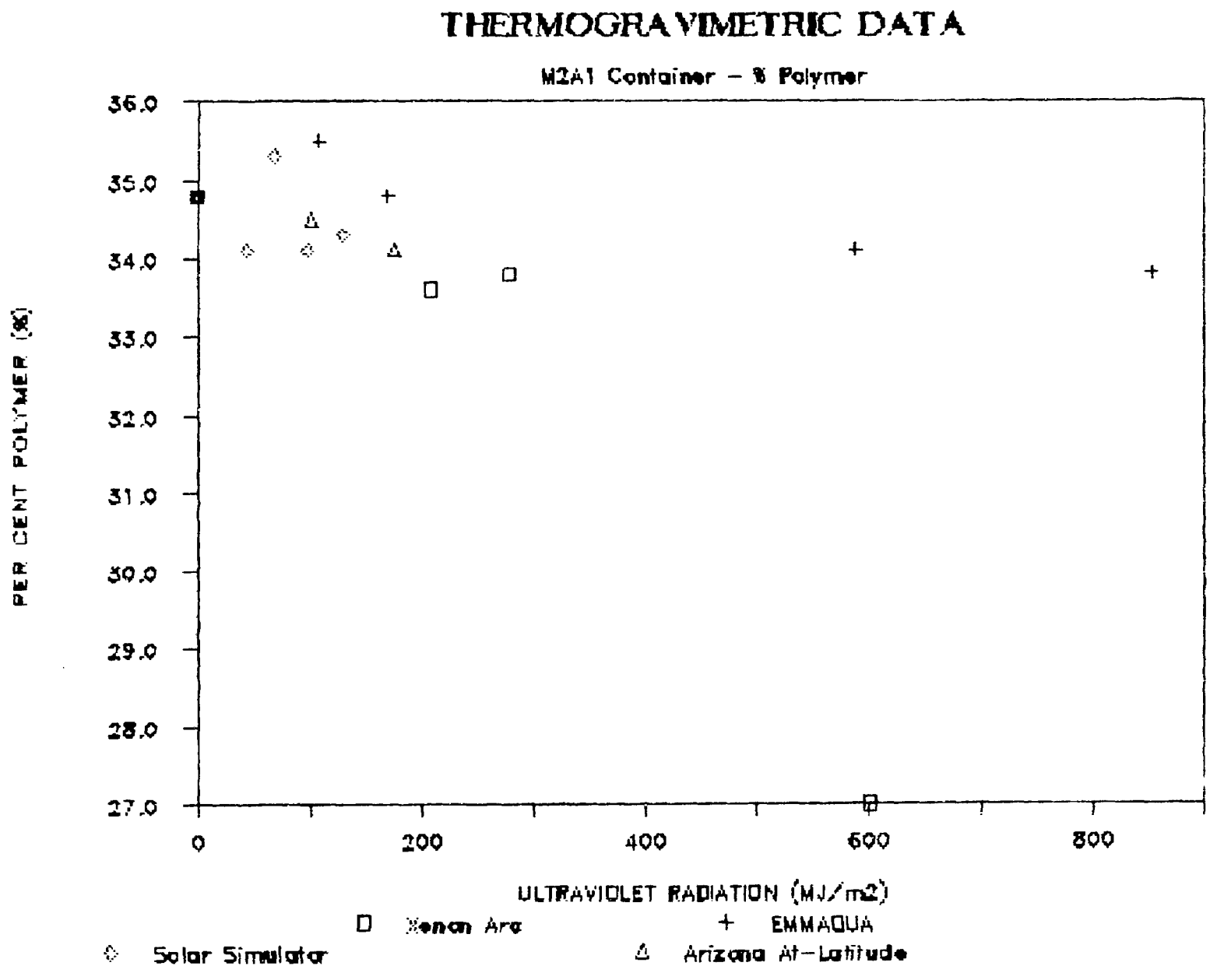

Figure 28: M2A1 Container Resin vs. Ultraviolet Radiation

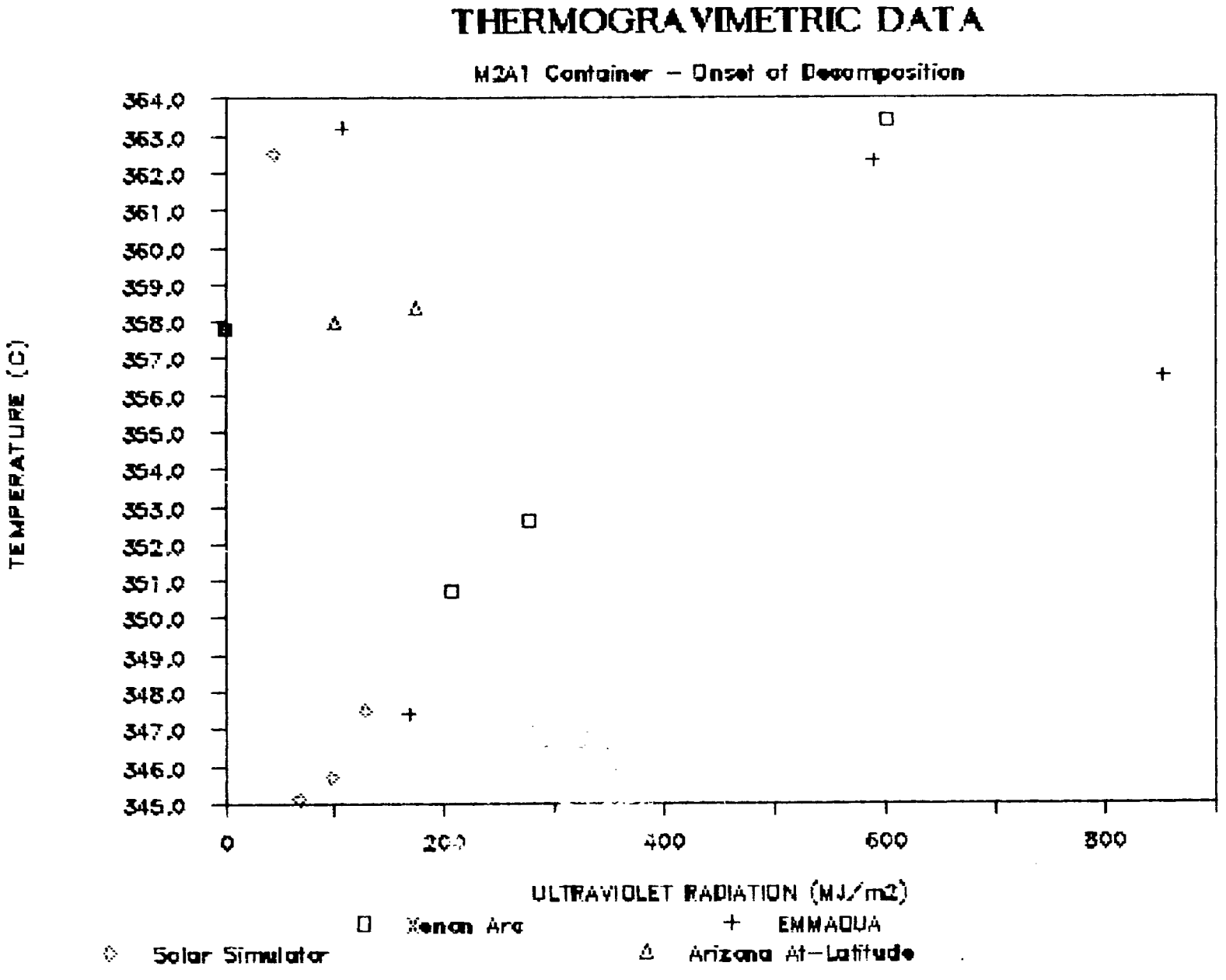

Figure 29: M2A1 Container Decomposition vs. Ultraviolet Radiation

4.7 Marlex CL-100 Tensile Strength Measurements

Tensile test data for the Marlex CL-100 material are exhibited in Table 18 and Figures 30 and 31. ASTM D638 Type IV specimens were tested at an extension rate of 5.1 cm per minute using an Instron Model 1123 Universal Test Machine in accordance with ASTM D638. Tensile strength and elongation at yield are reported, rather than at, the break point since the specimens typically necked down quite considerably during the tests. Tensile strength and elongation at the break point were therefore not reproducible.

The tensile strength of the Marlex CL-100 for the various exposure tests shown in Table 18 are generally within ±10% of the pre-exposure test values indicating that tensile strength remained fairly constant over the course of the exposure tests conducted. This is also supported by data for Marlex CL-100 reported in Reference 32 which indicated that tensile strength increased only 6% after approximately five years of exposure in Arizona. Over the same time period elongation was reported to decrease by 90%.

4.8 Optical Property Measurements

4.8.1 Colorimetric Measurements

CIE Y, x, and y colorimetric measurements were made on 155mm Propelling Charge container and M2A1 container materials using a Hunter Lab Model D25A-9 color difference meter with an Illuminant C light source following ASTM D2244. Using this measurement system, the daylight color of the test specimens are represented by points in a space formed by three rectangular coordinates representing the lightness scale, Y, and chromaticity scales x and y. The Y scale value describes relative "lightness", while the x and y scales describe "redness" and "greenness", respectively. Although other color coordinate systems could have been used, the Y, x, and y system was chosen on the basis of its use in speci-fying a number of Mil-Spec camouflage paint coatings.

4.8.2 Spectral Reflectance Measurements

Absolute hemispherical reflectance measurements were performed on samples after each exposure test interval. These measurements were made in accordance with ASTM E903. The measurements were made using a Beckman DK-2A Spectrophotometer with an Absolute integrating sphere for wall mounted specimens (Figure A1.3 of ASTM E903). Total reflectance measurements were obtained in the solar spectrum from 325nm to 2400nm at an incident angle of 20°. Air mass 1.5 solar absorptance was determined using the solar spectral distribution from ASTM E891. Reflectance data for 50 selected equal energy ordinates were averaged as a fraction and subtracted from unity. Solar absorptance values were calculated after each exposure interval.

Table 18
Marlex CL-100 Tensile and Elongation Data

Exposure Condition	Ultraviolet (MJ/m2)	Time at Maximum Temperature (hrs.)	Tensile Strength at Yield (psi)	Tensile Strength Std. Dev.	% Elongation at Yield (%)	Elongation at Yield Std. Dev.
Humidity Chamber		0.0	3959.0	160.0	8.0	0.4
at 60 C		429.0	3655.0	254.0	9.2	0.5
with 90%RH		693.0	3623.0	89.0	8.8	0.7
		1156.0	3838.0	359.0	9.0	0.8
		1757.0	3944.0	301.0	8.8	0.6
		3765.0	4380.0	33.0	8.0	0.0
Elevated Temperature		0.0	3959.0	160.0	8.0	0.4
at 71 C		720.0	4181.0	72.0	8.5	0.7
		1538.0	4328.0	176.0	8.2	0.4
		2138.0	4404.0	391.0	8.2	0.5
		5112.0	4246.0	121.0	7.2	0.0
EMMAUS	0.0	0.0	3959.0	160.0	8.0	0.4
	107.0	300.0	4130.0	58.0	8.2	0.4
	169.0	600.0	5040.0	107.0	7.7	0.5
	852.0	1950.0	3489.0	117.0	*	0.8
	588.0	1570.0	4260.0	122.0	8.4	*
	1154.0	2000.0	3487.0	160.0	8.0	0.5
Solar Simulator	0.0	0.0	3959.0	160.0	8.0	0.4
	43.5	307.0	3990.0	189.0	5.6	2.1
	67.6	477.0	3042.0	280.0	2.4	0.4
	97.8	690.0	2858.0	478.0	2.7	0.8
	128.6	908.0	3266.0	298.0	*	*
Arizona	0.0	0.0	3959.0	160.0	8.0	0.4
At-Latitude	101.0	1280.0	4187.0	60.0	7.9	0.2
	175.0	1750.0	4347.0	19.0	8.5	0.9
	295.0	2900.0	3895.0	300.0	6.0	1.6
Xenon Arc	0.0	0.0	3959.0	160.0	8.0	0.4
	658.0	2352.0	3521.0	170.0	*	*
	1062.9	3796.0	3601.0	127.0	*	*
	1110.2	3965.0	1987.0	223.0	*	*

* NOT MEASUREABLE

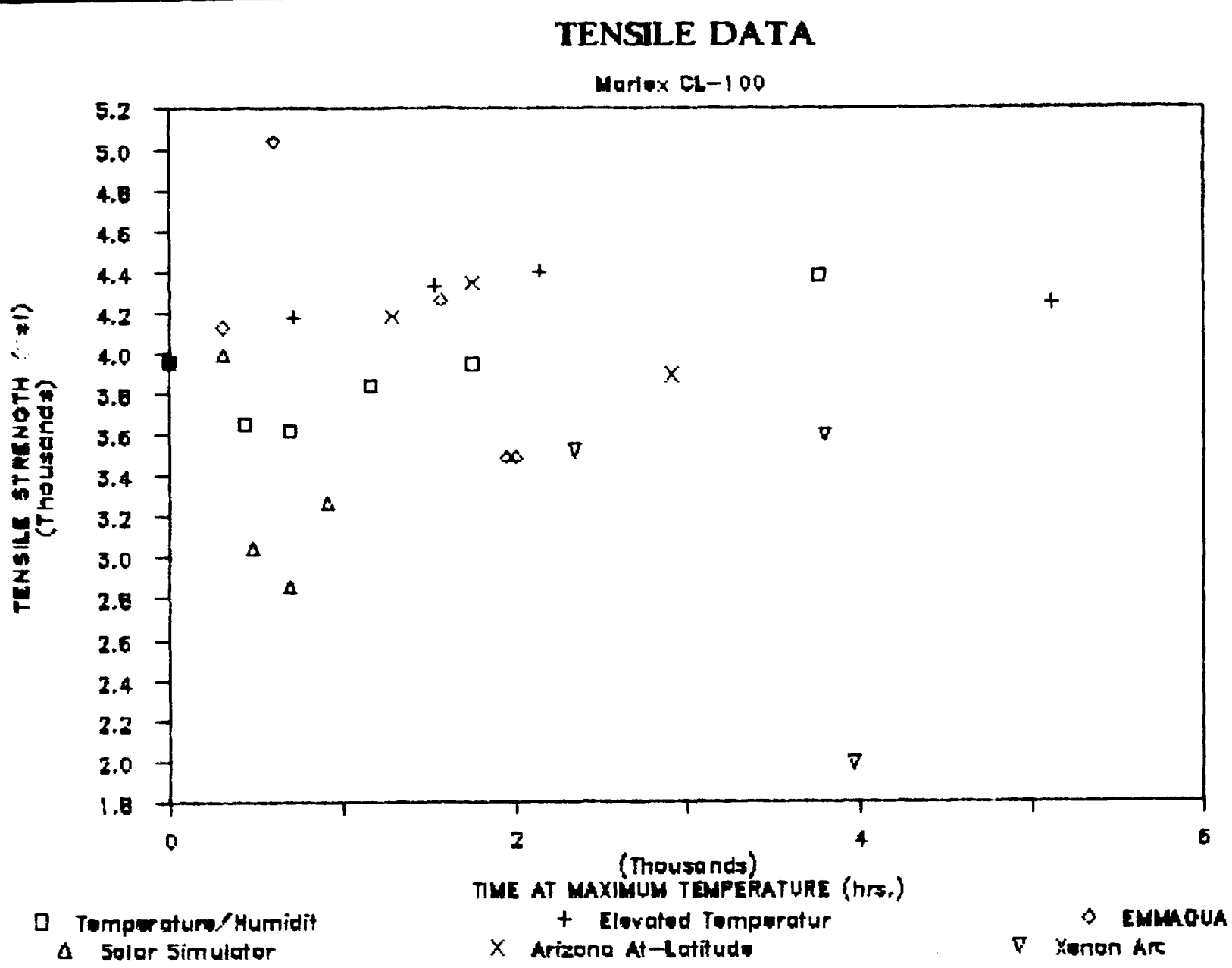

Figure 30: Marlex CL-100 Tensile Strength vs. Time

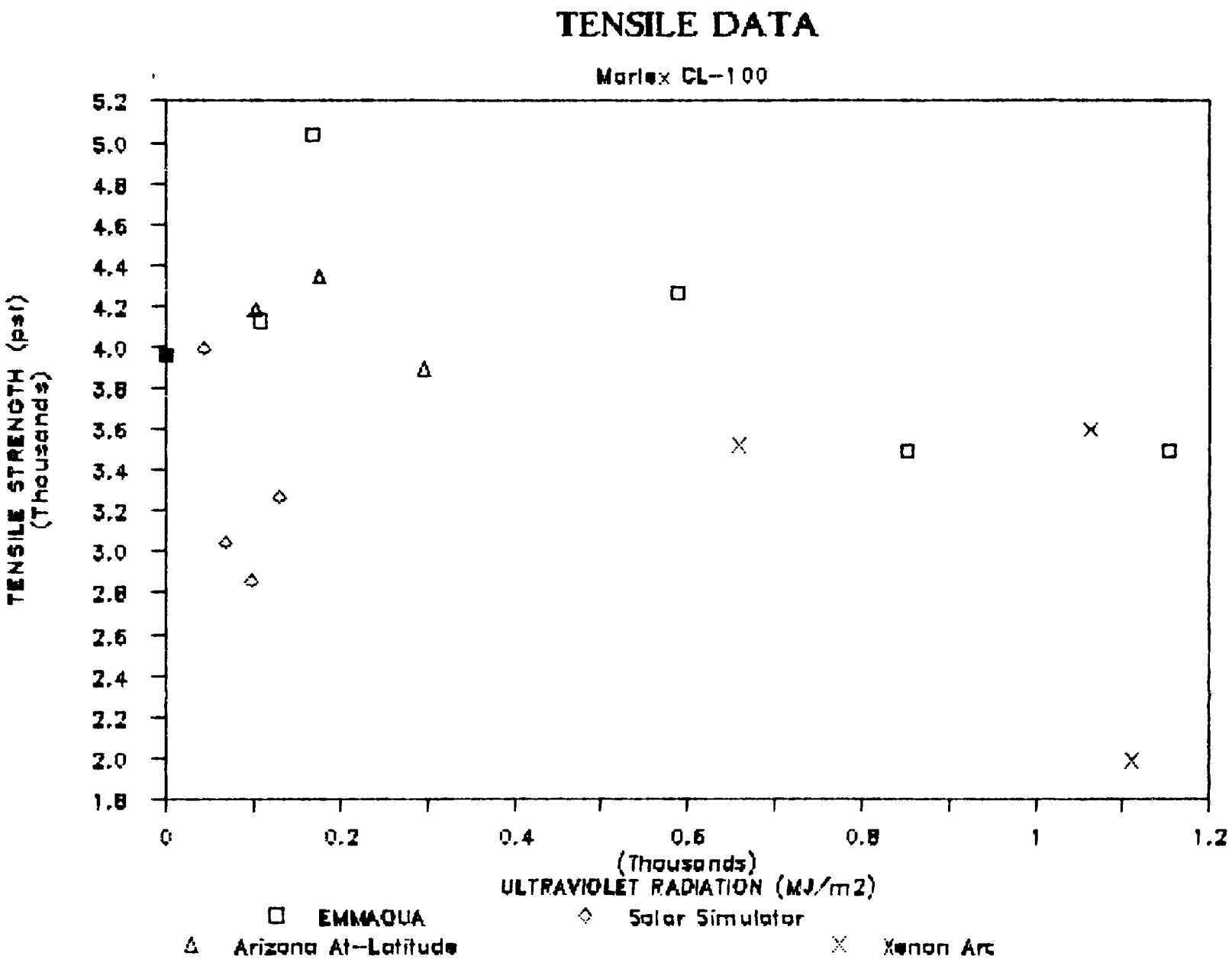

Figure 31: Marlex CL-100 Tensile Strength vs. Ultraviolet Radiation

Spectral reflectance measurements serve to indicate optical property changes in discrete wavelength regions of the spectrum. Property changes of this sort result from the interaction of the pigment and/or the binder with the environment. A typical change would be the development or change of an absorption band. A change in absorption in a particular wavelength region often can be related to a physical phenomenon at the surface of a material and can be modeled using the change in reflectance at the peak wavelength. Solar absorptance, although insensitive to all but major changes in discreet wavelength regions, is a measure of the broadband changes in the optical properties of material surfaces. Solar absorptance also indicates the extent to which a material will absorb solar radiation and thus be subject to solar radiation induced temperature change.

4.8.3 155mm Propelling Charge Container Material Measurements

Color data for 155mm Propelling Charge container material are presented in Table 19 and Figures 32 through 37. The Y coordinate data in Table 19 shows that the container material darkens in the early part of the environmental exposure tests before fading later on. Comparison of the Y, x, and y coordinate plots in Figures 32, 33, and 34 to Figures 35, 36, and 37 clearly shows the influence of ultraviolet on the surface of the container material and in fact the figures reflect the S-shape referred to in paragraph 2.5.1. The data plotted against time at temperature in Figures 35 through 37 however are widely scattered.

It is particularly interesting to compare the DSC data to the color data at the ultraviolet fluence at which surface cracks occurred. This suggests that the end of the induction phase for the surface of the container material at temperatures representing the extreme of the logistics chain, would occur outdoors in less than a two-year period. Further, the failure occurred shortly after the end of the induction phase. Thus, if the performance of the containers is found to be unacceptable with the presence of surface cracks, color measurements could be used to determine the acceptability of a container item and the change in color predictive of failure.

Unfortunately, the elevated temperature and elevated temperature/humidity data plotted against time, were not exposure tested long enough to exhibit a trend. Colorimetric properties must be characterized further before they could be used to predict or model performance. This is especially important since the DSC data and its relationship to cracking suggests that indoor storage, as shown by the elevated temperature and elevated temperature/humidity tests, would have an effect on the crystallinity of the HDPE which after a long period of time could change the rate at which surface cracking occurs either by thermal or photooxidative mechanisms.

155 Propelling Charge container spectral reflectance measurement and solar absorptance data are shown in Table 20. A spectral reflectance spectra for a pre-exposure test sample is shown in Figure 38. The lack of features, or the relative flatness, exhibited by the spectral

Table 19
155mm Propelling Charge Container Colorimetric Data

Exposure Conditions	Ultraviolet (MJ/m2)	Time at Maximum Temperature (hrs)	Y	x	y
Elevated Temperature at 71 C		0	12.57	0.3432	0.3504
		720	13.63	0.3415	0.3467
		1537.5	11.66	0.3402	0.3483
		2138	13.55	0.3337	0.3404
Humidity Chamber at 60 C with 90% RH		0	12.57	0.3432	0.3504
		429	14.11	0.3328	0.3463
		693	12.93	0.3432	0.3528
		1155.5	12.42	0.3446	0.3488
		1757.3	11.17	0.3433	0.3528
		3765	9.89	0.3515	0.3611
EMMAQUA	0	0	12.57	0.3432	0.3504
	106.7	300	10.58	0.3445	0.3511
	169.3	600	10.61	0.3489	0.3554
	588	1570	12.14	0.3424	0.3531
	852	1950	12.88	0.3389	0.341
	1261	1200	15.41	0.3329	0.3414
	1323	1500	15.66	0.3303	0.3405
Solar Simulator	0	0	12.57	0.3432	0.3504
	43.5	307	13.44	0.3428	0.3430
	67.6	477	10.70	0.3481	0.3475
	97.8	690	10.67	0.3488	0.3542
	128.6	908	11.36	0.3492	0.3564
Arizona	0	0	12.57	0.3432	0.3504
At-Latitude	101	1280	12.77	0.3396	0.344
	175	1750	9.96	0.3471	0.3559
	295	2900	10.64	0.3447	0.354
Xenon Arc	0	0	12.57	0.3432	0.3504
	882	2304	12.13	0.3386	0.3473
	1315	3152	17.81	0.3299	0.3375

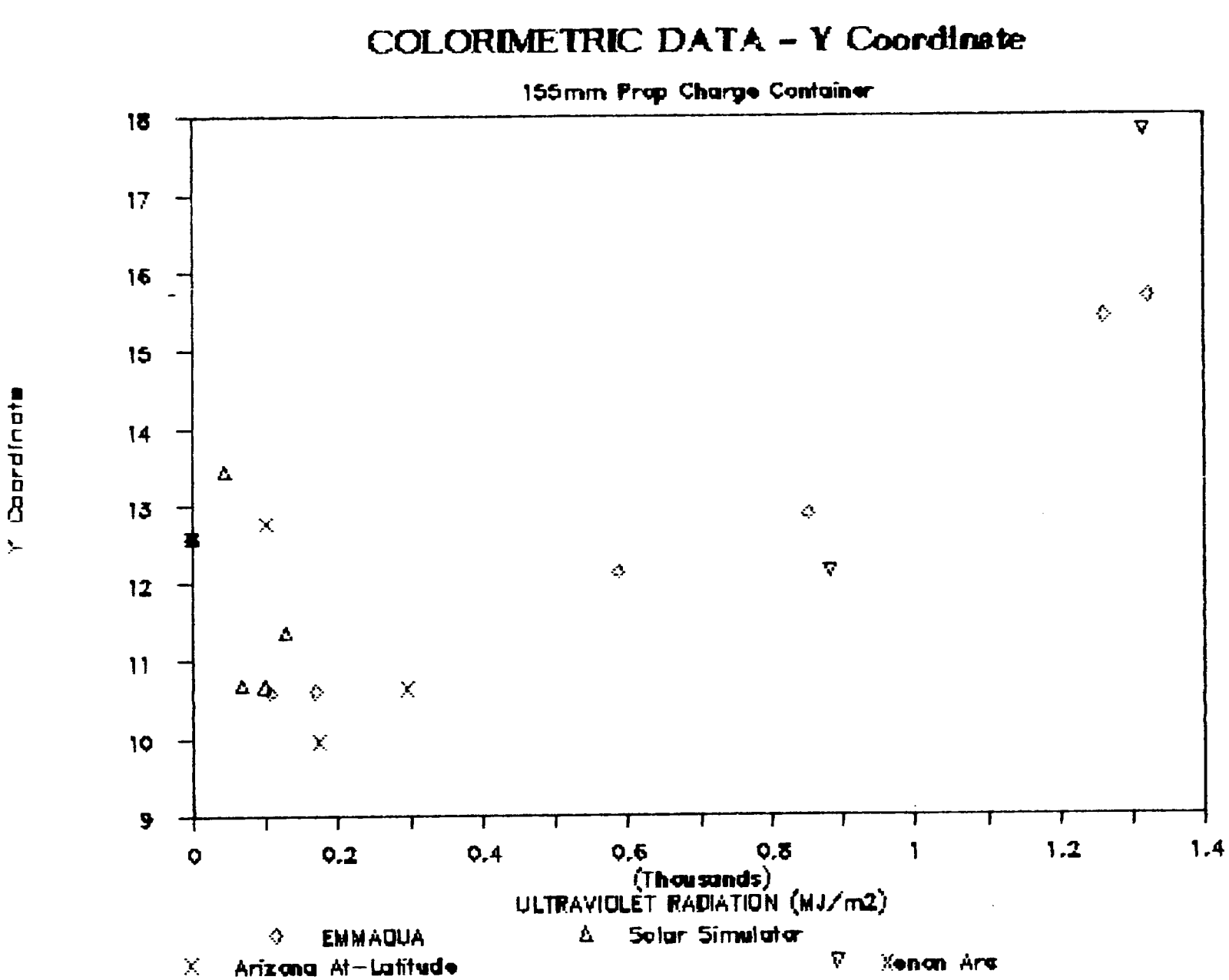

Figure 32: 155mm Propelling Charge Container Material Y Coordinate Data vs. Ultraviolet Radiation

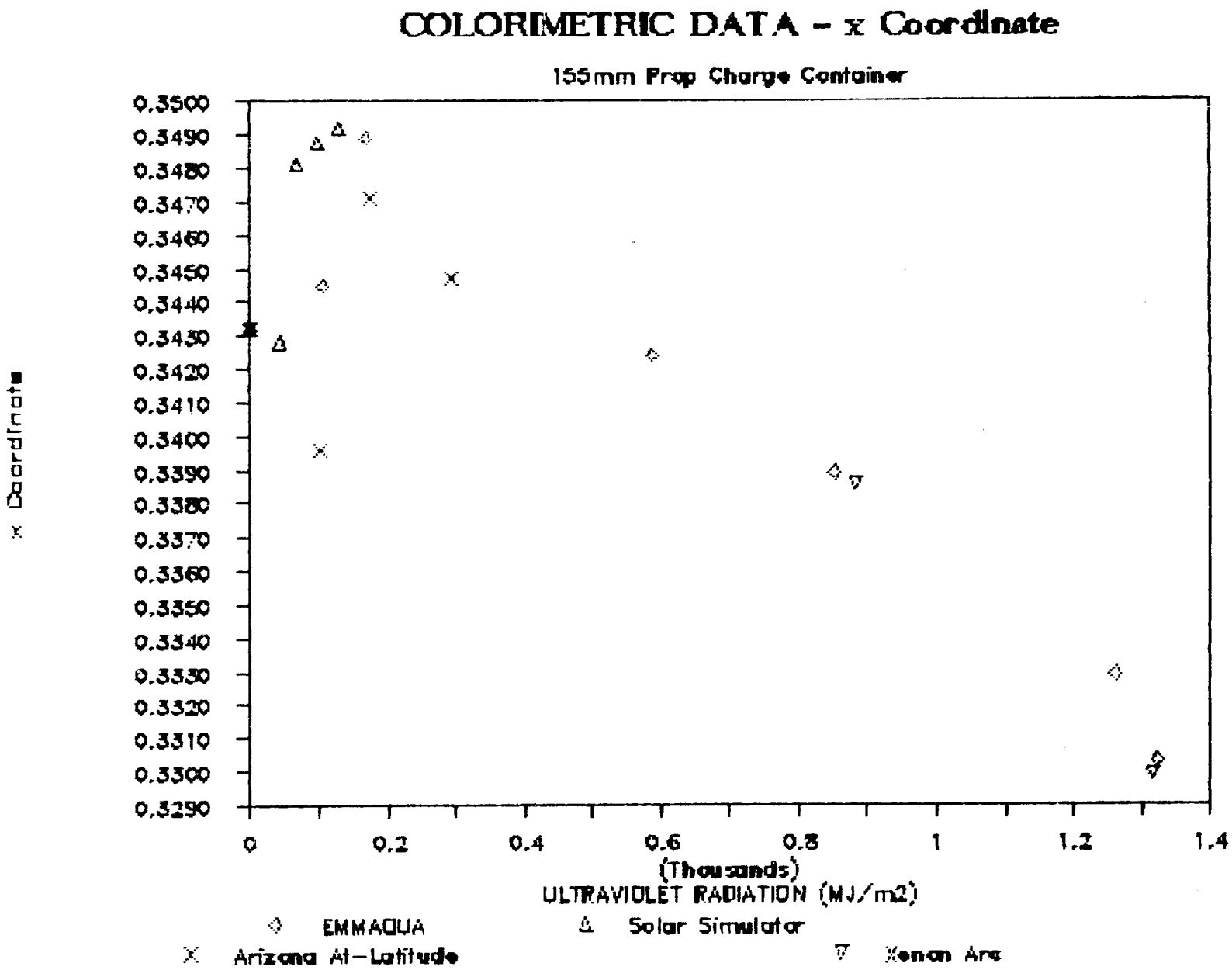

Figure 33: 155mm Propelling Charge Container Material x Coordinate Data vs. Ultraviolet Radiation

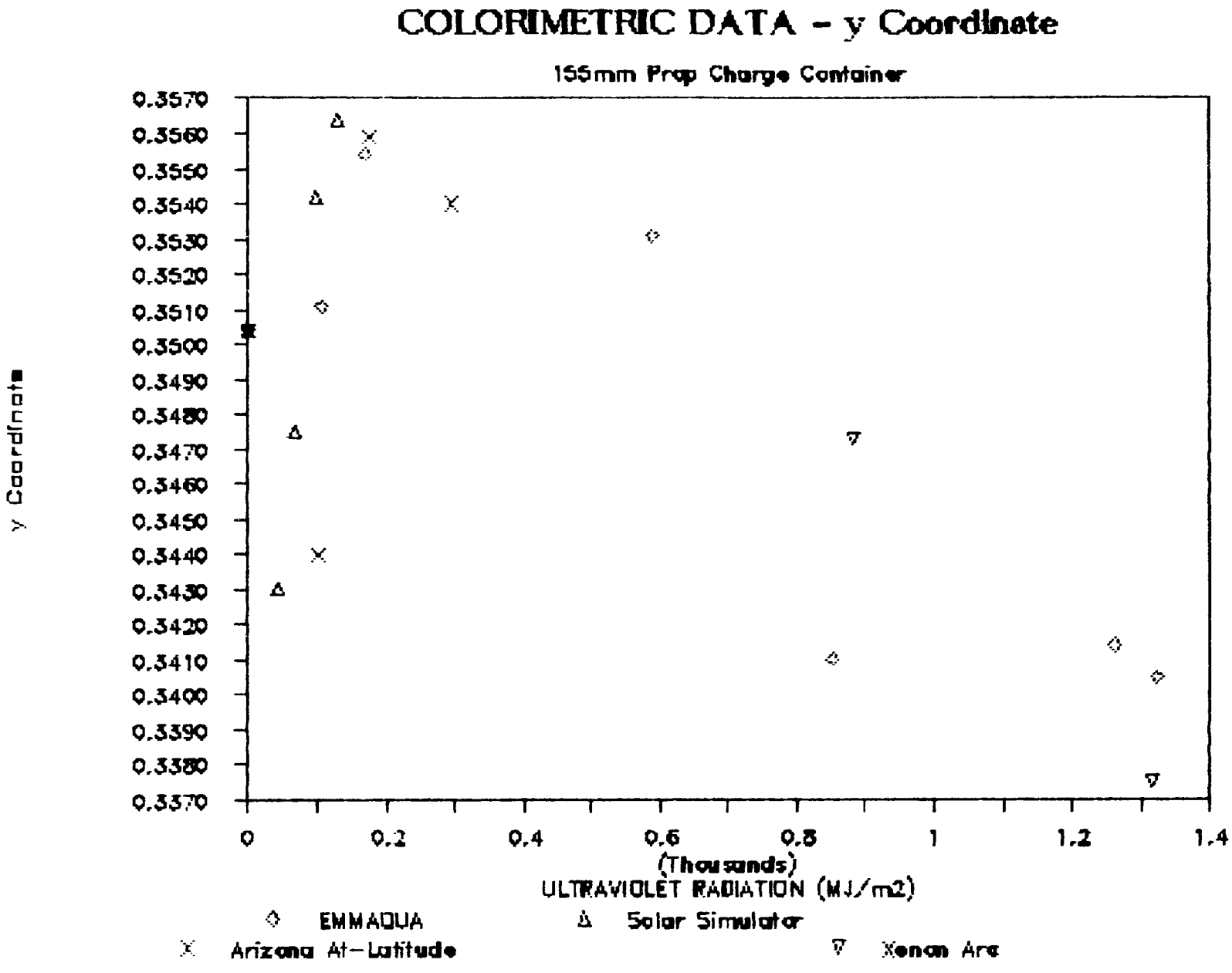

Figure 34: 155mm Propelling Charge Container Material y Coordinate Data vs. Ultraviolet Radiation

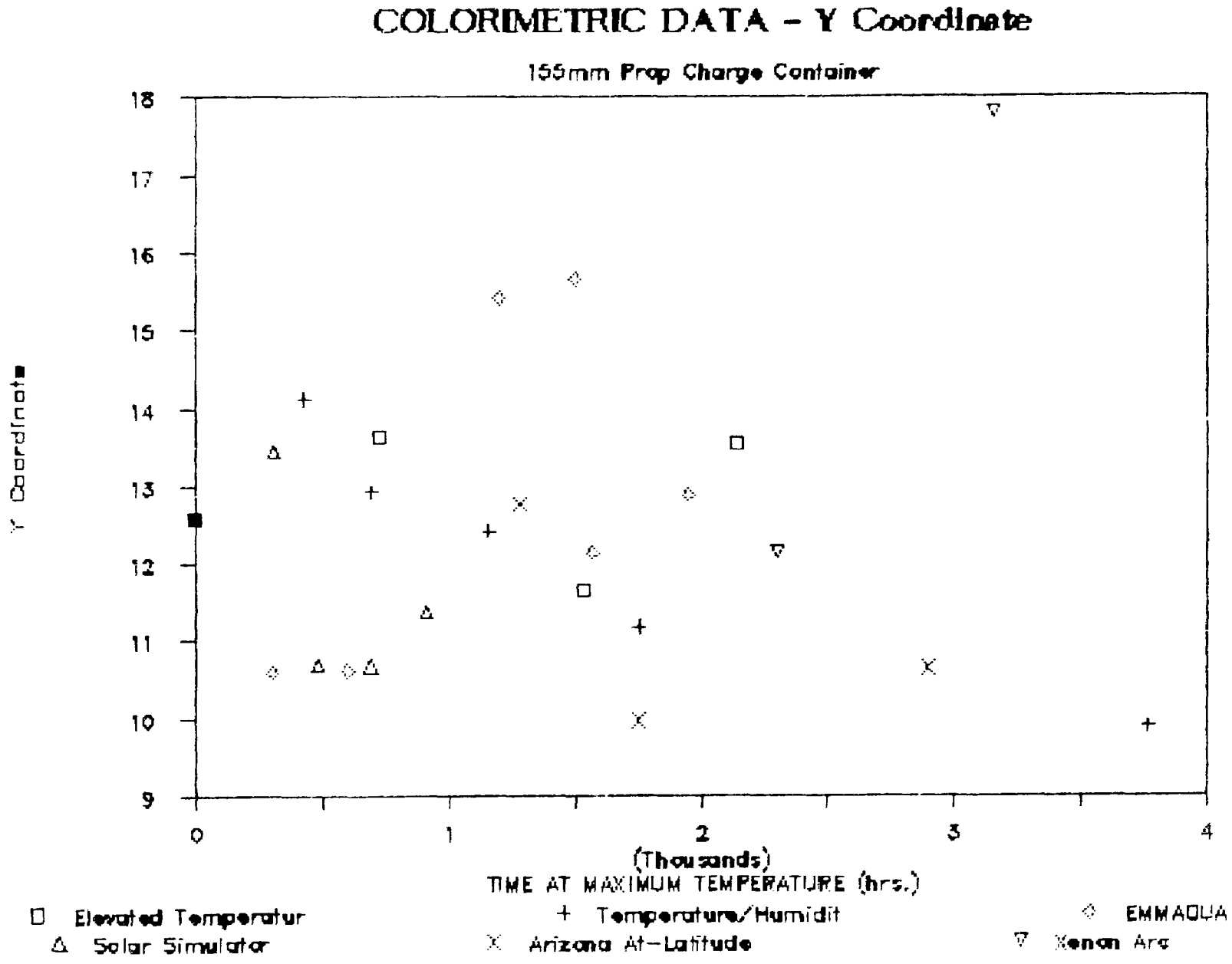

Figure 35: 155mm Propelling Charge Container Material Y Coordinate Data vs. Time at Temperature

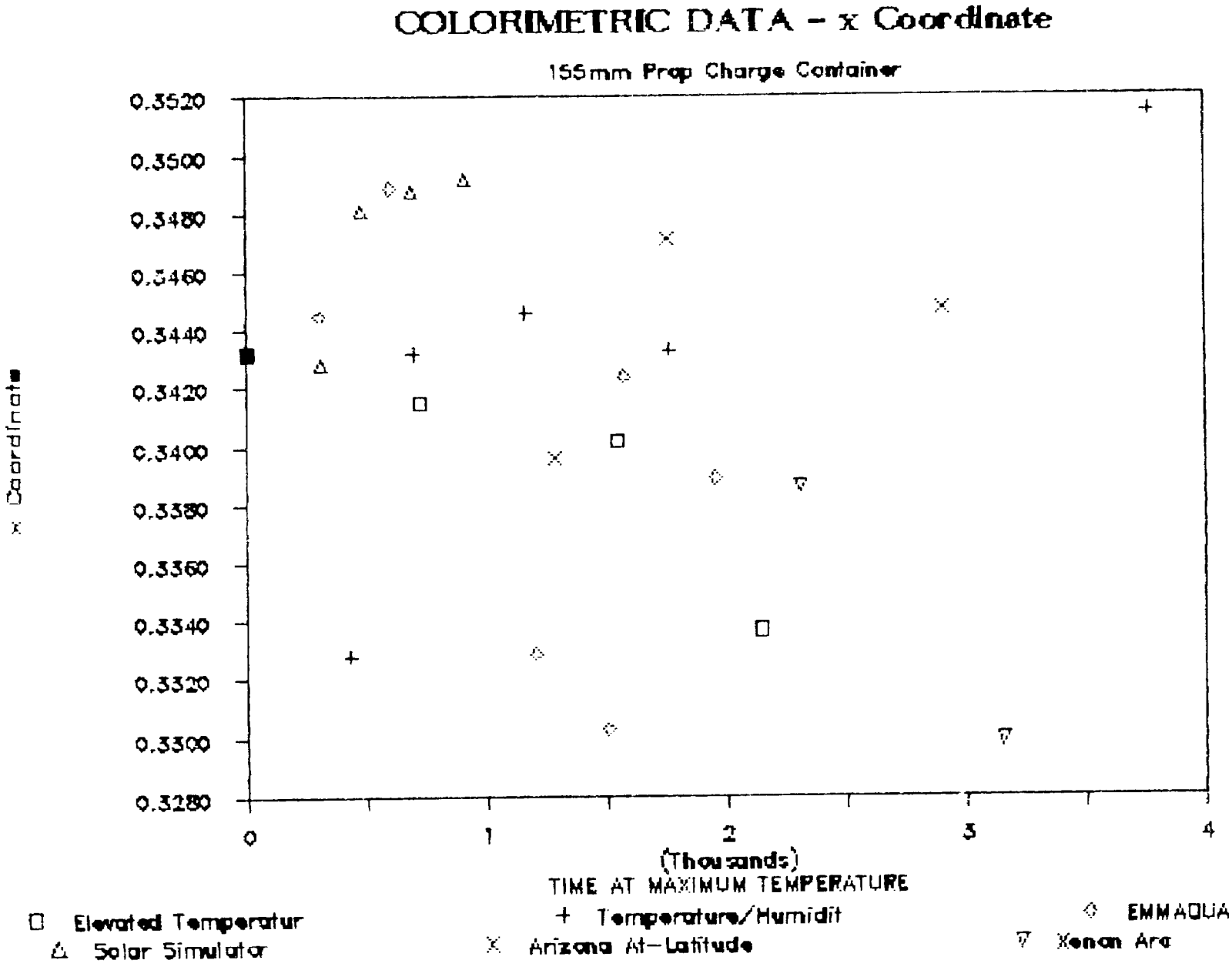

Figure 36: 155mm Propelling Charge Container Material x Coordinate Data vs. Time at Temperature

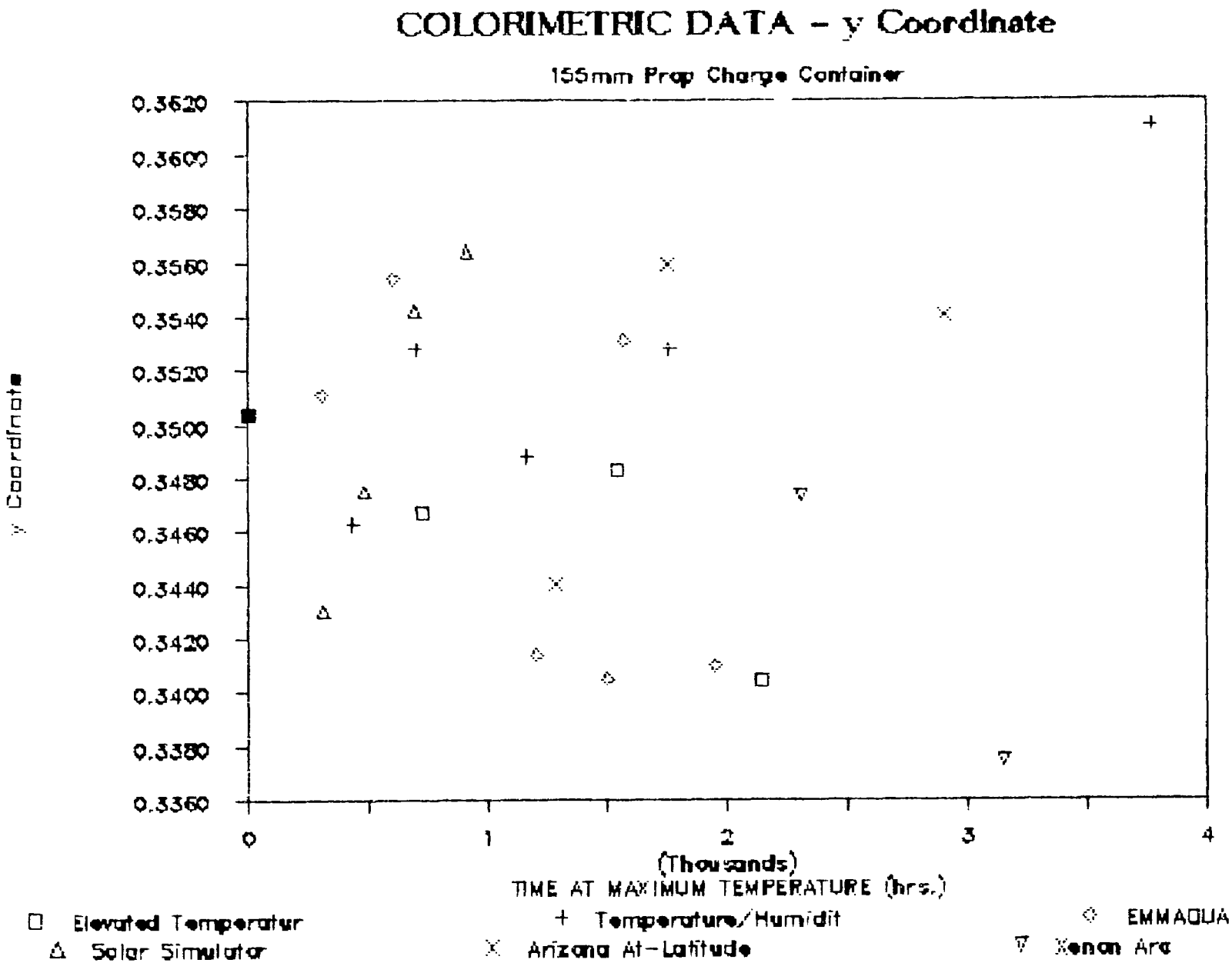

Figure 37: 155mm Propelling Charge Container Material y Coordinate Data vs. Time at Temperature

Table 20
155mm Propelling Charge Container Material
Air Mass 1.5 Solar Absorptance

Exposure Conditions	Ultraviolet (MJ/m^2)	Time at Maximum Temperature (hours)	Solar Absorptance
Elevated Temperature at 71°C		0	0.87
		720	0.88
		1538	0.88
		2138	0.88
Humidity Chamber at 60°C with 90%RH		0	0.87
		429	0.88
		693	0.89
		1156	0.88
		1757	0.88
		3765	0.88
EMMAQUA[6]	0	0	0.87
	107	300	0.88
	169	600	0.88
	588	1570	0.88
	852	1950	0.87
	1261	1200	0.91
	1323	1500	0.91
Solar Simulator	0	0	0.87
	43.5	307	0.87
	67.6	477	0.88
	97.8	690	0.88
	128.6	908	0.88
Xenon-Arc	0	0	0.87
	882.5	3152	0.82
	1315	4696	0.91
Arizona At-Latitude	0	0	0.87
	101	1280	0.87
	175	1750	0.87
	295	2900	0.93

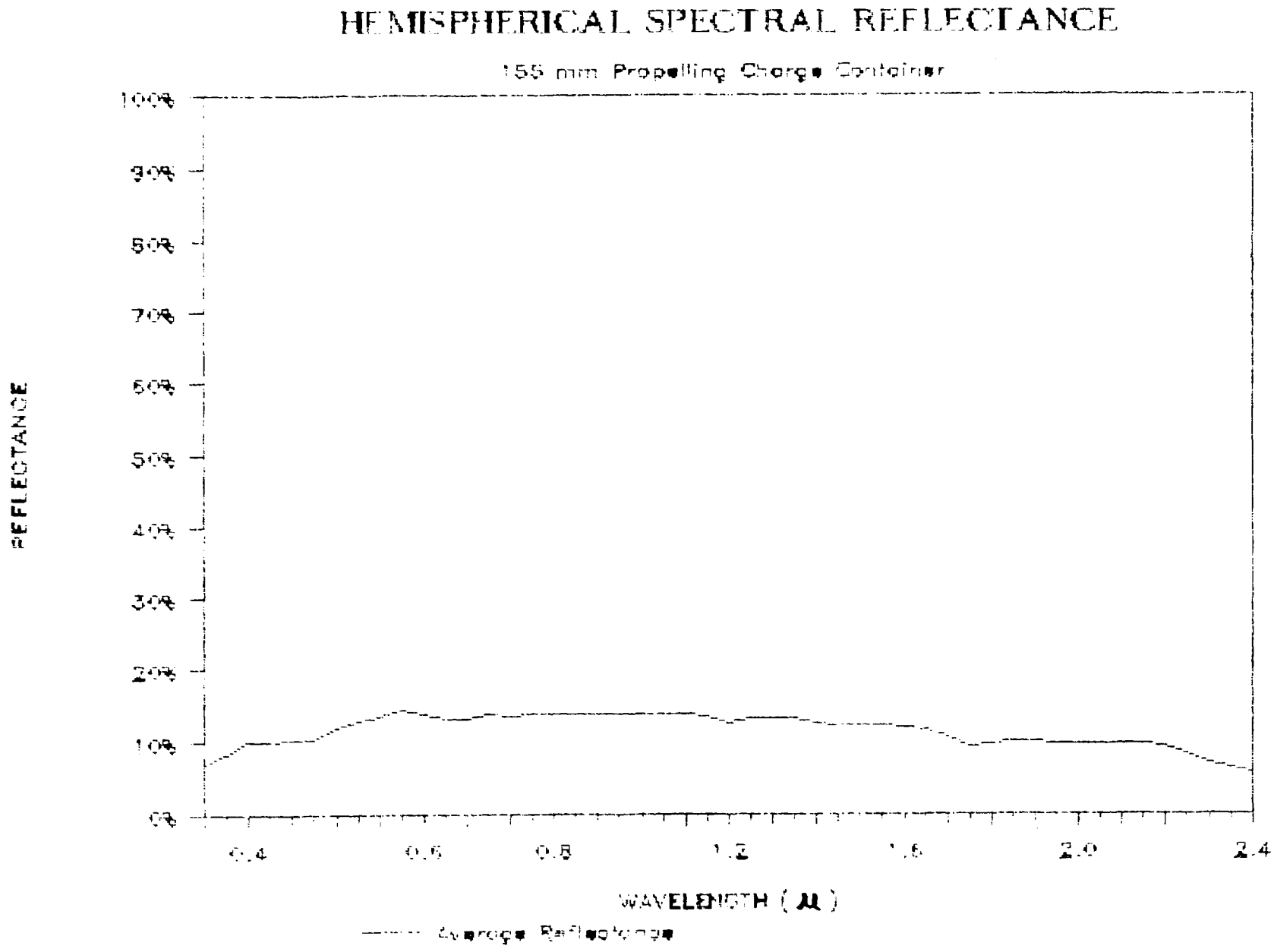

Figure 38: Spectral Reflectance of 155mm Propelling Charge Container Material

reflectance explains in part the small changes determined for the solar absorptance. That is, the development of absorption bands as a result of the exposure testing were not detected. Changes in the spectral reflectance occurred, but did so across the spectrum. The trends in color noted above could have been determined from spectral reflectance measurement data if integrated against the appropriate spectral distribution.

4.8.4 M2A1 Container Material Measurements

Color data for the M2A1 container material are presented in Table 21 and Figures 39 through 44. The data plotted against ultraviolet radiation in the figures reaches a plateau since the evolution of the fibers cause the color value of the material to approach that of the fibers. The data for the exposure tests without ultraviolet would not be expected to follow a similar trend since fiber blooming occurs as the resin matrix erodes. There is insufficient data to make a comparison of DSC determined compositional data to the colorimetric data although, consideration of the fiber blooming effect suggests that the start of the plateau noted in the colorimetric data represents the end of the induction stage for the surface of the composite material.

M2A1 container material spectral reflectance measurement data are shown in Table 22. A spectral reflectance spectra for pre-exposure test sample is shown in Figure 45. As noted for the 155mm Propelling Charge container material, the flatness exhibited by the spectral reflectance explains the small changes determined for the solar absorptance. Absorption bands as a result of the exposure testing also were not detected. Changes in the spectral reflectance occurred, but did so across the spectrum as indicated by the small change in solar absorptance values.

4.9 Full-Scale Item Tests

4.9.1 Arizona At-Latitude Exposure

Full-scale M2A1 and 155mm Propelling Charge container items were exposure tested with the test sample materials. The at-latitude exposure procedure was discussed in paragraph 4.1. The container items were exposed using the same schedule reported for the test sample materials.

Shortly before the end of the testing the 155mm Propelling Charge container exhibited surface cracks on those portions of the container which had a direct view of the sun. As mounted on the 34° south facing rack, two sides of the container did not have a view of the sun. One side was in direct contact with the rack and was shielded while the other side faced the ground at a 34° angle. The container item was mounted with its long dimension running east to west. Visual comparison of the exposure tested item to an unexposed container showed slight fading.

Table 21
M2A1 Small Ammo Container Colorimetric Data

Exposure Conditions	Ultraviolet (MJ/m2)	Time at Maximum Temperature (hrs)	Y	x	y
Elevated Temperature at 71 C		0	8.59	0.3384	0.3442
		720	8.75	0.3397	0.3436
		1538	9.07	0.3364	0.3440
		2138	10.06	0.3348	0.3421
Humidity Chamber at 60 C with 90% RH		0	8.59	0.3384	0.3442
		429	10.02	0.3335	0.3421
		693	9.54	0.3329	0.3414
		1156	8.13	0.3397	0.3484
		1757	7.99	0.3423	0.3509
		3765	9.68	0.3361	0.3435
EMMAQUA	0	0	8.59	0.3384	0.3442
	107	300	8.20	0.3411	0.3447
	169	600	9.12	0.3383	0.3452
	588	1570	16.77	0.3380	0.3495
	852	1950	18.82	0.3391	0.3480
	1261	1200	18.33	0.3409	0.3520
	1323	1500	17.66	0.3400	0.3437
Solar Simulator	0	0	8.59	0.3384	0.3442
	44	307	10.31	0.3341	0.3421
	68	477	10.17	0.3374	0.3455
	98	690	11.26	0.3342	0.3428
	129	908	10.12	0.3385	0.3468
Arizona At-Latitude	0	0	8.59	0.3384	0.3442
	101	1280	11.40	0.3374	0.3439
	175	1750	11.60	0.3343	0.3411
Xenon Arc	0	0	8.59	0.3384	0.3442
	601	2147	18.18	0.3223	0.3311

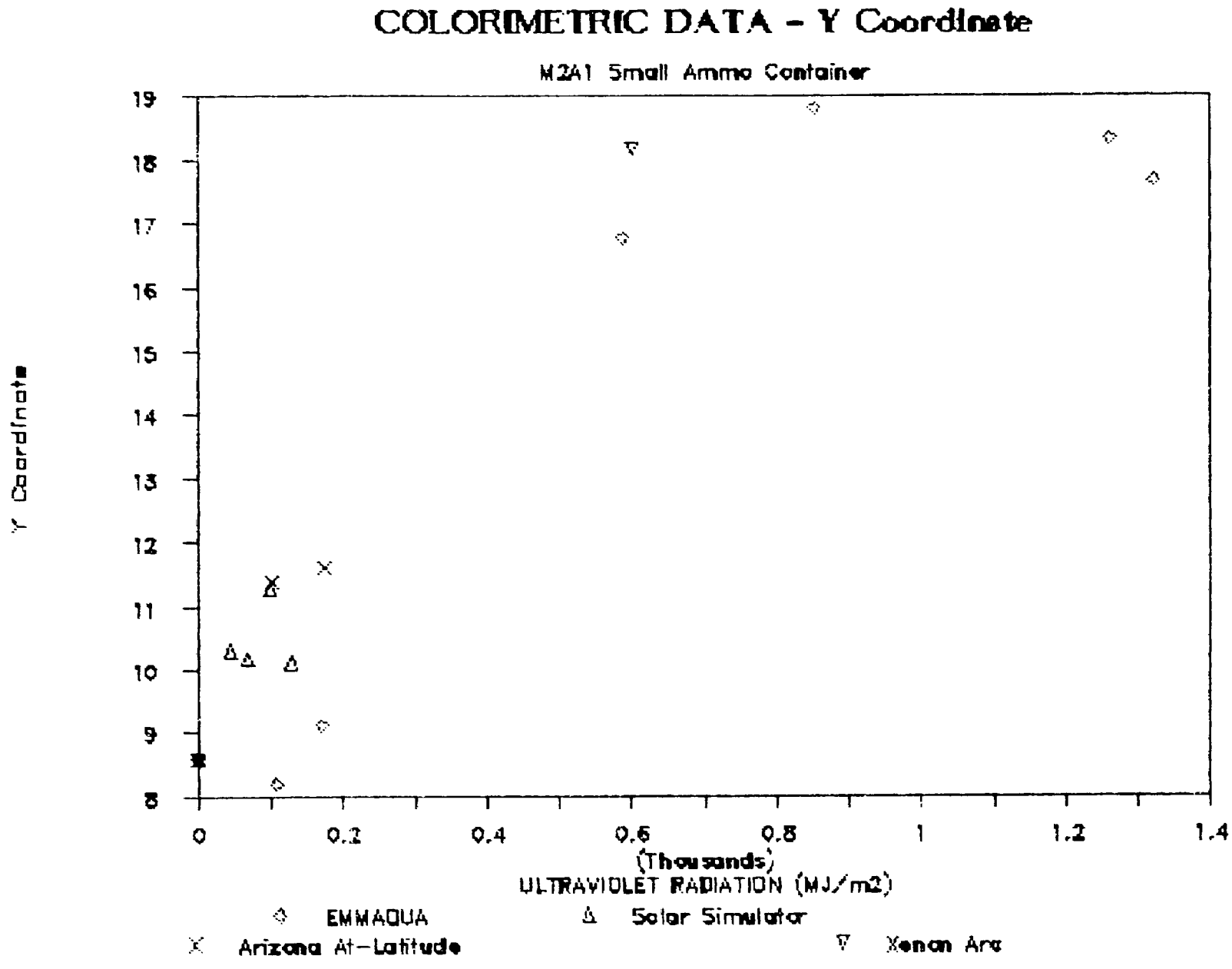

Figure 39: M2A1 Container Material & Coordinate Data vs. Ultraviolet Radiation

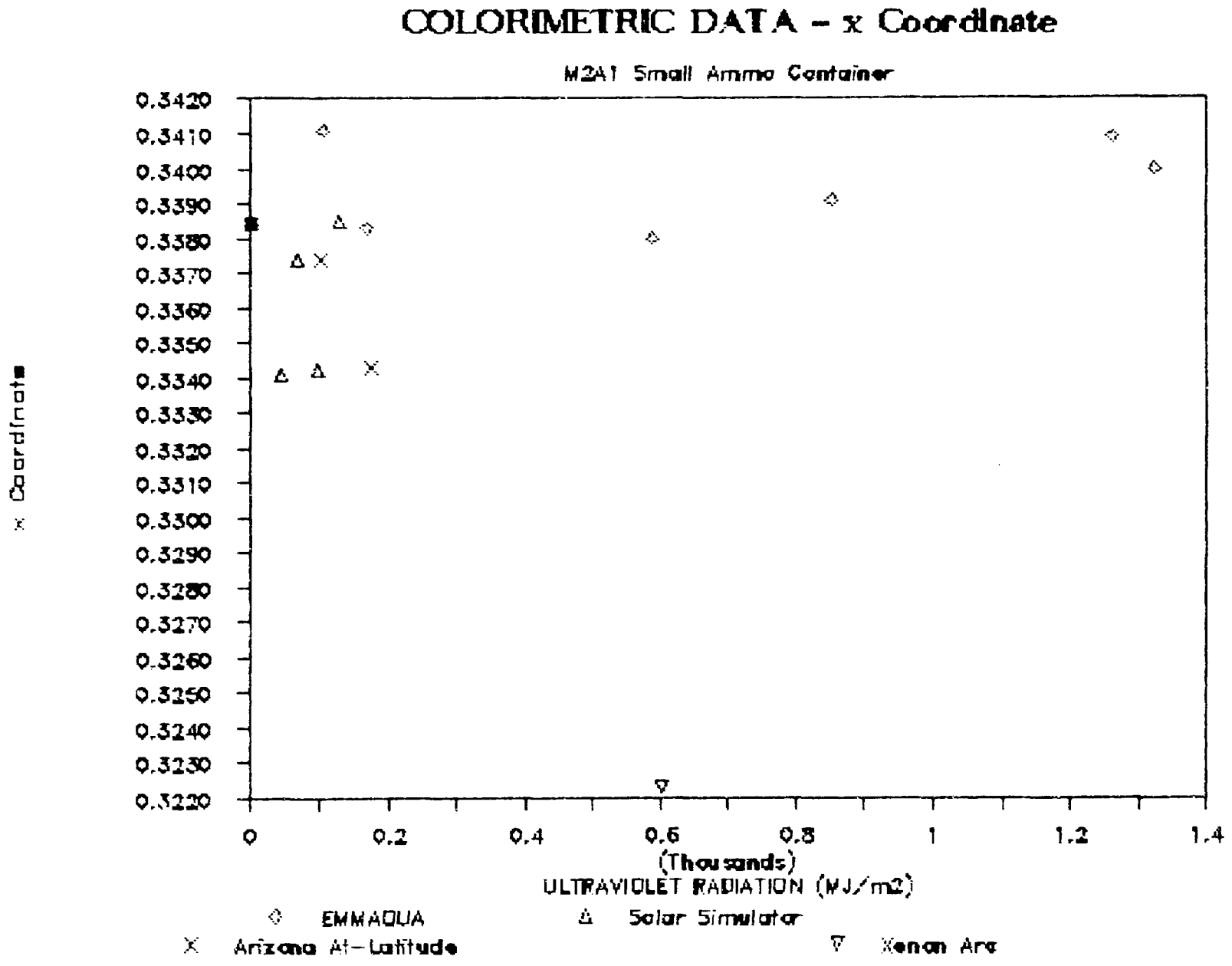

Figure 40: M2A1 Container Material x Coordinate Data vs. Ultraviolet Radiation

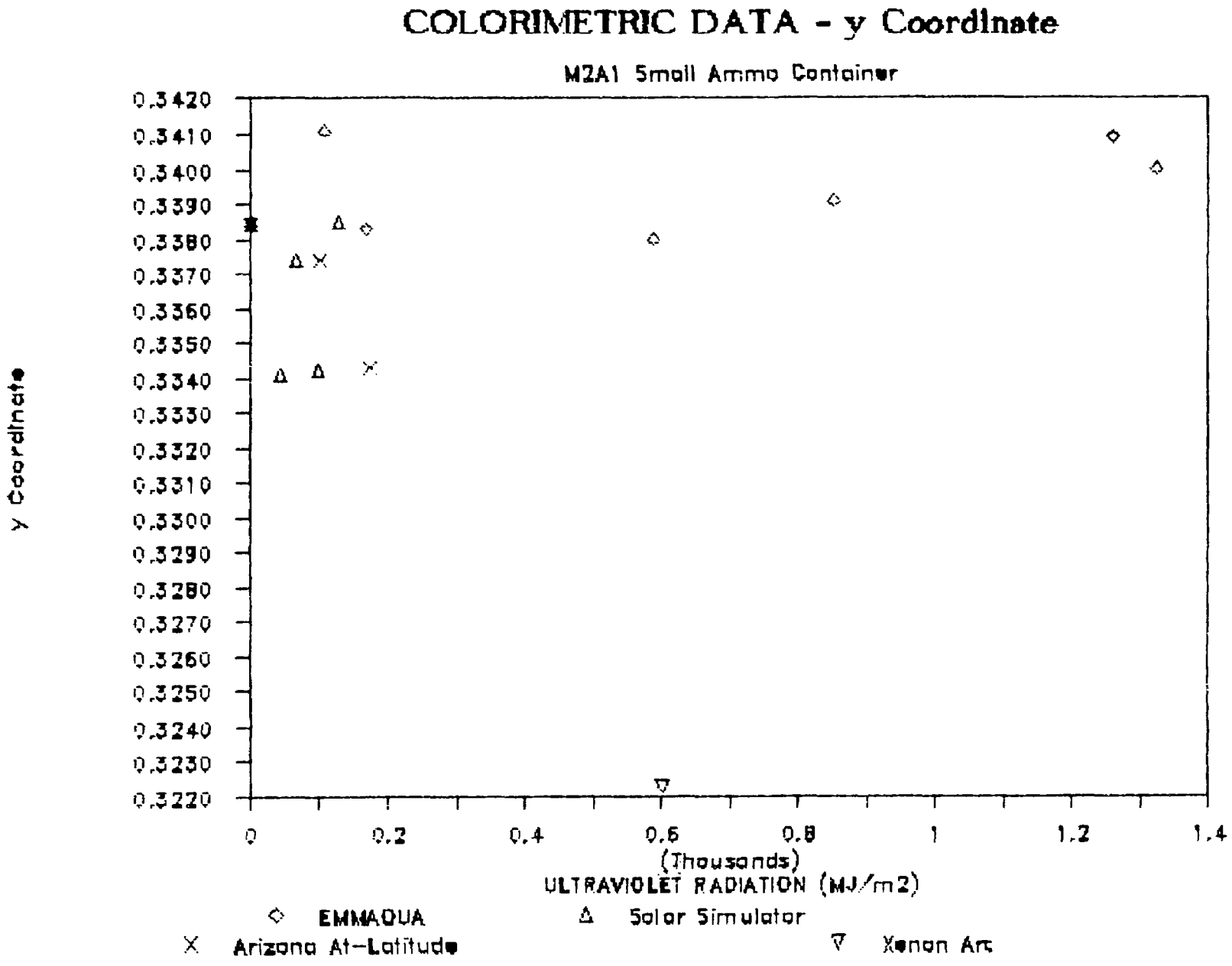

Figure 41: M2A1 Container Material y Coordinate Data vs. Ultraviolet Radiation

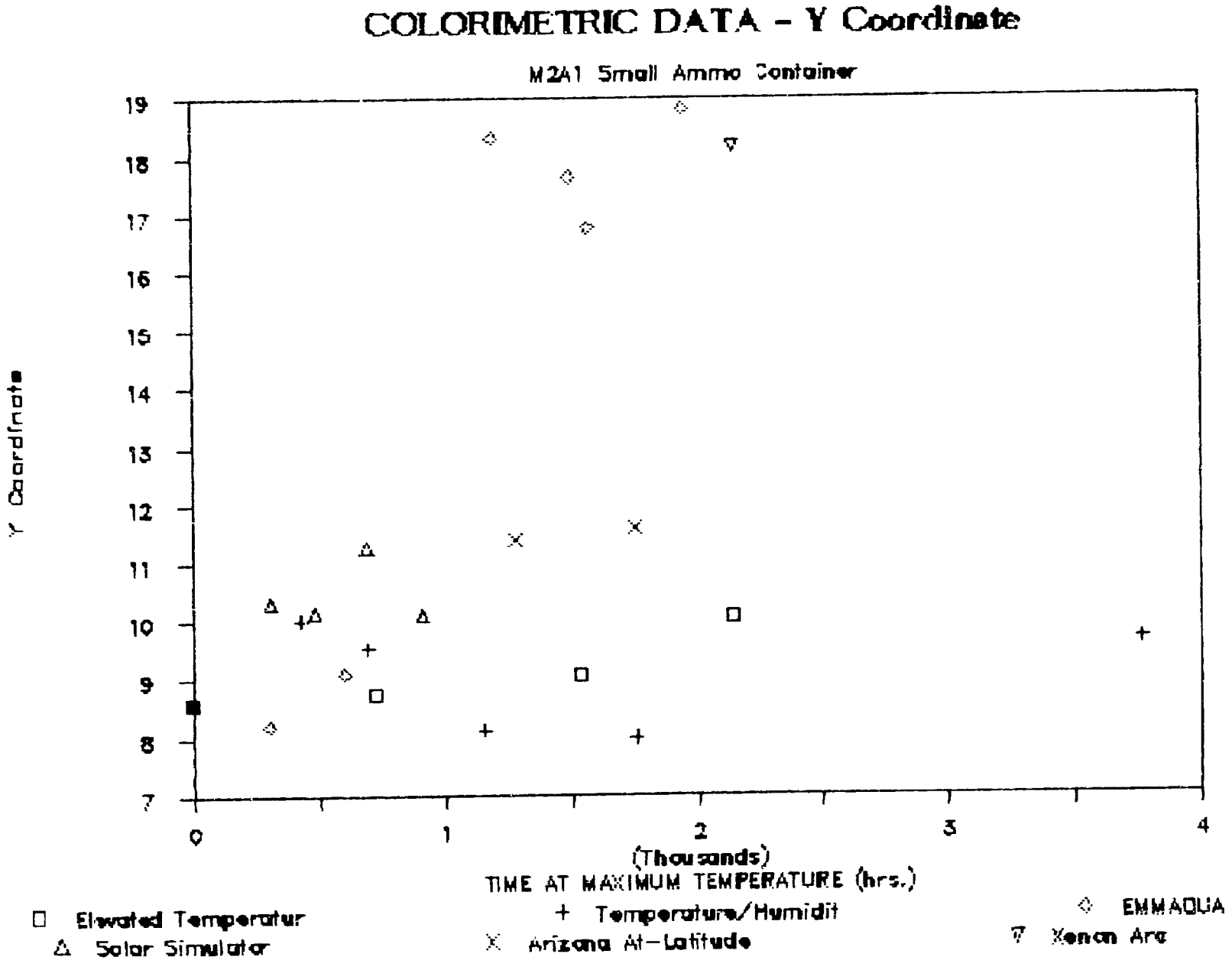

Figure 42: M2A1 Container Material Y Coordinate Data vs. Time at Temperature

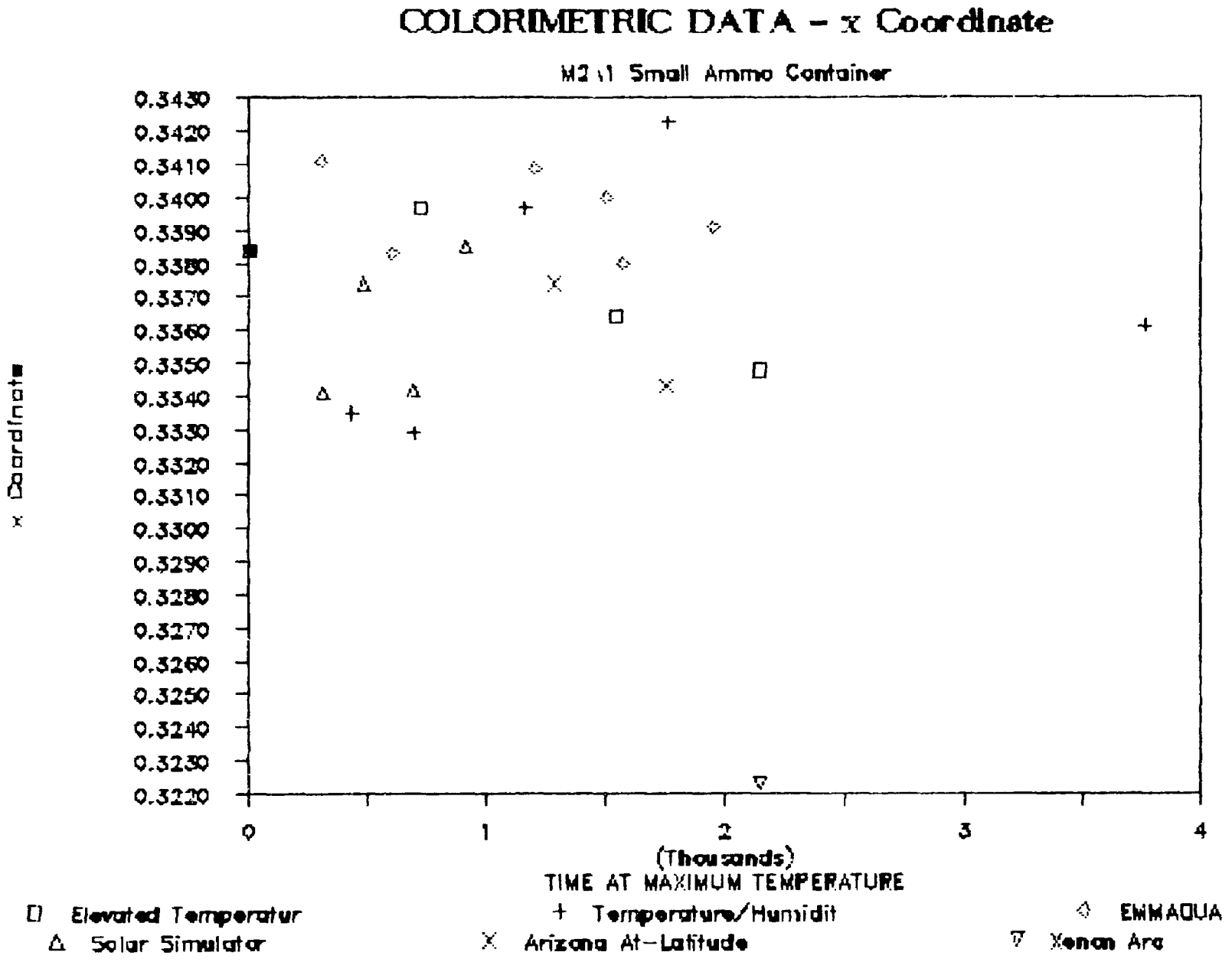

Figure 43: M2A1 Container Material x Coordinate Data vs. Time at Temperature

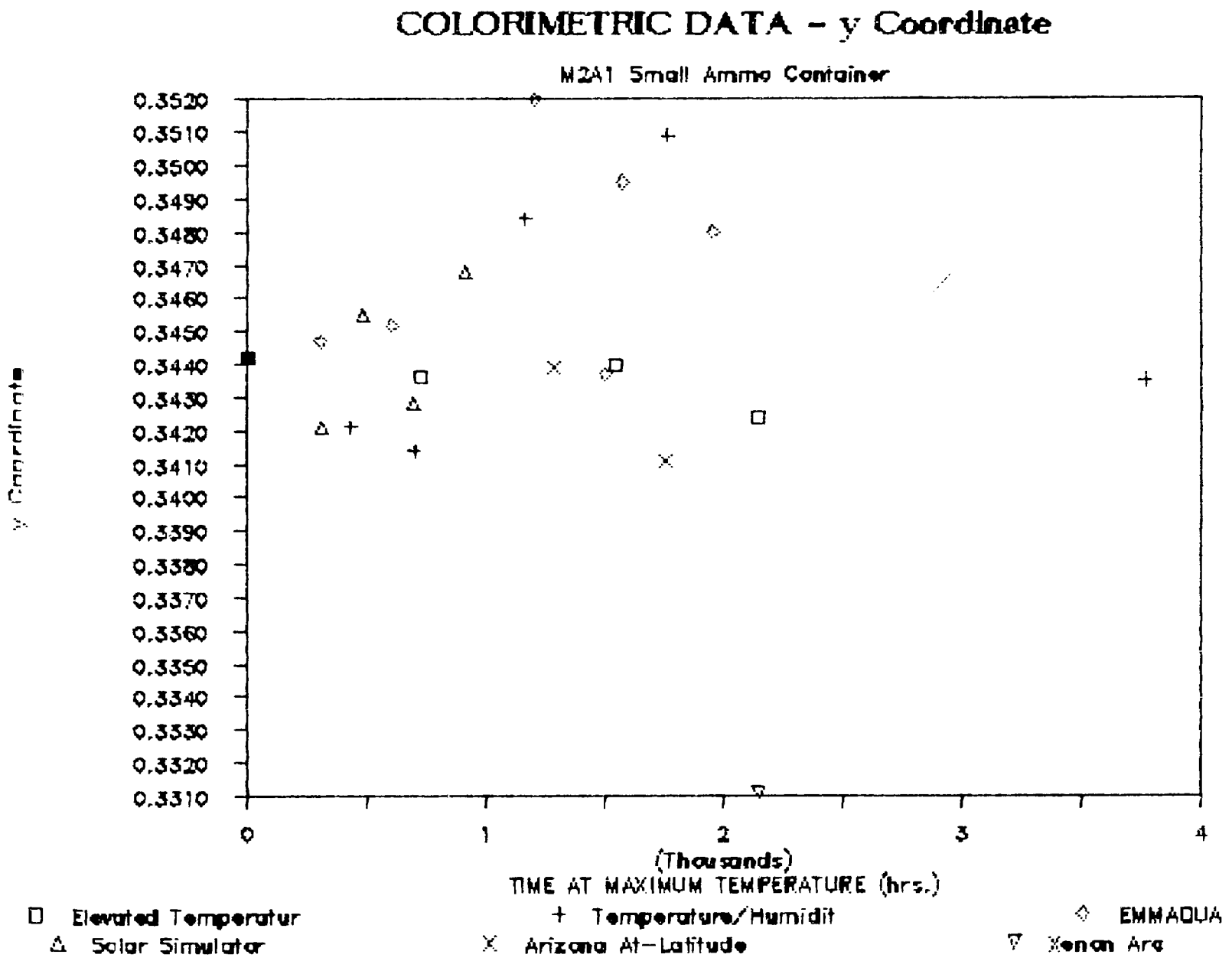

Figure 44: M2A1 Container Material y Coordinate Data vs. Time at Temperature

Table 22
M2A1 Container Material Air Mass 1.5 Solar Absorptance

Exposure Conditions	Ultraviolet (MJ/m^2)	Time at Maximum Temperature hrs.	Solar Absorptance
Elevated Temperature at 71°C		0	0.89
		720	0.9
		1538	0.89
		2138	0.89
Humidity Chamber at 60°C with 90%RH		0	0.89
		429	0.88
		693	0.91
		1156	0.89
		1757	0.9
EMMAQUA®	0	0	0.89
	107	300	0.9
	169	600	0.88
	588	1570	0.82
	852	1950	0.8
Solar Simulator	0	0	0.89
	43.5	307	0.89
	67.6	477	0.89
	97.8	690	0.88
	128.6	908	0.88
Xenon-Arc	0	0	0.89
	152	542	0.87
	601	2146	0.87
	1054	3764.3	0.89
Arizona-Latitude	0	0	0.89
	101	1280	0.89
	175	1750	0.87

Table 23
155mm Propelling Charge Container Moisture Gain Data

TEST SEQUENCE	TIME	ELAPSED TIME (HRS)	CONTAINER MOISTURE (G)	CONTAINER MOISTURE GAIN RATE (G/HR.)	CHAMBER VAPOR PRESSURE (DYN/CM2)	CONTAINER VAPOR PRESSURE (DYN/CM2)	CHAMBER CONTAINER PRESSURE DIFFERENCE (DYN/CM2)
TRIAL #6	155.5	0	0.4204		77.9	28.1	49.8
SOLAR RADIATION	164	8.5	0.4864	0.0077647		29.9	48
48C/80%RH	176.25	20.75	0.5174	0.0046746		31.8	46.1
	186.25	30.75	0.5468	0.0041105		33.6	44.3
	199.25	43.75	0.5812	0.0036754		35.7	42.2
	225.25	69.75	0.6215	0.0028831		37.8	40.1
	250.25	94.75	0.6602	0.0025308		40.1	37.8
	280.25	124.75	0.7032	0.0022669		42.5	35.4
	318.5	163	0.7465	0.0020006		45	32.9
	358.5	203	0.7923	0.0018320		47.6	30.3
	407.5	252	0.8407	0.0016678		50.3	27.6
SEPARATE RUN	617.5	0	0.7875		77.9	47.6	30.3
	700.5	83	0.8864	0.0011915		53.2	24.7
	751.5	134	0.94	0.0011380		56.3	21.6
	775.5	158	0.94	0.0009651		56.3	21.6
TRIAL #4	144.25	0	0.3114			19.4	58.5
SOLAR RADIATION	148.75	4.5	0.3542	0.0095111		22	55.9
48C/80%RH	153.25	9	0.3781	0.0074111		23.4	54.5
	156.75	12.5	0.3786	0.005376		24.9	53
	160.75	16.5	0.4294	0.0071515		26.5	51.4
	174	29.75	0.4558	0.0048537		28.1	49.8
	178.75	34.5	0.4849	0.0050289		29.9	48
	183.25	39	0.5158	0.0052410		31.6	46.3
TRIAL #6	39.75	0	0.2866		15	18.2	-3.2
DARK	41	1.25	0.3058	0.01536		19.4	-4.4
60C/20%RH	43.5	3.75	0.3262	0.01056		20.6	-5.6
	51.75	12	0.3477	0.0050916		22	-7
SEPARATE RUN	129.5	0	0.2867			17	-2
	130.5	1	0.3058	0.0191		19.3	-4.3
	133.25	3.75	0.3262	0.0105333		20.6	-5.6
	137.75	8.25	0.3477	0.0073939		22	-7
	141.25	11.75	0.3705	0.0071319		23.4	-8.4
	146	16.5	0.3948	0.0065515		24.9	-9.9
	150.5	21	0.4204	0.0063666		26.4	-11.4
TRIAL #6	853.75	0	0.9286		165	56.3	108.7
DARK	856.75	3	0.9786	0.0166666		59.5	105.5
60C/90%RH	869.75	16	1.0373	0.0067937		62.8	102.2
	884.25	30.5	1.0993	0.0055967		66.3	98.7
	903.25	49.5	1.1648	0.0047717		69.9	95.1
	922.25	68.5	1.2339	0.0044569		73.8	91.2
	946.25	92.5	1.307	0.0040908		77.9	87.1
	966.25	112.5	1.3841	0.0040488		82	83

Table 24

155mm Propelling Charge Container Graph Regression Information

SOLAR CYCLE 1ST GROUP REGRESSION

Regression Output:

Constant	-0.00562
Std Err of Y Est	0.000999
R Squared	0.746694
No. of Observations	10
Degrees of Freedom	8
X Coefficient(s)	0.000233
Std Err of Coef.	0.000047

SOLAR CYCLE LAST GROUP REGRESSION

Regression Output:

Constant	-0.01381
Std Err of Y Est	0.001157
R Squared	0.626297
No. of Observations	7
Degrees of Freedom	5
X Coefficient(s)	0.000393
Std Err of Coef.	0.000135

60°C 20%RH CYCLE 1ST GROUP REGRESSION

Regression Output:

Constant	0.022710
Std Err of Y Est	0.000049
R Squared	0.999953
No. of Observation	3
Degrees of Freedom	1
X Coefficient(s)	0.003948
Std Err of Coef.	0.000024

60°C/20%RH CYCLE 2ND GROUP REGRESSION

Regression Output:

Constant	0.021140
Std Err of Y Est	0.003252
R Squared	0.652529
No. of Observations	6
Degrees of Freedom	4
X Coefficient(s)	0.001497
Std Err of Coef.	0.000546

COMBINED SOLAR CYCLE DATA REGRESSION

Regression Output:

Constant	-0.00426
Std Err of Y Est	0.001056
R Squared	0.829285
No. of Observations	20
Degrees of Freedom	18
X Coefficient(s)	0.000205
Std Err of Coef.	0.000021

COMBINED 60°C/20%RH CYCLE DATA REGRESSION

Regression Output:

Constant	0.020153
Std Err of Y Est	0.003237
R Squared	0.582904
No. of Observations	9
Degrees of Freedom	7
X Coefficient(s)	0.001466
Std Err of Coef.	0.000468

60°C/90%RH CYCLE REGRESSION

Regression Output:

Constant	-0.03207
Std Err of Y Est	0.003375
R Squared	0.537379
No. of Observations	7
Degrees of Freedom	5
X Coefficient(s)	0.000408
Std Err of Coef.	0.000169

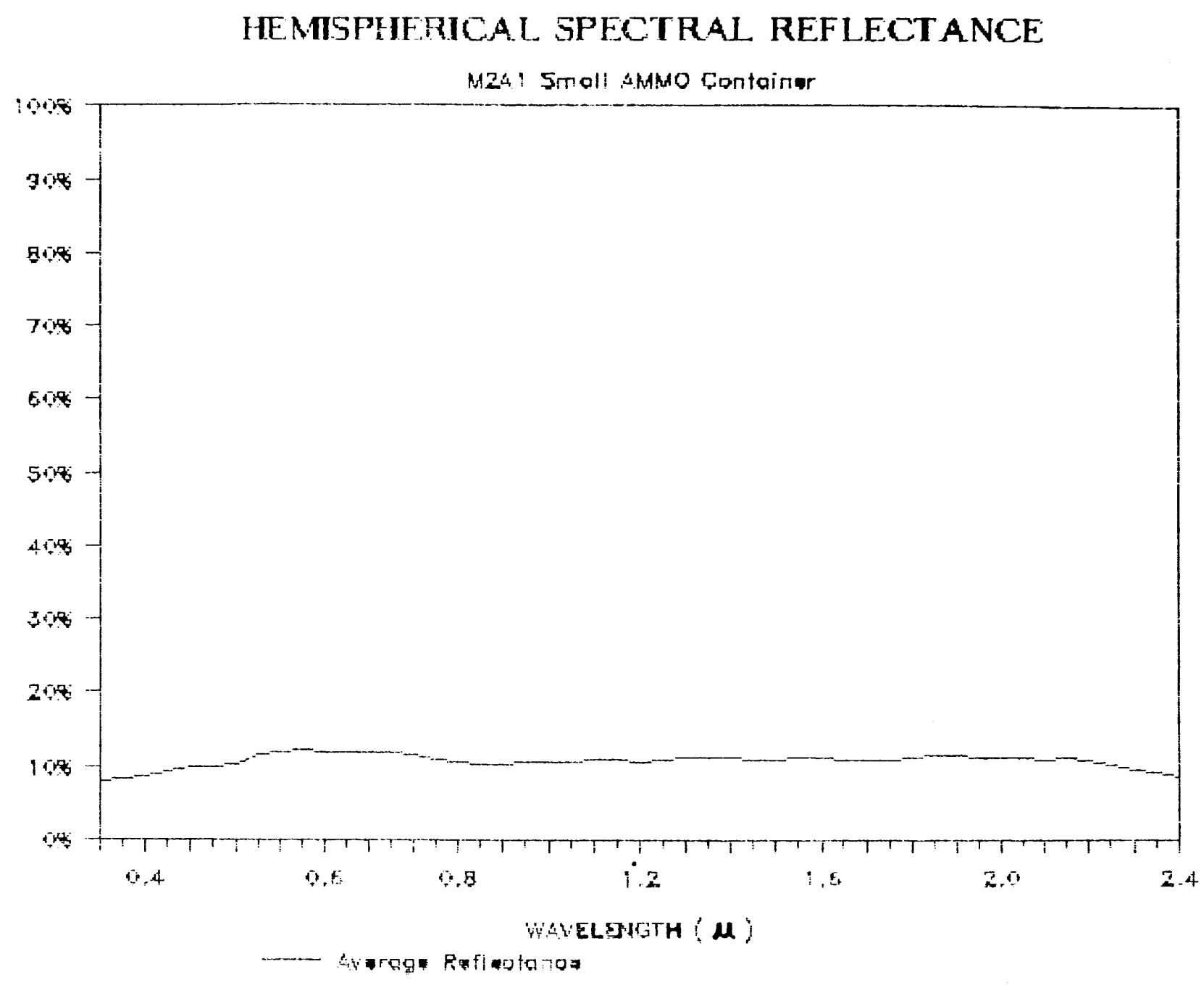

Figure 45: M2A1 Container Spectral Reflectance

The M2A1 container item was mounted on the rack also with its long dimension running east and west. The bottom of the container was attached to the rack. The handle was in a deployed position throughout the test rather than placing it flat against the top of the container lid. The container progressively faded and exhibited fiber bloom over the course of the test. The container lid was the most faded area, with fiber bloom most concentrated at corners. The sides of the container were also faded with fiber blooming decreasing in degree towards the bottom of the container. The plastic handle on the lid was badly cracked at the end of the test.

4.9.2 Environmental Chamber Tests

The environmental chamber test procedures, setup and results are reported in detail in Reference 46. The objectives of the full-scale item tests were to develop environmental chamber test procedures that could be used to predict the long-term performance of plastic ammunition containers. The objectives included accelerating the ageing process of container materials, determination of the container moisture vapor transmission rate, and determination of the container's ability to remain sealed.

Moisture vapor transmission rate constants and permeation constants are temperature dependent material properties. These constants generally increase logarithmically with increasing temperature. This is to be expected since water vapor pressure also increases with temperature in a logarithmic manner. Moisture vapor transmission rate is generally inversely dependent on thickness. The full-scale item tests and test data analysis attempted to normalize the effects of thickness and temperature by using chamber/container vapor pressure differential and the use of container volume to determine moisture gain and moisture gain rate.

The analysis of test data pursued the relationship of moisture gain in terms of grams per hour as a function of vapor pressure differential for the test conditions used. This is based on the concept of the rate of change in vapor pressure differential as function of time. This latter relationship is shown by equation 24 from Reference 48.

$$\ln(P/P_0) = -rt \qquad (24)$$

In equation 24,

P = water vapor pressure differential
P_0 = P at time zero
t = time
r = a rate constant derived from a material water vapor transmission rate constant.

In practice the weight of moisture in the container as a function of time was calculated using the humidity ratio and dry air volume from Reference 49 as determined from the container dew point and temperature. The vapor pressure of the container as a function of time was determined

likewise, while the vapor pressure of the test chamber was determined from the chamber calibration experiments. Finally, the vapor pressure differential between the test chamber and the container was calculated as a function of time from the vapor pressure data.

The amount of water occurring in the container during the course of environmental testing was calculated using equation 25,

$$\frac{W_s}{V_a} \quad V = W_{H_2O} \tag{25}$$

where W_s and V_a are the humidity ratio and dry air volume from Reference 49 and W_{H_2O} is the weight of water contained in the container air volume, V. W_s was obtained from Reference 49 at the measured dew point. V_a was obtained for the temperature measured inside the container during the test. Both values were obtained for temperatures to the nearest degree.

The total water content inside the container at a given time during the test was then associated with an elapsed time and test chamber vapor pressure. Elapsed time was determined by subtracting the given time in hours from time zero. Time zero was determined from data where the chamber and container conditions had stabilized. Water gain rate, in terms of grams per hour was then calculated by subtracting the moisture content of the container at a given time from the water content at time zero and dividing by the elapsed time. Container moisture vapor pressure was determined with the dew point temperature and the inside container temperature data. Vapor pressure differential as a function of time was calculated by subtracting the test chamber vapor pressure from the container vapor pressure at a given time during the test.

Moisture gain rate data was then plotted with their linear regressions as a function of vapor pressure differential. The regression line values were obtained using the natural logarithm of the moisture gain rates. The slope of the regression was taken to be the moisture vapor transmission rate constant over the vapor pressure range during the test. The rate constant was expressed in terms of grams of moisture per hour per dyne/cm^2. The calculated data are shown for both containers tested in the tables and figures in the following paragraphs.

4.9.2.1 155mm Propelling Charge Container Data Analysis

Moisture gain, moisture gain rate and vapor pressure data for a number of 155mm Propelling Charge container test cycles are shown in Table 23. Moisture gain rate was plotted as a function of vapor pressure differential. Table 24 exhibits linear regression analysis data used to prepare Figures 46 through 48.

The data regressions are shown over a vapor pressure differential of at least 100 dynes/cm^2, although the test data covers a significantly smaller range. This was done in order to compare the

change in rate of moisture gain for the different test cycle conditions. The use of the data regressions beyond the range covered by actual test data however is risky.

The data shown for different test cycles having identical test conditions, presented in Table 23, clearly suggests that moisture gain rate must be determined using long-term constant condition testing and that test conditions used to determine MVTR must be well inside the range of maximum instrument sensitivity. The considerable scatter shown for the last group of solar radiation data (Trial Run #4) and 60°C/20%RH test data indicate the effect of using short-term cycle data. Under these conditions the test chamber would have barely been stabilized when chamber conditions were changed. The data from the 60°C/90%RH and the second separate solar radiation cycles data shown in Table 23 present situations where, although long-term test cycles were used, the high moisture content of the container caused small changes in vapor pressure. These small changes decreased the precision by which vapor pressure differential could be determined.

The high R squared value obtained for the first solar radiation test cycle and the R squared value for all solar radiation test cycle data combined gives a high degree of confidence for the existence of the linear relationship between moisture gain rate and vapor pressure differential suggested in References 47 and 48. The test conditions, duration of the test, and the moisture content of the container during the test suggest that at least 200 hours of constant condition testing for a vapor pressure differential in the range of 30 to 60 dynes/cm^2 are required to obtain a reasonable measure of a moisture vapor transmission rate constant.

Comparison of the rate curves shown in Figures 46 through 47 and the Y-intercept (constant) values shown in Table 24 indicate that MVTR at any vapor pressure differential is dependent on the environmental conditions surrounding the container. This is expected since moisture permeation constants for many polymeric materials are temperature dependent.

The 60°C/20%RH chamber condition data shown in Figure 46 and the vapor pressure data in Table 24 show that although the vapor pressure differential was negative, moisture inside the container continued to increase. This indicates that water continued to desorb from the container material for the short period of time the test chamber was held at these conditions.

Figure 47 shows the effect of a large vapor pressure differential on the container during a time period when the container item contained a substantial quantity of water. Comparison of this test data to the solar radiation test data in Figure 48 shows that over a given period of time at the same temperature conditions, the container could continue to gain moisture even with a decrease in vapor pressure differential. This is due to the diffusion process and is important to the understanding of both outdoor and indoor daytime and nighttime temperature/humidity swings. Since the

slopes of the curves shown in Figures 47 and 48 are almost identical, the rate of moisture flow into the container is unlikely to change when the container is used in different moisture vapor pressure environments. However, as shown by the plot of the solar radiation cycle and 60°C/90%RH cycle regression lines in Figure 48, the moisture gain rate, or said another way, the flow of moisture, into the container can be different at the same vapor pressure differential at different temperatures.

Note that these comments can only be used to predict long-term performance of 155mm Propelling Charge Containers using several assumptions. These assumptions are that the moisture permeation constants of the container do not change as the materials age, the container remains sealed during its lifetime, and that palletization of the container items does not affect MVTR.

4.9.2.2 M2A1 Small Ammo Container Data Analysis

Moisture gain, moisture gain rate and vapor pressure data for two long-term cycles are shown for the M2A1 container in Table 25. The approach used to analyze the 155mm Propelling Charge container described in the previous paragraph was also used for the M2A1 container. Table 26 contains the linear regression data used to prepare Figures 49 through 52.

The relation of moisture gain rate and vapor pressure differential seen in the figures for the two test conditions used to evaluate the M2A1 container is strikingly different than was found for the 155mm Propelling Charge container. The solar radiation cycle data shown in Figure 28 and the small slope for the regression line noted in Table 26 suggests the container lost moisture. However, the large error associated with the slope could be taken to suggest that the moisture gain rate remained constant during the solar radiation cycle. The MVTR for the 60°C/90%RH cycle however, was quite similar to the 155mm container under the same test conditions. The difference between the performance of the two container items is thus the difference in MVTR caused by effect of temperature on the moisture permeability and diffusion coefficients of the materials comprising the two container items.

The obvious, and thus primary, difference between the materials used for the containers is the pigmentation and filler scheme. The polyester resin used for the M2A1 container was glass fiber reinforced and highly filled. The filler used consisted of a green pigment and $CaCO_3$. The filler and glass fibers were noted to be exposed by the effects of erosion during environmental exposure testing during the sample scale testing. The pigment and glass fibers at the surface of the container also presented a large surface area for the absorption and desorption of moisture. Simplifying the interpretation of the data for the case of the M2A1 container would liken the glass fiber and filler to a wick.

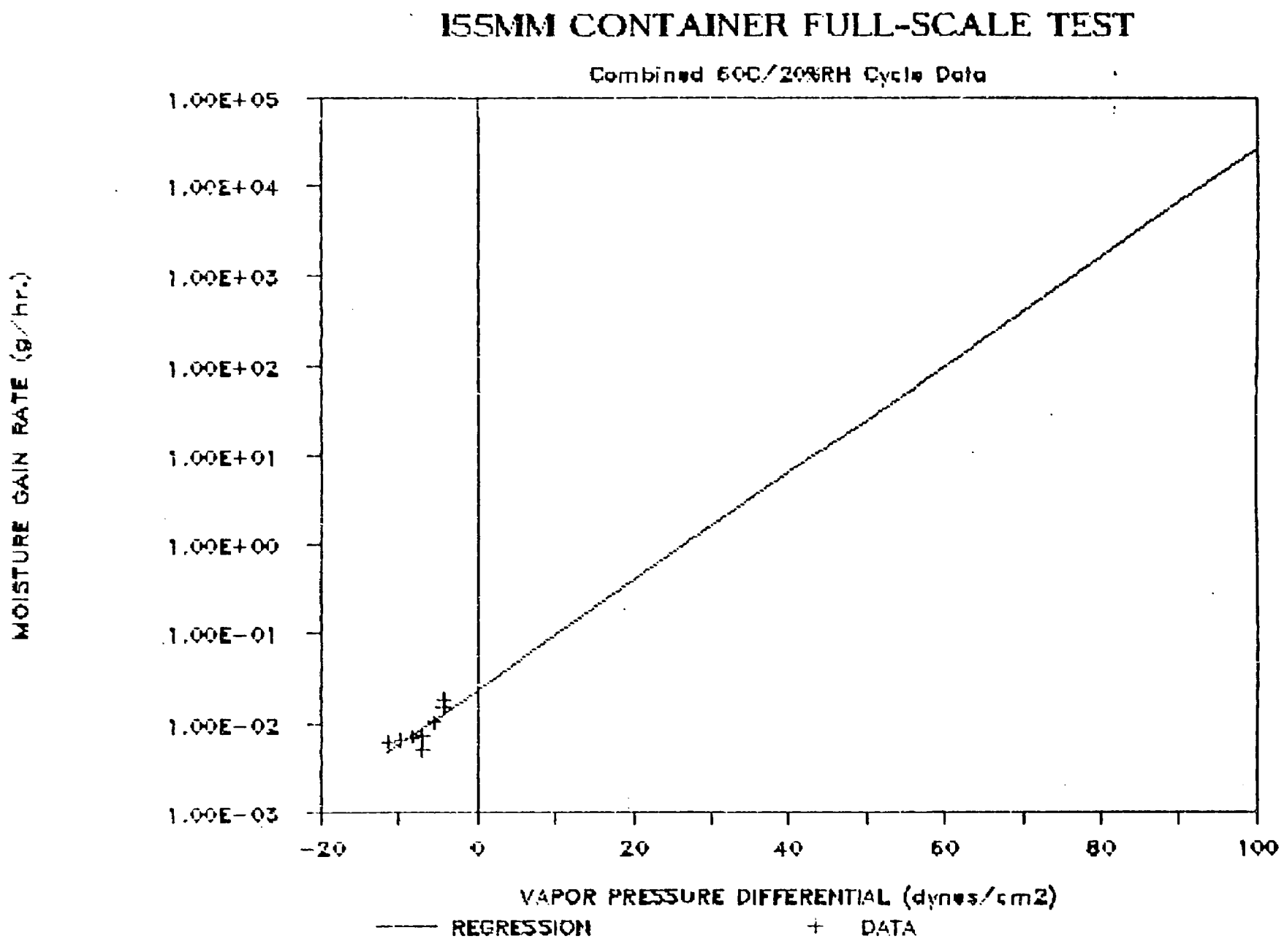

Figure 46: 60°C/20%RH Chamber Condition Data

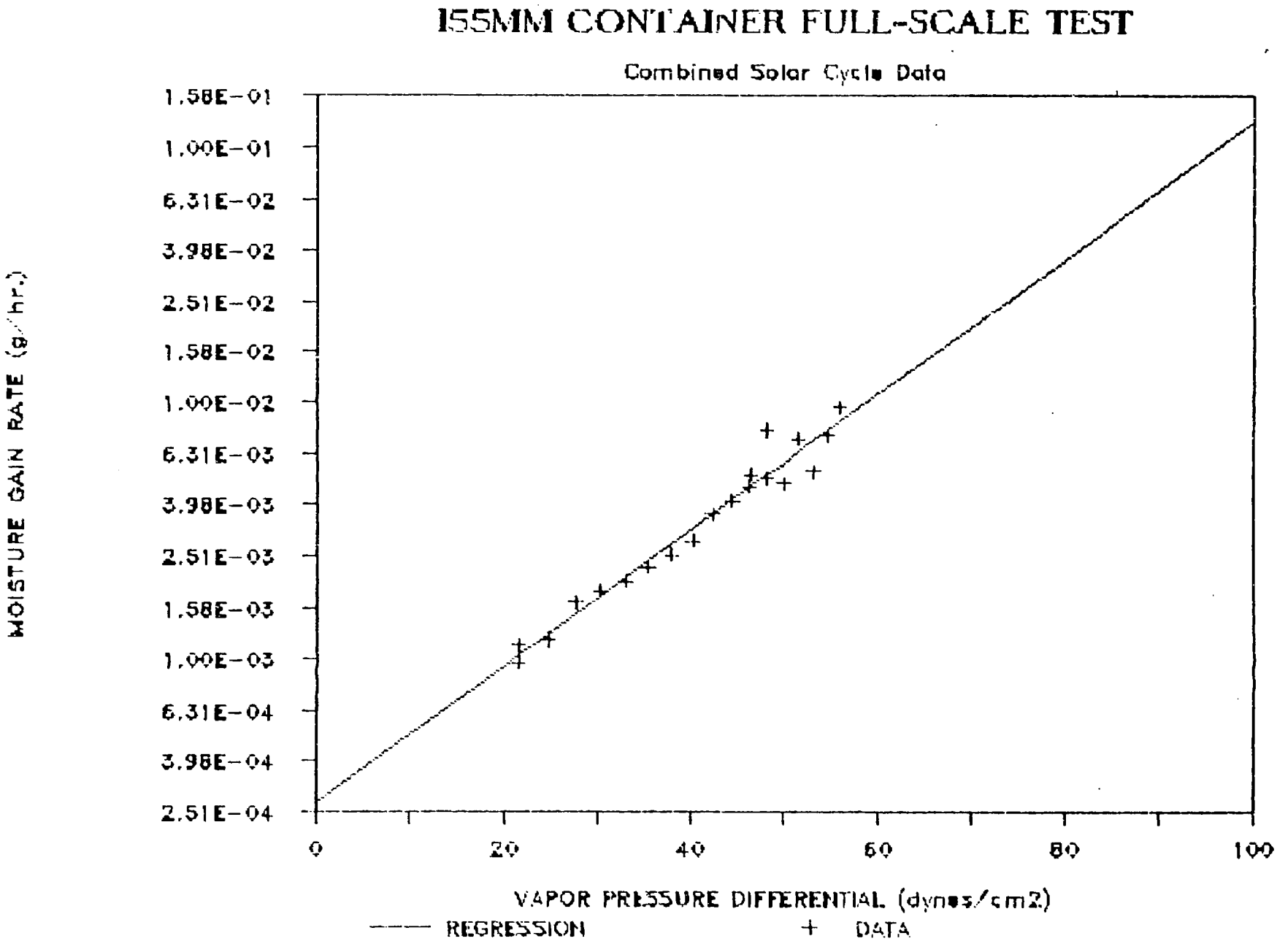

Figure 47: Solar Radiation Test Data

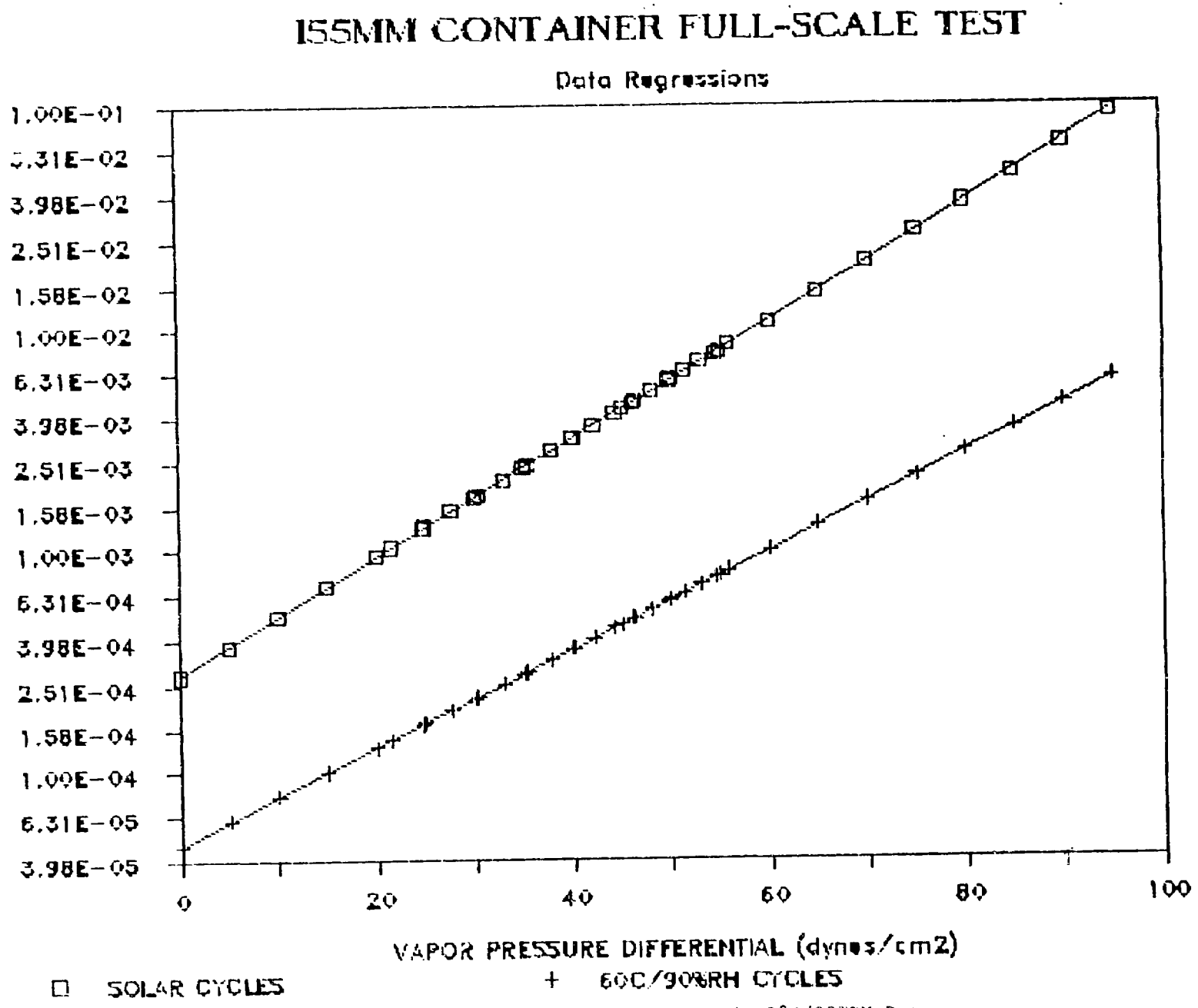

Figure 48: Regression Lines for Solar Cycle Data and 60°C/90%RH Data

Table 25
M2A1 Container Moisture Gain Data

TEST SEQUENCE	TIME	ELAPSED TIME(HRS)	CONTAINER MOISTURE (G)	CONTAINER MOISTURE GAIN RATE (G/HR.)	CHAMBER VAPOR PRESSURE (DYN/CM2)	CONTAINER VAPOR PRESSURE (DYN/CM2)	CHAMBER CONTAINER PRESSURE DIFFERENCE (DYN/CM2)
TRIAL #7	62	0	0.3069		165	62.8	102.2
DARK	63	1	0.3438	0.0369		70	95
60C/90%RH	64	2	0.3643	0.0287		73.8	91.2
	70	8	0.4085	0.0127125		82.1	82.9
	82	20	0.458	0.007555		91.1	73.9
	96	34	0.4849	0.0052352		95.9	69.1
	107	45	0.5132	0.0045844		101	64
	126	64	0.5432	0.0036921		106.3	58.7
	149	87	0.5749	0.0030804		111.8	53.2
	181	119	0.6084	0.0025336		117.5	47.5
	208	146	0.6438	0.0023075		123.5	41.5
	267.75	205.75	0.6813	0.0018196		129.8	35.2
SOLAR	301.75	0	0.7635		77.9	143.1	-65.2
RADIATION	381.75	80	0.6817	-0.001022		129.8	-51.9
48C/80RH	412.75	111	0.6442	-0.001074		123.5	-45.6
	444.75	143	0.6088	-0.001081		117.5	-39.6
	479.75	178	0.5752	-0.001057		111.8	-33.9
	531.75	230	0.5435	-0.000956		106.3	-28.4
	586.75	285	0.5135	-0.000877		100.1	-22.2
	636.75	335	0.4583	-0.000911		91.1	-13.2

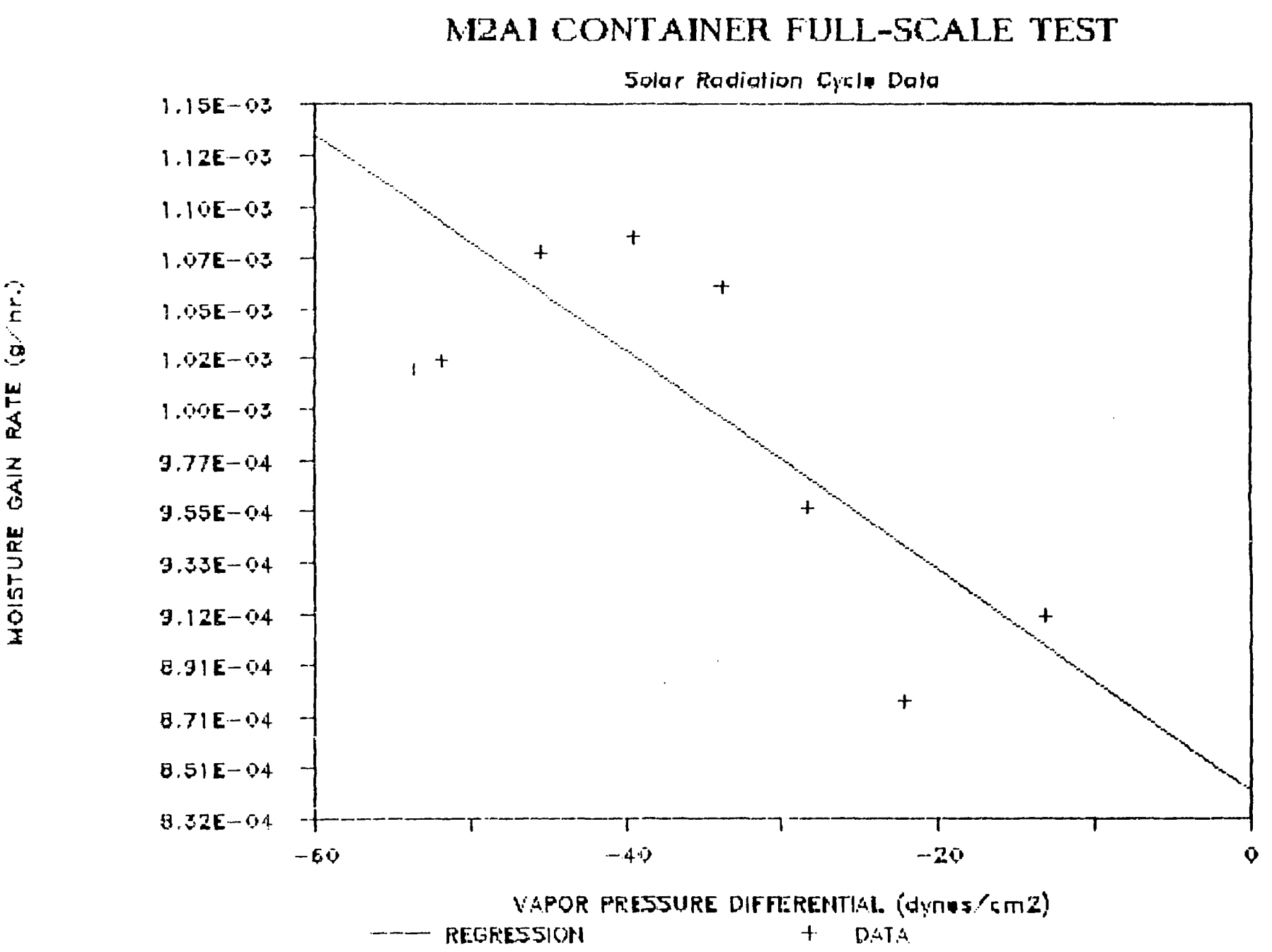

Figure 49: M2A1 ContainerSolar Cycle Data

During irradiation of the container the temperature increase caused by solar absorption mechanisms resulting in surface heating could be said to dry the container. The vapor pressure differential data in Table 25 and shown in Figure 49, is also negative; indicating an outflow of moisture. The solar radiation cycle was conducted subsequent to the 60°C/90%RH. This resulted in a substantial amount of moisture in the container at the start of the solar radiation cycle and accounts for the negative vapor pressure differential during the test.

The 60°C/90%RH data shown in Figure 50 shows moisture gain rate to increase with vapor pressure differential and by the slope and intercept of the regression in Table 26, MVTR for these conditions is approximately equal to the 155mm Propelling Charge container. A comparison of the two test conditions used for the M2A1 Container is shown in Figures 51 and 52. Figure 50 shows data regressions over the vapor pressure differential range occurring during the tests. Figure 52 shows the same regressions over the vapor pressure differential range used for the analysis of the 155mm Propelling Charge container. The decrease of moisture in the container during the solar radiation cycle suggests that the M2A1 container is quite permeable to moisture over a vapor pressure range caused by typical environmental test conditions. This is in contrast to the 155mm container where moisture gain continued to increase even when a negative vapor pressure differential occurred.

Table 26
M2A1 Container Graph Regression Information

SOLAR CYCLE REGRESSION
Regression Output:

Constant	-0.00093
Std Err of Y Est	0.000055
R Squared	0.619810
No. of Observations	7
Degrees of Freedom	5
X Coefficient(s)	0.000004
Std Err of Coef.	0.000001

60°C/90%RH CYCLE REGRESSION
Regression Output:

Constant	0.022[illegible]0
Std Err of Y Est	0.006701
R Squared	0.712920
No. of Observations	11
Degrees of Freedom	9
X Coefficient(s)	0.000505
Std Err of Coef.	0.000106

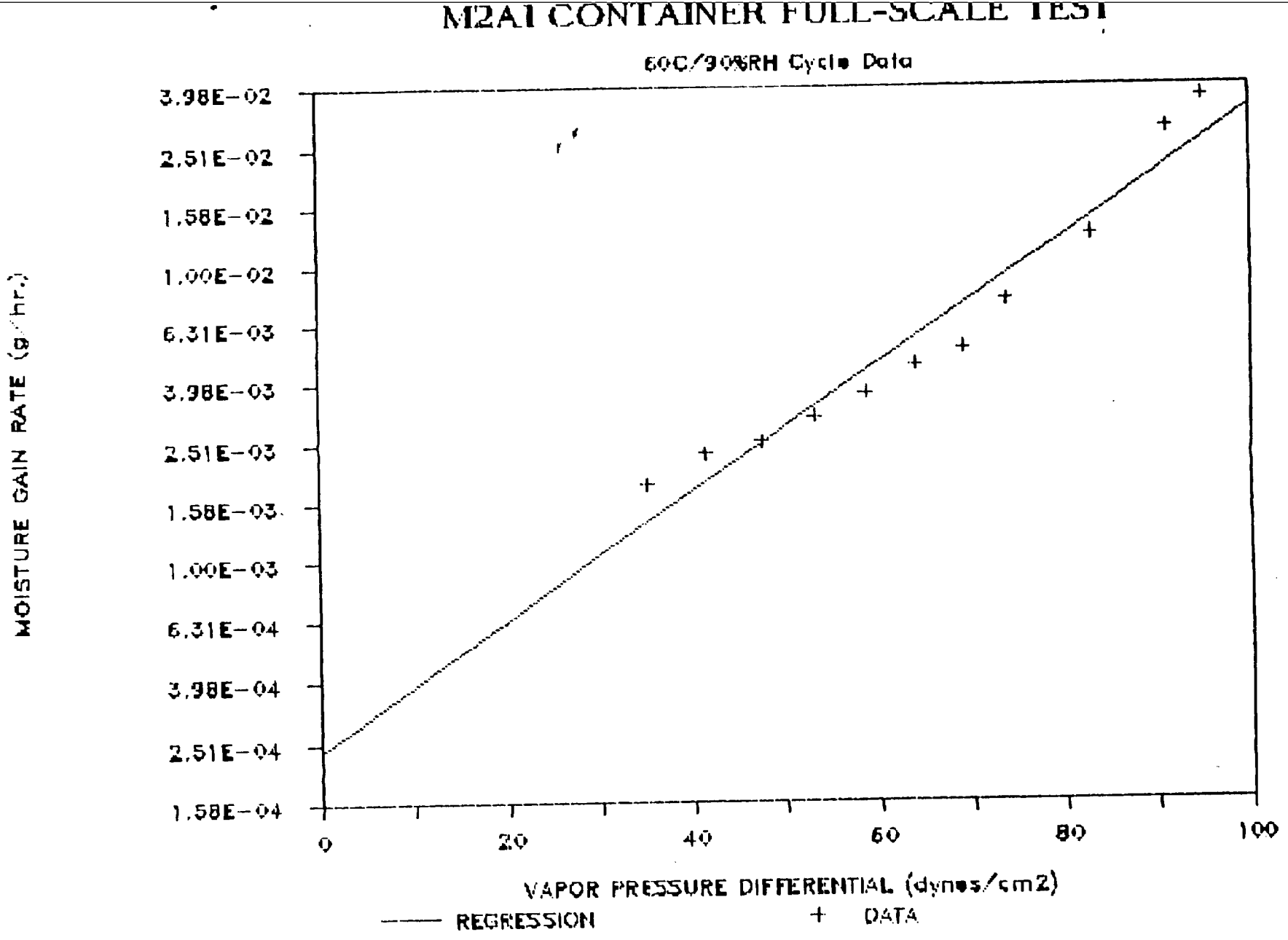

Figure 50: M2A1 Container Elevated Temperature/Humidity Data

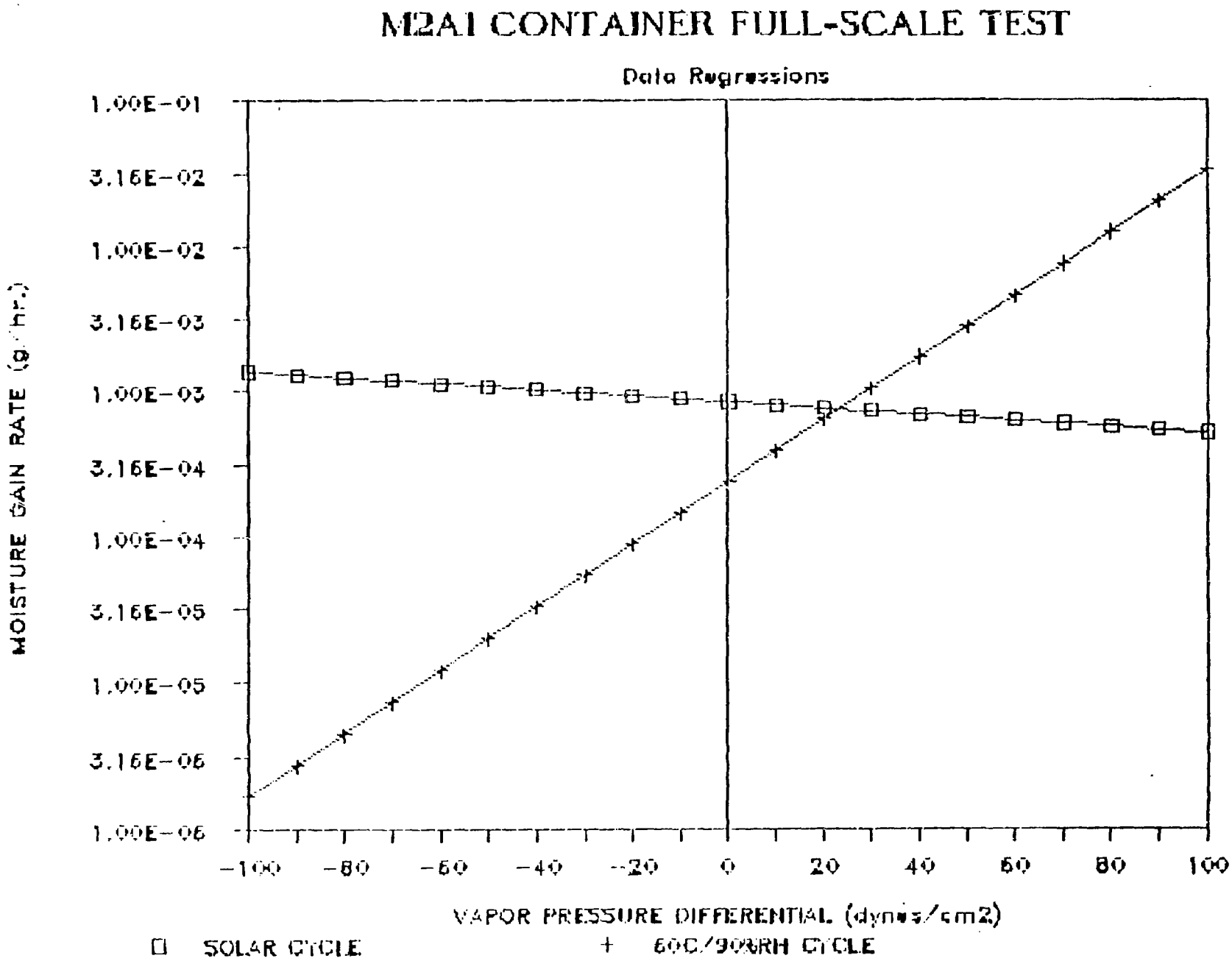

Figure 51: *Linear Regression Data Over Test Cycle Vapor Pressure Differential Range*

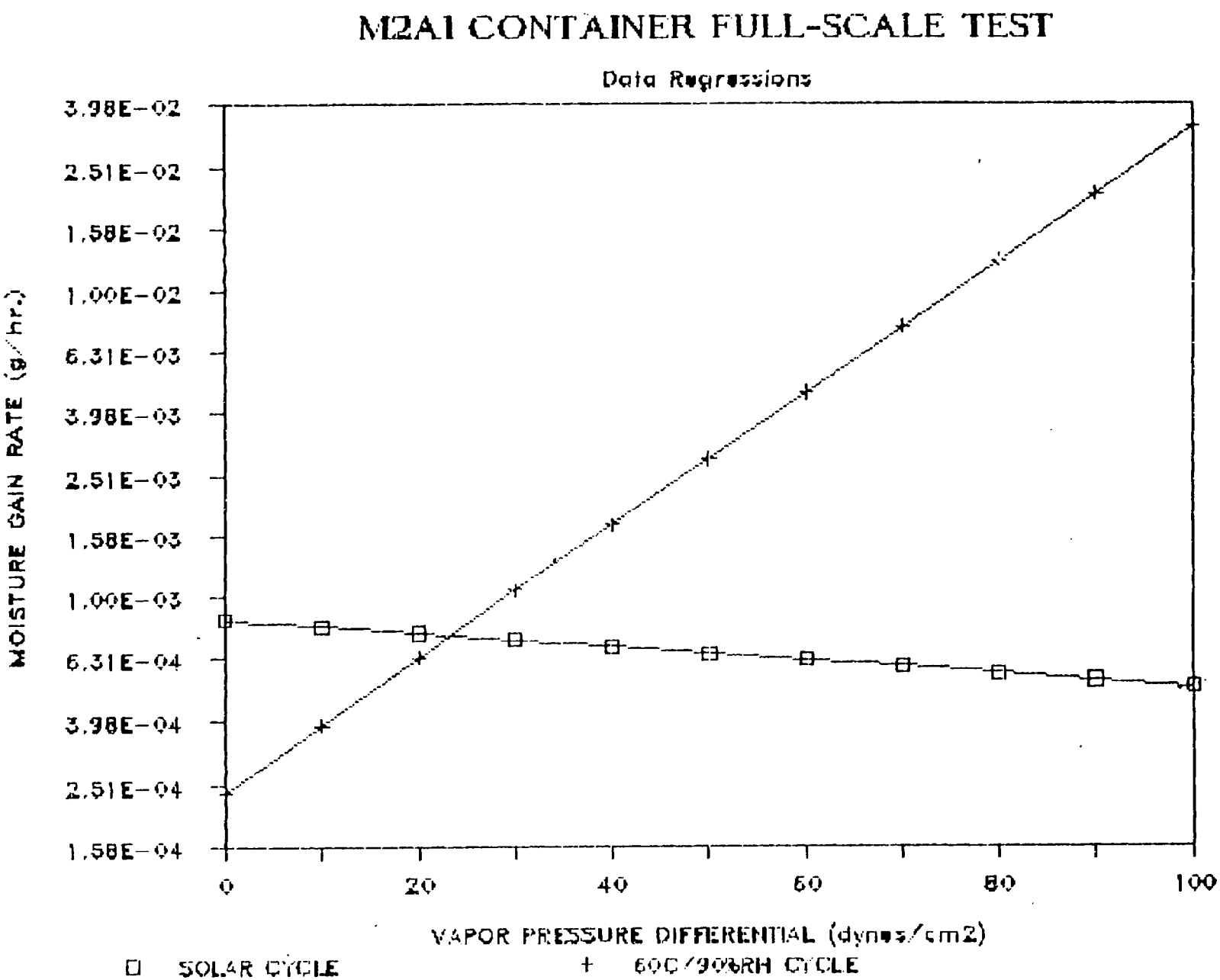

Figure 52: Linear Regression Data Over a Portion of the Vapor Pressure Differential Range

5.0 PERFORMANCE PREDICTION MODELS

5.1 Container Materials - General Discussion

The primary challenge to justifying the use of the two plastic materials studied during the project as ammunition packaging materials is the lack of performance requirements and data covering the required design life of the container items. Plastic materials, as with many engineering materials, are designed and formulated to meet particular specifications. Plastics, as raw materials, have and will change over a period of time in order to allow more efficient manufacturing processes and lower cost starting materials to be used to meet specification requirements. Testing of plastic materials and products manufactured from plastics must be ongoing over the production life of the manufactured goods in order to establish lot-to-lot and batch-to-batch differences and to ensure that the plastic materials used meet end use performance requirements. The requirement for plastic ammunition containers to function over a thirty-year period dictates that ageing tests be conducted on container materials prior to production as part of the container qualification program. This testing should also be conducted as part of container production acceptance testing on a lot-to-lot basis.

The fact that plastics are formulated to meet specifications that do not necessarily apply to their actual end use requires that performance property limits be established and that these properties be tested as a function of time. The establishment of an ongoing test program is critical to the successful use of plastics for items with a thirty-year lifetime requirement since unacceptable test results obtained after say ten or twenty years of ageing will identify problems for particular ammunition items before the end of their life cycle.

The project was faced with the problem of not having defined performance limits to which the test data as a function of exposure could be extended. Further, test sample materials, which could be used to obtain typical engineering property information during the course of the project, were not available. The significance and impact on the usefulness of the performance and lifetime prediction models presented are such that the models do not contain the degree of accuracy on which a major production program should be based and they cannot be used to meet the objective for a 10% certainty of performance over a thirty-year period without additional testing. However, they can be used to predict limits of probable acceptability for the materials tested, especially for the uncontrolled outdoor exposure period likely to occur during the container life cycle. The models, based on the actual degradation of the materials tested, can be used to predict the properties of these specific materials after being subjected to worst case conditions at the extreme conditions of the logistics chain. The extent to which this information can also be applied to the real use environment with any degree of certainty cannot be determined without further testing. However, the fact that the container materials and the full-scale items tested exhibited a measurable degree of failure after only a short

period of real-time exposure at a point early in their life cycle imposes a considerable doubt over the materials' appropriateness for ammunition packaging requiring a thirty-year certainty of performance capability.

The specific materials properties to be tested and the accelerated environmental conditions to be used, should be chosen on an individual basis for each specific material being considered for a particular application. The need for this approach is clearly seen by the test data presented in the preceding paragraphs for the two materials tested. The two materials are chemically and compositionally different and therefore reacted differently to the environmental tests conditions. The HDPE used for the 155mm Propelling Charge container was shown to be sensitive to ultraviolet both at the surface and in the bulk. The effects of the thermal and humidity environment, more typical of the indoor storage aspects of the logistics chain, were found to cause very different changes in the material. The degradation of the fiber reinforced polyester used for the M2A1 tended to limit itself at the surface during the time period over which the material and full-scale item were tested. The extent to which the surface would accelerate the degradation of the bulk of the material is unknown since the test data tended towards a plateau and the tests were ended before degradation could be measured in the bulk of the material. Obviously, these two materials, tested over equal time frames under similar conditions, react to the environment at different rates and therefore will require different accelerated test procedures to characterize their long-term performance characteristics.

This aspect of the design of an accelerated test program cannot be over stressed even in light of the U.S. Army's desire for a single test procedure for all plastics. Plastic materials are different "chemicals" and thus have different reaction kinetics and reaction rates. Plastics also are not homogeneous. They vary both in molecular weight distribution and compound formulation, although usually within standard manufacturing tolerances. These variations cause the lot-to-lot and batch-to-batch differences referred to. The effects of these variations must be well characterized.

The processing of plastic materials can also affect long-term performance. A trend of plastics production processing is to increase efficiency. The typical technique followed is to reduce cycle time or change processing temperatures. The net effect of this on the HDPE would be a change in the degree of crystallinity, while on the glass reinforced polyester a change in cross-link density. These properties, as shown by the data obtained during the project have a considerable effect on the rate of degradation. Indeed, the degradation rates observed during the project for the 155mm Propelling Charge container may have been quite different had the items had an annealing cycle or a controlled rate of cooling after the insertion of the fiberboard reinforcing tube component of the assembly. This in part could explain the significant differences noted in the DSC data between the elevated temperature testing conducted in a relatively low humidity environment and the elevated temperature/humidity testing. The crystallinity of HDPE is known to affect the fatigue resistance and thus, the

surface cracking observed after less than one year of outdoor exposure during this project since the degree of crystallinity affects b th the uptake in oxygen and fatigue resistance at the surface first and f llowed by the bulk (References 44 and 45).

5.1.1 155mm Propelling Charge Container HDPE

A feature of the measurement data, for virtually every property measured that was common to every test condition used, was the rate at which the property changed early in the tests being different from later stages of the tests. The test data presented in paragraph 4.0 exhibits the S-shape typical for the degradation of materials discussed in paragraph 2.0. The relative location of the end of the induction stage in this respect exhibited by the data, could be used as an indication of the relative degree of acceleration, especially since surface cracking occurred shortly after the end of the induction stage.

The general features of the trends shown by the data can be explained by the widely published effect of ultraviolet, temperature, moisture, and oxygen on polyethylene. Specifically, the data shows the effect of the uptake of oxygen. This feature of polyethylene is important to the design of an accelerated test and especially the interpretation of results since thickness, time at temperature, and ultraviolet flux and fluence all have a synergistic role in the degradation of the material.

The relationship of the crystalline phase to the amorphous phase of the polyethylene is the main factor which determines the properties of the polyethylene. The crystalline phase is inherently more stable to oxidation, however, the structural properties of the polymer rely on the amorphous region between crystallites. Therefore, an increase in crystallinity should not necessarily be interpreted as a positive indication since an increase in crystallinity generally results from either the crystallization of the amorphous region or by the decomposition of the amorphous region. The mechanism of surface cracking postulated for the ultraviolet exposure is therefore the decomposition of the amorphous region between crystallites. This postulation justified the subtraction of the effects of the crystalline component of the decomposition heat flow by the DSC measurements.

The rate of change in the decomposition heat flow property was found to be directly related to time at temperature for all of the exposure tests involving ultraviolet radiation, with the exception of the simulated solar radiation test. Interestingly for this test, the relationship did not hold for the data as a function of ultraviolet fluence. A possibility for this could relate to the crystallinity increasing and stabilizing the polyethylene at a rate greater than the decomposition of the amorphous region due to ultraviolet since the test being conducted at constant conditions and the possibility that the solar spectrum used, as described in Figure 3, may have been deficient in low wavelength ultraviolet. Further, the lack of surface cracking during the simulated solar test used

for sample materials and full-scale items is explained by the influence of water vapor on peroxide formation and the ultraviolet flux rate to hours of "daylight" which could, by the degradation mechanisms presented in equations 15 through 21, prevent further photoinduced degradation. This is possible since the container material was pigmented and especially thick compared to the sample materials reported on in literature.

These possibilities also explain in part why the at-latitude exposure heat flow degradation rates, conceivably conducted at lower temperatures, with respect to ultraviolet fluence were greater than the laboratory and EMMAQUA© exposure tests. The solar simulation test, although also having a high rate of increasing crystallinity had a slow rate of decomposition in the amorphous region. Further, none of the laboratory tests involved the temperature excursions in the surface or the bulk, which undoubtedly occurred during the real-time test.

The influence of even small temperature excursions as related to ultraviolet is seen by comparing the crystallization rates and decomposition rates of all tests involving ultraviolet. The Xenon and simulated solar tests were conducted using constant conditions. The Xenon radiation contained more low wavelength ultraviolet radiation than any of the other tests and thus would be expected to cause damage to the polymer at a greater rate than the other tests, especially on the basis of fluence. The fact that it did not shows the importance of time at temperature. Likewise, the EMMAQUA© test, with temperature excursions, did not produce the greatest rate of change on the basis of ultraviolet fluence although it also presented a high flux rate, or acceleration of ultraviolet radiation. The cause for the noted relationships being related to the uptake of oxygen are supported by discussions presented in References 44, 45, 50, and 51 and by noting the crystallization and decomposition rates for the elevated temperature tests conducted at ambient humidity conditions and the elevated temperature/humidity tests. The elevated temperature test exhibited the greater rate of change although in an opposite direction from the tests with ultraviolet radiation apparently due to the increase in crystallization resulting from the elevated temperature.

The apparent mechanism by which the "accelerated ultraviolet" tests did not produce acceleration of degradation in terms of ultraviolet fluence is the chemistry by which reactive species at the surface are quickly tied up and provide a protective barrier for the further reaction in the bulk of the material where thermal oxidative processes prevail. The change in physical properties at the surface resulting from changes in crystallinity thus could account for the occurrence of the surface cracks. This is shown by the DSC data in Table 14. However, the limiting values of the DSC data related to the occurrence of cracking obtained from the measurement samples taken from the surface as compared to the bulk suggest a failure point for engineering properties such as tensile and impact resistance. This property therefore provided the basis for the lifetime prediction analyses described in subsequent paragraphs and exhibited in Appendix D.

The influence of temperature excursions can be explained by the consideration of the creep properties of the material with regard to time/temperature superpositioning principles as derived from the W-L-F and Arrhenius equations as discussed in paragraph 2.4.1. The fatigue behavior of semi-crystalline polymers, such as polyethylene, depends on thermal history. Crack propagation depends not only on annealing temperature, but on the amorphous region containing tie molecules between crystallites. Thus, the choice of an accelerated test which does not affect the crystallinity of the polymer at a rate proportional to the rate that the real environment affects the amorphous region, cannot accelerate effects in a way that can be modelled.

One conclusion that can be made from the results of the project for the 155mm Propelling Charge container, and very probably for polyolefins in general, which is suggested in the cited references that describe the thickness of the samples used for other investigations, is that thickness must be included as a variable in the test matrix to determine the effects of the environment and accelerated testing on structural properties, including structural properties dependent on or originating at the surface.

The fact that surface cracking occurred very close to the end of the heat flow and color data induction periods which could be related to a bulk phenomenon complicates the development of a lifetime prediction model based on accelerated test data. It suggests that accurate lifetime prediction models should be based on real-time exposure tests conducted over a temperature regime covering the range of the logistics chain. Accelerated tests could be conducted concurrent with real-time tests for purposes of qualification and acceptance purposes for new materials and processes, however.

5.1.2 M2A1 Small Ammo Container Material

The thermal analysis data for the 155mm Propelling Charge container material was related to cracking, and thus brittleness, by associating the change in a property with the cracking phenomenon. The end of the induction period for this material was seen graphically in both thermal analysis data and colorimetric data and was applied to bulk properties. This analysis could not be applied to the M2A1 container material since, as shown in Table 15 and Figures 16 through 19, the properties that could be related to a physical property were not found to reach the end of the induction period. As noted in the discussion of the exposure tests with solar or simulated solar radiation in paragraph 4.0, fiber blooming was a main feature of the degradation of the material. The thermal analysis data suggests that this degradation was limited to the surface of the container and the container test samples. The extent to which these surface property changes can be related to the important functional properties of strength and impact resistance is not known. However, it is quite clear that in less than one year of outdoor exposure the M2A1 container exhibited a measurable degree of change. This information can be used to base further testing to determine

the effect of the observed changes on strength properties and on moisture vapor transmission rate properties. Performance prediction models could not be prepared for the M2A1 container material with the limited data available.

The container handle material was found to be sensitive to ultraviolet in outdoor and accelerated tests. The handle material was not subjected to the measurements described for the container materials but is a result of the exposure testing the handle material was so badly cracked that it is unlikely that the handle could function after even a short outdoor exposure. The metal hinge pins and pins used to retain the handle were also seen to exhibit slight corrosion.

5.2 155mm Propelling Charge Container Material Performance Prediction Model

The discussion of durability in paragraph 2.5 showed the temperature dependence of a property change for a material to be related to its activation energy. The mathematical treatment of property change as a function of temperature in paragraph 2.5 suggests that the activation energies for photodegradation will be lower than the activation energy for thermal degradation. Activation energies for thermal degradation processes are available in literature for many materials however, activation energies for photodegradation are limited to a few materials and are not widely published. A possible reason for this relates to the approaches typically taken to model degradation as a function of exposure testing.

Gross properties, such as engineering or appearance properties, are measured during typical exposure test programs. These properties are often dependent on many measurement parameters, especially the rate of testing for engineering properties, as well as the influence of the surface properties on bulk properties. Typical test programs generally do not account for surface and bulk property changes and only rarely consider thickness effects. The results of these test programs therefore have limited applicability to the prediction of performance for the material tested since the combination of the degree of degradation at the surface, the thickness of the material and the thermal history of the material affect the overall rate of degradation of performance as they relate to these properties. Thus, even if the test is carried through the saturation phase the rate of degradation could depend on the mechanism by which the material reached the rate controlling phase. In order to obtain an accurate rate and thus activation energy from experimental data using gross property measurements requires an extensive investigation of the effects of environmental factors on these properties. These environmental factors include time of year for outdoor exposures and time at temperature for indoor exposures.

Similar statements concerning thermal analysis data could be made. It is interesting however, to note that the relationship of the crystallinity to the amorphous region in a general sense explains the trends exhibited by the DSC data for the 155mm Propelling Charge container. The outdoor and accelerated ultraviolet tests suggest the relationship is more dependent on

time at temperature than on ultraviolet fluence while the temperature/humidity and elevated temperature test results indicate that moisture affected the rate of property change more than temperature. Thus, the use of DSC techniques allowed the study of the effects of different environments on the HDPE and how these environments affected polymer structure in reaching the rate controlling phase. Had the exposure tests been carried through the rate controlling phase, differences in rate could then be explained in terms of changes in the polymer structure rather than variation in the environment.

Fortuitously, the DSC measurements conducted on the HDPE correlated a material structural property with a measurement property, both thermal and photoactivation energies for HDPE were found in literature, the exposure tests were conducted at different temperatures, and a structural property failure which could be measured at the surface and in the bulk was found to occur near the end of the induction phase. This combination of results and events allowed a performance prediction modelling scheme to be developed which, although not as straight forward as the scheme described in paragraph 2.5 and therefore perhaps novel, resulted in a prediction of the range of time and the range of temperatures over which the 155mm Propelling Charge container material is expected to have a viable life.

The approach taken to prepare the performance prediction models, exhibited in Appendix D, involved studying the effects of apparent activation energy over the temperature range representative of the logistics chain on the Arrhenius relationships presented in paragraph 2.5. The results of this analysis, which used the rates of degradation determined experimentally during the project, allowed the determination of a range of time over which the HDPE material used for the 155mm Propelling Charge container would be expected to retain structural properties when stored outdoors or indoors in several different environments. The failure or endpoint used for the models was based on the adjusted heat flow values discussed previously and is interpreted to indicate the point at which the container material would be expected to easily crack well into the bulk of the material.

Equations 26 and 27 were used to calculate property values as a function of time or ultraviolet fluence for the plots shown in Appendix D.

$$k_1 = k_0 \frac{e^{-E_a/RT_1}}{e^{-E_a/RT_0}} \qquad (26)$$

$$P_1 = P_0 - k_1 \cdot t \qquad (27)$$

Table 27
Activation Energy Values Used
for
155mm Propelling Charge Container Performance Prediction Models

Activation Energy (CAL/MOLE)	Type	Source of Value	Comment
4633.1	Photo	Experimental Data	-
7000	Photo	Reference 41	-
9500	Photo	Arbitrary Value	Value used to test effect of Activation Energy on Model
12000	Thermal	Arbitrary Value	Value used to test effect of Activation Energy on Model
26000	Thermal	Reference 19	-

Tabl 28
155mm Propelling Charge Container Material
Performance Prediction Model Summary

Indoor Storage Environment

Conditions	Model Activation Energy (CAL/MOLE)	Environmental Temperature Range (°C)	Lifetime Prediction
Dry	12000	0 - 30	Greater than 34 years
	26000	0 - 30	Greater than 34 years
Humid	12000	0 - 30	17 to 34 years
	26000	0 - 30	Greater than 34 years
		Outdoor Storage	
-	4633.1	20 - 60	1 to 2 years (300 to 800 MJ/m^2 ultraviolet)
-	7000	20 - 60	1 to 4 years (300 to 1200 MJ/m^2 ultraviolet)
-	9500	20 - 60	1 to 5 years (300 to 1700 MJ/m^2 ultraviolet)

In equation 26, k_1 is the rate of change at temperature T_1, E_a is the apparent activation energy, R is the gas constant, and k_0 is the rate of change at T_0. P_1 is the calculated property value at T_1 in equation 27, determined from linear regressions of measurement data obtained during the project and may be found in Tables 12 and 13. The origins of the activation energy values used are shown in Table 27. The temperature values used to prepare the models covered the range of temperatures expected to occur in the logistics chain. A summary of the performance prediction models for a number of generalized storage conditions is shown in Table 28.

5.3 Container Moisture Gain

5.3.1 155mm Propelling Charge Container

The effect of moisture gain on the functional lifetime of the 155mm Propelling Charge container cannot be determined until the unacceptable limit of moisture inside the container is determined. The test data obtained during the project indicate that the unpalletized 155mm Propelling Charge container retains its seal. However, when outside vapor pressure conditions exceed the vapor pressure at the time of loading, for example when stored in a tropical environment, there will be a net increase in moisture inside the container. This is especially true during daytime periods when the vapor pressure of the storage environment is likely to exceed the vapor pressure inside the container in many geographic locations in the logistics chain. The integrity of the container seal and the wall thickness of the container also contributed to the net increase of moisture as shown by the tests having low outside vapor pressure. The results of these tests indicated that the container walls continued to desorb moisture into the container with time.

As reported in Reference 46, the 155mm Propelling Charge container test item was sealed under conditions of 20°C/50%RH or at a vapor pressure of approximately 7.5 dynes/cm^2. The solar cycle test conditions used a vapor pressure outside the container of approximately 81 dynes/cm^2 while the vapor pressure during the 60°C/90%RH cycle was approximately 166 dynes/cm^2. The moisture gain rates shown in Table 24 show that the container gained moisture during the 60°C/90%RH cycle at a rate approximately two times greater than during the solar cycles. Comparison of these data to the 60°C/20%RH cycle where the outside vapor pressure was determined to be 16.9 dynes/cm^2 shows the driving effect of temperature on moisture gain by desorption.

Thus, one conclusion to be made for the 155mm Propelling Charge container is that the moisture content will tend to increase with time in both temperate and humid environments where the moisture vapor pressure environment is greater than at the load plant environment. Daytime and nighttime temperature and humidity swings in temperate and humid environments would obviously tend to slow down the moisture gain rate, however the test data suggest that even under real conditions there will be a net gain.

The extent to which the moisture gain rate can be modelled will depend on obtaining more detailed temperature and humidity data for the indoor storage environments. The logistics chain study indicated that the storage bunkers were not specifically controlled. This suggests that there would be daytime and nighttime temperature and humidity swings but not as great as in the outdoor environment.

The 60°C/90%RH test conditions used represented the extreme of the logistics chain environment. As a constant condition test it also indicates the limit to which elevated temperature/humidity tests for the evaluation of the effects of moisture can realistically be accelerated. The degree of acceleration could be determined by the change in moisture gain rate resulting at lower outside moisture vapor pressures and applied to a prediction model by quantifying the daytime and nighttime changes in moisture vapor pressure on a time basis to adjust the moisture gain in the container.

5.3.2 M2A1 Small Ammo Container

The effect of moisture gain on the functional lifetime of the M2A1 container also cannot be determined until after an allowable limit of moisture inside the container has been established. The test data obtained for the M2A1 container indicates that it is less well-sealed than the 155mm Propelling Charge container but because of this the container might not exhibit an overall net gain of moisture, especially during outdoor exposure in low humidity environments. This is seen by the moisture gain rate data in Table 26 where the rate of moisture gain during the solar cycle was two orders of magnitude slower than during the high humidity test.

The modelling concept discussed for the 155mm Propelling Charge container could be applied to the M2A1 container. However, the results of the testing and the degree of acceleration must be interpreted differently in view of the significant difference in moisture gain rate between high and low moisture vapor pressure regimes. The contents of the M2A1 container are likely to experience a cyclic humidity environment in both hot, dry, and temperate environments. Under the conditions presented by the container in these environments, the contents would be subjected to the effects of absorption and desorption of moisture.

The degree of acceleration for the M2A1 container would result from test conditions which would allow the contents of the container to be subjected to these absorption and desorption effects. This is in direct contrast to the 155mm container where a constant condition test apparently would produce the greatest acceleration. The specific test conditions which would produce acceleration for the M2A1 container were not established during the project. The conditions most likely to produce realistic acceleration, as suggested by the test data available, would involve a cyclic test which would allow the container to desorb moisture during a low vapor pressure cycle. As seen from the test data presented in Reference 46 each leg of the test cycle could be as long as several hundred hours.

6.0 SUMMARY AND CONCLUSIONS

6.1 Summary

The objective of the work reported was to develop a test methodology based on ammunition packaging container logistics which would result in accurate life cycle performance models for plastic ammunition packaging. Ideally, the methodology would involve a single series of tests which would be applicable to all plastic packaging materials and full-scale container items. The HDPE 155mm Propelling Charge container and the glass reinforced polyester M2A1 Small Ammo container were used during the project to study the performance of materials and the respective container items during accelerated and real-time environmental tests. The test procedures used during the course of the project focused on Mil-Std and commercially accepted practices which are generally used for products with shorter life cycles. These procedures are based on years of experience and thus serve as a basis for developing the methodology needed to extend test results to thirty-year time frames. The analytical portion of the work effort addressed identifying the areas of current state-of-the-art testing methodology that require change in order to develop long-term performance models.

A variety of materials property measurement techniques were also evaluated during the course of the project. These techniques included thermal property, engineering property, and optical property measurement procedures. The measurement data quantified property changes resulting from environmental exposure testing and were used to prepare performance prediction models. The sensitivity of the thermal analysis and optical properties measurements provided data which could be modelled even after short term testing. The tensile and elongation tests conducted on Marlex CL-100 HDPE showed that although these properties changed, the environmental tests were not conducted long enough to derive a meaningful model by itself. However, in combination the results of the project show that specific materials' characteristics and specific container designs must be used to determine the detailed test procedures to be followed in order to develop performance prediction models. The results further show that it is unlikely that one series of tests and one material property can be used to prepare models. These conclusions are made by comparing in a relative sense, the performance of the 155mm Propelling Charge container HDPE, the Marlex CL-100 HDPE, and the glass reinforced polyester in the M2A1 container. Both the Marlex CL-100 and the 155mm Propelling Charge container polyethylene became embrittled during the testing as evidenced by the changes in strength and elongation for the Marlex CL-100 and by the decrease in the amorphous nature of the 155mm Propelling Charge container material. The M2A1 container material exhibited significant changes in appearance during the testing but changes related to changes in structural performance were not measurable.

The results of the moisture vapor transmission rate testing of the two container items also supports the conclusion that a single series of tests for all container items is not appropriate for the final test plan. The characteristics of the 155mm Propelling Charge container suggest moisture

will slowly be gained over long periods of time whereas the M2A1 container will gain and lose moisture depending on the environment. The test procedures used to evaluate these different characteristics necessitate different environmental test procedures in order to quantify the effects on the ammunition items.

The specific accomplishment of the project resides in forming the basis for the Volume II Test Plan by providing specific examples of the use environmental test data to prepare performance prediction models. The data obtained and the resulting analyses for the two container items tested also serve as the basis for continued testing for these items. The results of the project suggest that a test plan, in a generic sense, is feasible. However, the actual test procedures followed, the specific properties measured and the analysis of test data must be on a materials specific and container item specific basis. The results of this project show that it is unlikely that a single test or series of tests will result in sufficient data to develop life cycle prediction models covering a thirty-year period.

6.2 155mm Propelling Charge Container

The results of the 155mm Propelling Charge container material tests indicate that the HDPE used for the container will not meet the requirements for a two-year uncontrolled outdoor exposure in extreme desert and tropic environments. This is due to the sensitivity of the material to ultraviolet radiation at high temperatures. The extent to which the wall thickness of the container would provide adequate protection from physical abuse such as impact or palletization loads was not measured directly. However, the performance prediction model used was based on the rate of a property change measured in the bulk as a function of exposure testing which showed a clear relationship to the cracking phenomenon at the surface. The results of tests without solar radiation indicate that the HDPE material is more sensitive to hot and humid environments than to hot and dry environments.

The performance prediction models prepared for the material were derived by applying the Arrhenius equation to the measured rate of a property change at temperatures representative of the logistics chain. The activation energy of the HDPE used to prepare the model for the 155mm Propelling Charge container was not specifically determined during the course of the project. However, several activation energies, taken from literature and derived from experimental data by analysis, were used to evaluate the effect of this property on the model. The range of activation energies used showed little effect on the predicted lifetime for temperatures at the high temperature end of the logistics chain environment involving outdoor exposure. The study showed that the lifetime of the container material was also not greatly affected by the activation energy value for dry indoor climates but did show an effect for hot humid indoor environments.

The expected lifetime of the container material in the outdoor environment was predicted to range between one and five years in temperate and hot climates. The lifetime of the container material stored indoors was

predicted to be greater than 34 years in dry climates and in a range between 17 and 34 years in humid climates. These predictions do not include the effects of palletization loads, the long-term effects of typical temperature swings on palletized containers or the effects of maintenance and transportation environments, all of which could shorten the life of the container. The performance predictions for the container material also do not include the long-term ageing effects of the seal.

The accuracy of the predictions cannot be established at this time since the activation energies related to photodegradation and thermal degradation of the material were not actually determined. The range of activation energies used to test the models however, does lend a degree of confidence in the resulting predictions from the standpoint that the models predict the failure of the material in less than one year of real-time outdoor exposure and is supported by test data. Further, the models were based on test data obtained in a temperature range representative of the end use environment. This also would tend to minimize error. A discussion of the effects of errors in activation energy on scaled temperature tests is given in Reference 18. This analysis showed that the greater the difference between the service temperature and the accelerated test temperature, the more accurate activation energy had to be in order to produce reliable lifetime predictions. A small difference in temperatures between real and accelerated conditions would require that the activation energy be determined to within 300 calories per mole in order to determine a rate with a 10% error.

The tests conducted on the models used activation energies different by several thousand calories per mole. Large differences in activation energy over the logistics chain temperature range did not cause a major change in the predicted lifetime at least in respect to the design life requirements for a two-year uncontrolled outdoor storage and a thirty-year service life. The accuracy of the models presented therefore depend greatly on the degradation rates measured for the HDPE being representative for the material and manufacturing process parameters used.

The test samples used during the project were taken from two containers. However, test data was obtained with a reasonable variance. Thermal analysis measurements did show that the thermal history of the material could affect results. This aspect of the test results being related to the degradation rate causes one of the two areas of concern in using the models.

The possibility for a different thermal history for container items even in the same lot of items relates to the size and mass of the container. Different cool down rates after molding could occur as a result of plant environment or handling after the molding cycle. Palletized containers could be insulated by items on the outside of the pallet and thus be subjected to a different thermal profile and as suggested in Reference 44 cause creep and fatigue failure to occur at different rates.

The second area of concern involves the extrapolation of materials property data in the induction phase to a poorly characterized point in the

rate controlling phase. This was required primarily for the tests without solar radiation and relates specifically to the short duration of the tests. The measurement data was concentrated in the induction phase where, because of the action of stabilizers, test data are often scattered. Further, degradation rates were determined using linear regression through the induction phase.

The moisture vapor transmission rate testing cannot be related to a lifetime prediction model at this time because an acceptable limit for the amount of moisture inside the container is not available. Test procedures have been established which resulted in moisture gain rate as a function of vapor pressure differential. This rate could be used to prepare a model which would predict the amount of water inside the container with respect to time in a specific moisture vapor pressure environment.

Caution should also be used when applying the results of the moisture gain data to a prediction model. Only one container item was tested. Further, the effects of container age, the torque used to seal the cap and effects of moisture brought into the container by the contents were not investigated. Therefore the extent to which the data obtained is actually representative of the container design has not been established.

6.3 M2A1 Small Ammo Container

The approach taken to determine the functional lifetime of the fiberglass reinforced polyester material used for the M2A1 container focused on measuring changes in the glass, filler, and polymer content of the material as a function of the exposure testing. The results of this testing were inconclusive in that little measurable change occurred over the duration of the tests conducted. A performance prediction model could not be developed using the data available.

The mode of degradation resulting after less than one year of outdoor desert exposure was typical for fiber reinforced composites. The effect of the noted surface degradation on the ability of the container to provide protection to its contents was not tested. The results of the tests do give the conditions and time frame required on which to base further accelerated testing however.

The results also show that the container handle material is not environmentally stable. Since the container handle is directly related to the function of the container and it is directly exposed to the environment it should be included in any future testing.

6.4 Container Test Plan

The data and analysis contained in this volume have been used as the basis for the container test plan described in Volume II. The test plan is applicable to plastic ammunition packaging containers from the concept

stage through production and addresses materials issues as well as functional properties. Foremost to the success of the test plan will be the definition of the limits of acceptability in regards to material properties and the function of the container design. These definitions were not available during this project and therefore hindered the success of the project if only by making the significance of the results difficult to judge.

The modes of degradation and the degree of degradation recognized for the 155mm Propelling Charge container and the M2A1 container in less than one year of realtime exposure testing clearly suggests that the containers and container materials be subjected to additional testing before they are used for production items. The status of the testing of these two containers will be summarized with suggestions for additional testing in the following paragraph.

The performance of the container materials during the project shows that realtime outdoor testing is a viable and low cost means to screen materials for suitability in ammunition container packaging applications. An ongoing realtime test program integrated with a materials qualification program for packaging materials intended for longterm use should be considered. Using this approach a materials database would be developed which could serve as a materials selection guide and as a reference for evaluating accelerated test results. Container manufacturers would be required to select materials from a qualified materials listing and submit test and evaluation sample materials prior to production or changing formulations for production use. A similar approach could be used for changes in manufacturing processes and conditions.

The accelerated test results reported showed two areas that must be addressed by the test plan. First, typical Mil-Std-810 and state-of-the-art accelerated tests do not necessarily accelerate effects which can be modelled to a realtime base. This is particularly true for Mil-Std-810 testing which generally cover less than one month of realtime even when conducted 24 hours per day. The potential for misleading data are seen by comparing the results of the laboratory accelerated tests conducted on the HDPE materials, which were found to exhibit a failure near the end of the induction period, to the realtime outdoor tests.

The second area to be addressed by the test plan is the selection of appropriate test conditions and measurement techniques. The importance of this area is seen by comparing the performance of the HDPE and the reinforced polyester materials. Both materials exhibited a visual change as a result of several of the exposure tests which intuitively suggest that the functional performance of both materials was detrimentally affected by the exposure testing. The degradation of M2A1 container material could not be measured and related to a structural property change for the duration of the tests conducted. This implies that either the wrong measurement technique was used or that the material was degrading at a slower rate than the HDPE under the same conditions. In this latter case accelerated testing of the M2A1 container material must use different accelerated test conditions or be subjected to a longer test in order to model performance.

Further, since the test data, normalized to a time at temperature scale or to an ultraviolet fluence scale, showed promise for the development of performance prediction models, it is likely that the use of typical temperature/hu[illegible] cycle tests would have caused less degradation than the constant con[illegible]ests used. This conclusion is made since the test items would not have [illegible]nt as long a period of time at maximum temperature in a cyclic test.

Materials degradation is often related to diffusion processes. In order to obtain the required accuracy for the lifetime and performance prediction models resulting from accelerated tests, the tests must be conducted near the service temperature. This requires a tradeoff of test time, or acceleration, for accuracy. This is particularly important for materials, such as HDPE, used in a thick cross section.

This same test philosophy relates to functional testing such as moisture vapor transmission. The study of the logistics chain environment shows a broad range of conditions which are characterized by average features of temperature, moisture, and solar radiation. The response of materials and items to a range of conditions over a long period of time results in a range of performance levels dependent on the conditions that actually occur. Thus, a sampling plan to provide a statistical base for performance prediction over the range of environments must also be developed.

6.5 155mm Propelling Charge Container and M2A1 Small Ammo Container Test Status

6.5.1 155mm Propelling Charge Container

Test procedures and performance prediction models were developed for the 155mm Propelling Charge container material and for the container item. The material performance model covered a range of environments and was extended over a thirty-year period. By nature of the fact that only several containers were tested and material performance was evaluated over a short period of time, the accuracy of the models cannot be determined. Further, no limits of acceptability for container material performance or moisture gain have been established. Therefore the true end-of-life cannot be identified from the models.

These shortcomings provide the starting point for improving confidence in the test approach and the models developed. Obviously many more containers must be tested to confirm the models and to quantify inherent performance variability. The results of this project suggest that testing could be accomplished in a relatively short period of time which would prove the models for the extreme environments of the logistics chain.

Concurrent with this recommended additional effort is the definition of performance limits. The material performance models could be

proven using test items subjected to the recommended additional tests. Moisture gain acceptability could be established by testing the metal containers currently in production.

The approach taken during this project used actual container items as test specimens and applied test results to the Arrhenius equation. In order to determine the effect of manufacturing processes and thermal history on the performance models, the activation energies of the container material must be accurately determined. Concurrent with this effort should be the evaluation of engineering properties such as impact resistance and tensile strength.

The weight of loaded containers and the palletization scheme intended for the containers suggests the long-term effects of the seal on the container material should also be studied.

6.5.2 M2A1 Small Ammo Container

The M2A1 container and container material were subjected to the same exposure test procedures used to evaluate the 155mm Propelling Charge container. As noted previously, a modelable degradation could not be measured. The nature of the degradation however, could adversely affect both strength and moisture vapor transmission properties. Thus, the test status for the M2A1 container and its materials is less advanced than for the 155mm Propelling Charge container.

The starting point for further testing of the M2A1 container would be to determine the effect of surface degradation on structural properties such as impact resistance. If it can be shown that the container retains functional integrity even with a considerable degree of fiber bloom, then additional test efforts should involve conducting longer duration tests in order to reach the rate controlling stage of the material's degradation. The other additional tests and comments described in paragraph 6.4.1 for the 155mm Propelling Charge Container also apply to the M2A1 container.

(THIS PAGE LEFT BLANK)

7.0 REFERENCES

1. Wernstedt, F.L., World Climatic Data. Climatic Data Press, 1972.

2. Pearce, E.A. and Smith, C.G., World Weather Guide. New York Times Book Co., 1984.

3. Korean Energy Research Center. "Present Analysis of the Sunlight Energy Sources of Korea." Report No. KE-84-21, Volume II, 1984.

4. Palz, W. ed., European Solar Radiation Atlas - Vol. I. Commission of European Communities, 1984.

5. Gale Research Co., Climates of the States - Vol. I and II, 3rd edition, NOAA, 1985.

6. Knapp, C.L., Stoffel, T.C. and Whittaker, S.D., Insolation Data Manual. Solar Energy Research Institute. Golden, Co., 1980.

7. Rudloff, W., World Climates. Wissenschaftliche Verlags Gesellschaft, Stuttgart, 1981.

8. Personal Communication. Mr. Weingarten of the Tropic Test Center at Fort Clayton, Panama.

9. MIL-STD-210B, "Climatic Extremes for Military Equipment." 15 December 1973.

10. AR-70-38, "Research, Development, Test and Evaluation of Material for Extreme Climatic Conditions". 1 September 1979.

11. Pratt, C.F., "Selecting Plastics for Tough Working Environments". Plastics Engineering, August 1978.

12. Ghaemy, M. and Scott, G., "Photo- and Thermal- Oxidation of ABS: Correlation of Loss of Impact Strength with Degradation of the Rubber Component". Polymer Degradation and Stability, Vol. 3, No. 3, May 1981.

13. Toop, D.J., "Theory of Life Testing and Use of Thermogravimetric Analysis to Predict the Thermal Life of Wire Enamels". IEEE Transactions on Electrical Insulation, Vol. EI-6, No. 1, March 1971.

14. Lamarre, L., "Characterization of Aged Electrical Insulation Materials by Viscoelastic Methods". Sampe Journal, July/ August 1986.

15. Sacher, R.E., "Novel Techniques for Measuring Field Service Deterioration of Composite Materials". Proceedings of the TTCP-3 Critical Review Techniques for the Characterization of Polymeric Materials. AMMRC MS-77-2. January 1977.

16. Gillen, K.T., Clough, R.L., and Quintana, C.A., "Modulus Profiling of Polymers". Polymer Degradation and Stability. Vol. 17, 1987.

17. Sichina, W.J., "A Practical Technique for Predicting Mechanical Performance and Useful Lifetime of Polymeric Materials". American Laboratory, January 1988.

18. Flynn, J.H. and Dickens, B., "Application of New Kinetic Techniques to the Lifetime Prediction of Polymers from Weight Loss Data". Durability of Macromolecular Materials, ACS Symposium No. 95, American Chemical Society, Washington, D.C. 1979.

19. Turi, E.A., Thermal Characterization of Polymeric Materials, Academic Press, Inc. New York, 1981.

20. Nielsen, L.E., Mechanical Properties of Polymers and Composites. Vol. I. Marcel Dekker, Inc. New York, 1974.

21. Blaine, R.L., "Estimation of Polymer Lifetime by TGA Decomposition Kinetics". DuPont Instruments Application Brief No. TA-84.

22. Harris, A.P., "A Method for Predicting Results of Humidity Tests". Journal of Environmental Sciences. November/ December 1986.

23. American Society of Heating, Refrigerating and Air Conditioning Engineers. ASHRAE 1985 Fundamentals, Chapter 6, 1985.

24. Hardcastle, H.K., "The Effects of Environments on Physical Characteristics of Selected Plastic Materials -- A Literature Survey". DSET Report No. R2970-5, December 1986. U.S. Army Contract No. DAAA-021-86-C-0275.

25. Clark, D.T. and Munro, H.S., "Surface Aspects of the Photo-degradation of Bisphenol A Polycarbonate in Oxygen and Nitrogen Atmospheres as Revealed by E.S. CA.," Polymer Degradation and Stability, Volume 4, No. 6, 1982.

26. Munro, H.S. and Allaker, R.S., "Wavelength Dependence of the Surface Photooxidation of Disphenol A Polycarbonate," Polymer Degradation and Stability, Vol. 11, No. 4, 1985.

27. Lemair, J., Gardette, J., Rivation, A., and Roger, A., "Dual Photo-chemistries in Aliphatic Polyamides, Bisphenol A Polycarbonate and Aromatic Polyurethanes -- a Short Review," Polymer Degradation and Stability, Vol. 5, No. 1, 1985.

28. Pitman, G.L., Ward, I.M., and Duckett, R.A., "The Effects of Thermal Pretreatment and Molecular Weight on the Impact Behavior of Polycarbonate," Journal of Materials Science, Vol. 13, No. 10, 1978.

29. Skowronski, T.A., Rabek, J.F., and Ranby, B., "Photooxidation of Copolymers of Butadiene and Acrylonitrile," Polymer Degradation and Stability, Vol. 5, No. 3, 1983.

30. Wyzgoski, M.G., "Effects of Oven Ageing on ABS," Polymer Engineering and Science, Vol. 16, No. 4, 1976.

31. Geuskens, G., and Bastin, P., "Photooxidation of Polymers: Part VI -- Influence of Thermal Oxidation on the Photooxidative Stability of a Styrene-Acrylonitrile Copolymer", Polymer Degradation and Stability, Vol. 4, No. 2, 1982.

32. Modern Plastics Encyclopedia, McGraw-Hill, Inc., New York, October, 1986, Vol. 63, No. 10A.

33. Hellinek, H.H.G., "Fundamental Degradation Processes to Outdoor Exposure of Polymers," in Weatherability of Plastic Materials, J.K. Kamal, ed., Applied Polymer Symposium No. 4, Interscience, NY, 1967.

34. Scott, G., "Mechanisms of Photodegradation and Stabilization of Polyolefins", in Ultraviolet Light Induced Reactions in Polymers, S.S. Labana, ed., American Chemical Society Symposium No. 25, Washington, D.C., 1976.

35. Munro, H.S., and Allaker, R.S., "An ESCA Study of the Thermal Oxidation of Low Density Polyethylene", Polymer Degradation and Stability Vol. 15, No. 4, 1986.

36. Scott, G., "Developments in the Photooxidation and Photostabilization of Polymers," Polymer Degradation and Stability, Vol. 10, No. 2, 1985.

37. Allen, N.S., and Fatinikun, K.O., "Destruction of Carbonyl and Hydroperoxide Groups in Oxidized Polypropylene: Effect on Photooxidation," Polymer Degradation and Stability, Vol. 3, No. 5, 1981.

38. Allen, N.S., and Fatinikun, K.O., et al, "Some Important Factors Which Influence the Photooxidation of Polypropylene," Polymer Degradation and Stability, Vol. 4, No. 1, 1982.

39. Allen, N.S., and Fatinikun, K.O., et al, "Photooxidation of Polypropylene: Relationship Between Unsaturation and Induction Period," Polymer Degradation and Stability, Vol. 4, No. 2, 1982.

40. MIL-HDBK-17A, "Plastics for Aerospace Vehicles Part 1," Reinforced Plastics, Department of Defense, January 1971.

41. Davis, A., and Sims, D., Weathering of Polymers, Applied Science Publishers, New York, 1983.

42. Pritchard, G., and Taneja, N., "Nature and Extent of Water Damage in Glass Laminates," Proceedings of the 29th Annual Conference on Reinforced Composites.

43. Blaine, R.L., "Polymer Crystallinity" DuPont Instruments Application Brief No. TA-12.

44. Runt, J., Jacq, M., Yen, J.T., and Gallagher, K.P., "Morphology and Fatigue Crack Propagation in Crystalline Polymers." Polymer Preprints Vol. 29, No. 2. September 1988. American Chemical Society.

45. Hawkins, W.L., "Polymer Degradation and Stabilization." Polymers-Properties and Applications No. 8. Springer-Verlag, Berlin. 1984.

46. Brzuskiewicz, J.E., "Full-Scale Plastic Ammunition Container Testing." DSET Report No. R2970-21, July 1988. U.S. Army Contract No. DAAA-21-86-C-0275.

47. Harris, A.P., "A Method For Predicting Results of Humidity Tests." Journal of Environmental Sciences. November/December 1986.

48. Kolyer, J.M., "Rate of Moisture Permeation Into Elastomer-Sealed Electronic Boxes." Sampe Journal. May/June 1986.

49. Ashrae 1985 Fundamentals. American Society of Heating, Refrigerating and Air-Conditioning Engineers, Inc., Chapter 6. 1985.

50. Shlyapnikov, Y.A., Marin, A.P., and Kiryuskin, S.G., "Temperature Dependence of Inhibited Oxidation Parameters of Polyethylene." Polymer Degradation and Stability. Vol. 17, p.265-272, 1987.

51. Kramer, E. and Koppelmann J., "Studies of the Autoxidation of Polybutylene and Crosslinked Polyethylene by Isothermal Long-Term DTA." Polymer Degradation and Stability. Vol. 14, p.p.333-339, 1986.

APPENDIX A

AMMUNITION ITEM LOGISTICS

(THIS PAGE LEFT BLANK)

81mm MORTAR ROUND

U.S. ITEM MANAGER

Mr. Frank Woodard
AMCCOM
Defense Ammunition Directorate
Telephone (309) 782-3261

ROYAL ORDNANCE ITEM MANAGER

Dr. Richard Smith
Telephone (02) 913-2211, ext.4040

KEY

AP	= Armor Piercing	HEAT	= High Explosive Anti-Tank
DS	= Discarding Sabot	WP	= White Phosphorous
FS	= Fin Stabilized	HEP	= High Explosive Plastic

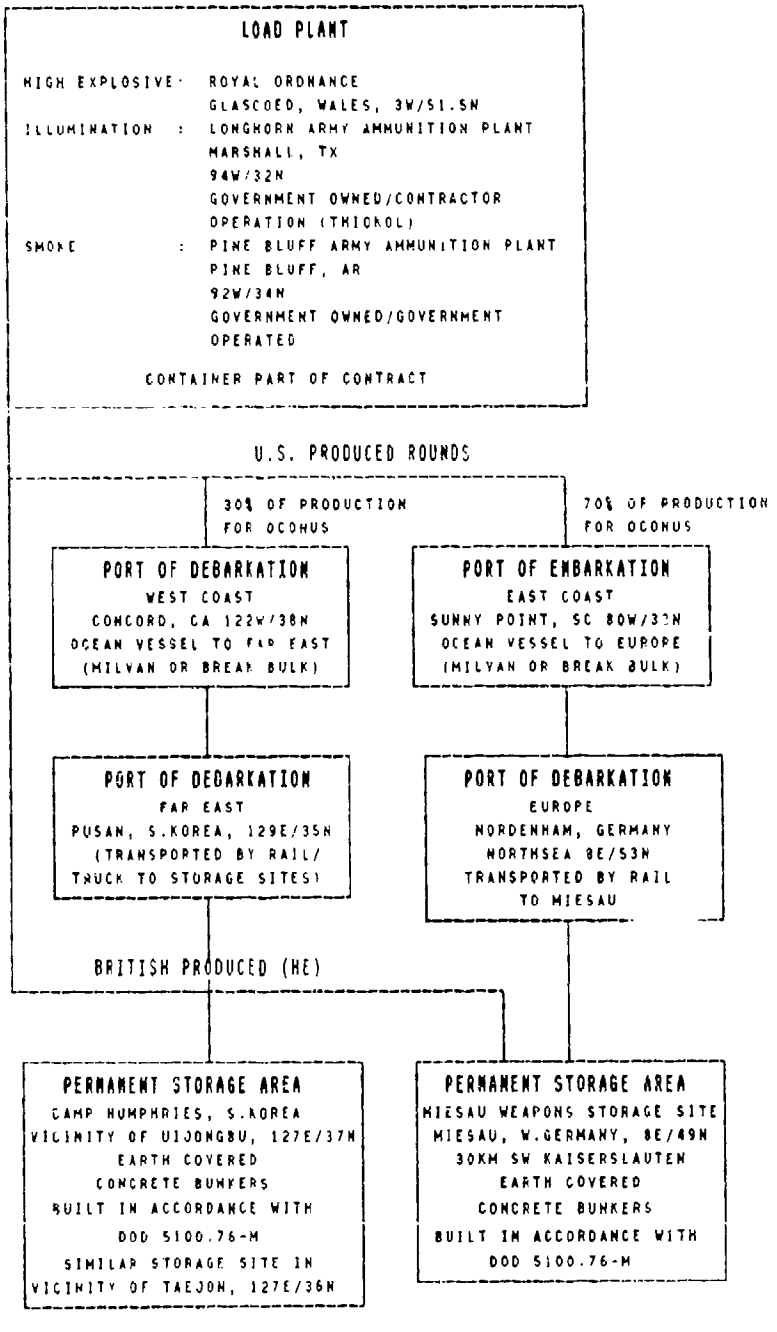

The round is packed on the assembly line as a part of the loading procedure. The British HE round is packed one per plastic container and three plastic containers per steel box. U.S. produced illumination and smoke rounds are packed one per fiber container and three fiber containers per wooden box. There is no moisture testing requirements at packing (see MSG PMAMMO Log 2410302 Feb. 86). Containers are palletized for shipment/15 boxes per pallet. Short term storage at load plant (up to one (1) year) is possible. Items are shipped primarily by rail, some by truck to port of embarkation. More than 75% of production goes to war reserve with 60% going OCONUS.

Items are generally in a ship hold environment -- dry with sealed hatches for up to 3 days during shipment to Germany and up to 19 days during shipment to South Korea. Items may remain in port for up to 7 days.

Unprotected storage, if any, will probably be at the Miesau site in Europe and at the Taejon site in Korea since the preposition stock sites are in territory subject to espionage activity. The basic load of mortar ammunition is kept in boxes in bunkers (on pallets) or on vehicles. The basic load that is kept on vehicles will be kept in packs but protected by canvas or in the case of mechanized divisions, in armored personnel carriers. Unlike tank rounds, mortar rounds are not broken out until needed for firing.

Average length of storage for mortar stocks is 15-20 years.

Stockpile testing schedule:

<5 years old	2 year cycle
>5 years old	ILL (3 years)
	Smoke (5 years)
	HE unfuzed (5 years)

Containers undergo care and preservation by the ammunition maintenance personnel after inspection in accordance with SB 742-1.

2.75 IN. ROCKET

ITEM MANAGER
BEV SWANSON, AMCCOM
TEL (309) 782-4290

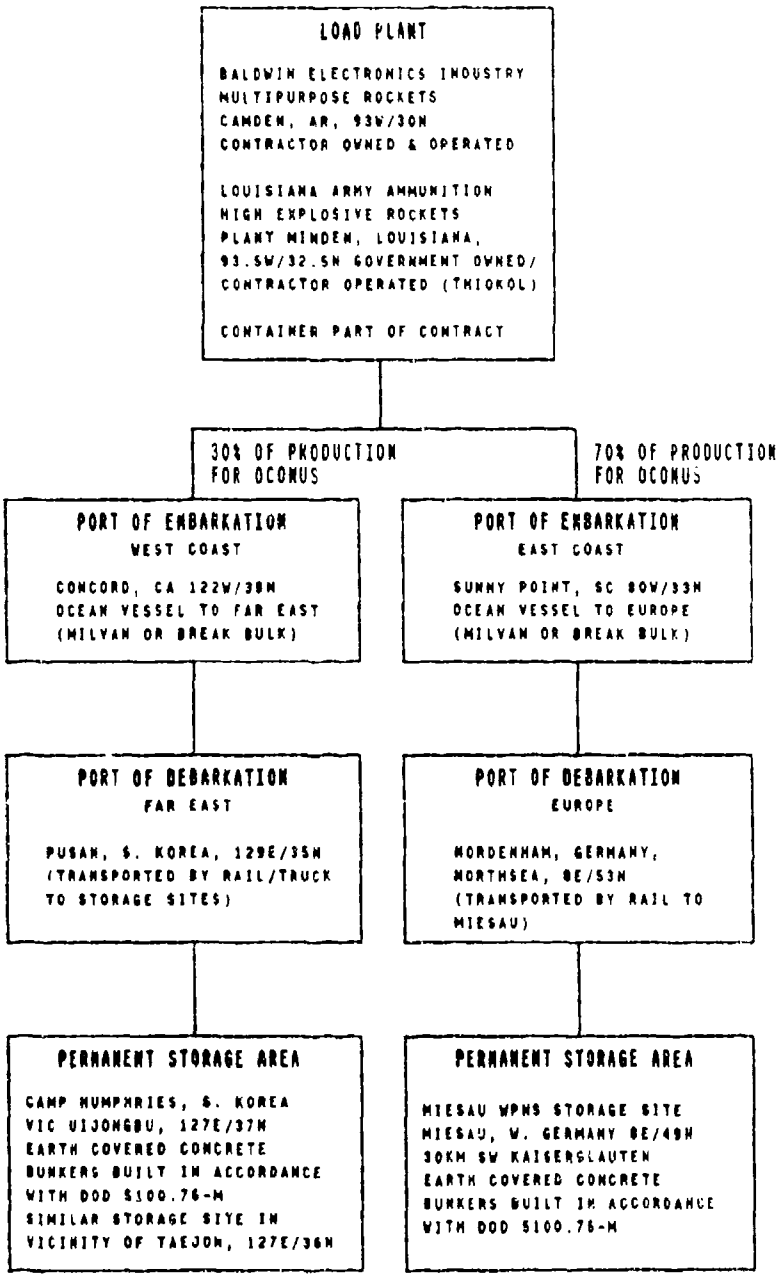

Rockets are packed on the assembly line as part of the loading procedure; one per fiber container and four (4) fiber containers per wooden box. Wooden boxes are palletized; 48 boxes per pallet short term storage at load plant presently does not exceed 90 days. Shipped from load plant to port of embarkation by rail or truck. 60% of production goes OCONUS.

Items are generally in a ship hold environment -- dry with sealed hatches for up to 13 days during shipment to Germany and up to 18 days during shipment to S. Korea. Items may remain in port for up to 7 days. High temperature and high humidity conditions could occur if a southern route is taken.

With the advent of the armed Helicopter concept, the 2.75 Rocket has become much more in demand and is not stored in great quantity. The present stockpile is tested every year (each type) so that a pattern of reliability can be determined. The frequency may change after reliability is determined.

Containers undergo care and preservation by the ammunition maintenance personnel after inspection in accordance with S6742-1.

5.56/7.62mm
SMALL CALIBER ROUNDS

ITEM MANAGER
Dick Green
AMCCOM
Tel (309) 782-3150

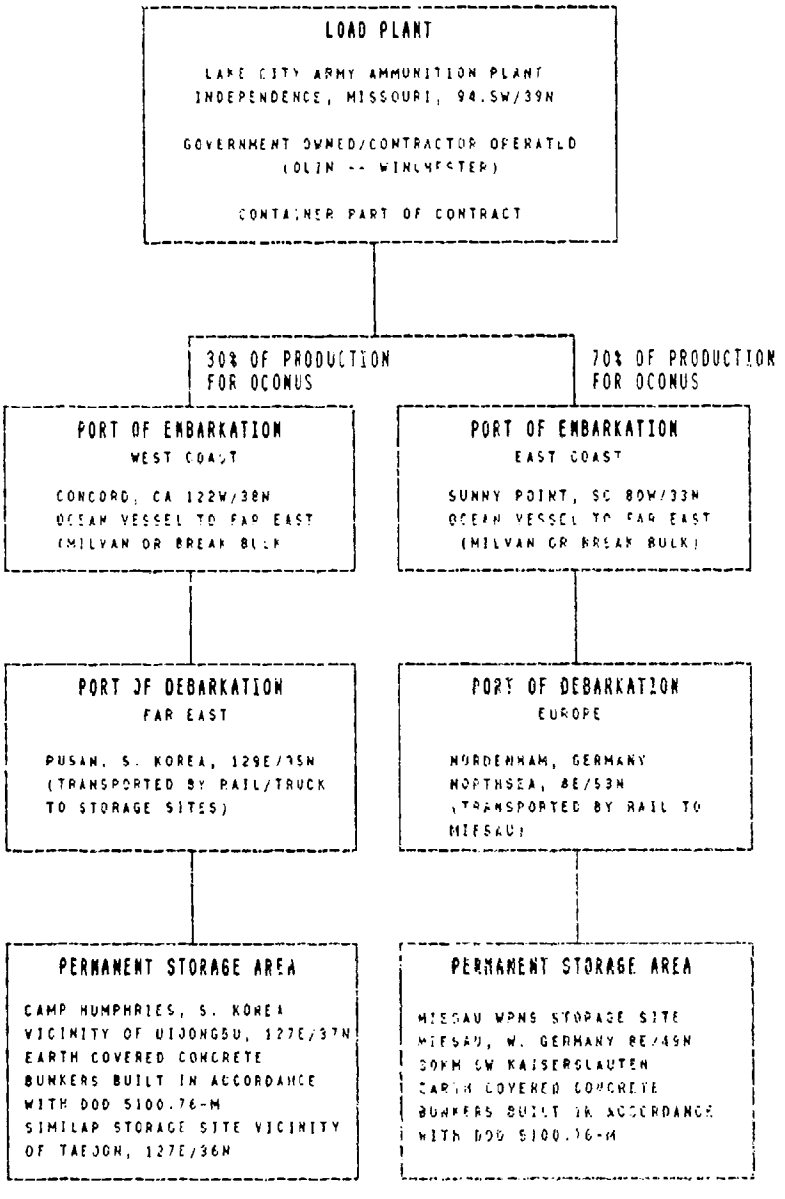

The Rounds are packed on the assembly line as part of the loading procedure. The 5.56mm line is totally automated from raw materials to packing in container. 5.56mm are put in metal M2A1 containers. The 7.62mm line is only partially automated. They are packed in metal M2A1 or M19 containers.

Two metal containers are packed in a wire wrapped wooden box. Some wire wraps have four (4) metal containers. Wire wrapped boxes are palletized; 40 boxes per pallet short term storage at load plant (up to one year) is possible. Items are shipped from load plant to port of embarkation by rail or truck. More than 75% of production goes to war reserve, with 60% going OCONUS.

Items are generally in a ship hold environment -- dry with sealed hatches for up to 12 days during shipment to Germany up to 19 days during shipment to S. Korea. Items may remain in port for up to 7 days.

Basic loads of small arms ammunition are kept in containers and in protected storage sites until required for combat. It is the philosophy and policy of the Defense Ammunition Director and AMCCOM that new production items are put into war reserve stocks and old stocks rotated out to the training stocks. This is common practice, but is left up to theatre commander as to its implementation.

Average length of storage for small arms war reserve stocks at the present time is 15-20 years.

5.56/7.62mm ammunition stockpile is tested every 5 years.

Containers undergo care and preservation by the ammunition maintenance personnel after inspection in accordance with SB 742-1.

105mm TANK ROUND

ITEM MANAGER
Mr. Frank Woodard
AMCCOM
Defense Ammunition Directorate
Tel (309) 782-3261

KEY			
AP	= Armor Piercing	HEAT	= High Explosive Anti-Tank
DS	= Discarding Sabot	WP	= White Phosphorous
FS	= Fin Stabilized	HEP	= High Explosive Plastic

LOAD PLANT

MILAN ARMY AMMUNITION PLANT
MILAN, TN; 89W/36N
GOVERNMENT OWNED/CONTRACTOR OPERATED
(MARTIN-MARIETTA)

CONTAINER PART OF CONTRACT

The round is packed on the assembly line as a part of the loading procedure. Rounds are packed one per fiber tube and two fiber tubes per wooden box. If new metal containers with square supports are used, there will be one fiber tube per metal container. There is no moisture testing requirement at packing (MSG PMAMMO Log 241030Z Feb 86). Containers are palletized for shipment, 15 boxes per pallet. Short term storage at load plant (up to one (1) year) is possible. Items are shipped primarily by rail (some in Milvan), some by truck to port of embarkation. More than 75% of production goes to ware reserve with 60% going OCONUS.

60% OF PRODUCTION FOR OCONUS

PORT OF EMBARKATION

SUNNY POINT, SC 80W/33N
OCEAN VESSEL TO EUROPE
(MILVAN OR BREAK BULK)

Items are generally in a ship hold environment -- dry with sealed hatches for up to 13 days. Items may remain in port for up to 7 days.

PORT OF DEBARKATION

NORDENHAM, GERMANY
NORTHSEA 8E/53N

TRANSPORTED PRIMARILY BY RAIL, SOME BY TRUCK TO MEISAU STORAGE SITE

85% of the stock is stored here or in prepositon supply points (PSP) in V Corps or VII Corps; 15% of this stock is carried as a basic load on tanks, out of containers, in ready racks. PSPs are of the same construction as Miesau.

The stocks at Miesau are never intended to be out of bunker storage, but if there is to be a two-year unprotected storage, this would be the place to consider since the PSPs are kept in bunker storage for both weather and security. The prime consideration is security. The tank carried basic load is never intended to go back into protected/sealed storage. It is removed from the tanks once a year for approximately two weeks and placed in temporary storage at the training site and returned to the tanks after completion of training firings. It is inspected each time and renovated as necessary.

The PSP environment should be considered in areas limited to longitudes 6E thru 12E and latitudes 48N thru 52N.

Average length of storage at present:

L36-Original APDS	-- British Made (67/68)	20 years
M774	-- U.S. Made	10 years
M833	-- U.S. Made (just in production)	no history

PERMANENT STORAGE AREA

MEISAU WEAPONS STORAGE SITE
MEISAU, W. GERMANY 8E/49N
30KM SW KAISERSLAUTERN

EARTH COVERED CONCRETE BUNKERS
BUILT IN ACCORDANCE WITH DOD
5100.76-M

Stockpile testing schedule:

AP & WP		5 year cycle
HEP		4 year cycle
APFS, HEAT, APDF	> 5 years old	3 year cycle
	< 5 years old	2 year cycle

Containers undergo care and preservation (painting, etc.) by ammunition maintenance personnel in accordance with inspection procedure SB-742-1.

The overwhelming preponderance of armor and mechanized divisions in Europe, make this environment one to be considered for the 105mm tank round. Far East environments have the same logistics as the 81mm mortar round.

155mm PROPELLING CHARGE

ITEM MANAGER
Gerry Price, AMCCOM
Tel (309) 782-3358

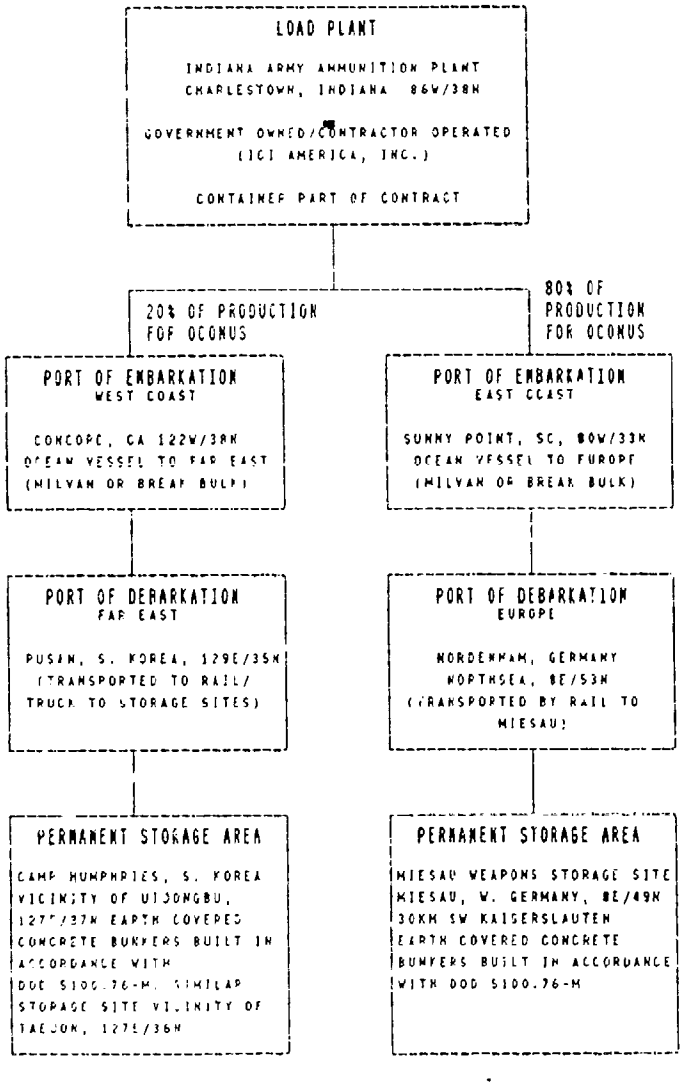

The charges are packed in containers as part of loading plant assembly line process. There are several models of propelling charges. However, since all are handled similarly. The single charge containers are used as the model. The charge is wrapped with a single face corrugated fiberboard and inserted into a cylindrical steel container. The cover for the container contains a rubber gasket for sealing the container against moisture. There is no moisture testing requirements at packing (see MSG PM AMMO LOG 2410302 FEB 86). The containers are then palletized. The present round-end containers are palletized 25 per pallet and the proposed square end container will have 36 per pallet. Short term storage at load plant (up to 90 da,) is possible. Items are shipped by rail or truck to port of embarkation. More than 75% of production goes to war reserve with 60% going OCONUS.

Items are generally in a ship hol environment -- dry with sealed hatches for up to 13 days during shipment to Germany and up to 19 days during shipment to S. Korea. Items may remain in port up to 7 days.

15% of stock is carried with the units as basic load. It is kept in metal containers, either under canvas or in the accompanying light armored vehicle or on the self-propelled Howitzer itself. The charges are not broken out of the metal container until needed. Propelling charges are not normally stored outside. If unprotected storage is to be considered, it should be in the Miesau weapons storage area environment. PSP environment should be considered in areas limited to longitudes 6E thru 12E and latitudes 48N thru 52N.

The average length of storage is 10 to 15 years. Stockpile testing is conducted on a 4- to 5-year cycle based on history of reliability. Care and preservation performed as required in accordance with inspection procedure SB 742-1. Empty containers are not returned from OCONUS.

(THIS PAGE LEFT BLANK)

APPENDIX B

LOGISTICS CHAIN CLIMATE DATA

(THIS PAGE LEFT BLANK)

TAEJON, SOUTH KOREA

Location: 36N, 127E

Elevation: About 60 m (About 200 ft)[3]

Taejon is located in west central South Korea approximately 150 km (93 mi) south of Seoul. The estimated average temperature is 11°C (52°F), the estimated average relative humidity is 69%, and the estimated average annual precipitation is 133 cm (52 in). The estimated highest and lowest temperatures recorded during a 22 year period are 37°C (99°F) and -24°C (-12°F), respectively.[1]

Month	Avg. Temperature[1] Max. °C	Max. °F	Min. °C	Min. °F	Mean °C	Mean °F	R.H.[1] %	Total Precip.[2] (cm)	(in)	Avg. Daily Radiation[3] (MJ/m^2)	(BTU/ft2)
Jan.	0	32	-9	15	-5	24	65	2.7	1.1	7.5	663
Feb.	3	37	-7	20	-2	29	62	3.0	1.2	10.3	906
Mar.	8	47	-2	29	3	38	62	4.3	1.7	12.5	1097
Apr.	17	62	5	41	11	52	65	9.5	3.7	14.7	1292
May	22	72	11	51	17	62	69	9.2	3.6	16.5	1455
June	27	80	16	61	22	71	71	17.3	6.8	17.7	1562
July	29	84	21	70	25	77	79	33.2	13.1	14.2	1254
Aug.	31	87	22	71	27	79	76	26.0	10.2	14.1	1238
Sep.	26	78	15	59	21	69	72	15.5	6.1	12.8	1131
Oct.	19	67	7	45	13	56	68	4.9	1.9	10.7	938
Nov.	11	51	0	32	6	42	68	4.4	1.7	6.8	600
Dec.	3	37	-7	20	-2	29	66	3.2	1.3	6.3	558
TOTALS								133.2	52.4		
AVERAGES	16	61	6	43	11	52	69			12.0	1058

[1]Temperature data from World Climatic Data, Frederick L. Wernstedt, Climatic Data Press, 1972 (ASU Library) contains average daily temperature data for 82 South Korean locations. Unfortunately, Taejon is not one of them. Data from five cities within 50 km (31 mi) of Taejon are listed below along with data for Seoul, 150 km (93 mi) north of Taejon.

Average Daily Temperature

	J	F	M	A	M	J	J	A	S	O	N	D
Cochiwon	-4°C	-2°C	4°C	11°C	16°C	21°C	25°C	26°C	20°C	13°C	6°C	-1°C
	24°F	29°F	39°F	51°F	62°F	70°F	77°F	78°F	68°F	56°F	43°F	31°F
Kongju	-4°C	-1°C	5°C	11°C	17°C	22°C	26°C	26°C	20°C	14°C	7°C	0°C
	26°F	31°F	40°F	52°F	63°F	72°F	79°F	79°F	69°F	57°F	44°F	32°F
Nonsan	-3°C	0°C	5°C	12°C	18°C	22°C	26°C	27°C	21°C	14°C	11°C	1°C
	27°F	32°F	42°F	53°F	64°F	72°F	79°F	80°F	70°F	57°F	51°F	34°F

Average Daily Temperature

	J	F	M	A	M	J	J	A	S	O	N	D
Muju	-4°C	-2°C	4°C	11°C	17°C	21°C	26°C	26°C	19°C	13°C	6°C	0°C
	25°F	29°F	40°F	51°F	62°F	71°F	78°F	78°F	67°F	55°F	43°F	33°F
Poun	-4°C	-2°C	4°C	11°C	16°C	21°C	25°C	26°C	20°C	13°C	6°C	-1°C
	25°F	28°F	39°F	51°F	62°F	70°F	78°F	78°F	68°F	55°F	43°F	31°F
Seoul	-5°C	-2°C	4°C	11°C	16°C	21°C	25°C	25°C	20°C	13°C	6°C	-1°C
	23°F	29°F	39°F	51°F	61°F	69°F	76°F	78°F	69°F	56°F	43°F	30°F

This data would indicate that temperature data for Taejon would be very similar to Seoul. The data reported in the table is for Seoul (elevation 87 m [285 ft], 37° 34'N, 126° 58'E) from p. 281 of World Weather Guide, E. A. Pearce and C. G. Smith, New York Times Book Company, 1984 (ASU Library). The average and extremes for temperature and humidity are based on a 22 year period ending in 1980. The mean daily temperature was taken to be the average between the maximum and minimum temperatures. Humidity at Seoul was recorded at 0530 and 1330 hours. The humidity reported is an average of these two values.

[2]The five locations within 50 km (31 mi) of Taejon listed in explanation (1) above report the following average monthly precipitation.

Average Precipitation by Month

City	J	F	M	A	M	J	J	A	S	O	N	D
Cochiwon	1.9cm	2.3cm	3.0cm	6.4cm	7.2cm	11.0cm	32.1cm	19.8cm	12.4cm	3.4cm	3.5cm	2.7cm
	.8in	.9in	1.2in	2.5in	2.8in	4.3in	12.6in	7.8in	4.9in	1.3in	1.4in	1.1in
Kongju	2.7cm	3.0cm	4.3cm	9.5cm	9.2cm	17.3cm	33.2cm	26.0cm	15.5cm	4.9cm	4.4cm	3.2cm
	1.1in	1.2in	1.7in	3.7in	3.6in	6.8in	13.1in	10.2in	6.1in	1.9in	1.7in	1.3in
Nonsan	2.1cm	2.0cm	3.5cm	8.0cm	8.0cm	15.8cm	28.0cm	24.2cm	13.4cm	4.4cm	3.8cm	3.0cm
	.8in	.8in	1.4in	3.2in	3.2in	6.2in	11.0in	9.5in	5.3in	1.7in	1.5in	1.2in
Muju	2.4cm	2.9cm	4.0cm	7.7cm	7.6cm	16.0cm	24.5cm	20.2cm	13.6cm	4.2cm	4.1cm	3.3cm
	.9in	1.1in	1.6in	3.0in	3.0in	6.3in	9.7in	8.0in	5.4in	1.7in	1.6in	1.3 in
Poun	2.3cm	2.6cm	4.0cm	8.5cm	8.4cm	15.8cm	30.5cm	20.5cm	12.5cm	4.3cm	4.4cm	3.0cm
	.9in	1.0in	1.6in	3.4in	3.3in	6.2in	12.0in	8.1in	4.9in	1.7in	1.7in	1.2in

Since Kongju (36° 28'N, 127° 08'E) has reported the greatest precipitation, these values were taken to represent Taejon. The source is World Climatic Data, Frederick L. Wernstedt, Climatic Data Press, 1972. The reporting period is 1942-1972.

[3]Horizontal radiation data is from p. 79 of the Present Analysis of the Sunlight Energy Sources of Korea, KE-84-21, Volume II (Appendix), Korean Energy Research Center, 1984 (provided by SERI). The data reported is from measurements at Kongju, about 35 km (22 mi) north of Taejon for the years 1983 and 1984. This source reports the elevation of Kongju as 59 m.

UIJONGBU, SOUTH KOREA

Location: 37°45'N, 127°00'E

Elevation: Near Sea Level

Uijongbu is located in the northern portion of South Korea, approximately 30 km (19 mi) north of Seoul. The estimated average temperature is 11°C (52°F), the estimated average relative humidity is 69%, and the estimated average annual precipitation is 133 cm (52.5 in). The estimated highest and lowest temperatures recorded during a 22 year period are 37°C (99°F) and -24°C (-12°F), respectively[1].

Month	Avg. Temperature[1] Max.		Min.		Mean		R.H.[1] %	Total Precip.[2] (cm)	(in)	Avg. Daily Radiation[3] (MJ/m^2)	(BTU/ft2)
	°C	°F	°C	°F	°C	°F					
Jan.	0	32	-9	15	-5	24	65	2.1	0.8	7.3	644
Feb.	3	37	-7	20	-2	29	62	2.1	0.8	9.7	853
Mar.	8	47	-2	29	3	38	62	3.6	1.4	12.7	1120
Apr.	17	62	5	41	11	52	65	7.8	3.1	14.8	1301
May	22	72	11	51	17	62	69	10.4	4.1	15.2	1342
Jun.	27	80	16	61	22	71	71	13.4	5.3	16.3	1432
July	29	84	21	70	25	77	79	41.0	16.1	12.2	1078
Aug.	31	87	22	71	27	79	76	27.3	10.7	12.4	1096
Sep.	26	78	15	59	21	69	72	14.3	5.6	13.3	1171
Oct.	19	67	7	45	13	56	68	4.3	1.7	10.4	916
Nov.	11	51	0	32	6	42	68	4.3	1.7	7.0	616
Dec.	3	37	-7	20	-2	29	66	2.8	1.1	5.9	522
TOTAL								133.4	52.4		
AVERAGES	16	61	6	43	11	52	69			11.4	1008

[1]Temperature and humidity data is from p.281 of World Weather Guide, E.A. Pearce and C.G. Smith, New York Times Book Company, 1984 (ASU Library). The reported weather is for Seoul (elevation 87m [285 ft], 37°34'N, 126°58'E). The averages and extremes for temperature, humidity and precipitation are based on a 22 year period ending in 1980. The mean daily temperature was taken to be the average between the maximum and minimum temperatures. Humidity was recorded at 0530 and 1330 hours. The humidity reported is an average of these two values.

[2]Precipitation data is from World Climatic Data, Frederick L. Wernstedt, Climatic Data Press, 1972. The station reported is Uijongbu and represents 1942 to 1972 data.

[3]Horizontal radiation data is from p. 55 of the Present Analysis of the Sunlight Energy Sources of Korea, KE-84-21, Volume II (Appendix), Korean Energy Research Center, 1984 (provided by SERI). The data reported is from measurements at Seoul, about 30 km (19 mi) south of Uijongbu, for the years 1983 and 1984.

PUSAN, SOUTH KOREA

Location: 35°06'N, 129°01'E

Elevation: Near Sea Level

Pusan is located in southeastern Korea on the Pacific Ocean. The average temperature is 14°C (57°F), the average relative humidity is 66%, and the average annual precipitation is 137 cm (53 in). The highest and lowest temperatures recorded during a 29 year period are 36°C (96°F) and -14°C (7°F), respectively[1].

Month	Avg. Temperature[1] Max.		Min.		Mean		R.H.[1] %	Total Precip.[1] (cm)	(in)	Avg. Daily Radiation[2] (MJ/m^2)	(BTU/ft2)
	°C	°F	°C	°F	°C	°F					
Jan.	6	43	-2	29	2	36	49	4.3	1.7	11.3	997
Feb.	7	45	-1	31	3	38	53	3.6	1.4	13.6	1197
Mar.	12	53	3	37	8	45	58	6.9	2.7	16.6	1462
Apr.	17	62	8	47	13	55	66	14.0	5.5	18.3	1611
May	21	69	13	55	17	62	67	13.2	5.2	19.8	1744
Jun.	24	75	17	62	21	69	77	20.1	7.9	18.4	1620
July	27	81	22	71	25	76	83	29.5	11.6	70.6	1494
Aug.	29	85	23	73	26	79	79	13.0	5.1	18.1	1598
Sep.	26	78	18	65	22	72	73	17.3	6.8	15.2	1338
Oct.	21	70	12	54	17	62	64	7.4	2.9	14.2	1248
Nov.	15	59	6	43	11	51	61	4.1	1.6	10.7	942
Dec.	9	48	1	33	5	41	57	3.1	1.2	10.5	927
TOTAL								136.5	53.6		
AVERAGES	18	64	10	50	14	57	66			15.3	1348

[1]Temperature, humidity, and precipitation data is from page 281 of World Weather Guide, E.A. Pearce and C.G. Smith, New York Times Book Company, 1984 (ASU Library). The reported weather is for Pusan. The averages and extremes for temperature, humidity and precipitation are based on a 29 year period ending in 1980. The mean daily temperature was taken to be the average between the maximum and minimum temperatures. Humidity was recorded at 0530 and 1330 hours. The humidity reported is an average of these two values.

[2]Horizontal radiation data is from p. 151 of the Present Analysis of the Sunlight Energy Sources of Korea, KE-84-21, Volume II (Appendix), Korean Energy Research Center, 1984 (provided by SERI). The data reported is from measurements at Pusan for the years 1983 and 1984.

NORDENHAM, GERMANY

Location: 53N, 8E

Elevation: Sea Level

Nordenham is located on the North Sea in northern Germany about 100 km (62 mi) west of Hamburg. The estimated average temeprature is 9°C (48°F), the estimated average relative humidity is 79%, and the estimated average annual precipitation is 72 cm (28 in). The estimated highest and lowest temperatures recorded during a 30 year period ending in 1980 is 36°C (97°F) and -29°C (-20°F), respectively.[1]

Month	Avg. Temperature[1] Max. °C	Max. °F	Min. °C	Min. °F	Mean °C	Mean °F	R.H.[1] %	Total Precip.[2] (cm)	(in)	Avg. Daily Radiation[3] (MJ/m^2)	(BTU/ft2)
Jan.	2	36	-2	28	0	32	87	5.7	2.2	2.1	184
Feb.	3	37	-2	28	1	33	85	4.8	1.9	4.4	386
Mar.	7	44	-1	31	3	38	78	4.2	1.7	8.7	767
Apr.	13	55	3	38	8	47	73	5.0	2.0	14.5	1274
May	18	64	7	45	13	55	69	5.6	2.2	18.0	1585
June	21	69	11	51	16	60	70	5.9	2.3	21.0	1852
July	22	73	13	55	18	64	74	9.2	3.6	18.6	1643
Aug.	22	72	12	54	17	63	76	7.9	3.1	16.5	1458
Sep.	19	66	10	49	15	58	78	6.0	2.4	10 7	946
Oct.	13	55	6	43	10	49	83	5.8	2.3	5.8	514
Nov.	7	45	3	37	5	41	88	6.0	2.4	2.5	223
Dec.	4	39	0	31	2	35	89	5.4	2.1	1.6	141
TOTALS								71.5	28.1		
AVERAGES	13	55	5	41	9	48	79			10.4	917

[1]Temperature and humidity data is from p. 367 of World Weather Guide, E. A. Pearce and C. G. Smith, New York Times Book Company, 1984 (ASU Library). The reported weather is for Hamburg, Germany, a full 100 km (62 mi) east of Nordenham. The averages and extremes are based on a 30 year period ending in 1980. The mean daily temperature was taken to be the average between the maximum and minimum temperatures. The closest city for which any data could be found is Bremen, about 30 km (19 mi) south of Nordenham. Only averages could be found at Bremen. A comparison of averages (1942-1972) for Bremen and Hamburg from p. 191 and 192 of World Climatic Data, Frederic .. Wernstedt, Climatic Data Press, 1972, is as follows:

	J	F	M	A	M	J	J	A	S	O	N	D
Hamburg	0°C	0°C	3°C	8°C	13°C	16°C	17°C	17°C	14°C	9°C	5°C	2°C
	32°F	33°F	38°F	46°F	55°F	60°F	63°F	62°F	57°F	48°F	41°F	35°F
Bremen	1°C	1°C	4°C	8°C	13°C	16°C	17°C	17°C	14°C	9°C	5°C	2°C
	33°F	34°F	39°F	47°F	55°F	61°F	63°F	63°F	57°F	49°F	42°F	36°F

The above data would indicate that temperature data for Bremen would be similar to Hamburg. It is also expected that Nordenham data would be very similar to Hamburg because of the moderating influence of the North Sea. Humidity data at Hamburg was recorded at 0630 and 1330 hours. The humidity reported is an average of these two values.

[2]The precipitation data is from p. 191 of World Climatic Data, Frederick L. Wernstedt, Climatic Data Press, 1972 (ASU Library). The data reported is for Bremen (elevation 4 m [13 ft]), about 30 km (19 mi) south of Nordenham and covers the period 1942-1972.

[3]The radiation data is from European Solar Radiation Atlas, Vol. 1, W. Palz, ed. Commission of European Communities, 1984 (DSET Library). The data reported is for Bremerhaven, about 5 km (3 mi) east of Nordenham. The reporting period is 1966-1975.

MARSHALL, TX

Location: 32° 32'N, 94° 21'W

Elevation: 107 m (352 ft)

Marshall is located in east Texas about 30 km (19 mi) from the Louisiana border and about 70 km (43 mi) west of Shreveport, LA. The average temperature is 18°C (64°F), the estimated average relative humidity is 72%, and the average annual precipitation is 118 cm (46 in). The highest and lowest temperatures recorded (1951-1980) were 43°C (110°F) in August of 1962, and -16°C (4°F) in February of 1951, respectively.[1]

Month	Avg. Temperature[1] Max. °C	Max. °F	Min. °C	Min. °F	Mean °C	Mean °F	R.H.[2] %	Total Precip.[1] (cm)	(in)	Avg. Daily Radiation[3] (MJ/m^2)	(BTU/ft2)
Jan.	13	55	1	33	7	44	73	10.5	4.1	8.7	762
Feb.	15	60	3	37	9	48	69	9.4	3.7	11.8	1038
Mar.	20	67	6	43	13	55	68	10.1	4.0	15.2	1342
Apr.	25	76	12	53	18	65	70	13.0	5.1	18.3	1613
May	29	83	16	61	22	72	73	12.3	4.9	21.4	1886
June	32	90	20	68	26	79	73	9.5	3.7	23.4	2065
July	35	94	22	72	28	83	72	8.4	3.3	22.9	2014
Aug.	34	94	21	70	28	82	72	6.1	2.4	21.3	1877
Sep.	31	88	18	65	25	77	73	10.4	4.1	17.6	1554
Oct.	26	79	11	53	19	66	71	8.1	3.2	14.8	1304
Nov.	19	67	6	42	12	54	73	9.5	3.8	10.5	929
Dec.	15	59	2	36	8	47	74	10.4	4.1	8.3	731
TOTALS								117.7	46.4		
AVERAGES	24	76	12	53	18	64	72			16.2	1426

[1]Temperature and Precipitation data is from p. 1080 of Climates of the States, Vol. 2, National Oceanic and Atmospheric Administration, 3rd ed., 1985, Gale Research Company, Detroit, MI (DSET Library). The weather station reported is Marshall, TX. The averages and extremes for temperature and precipitation are based on the period 1951-1980.

[2]Humidity data is from the same source as (1) (Vol. 1, p. 472), but since humidity data is not published for Marshall, TX, this data is for Shreveport, LA (32° 28'N, 93° 49'W, elevation 77 m [254 ft]) 70 km (43 mi) east of Marshall, TX. Humidity is recorded at 0600, 1200, 1800, and 2400 hours. The average humidity is the mean of these four values. The averages are based on a 31 year period ending in 1980.

[3]Radiation data is from p. 95 of the Insolation Data Manual, Connie L. Knapp, Thomas L. Stoffel, and Stephen D. Whittaker, Solar Energy Research Institute, Golden, CO, 1980 (ASU Library). The radiation data is for Shreveport, LA.

SUNNY POINT, SC

Location: Approx. 33°N, 80°W (vicinity of Charleston)

Elevation: Near Sea Level

Sunny Point is located on the Atlantic Ocean near Charleston. The average temperature is 18°C (65°F), the average relative humidity is 75%, and the average annual precipitation is 131 cm (52 in). The highest and lowest temperatures recorded (1951-1980) were 39°C (102°F), in June, 1944, and -13°C (9°F) in December, 1962, respectively.[1]

Month	Avg. Temperature[1] Max. °C	Max. °F	Min. °C	Min. °F	Mean °C	Mean °F	R.H.[1] %	Total Precip.[1] (cm)	(in)	Avg. Daily Radiation[2] (MJ/m^2)	(BTU/ft^2)
Jan.	15	59	3	37	9	48	73	8.5	3.3	8.5	744
Feb.	16	61	4	38	10	50	69	8.6	3.4	11.3	995
Mar.	20	68	7	45	14	57	70	11.1	4.4	15.2	1339
Apr.	24	76	11	53	18	64	71	6.6	2.6	19.7	1732
May	28	83	16	61	22	72	75	11.2	4.4	21.1	1860
June	31	87	20	68	25	78	77	16.6	6.6	20.9	1844
July	32	89	22	72	27	81	80	18.6	7.3	20.4	1799
Aug.	32	89	22	71	27	80	81	16.5	6.5	18.0	1585
Sep.	29	85	19	67	24	76	81	12.5	4.9	15.8	1394
Oct.	25	77	13	55	19	67	78	7.4	2.9	13.5	1193
Nov.	20	69	7	45	14	57	75	5.5	2.2	10.6	934
Dec.	16	61	4	39	10	50	73	7.9	3.1	8.2	721
TOTAL								131.0	51.6		
AVERAGE	24	75	12	54	18	65	75			15.3	1345

[1]Temperature, humidity, and precipitation data is from p. 992 of Climate of the States, Vol. 2, National Oceanic and Atmospheric Administration, 3rd ed., 1985, Gale Research Company, Detroit, MI (DSET library). The weather station reported is the Charleston Municipal Airport, 32°54'N, 80°02'W, elevation 12 m (39 ft) above sea level. The averages and extremes for temperature, precipitation, and humidity are based on the period 1951-1980. Humidity is recorded at 0600, 1200, 1800, and 2400 hours; the average daily humidity is the mean of these four values.

[2]The radiation data is from p. 195 of the Insolation Data Manual, Connie L. Knapp, Thomas J. Stoffel, and Stephen D. Whittaker, Solar Energy Research Institute, Golden, CO, 1980. The weather station reported is Solmet Station No. 13880 at the same latitude, longitude, and elevation as in (1) above.

GLASCOED WALES

Location: Approximately 51.5°N, 3°W (vicinity of Newport)

Elevation: Near sea level

Glascoed, Wales is located in southern Wales near Newport at the mouth of the Severn River. The estimated average temperature is 11°C (51°F), the estimated average relative humidity is 81%, and the estimated average annual precipitation is 106.5cm (42 in.). The highest and lowest temperatures recorded (about 1950-1980) were 33°C (91°F) and -17°C (2°F), respectively.[1]

Month	Avg. Temperature[1] Max. °C	Max. °F	Min. °C	Min. °F	Mean °C	Mean °F	R.H.[1] %	Total Precip.[1] (cm)	(in)	Avg. Daily Radiation[2] (MJ/m^2)	(BTU/ft²)
Jan.	7	45	2	35	5	40	89	10.6	4.3	2.3	206
Feb.	7	45	2	35	5	40	87	7.2	2.8	4.5	397
Mar.	10	50	3	38	7	44	82	6.3	2.5	8.5	751
Apr.	13	56	5	41	9	49	74	6.5	2.6	11.8	1040
May	16	61	8	46	12	54	74	7.6	3.0	15.8	1393
June	19	66	11	52	15	59	73	6.3	2.5	18.4	1620
July	20	69	12	54	16	61	76	8.9	3.5	17.4	1532
Aug.	21	69	13	55	17	62	78	9.7	3.8	13.7	1210
Sep.	18	64	11	51	15	58	81	9.9	3.9	10.2	902
Oct.	14	58	8	46	11	52	85	10.9	4.3	6.0	533
Nov.	10	51	5	41	8	46	88	11.6	4.7	3.4	298
Dec.	8	46	3	37	7	42	89	10.8	4.3	2.1	181
TOTAL								106.5	42.2		
AVERAGES	14	57	7	44	11	51	81			9.5	841

[1]Temperature, humidity, and precipitation data is from p. 375 of World Weather Guide, E. A. Pearce and C. G. Smith, New York Times Book Company, 1984 (ASU library). The reported weather is for Cardiff, Wales, 52°29'N, 1°56'W, elevation 163m (535 ft), about 20 km (12 mi) southwest of Newport along the mouth of the Severn. The averages and extremes for temperature, humidity, and precipitation are based on a 30 year period ending in 1980. It is most likely that a maximum-minimum type thermometer was used since the mean daily temperature is not reported. For this table, the mean was taken to be the average between maximum and minimum temperatures. The humidity was recorded at 0900 hours.

[2]The radiation data is from p. 80 of European Solar Radiation Atlas, vol 1, W. Palz, ed., Commission of European Communities, 1984 (DSET library). The weather station reported in Malvern, England, 52°06'N, 2°18'W, elevation 63m, (207 ft) about 60km (37 mi) northeast of Newport.

MILAN, TN

Location: 34° 56'N, 88° 46'W

Elevation: 131m (430 ft)

Milan is located in the Mississippi River Valley in western Tennessee about 80 km (50 mi) east of the Mississippi River and 160 km (99 mi) northeast of Memphis. The average temperature is 15°C (59°F), the estimated average relative humidity is 69%, and the average annual precipitation is 135 cm (53 in). The highest and lowest temperatures recorded (1951-1980) were 42°C (108°F) in July, 1952, and the lowest -31°C (23°F) in February, 1962, respectively.[1]

Month	Avg. Temperature[1] Max. °C	Max. °F	Min. °C	Min. °F	Mean °C	Mean °F	R.H.[2] %	Total Precip.[1] (cm)	(in)	Avg. Daily Radiation[3] (MJ/m^2)	(BTU/ft2)
Jan.	8	46	-3	26	2	36	71	11.8	4.6	7.7	683
Feb.	10	50	-2	29	4	40	68	11.5	4.5	10.7	945
Mar.	15	59	3	38	9	49	65	14.5	5.7	14.5	1278
Apr.	22	71	9	48	15	60	64	13.2	5.2	18.6	1639
May	26	79	14	56	20	68	67	13.1	5.1	21.4	1885
June	30	87	18	64	24	76	69	10.8	4.3	23.2	2045
July	32	90	20	68	26	79	70	10.0	3.9	22.4	1972
Aug.	32	89	19	66	25	78	70	9.8	3.9	20.7	1824
Sep.	29	83	15	59	22	71	71	9.9	3.9	16.7	1471
Oct.	23	73	8	46	15	59	68	6.8	2.7	13.7	1205
Nov.	15	60	3	37	9	48	68	11.4	4.5	9.3	817
Dec.	10	50	-1	30	4	40	70	12.1	4.8	7.1	629
TOTALS								134.9	53.1		
AVERAGES	21	70	9	47	15	59	69			15.5	1366

[1]Based on an average of data taken at Milan, TN from 1951 to 1980. The data was obtained from p. 1031 of Climates of the States, Vol. 2, National Oceanic and Atmospheric Administration, 3rd ed., 1985, Gale Research Company, Detroit, MI (DSET Library).

[2]Since humidity data is not published for Milan, this data is for Memphis, TN (elevation 79 m [258 ft]), about 160 km (99 mi) SW of Milan. Since both Milan and Memphis are in the western (flat) portion of Tennessee, it is not expected that there would be significant differences between the humidity in Milan and Memphis. This data is from the same source as 1 (p. 1037). Humidity at Memphis is recorded at 0600, 1200, 1800, and 2400 hours. The average humidity is the mean of these four recorded values. The averages are based on a 44 year period ending in 1980. (DSET Library).

[3]Radiation data is from the Insolation Data Manual, Connie L. Knapp, Thomas L. Stoffel, and Stephen D. Whittaker, Solar Energy Research Institute, Golden, CO, 1980. The radiation data is for Memphis (ASU Library).

CAMDEN, AR

Location: 33°36'N, 92°49'W

Elevation: 35m (116 ft)

Camden is located in the Mississippi River Valley in southern Arkansas about 140 km (87 mi) south of Little Rock and about 140 km (87 mi) west of the Mississippi River. The average temperature is 17°C (63°F), the estimated average relative humidity is 70%, and the average annual precipitation is 128 cm (50 in). The highest and lowest temperatures recorded (1951-1980) were 44°C (111°F) in July of 1954 and -22°C (-8°F) in February of 1951, respectively.[1]

Month	Avg. Temperature[1] Max. °C	Max. °F	Min. °C	Min. °F	Mean °C	Mean °F	R.H.[2] %	Total Precip.[1] (cm)	(in)	Avg. Daily Radiation[3] (MJ/m^2)	(BTU/ft2)
Jan.	12	54	-1	31	6	42	70	11.1	4.4	8.3	731
Feb.	15	59	1	34	8	47	67	10.0	3.9	11.4	1003
Mar.	20	67	5	41	12	54	65	12.4	4.9	14.9	1313
Apr.	25	77	11	51	18	64	67	13.0	5.1	18.3	1611
May	28	83	15	59	22	71	72	12.0	4.7	21.9	1929
June	32	90	19	67	26	78	70	9.3	3.7	23.9	2107
July	34	94	21	70	28	82	72	10.4	4.1	23.1	2032
Aug.	34	93	20	69	27	81	71	7.8	3.1	21.1	1861
Sep.	31	87	17	62	24	75	74	11.4	4.5	17.2	1518
Oct.	25	78	10	49	18	64	70	7.0	2.8	13.9	1228
Nov.	19	66	4	40	11	53	71	11.6	4.6	9.6	847
Dec.	14	57	1	33	7	45	71	11.7	4.6	7.6	674
TOTALS								127.7	50.3		
AVGS	24	75	10	51	17	63	70			15.9	1404

[1]Temperature and precipitation data is from p. 64 of Climates of the States, Vol. 1, National Oceanic and Atmospheric Administration, 3rd ed., 1985, Gale Research Company, Detroit, MI (DSET Library). The weather station reported is Camden. The averages and extremes for temperature and precipitation are based on the period 1951-1980.

[2]Humidity data is from the same source as (1) (p. 77), but since humidity data is not published for Camden, this data is for Little Rock, 140 km (87 mi) north of Camden. Humidity is recorded at 0600, 1200, 1800, and 2400 hours. The average humidity is the mean of these four values. The averages are based on a 23 year period ending in 1980.

[3]Radiation data is from p. 28 of the Insolation Data Manual, Connie L. Knapp, Thomas L. Stoffel, and Stephen D. Whittaker, Solar Energy Research Institute, Golden, CO, 1980 (ASU Library). The radiation data is for Little Rock.

MINDEN, LA

Location:32°36'N, 93°18'W

Elevation:76 m (250 ft)

Minden is located in northwestern Louisiana about 50 km east of Shreveport. The average temperature is 18°C (64°F), the estimated average relative humidity is 72%, and the average annual precipitation is 123 cm (48 in). The highest and lowest temperatures recorded (1951-1980) were 42°C (108°F) in August of 1951 and -18°C in (0°F) January of 1962, respectively.[1]

Month	Avg. Temperature[1] Max. °C	Max. °F	Min. °C	Min. °F	Mean °C	Mean °F	R.H.[2] %	Total Precip.[1] (cm)	(in)	Avg. Daily Radiation[3] (MJ/m^2)	(BTU/ft2)
Jan.	13	56	1	34	7	45	73	11.1	4.4	8.7	762
Feb.	16	61	3	37	9	49	69	10.2	4.0	11.8	1038
Mar.	20	68	6	43	13	56	68	11.1	4.4	15.2	1342
Apr.	25	77	12	53	18	65	70	11.7	4.6	18.3	1613
May	29	83	16	61	22	72	73	13.8	5.4	21.4	1886
June	32	90	20	68	26	79	73	9.6	3.8	23.4	2065
July	34	93	22	71	28	82	72	10.8	4.3	22.9	2014
Aug.	34	93	21	70	28	82	72	7.6	3.0	21.3	1877
Sep.	31	88	18	64	25	76	73	8.3	3.3	17.6	1554
Oct.	26	79	11	52	19	65	71	6.4	2.5	14.8	1304
Nov.	20	67	6	42	13	55	73	10.7	4.2	10.5	929
Dec.	15	59	2	36	9	47	74	11.3	4.4	8.3	731
TOTALS								122.6	48.3		
AVERAGES	25	76	11	53	18	64	72			16.2	1426

[1]Temperature and precipitation data is from p. 466 of Climates of the States, Vol. 2, National Oceanic and Atmospheric Administration, 3rd ed., Gale Research Company, Detroit, MI (DSET Library). The weather station reported is Minden. The averages and extremes for temperature and precipitation are based on the period 1951-1980.

[2]Humidity data is from the same source as (1) (p. 472), but since humidity is not published for Minden, this data is for Shreveport (32° 28'N, 93° 49'W, elevation 77 m [254 ft]), about 50 km (31 mi) west of Minden. Humidity is recorded at 0600, 1200, 1800, and 2400 hours. The average humidity is the mean of these four values. The averages are based on a 31 year period ending in 1980.

[3]Radiation data is from p. 95 of the Insolation Data Manual, Connie L. Knapp, Thomas L. Stoffel, and Stephen D. Whittaker, Solar Energy Research Institute, Golden, CO, 1980 (ASU Library). The radiation data is for Shreveport, LA.

INDEPENDENCE, MO

Location: 39°N, 94.5°W

Elevation: Approx. 250m (820 ft)

Independence is located near Kansas City at the western edge of Missouri. The average temperature is 14°C (56°F), the average relative humidity is 64%, and the average annual precipitation is 75 cm (29 in). The highest and lowest temperatures recorded (1951-1980) were 43°C (109°F) in July of 1980 and -26°C (-14°F) in January of 1982, respectively.[1]

Month	Avg. Temperature[1] Max. °C	Max. °F	Min. °C	Min. °F	Mean °C	Mean °F	R.H.[1] %	Total Precip.[1] (cm)	(in)	Avg. Daily Radiation[2] (MJ/m^2)	(BTU/ft2)
Jan.	3	37	-7	19	-2	28	66	2.5	1.0	7.4	648
Feb.	6	44	-4	25	1	34	65	2.7	1.1	10.2	895
Mar.	12	54	1	34	6	44	60	5.4	2.1	13.7	1203
Apr.	20	67	8	46	14	57	58	6.8	2.7	17.9	1575
May	25	77	14	57	19	67	63	8.7	3.4	21.3	1873
June	30	85	19	66	24	76	68	10.5	4.1	23.6	2080
July	33	91	22	71	27	81	64	8.9	3.5	23.9	2102
Aug.	32	89	21	69	26	79	65	8.0	3.2	21.1	1862
Sep.	27	81	16	61	22	71	66	8.5	3.3	16.5	1452
Oct.	21	71	9	49	15	60	61	6.5	2.6	12.4	1092
Nov.	13	55	1	34	7	45	67	3.1	1.2	8.4	737
Dec.	6	43	-4	26	1	34	69	2.9	1.1	6.4	562
TOTAL								74.5	29.3		
AVGS	19	66	8	47	14	56	64			15.2	1340

[1]Temperature, humidity and precipitation data is from p. 632 of Climates of the States, Vol. 2, National Oceanic and Atmospheric Administration, 3rd ed., 1985, Gale Research Company, Detroit, MI (DSET Library). The weather station reported is the downtown Kansas City airport, 39° 07'N, 94° 36'W, elevation 226 m (742 ft). The averages and extremes for temperature, precipitation, and humidity are based on the period 1951-1980. Humidity is recorded at 0600, 1200, 1800, and 2400 hours; the average daily humidity is the mean of these four values.

[2]The radiation data is from p. 116 of the Insolation Data Manual, Connie L. Knapp, Thomas J. Stoffel, and Stephen D. Whittaker, Solar Energy Research Institute, Golden, CO, 1980 (ASU Library). The weather station reported is Kansas City.

48N to 52N, 6E to 12E
(Excluding East Germany)

TEMPERATURE

Three sources (referenced as (1), (2), and (3)) were found to contain significant data. The variety of this data is described below:

Source	# Cities	Avg. Daily Temps.	Max/Min Temps.	Extreme Temps.
(1)	4	Yes	Yes	Yes
(2)	7	Yes	Yes	No
(3)	134	Yes	No	No

Using source (3) which only contains average daily temperatures (by month), the warmest cities within the designated area are as follows:

City	Latitude	Longitude	Elevation		Avg. Temps. July		Entire Year	
			(m)	(ft)	(°C)	(°F)	(°C)	(°F)
Koblenz	50°21'N	7°36'E	66	217	19.1	66.4	10.5	50.9
Leverkusen	51°02'N	6°59'E	44	144	18.6	65.5	10.3	50.5
Freiberg	48°01'N	7°51'E	259	850	19.4	66.9	10.3	50.5
Frankfurt	50°07'N	8°40'E	103	338	19.4	66.9	10.2	50.4
Dusseldorf	51°13'N	6°45'E	36	118	18.4	65.1	10.2	50.4

Source (1) contains the most complete information since it also includes temperature extremes. Frankfurt is one of the cities listed in source (1) and it is one of the warmest cities in West Germany based on source (3).

Using a similar approach, the coldest cities within the designated area based on source (3) are listed in the following table:

City	Latitude	Longitude	Elevation		Avg. Temps. Jan.		Entire Year	
			(m)	(ft)	(°C)	(°F)	(°C)	(°F)
Hof	50°19'N	11°55'E	471	1545	-2.9	26.8	6.7	44.1
Kahler Asten	51°11'N	8°29'E	836	2743	-3.1	26.4	5.0	41.0
Tenschnitz	50°24'N	11°23'E	622	2041	-3.6	25.5	6.2	43.2
Wasserkuppe	50°30'N	9°57'E	920	3018	-3.9	25.0	4.8	40.6

None of the four cities listed above are included in source (1). However, it is surprising that only a 6°C difference exists between the coldest and warmest locations within the entire designated area.

Of the four cities listed in source (1), the coolest is Munich.

Munich	48°10'N	11°30'E	515	1690	-2.1	28.2	7.9	46.2

Munich is approximately 2°C warmer than the four cities listed above.

Using Munich and Frankfurt as a guide, we could use source (1) to estimate the following temperature extremes:

Highest recorded: 38°C (101°F) (Frankfurt, July)
Lowest recorded: -30°C (-21°F) (Munich, February)

The complete temperature data for these two cities are listed in the following tables:

	FRANKFURT (WARM)								MUNICH (COLD)							
	Highest		Avg. Daily				Lowest		Highest		Avg. Daily				Lowest	
Month	Recorded		Max.		Min.		Recorded		Recorded		Max.		Min.		Recorded	
	°C	°F	°C	°F	°C	°F	°C	°F	°C	°F	°C	°F	°C	°F	°C	°F
Jan.	14	57	3	38	-2	29	-24	-11	16	62	1	35	-5	23	-29	-20
Feb.	18	65	5	41	-1	30	-19	-3	20	68	3	38	-5	23	-30	-21
Mar.	24	75	11	51	2	35	-8	17	24	74	9	48	-1	30	-18	0
Apr.	31	87	16	60	6	42	-4	26	29	84	14	56	3	38	-16	3
May	34	94	20	69	9	49	-2	29	31	87	18	64	7	45	-6	22
Jun.	38	101	23	74	13	55	4	39	35	94	21	70	11	51	3	37
Jul.	38	101	25	77	15	58	8	46	35	95	23	74	13	55	5	40
Aug.	38	100	24	76	14	57	7	44	36	96	23	73	12	54	3	38
Sep.	34	94	21	69	11	52	1	33	32	90	20	67	9	40	-3	28
Oct.	26	78	14	58	7	44	-4	25	28	82	13	56	4	40	-6	21
Nov.	19	65	8	47	3	38	-7	19	20	67	7	44	0	33	-12	10
Dec.	14	56	4	39	0	32	-18	0	16	60	2	36	-4	26	-22	-8

The Frankfurt and Munich data reported are from source (1) and represent 29 years of data ending in 1980.

If the designated area were expanded to include West Germany south of latitude 48°N (German Alps), the cold temperatures would decrease by 10° to 15°C (18 to 27°F).

HUMIDITY

Surprisingly, the humidity listed for the cities in source (1) all have almost identical relative humidity averages:

	(29) Frankfurt		(27) Freiberg		(28) Kassel		(29) Munich	
Month	0630h	1330h	0630h	1330h	0630h	1320h	0700h	1400h
Jan.	86	77	85	78	87	81	87	77
Feb.	86	70	85	72	87	75	87	71
Mar.	84	57	83	60	87	64	86	61
Apr.	79	51	80	56	83	58	82	55
May	78	50	81	57	82	55	81	57
Jun.	78	52	81	60	82	56	80	58
Jul.	81	53	80	58	85	58	81	57
Aug.	85	54	84	59	88	57	85	58
Sep.	89	60	88	63	91	62	89	61
Oct.	91	68	90	70	92	70	91	68
Nov.	89	77	88	76	89	79	92	78
Dec.	88	81	86	79	89	84	90	82

The data reported is from source (1). The number above each city is the number of years of data used to obtain the reported averages. The extreme humidity should be taken as 100%.

PRECIPITATION

Source (3) contains average monthly precipitation for 104 cities within the designated area. The city with the highest annual precipitation is Treiberg (elevation 683m [2241 ft], 48°00'N, 9°14'E):

Month	Average Total Precip.	
	cm	in
Jan.	15.7	6.2
Feb.	13.4	5.3
Mar.	9.9	3.9
Apr.	9.5	3.7
May	10.2	4.0
Jun.	13.7	5.4
Jul.	13.2	5.2
Aug.	13.3	5.2
Sep.	11.8	4.7
Oct.	11.4	4.5
Nov.	12.8	5.0
Dec.	11.2	4.4
TOTALS	146.1	57.5

The reported data is based on a 30 year period.

RADIATION

Source (4) contains radiation data for 41 stations within the designated area. Of these stations, the greatest annual radiation occurs in Augsberg, latitude 48°26'N, longitude 10°56'W, elevation 461 m (1512 ft). Data for Augsburg based on recordings of radiation from 1966 to 1975 are as follows:

Month	Avg. Daily Radiation	
	MJ/m^2	BTU/ft^2
Jan.	3.9	347
Feb.	6.7	587
Mar.	10.7	940
Apr.	15.1	1330
May	18.6	1641
Jun.	19.6	1728
Jul.	20.1	1774
Aug.	16.5	1450
Sep.	13.6	1200
Oct.	7.9	699
Nov.	4.3	382
Dec.	3.1	273
TOTAL	11.7	1031

SOURCES

(1) World Weather Guide, E.A. Pearce and C.G. Smith, New York Times Book Company, 1984 (ASU Library)

(2) World Climates, Willy Rudloff, Wissenschaftliche Verlagsgesellschaft, Stuttgart, 1981 (ASU Library)

(3) World Climatic Data, Frederick L. Wernstedt, Climatic Data Press, 1972 (ASU Library)

(4) European Solar Radiation Atlas, Volume 1, W. Palz, Editor, Commission of the European Communites, Brussels and Luxembourg, 1984 (DSET Library)

CHARLESTOWN, IN

Location: Approx. 38°N, 86°W

Elevation: Approx. 150m

Charlestown is located in southern Indiana about 30km (19 mi) north of Louisville and the Ohio River. The average temperature is 13°C (56°F), the average relative humidity, 69%, and the average annual precipitation 111 cm (44 in). The highest and lowest temperatures recorded (1951-1980) were 41°C (105°F) in July of 1954 and -29°C (-20°F) in January of 1963, respectively.[1]

Month	Avg. Temperature[1] Max. °C	Max. °F	Min. °C	Min. °F	Mean °C	Mean °F	R.H.[1] %	Total Precip.[1] (cm)	(in)	Avg. Daily Radiation[2] (MJ/m^2)	(BTU/ft2)
Jan.	5	41	-4	24	11	53	70	8.6	3.4	6.2	546
Feb.	7	45	-3	27	2	36	68	8.2	3.2	9.0	789
Mar.	13	55	2	35	7	45	65	12.0	4.7	12.5	1102
Apr.	20	68	8	46	14	57	62	10.4	4.1	16.6	1467
May	25	76	13	55	19	65	67	10.5	4.2	19.5	1720
June	29	84	17	63	23	74	70	9.1	3.6	21.6	1904
July	31	88	20	68	25	78	71	10.4	4.1	20.9	1838
Aug.	30	87	19	66	25	76	72	8.4	3.3	19.1	1680
Sep.	27	81	15	59	21	70	74	8.5	3.4	15.4	1361
Oct.	21	69	8	46	14	58	70	6.7	2.6	11.8	1042
Nov.	13	56	3	37	8	46	70	8.9	3.5	7.4	652
Dec.	7	45	-2	29	3	37	70	8.8	3.5	5.5	488
TOTAL								110.5	43.6		
AVERAGES	19	66	8	46	13	56	69			13.8	1216

[1]Temperature, humidity, and precipitation data is from p. 451 of Climate of the States, vol. 1, National Oceanic and Atmospheric Administration, 3rd ed., 1985, Gale Research Company, Detroit, MI (DSFT library). The weather station reported is Louisville (38°11'N, 85°44'W, elevation 145 m [477 ft]), about 30km (19 mi) south of Charlestown. The averages and extremes for temperature, precipitation, and precipitation are based on a 23 year period ending in 1980. Humidity is recorded at 0100, 0700, 1300, and 1900 hours. The average daily humidity is the mean of these four values.

[2]The radiation data is from p. 91 of the Insolation Data Manual, Connie L. Knapp, Thomas J. Stoffel, and Stephen D. Whittaker, Solar Energy Research Institute, Golden, CO, 1980. The weather station reported is Louisville, KY., latitude, longitude, and elevation as in (1) above.

MIESAU, WEST GERMANY

Location: 49N, 8E

Elevation: 232 m (761 ft)[4]

Miesau is located in southwestern Germany about 40 km (25 mi) northeast of Saarbrucken (elevation 188 m [616 ft]) on the French border, and about 30 km (19 mi) southwest of Kaiserslautern (elevation 280 m [918 ft]). The estimated average temperature is 11°C (51°F), the estimated average relative humidity is 74%, and the estimated average annual precipitation is 77 cm (30 in). The estimated highest and lowest temperatures recorded during a 30 year period are 38°C (101°F) and -24°C (-11°F), respectively.[1]

Month	Avg. Temperature[1] Max.		Min.		Mean		R.H.[1] %	Total Precip.[2] (cm)	(in)	Avg. Daily Radiation[3] (MJ/m^2)	(BTU/ft2)
	°C	°F	°C	°F	°C	°F					
Jan.	3	38	-2	29	1	34	82	7.5	3.0	2.6	232
Feb.	5	41	-1	30	2	36	78	6.3	2.5	5.5	484
Mar.	11	51	2	35	7	43	71	4.6	1.8	9.0	791
Apr.	16	60	6	42	11	51	65	5.5	2.2	13.5	1186
May	20	69	9	49	15	59	64	5.7	2.2	17.3	1523
June	23	74	13	55	18	65	65	6.9	2.7	18.6	1643
July	25	77	15	58	20	68	67	6.7	2.6	18.5	1628
Aug.	24	76	14	57	19	66	70	7.7	3.0	15.5	1366
Sep.	21	69	11	52	16	61	75	6.5	2.6	11.9	1045
Oct.	14	58	7	44	11	51	80	5.8	2.3	6.7	593
Nov.	8	47	3	38	6	43	83	6.7	2.6	3.2	279
Dec.	4	39	0	32	2	36	85	6.9	2.7	2.1	188
TOTALS								76.8	30.2		
AVERAGES	15	58	6	43	11	51	74			10.4	915

[1]Temperature and humidity data is from p. 371 of World Weather Guide, E. A. Pearce and C. G. Smith, New York Times Book Company, 1984 (ASU Library). The reported weather is for Frankfurt, a full 150 km (93 mi) northeast of Miesau. The closest cities for which any data could be found are Kaiserlautern and Saarbrucken. Only averages could be found at these locations. A comparison of averages (1942-1972) for Kaiserlautern, Saarbrucken, Frankfurt, and Nancy (in France, 150 km southwest of Miesau) from p. 185, 192, 193, and 195 of World Climatic Data, Frederick L. Wernstedt, Climatic Data Press, 1972 (ASU Library), is as follows:

	J	F	M	A	M	J	J	A	S	O	N	D
Kaiserlautern	0°C	1°C	5°C	8°C	13°C	16°C	18°C	17°C	14°C	9°C	5°C	1°C
	32°F	33°F	40°F	47°F	55°F	61°F	64°F	62°F	57°F	48°F	40°F	34°F
Saarbrucken	1°C	2°C	6°C	10°C	14°C	17°C	19°C	18°C	15°C	10°C	6°C	2°C
	34°F	36°F	42°F	50°F	57°F	63°F	66°F	64°F	59°F	50°F	42°F	36°F
Frankfurt	1°C	2°C	6°C	10°C	15°C	18°C	19°C	19°C	15°C	10°C	6°C	2°C
	33°F	35°F	43°F	51°F	58°F	64°F	67°F	66°F	59°F	50°F	42°F	36°F
Nancy, FR	1°C	2°C	6°C	9°C	13°C	16°C	18°C	18°C	15°C	10°C	5°C	2°C
	34°F	36°F	42°F	49°F	56°F	61°F	65°F	64°F	59°F	50°F	42°F	35°F

Very complete data is available for Frankfurt and Nancy. The Frankfurt data is very similar to Saarbrucken which is close to Miesau. The averages and extremes are based on a 29 year period ending approximately in 1980. The mean daily temperature was taken to be the average between the maximum and minimum temperatures. Humidity data at Frankfurt was recorded at 0630 and 1330 hours. The humidity reported is the average of these two values.

[2]The precipitation data is from p. 195 of World Climatic Data, Frederick L. Wernstedt, Climatic Data Press, 1972 (ASU Library). The data reported is for Saarbrucken (elevation 188 m (616 ft), about 40 km (25 mi) southwest of Miesau and covers the period 1942-1972. Saarbrucken was chosen instead of Kaiserslautern because Saarbrucken receives about 10% more precipitation.

[3]The radiation data is from European Solar Radiation Atlas, Vol. 1, W. Palz, ed., Commission of European Communities, 1984 (DSET Library). The data reported is for Saarbrucken.

[4]The elevation of Miesau was obtained from Jasper Griggs.

PINE BLUFF, ARKANSAS

Location: 34°13'W, 92°01'W

Elevation: 66 m (215 ft)

Pine Bluff is located in the Mississippi River valley in west central Arkansas about 75 km (47 mi) west of the Mississippi River and 50 km (31 mi) southeast of Little Rock. The average temperature is 18°C (64°F), the estimated average relative humidity is 70%, and the average annual precipitation is 128 cm (50 in). The highest and lowest temperatures recorded (1951-1980) were 43°C (110°F) in July and August of 1954 and -18°C (-1°F) in January of 1966, respectively.[1]

Month	Avg. Temperature[1] Max. °C	Max. °F	Min. °C	Min. °F	Mean °C	Mean °F	R.H.[2] %	Total Precip.[1] (cm)	(in)	Avg Daily Radiation[3] (MJ/m^2)	(BTU/ft2)
Jan.	12	53	1	33	6	43	70	11.2	4.4	8.3	731
Feb.	14	58	2	36	8	47	67	11.0	4.4	11.4	1003
Mar.	19	66	6	43	13	55	65	12.9	5.1	14.9	1313
Apr.	25	76	12	53	18	65	67	13.4	5.3	18.3	1611
May	28	83	16	61	22	72	72	14.3	5.6	21.9	1929
June	32	90	20	68	26	79	70	7.7	3.1	23.9	2107
July	34	94	22	72	28	83	72	9.2	3.6	23.1	2032
Aug.	34	93	21	70	28	82	71	7.8	3.1	21.1	1861
Sep.	30	87	18	64	24	75	74	9.6	3.8	17.2	1518
Oct.	25	77	11	52	18	65	70	8.1	3.2	13.9	1228
Nov.	18	65	6	42	12	53	71	10.5	4.2	9.6	847
Dec.	13	56	2	36	8	46	71	12.0	4.7	7.6	674
TOTALS								127.7	50.3		
AVERAGES	24	75	11	53	18	64	70			15.9	1404

[1]Temperature and precipitation data is from p. 73 of Climates of the States, Vol. 1, National Oceanic and Atmospheric Administration, 3rd ed., 1985, Gale Research Company, Detroit, MI (DSET Library). The weather station reported is Pine Bluff. The averages and extremes for temperature and precipitation are based on the period 1951-1980.

[2]Humidity data is from the same source as (1) (p. 77) but since humidity data is not published for Pine Bluff, this data is for Little Rock, AR (34° 44'N, 92° 14'W, elevation 78 m [257 ft]), about 50 km (31 mi) northwest of Pine Bluff. Humidity is recorded at 0600, 1200, 1800, and 2400 hours. The average humidity is the mean of these four values. The averages are based on a 23 year period ending in 1980.

[3]Radiation data is from p. 28 of the Insolation Data Manual, Connie L. Knapp, Thomas L. Stoffel, and Stephen D. Whittaker, Solar Energy Research Institute, Golden, CO, 1980 (ASU Library). The radiation data is for Little Rock.

CONCORD, CA

Location: 38°N, 122°W

Elevation: Near Sea Level

Concord is located in the San Francisco Bay area about 25 km (16 mi) east of Richmond and 30 km (19 mi) northeast of Oakland. The estimated average temperature is 15°C (58°F), the estimated average relative humidity is 75%, and the estimated average annual precipitation is 56 cm (22 in). The estimated highest and lowest temperatures recorded during the period 1951-1980 were 42°C (107°F) and -4°C (24°F), respectively.[1]

Month	Avg. Temperature[1] Max. °C	Max. °F	Min. °C	Min. °F	Mean °C	Mean °F	R.H.[2] %	Total Precip.[1] (cm)	(in)	Avg. Daily Radiation[3] (MJ/m^2)	(BTU/ft2)
Jan.	14	57	6	42	10	50	73	12.6	5.0	8.0	708
Feb.	16	62	7	45	12	53	74	8.5	3.3	11.5	1018
Mar.	17	63	8	46	13	55	70	6.8	2.7	16.5	1456
Apr.	19	66	9	48	14	57	71	4.4	1.7	21.8	1922
May	20	69	11	51	16	60	77	0.8	0.3	25.1	2211
June	21	70	12	54	17	62	80	0.3	0.1	26.7	2350
July	21	70	13	55	17	62	82	0.2	0.1	26.4	2323
Aug.	21	70	13	56	17	63	82	0.2	0.1	23.3	2053
Sep.	23	74	14	56	18	65	75	0.8	0.3	19.3	1701
Oct.	22	72	12	53	17	63	69	3.1	1.2	13.8	1212
Nov.	18	65	9	48	13	56	73	7.2	2.8	9.3	822
Dec.	15	58	6	43	10	51	72	10.6	4.2	7.3	647
TOTALS								55.5	21.8		
AVERAGES	19	66	10	50	15	58	75			17.4	1535

[1]Temperature and precipitation data is from p. 112 of Climates of the States, Vol. 1, National Oceanic and Atmospheric Administration, 3rd ed., 1985, Gale Research Company, Detroit, MI (DSET Library). The weather station reported is Richmond (37° 56'N, 122° 21'W, elevation 17 m [55 ft]) about 25 km (16 mi) west of Concord. The averages and extremes for temperature and precipitation are based on the period 1951-1980.

[2]Humidity data is from the same source as (1) (p. 129), but since humidity data is not published for Richmond, this data is for San Francisco (Mission Dolores, elevation 22m [75 ft], 37° 46'N, 122° 26'W), about 40 km (25 mi) southwest of Concord. Humidity is recorded at 0400, 1000, 1600, and 2200 hours. The average humidity is the mean of these four values. The averages are based on the period 1951-1980.

[3]Radiation data is from p. 39 of the Insolation Data Manual, Connie L. Knapp, Thomas L. Stoffel, and Stephen D. Whittaker, Solar Energy Reserach Institute, Golden, CO, 1980 (ASU Library). The radiation data is for Oakland, CA, about 30 km (19 mi) southwest of Concord.

CANAL ZONE, PANAMA

Location: 9°N, 80°W
Elevation: Near Sea Level

The Canal Zone in Panama is at the southeastern tip of Central America about 320 km (200 mi) northwest of the Columbian border. The average annual temperature is 27°C (80°F), the average relative humidity is 88%, and the average annual precipitation is 177 cm (70 in). The highest and lowest temperatures recorded during a 34 year period ending in 1980 were 36°C (97°F) and 17°C (63°F), respectively.[1]

Month	Average Temperature[1] Max. °C	Max. °F	Min. °C	Min. °F	Mean °C	Mean °F	R.H.[1] (%)	Total Precip.[2] (cm)	(in)	Avg. Daily Radiation[3] (MJ/m^2)	(BTU/ft^2)
Jan.	31	88	22	71	27	80	86	9.2	3.6	18.9	1663
Feb.	32	89	22	71	27	80	83	4.2	1.7	20.5	1803
Mar.	32	90	22	72	27	81	80	3.0	1.2	20.4	1799
Apr.	31	87	23	74	27	81	81	14.3	5.6	18.7	1648
May	30	86	23	74	27	80	88	33.1	13.0	15.3	1349
Jun.	31	87	23	74	27	81	90	35.4	13.9	13.3	1169
Jul.	31	87	23	74	27	81	91	34.5	13.6	14.7	1298
Aug.	30	86	23	74	27	80	91	37.8	14.9	14.2	1254
Sep.	29	85	23	74	26	80	91	30.1	11.9	14.0	1231
Oct.	29	85	23	73	26	79	91	41.8	16.5	13.3	1176
Nov.	29	85	23	73	26	79	92	48.5	19.1	13.9	1228
Dec.	31	87	23	73	27	80	90	26.1	10.3	16.7	1475
Totals								318.0	125.3		
Averages	31	87	23	73	27	80	88			16.2	1424

[1]Temperature, humidity and precipitation data is from p. 196 of World Weather Guide, E.A. Pearce and C.G. Smith, New York Times Book Company, 1984 (ASU Library). The reported weather is for Balboa Heights, Panama (8° 57'N, 79° 33'W, elevation 33m [118 ft.]). The averages and extremes for temperature and humidity are based on a 34 year period ending in 1980. The mean daily temperature was taken to be the average between the maximum and minimum temperatures. Humidity was recorded at 0730 and 1930 hours. The humidity reported is an average of these two values.

[2]Precipitation data is from a 3-5-87 telephone call with Mr. Weingarten of the Tropic Test Center, Fort Clayton, Panama. The data presented is for the Atlantic side of the Canal Zone, which receives about twice as much rainfall as the Pacific side.

[3]Radiation data is from the same source as note 2 above. The data presented is for the Pacific side of the Canal Zone which receives more radiation than the Atlantic side.

YUMA, ARIZONA

Location: 32° 40'N, 114° 36' W
Elevation: 59 m (141 ft)

Yuma is located in southwestern Arizona about 300 km (185 mi) southwest of Phoenix. The average temperature is 23°C (74°F), the average relative humidity is 37%, and the average annual precipitation is 7 cm (3 in). The highest and lowest temperatures recorded (1951-1980) were 49°C (120°F) in August of 1981 and -4°C (24°F) in January of 1971, respectively.[1]

Month	Average Temperature[1] Max. °C	Max. °F	Min. °C	Min. °F	Mean °C	Mean °F	R.H.[1] (%)	Total Precip.[1] (cm)	(in)	Avg. Daily Radiation[2] (MJ/m^2)	(BTU/ft^2)
Jan.	20	69	6	43	13	56	43	1.0	0.4	12.4	1096
Feb.	23	74	8	46	16	60	40	0.7	0.3	16.4	1443
Mar.	25	77	10	50	18	64	36	0.5	0.2	21.8	1919
Apr.	30	86	13	56	22	71	31	0.3	0.1	27.4	2413
May	34	94	17	63	26	78	29	0.1	0.0	31.0	2728
Jun.	39	103	22	71	31	87	27	0.0	0.0	31.9	2814
Jul.	42	107	27	80	34	94	36	0.4	0.2	27.8	2453
Aug.	41	105	26	80	34	92	39	1.1	0.4	26.4	2329
Sep.	39	101	23	73	31	87	40	0.6	0.3	23.3	2051
Oct.	33	91	17	62	25	76	38	0.7	0.3	18.4	1623
Nov.	25	77	10	50	18	64	41	0.5	0.2	13.8	1215
Dec.	21	69	7	44	14	57	46	0.9	0.3	11.4	1000
Totals								6.7	2.7		
Averages	31	88	15	60	23	74	37			21.8	1924

[1]Temperature, humidity and precipitation data is from p. 54 of Climates of the States, Vol. 1, National Oceanic and Atmospheric Administration, 3rd ed., 1985, Gale Research Company, Detroit, MI (DSET Library). The weather station reported is the Yuma International Airport (32° 40'N, 114° 36'W, elevation 59 m [194 ft]). The averages and extremes for temperature, precipitation and humidity are based on the period 1951-1980. Humidity is recorded at 0500, 1100, 1700, and 2300 hours. The average daily humidity is the mean of these four values.

[2]The radiation data is from the Insolation Data Manual, Connie L. Knapp, Thomas J. Stoffel, and Stephen D. Whittaker, Solar Energy Research Institute, Golden, CO, 1980. The weather station reported is the Yuma International Airport.

NEW ORLEANS, LOUISIANA

Location: 30°N, 90°W
Elevation: Sea Level

New Orleans is located near the southern end of the Mississippi River on the Gulf of Mexico in southern Louisiana. The average temperature is 20°C (68°F), the average relative humidity is 76%, and the average annual precipitation is 152 cm (60 in). The highest and lowest temperatures recorded (1951-1980) were 39°C (102°F) in August of 1980 and -10°C (14°F) in December of 1983, respectively.[1]

Month	Average Temperature[1] Max °C	Max °F	Min °C	Min °F	Mean °C	Mean °F	R.H.[1] %	Total Precip.[1] (cm)	(in)	Avg. Daily Radiation[2] (MJ/m^2)	(BTU/ft^2)
Jan.	17	62	6	43	11	52	77	12.6	5.0	9.5	835
Feb.	18	65	7	45	13	55	69	13.3	5.2	12.6	1112
Mar.	22	71	11	52	16	61	73	12.0	4.7	16.1	1415
Apr.	26	79	15	59	20	69	74	11.4	4.5	20.2	1780
May	29	85	19	65	24	75	75	12.9	5.1	22.3	1968
Jun.	32	90	22	71	27	80	76	11.7	4.6	22.7	2004
Jul.	33	91	23	74	28	82	80	17.1	6.7	20.6	1814
Aug.	32	90	23	73	28	82	80	15.3	6.0	19.5	1717
Sep.	30	87	21	70	26	79	79	14.9	5.9	17.2	1514
Oct.	26	80	15	59	21	69	76	6.7	2.7	15.2	1335
Nov.	21	70	10	50	16	60	76	10.3	4.0	11.0	973
Dec.	18	64	7	45	13	55	77	13.4	5.3	8.8	779
Totals								151.6	59.7		
Averages	25	78	15	60	20	68	76			16.3	1437

[1]Temperature, humidity, and precipitation data is from p. 472 of Climates of the States, Vol. 1, National Oceanic and Atmospheric Administration, 3rd ed., 1985, Gale Research Company, Detroit, MI (DSET Library). The weather station reported is the New Orleans International Airport (29° 59'N, 90° 15' W, elevation 1 m [4 ft]). The averages and extremes for temperature, precipitation and humidity are based on the period 1951-1980. Humidity is recorded at 0600, 1200, 1800 and 2400 hours. The average daily humidity is the mean of these four values.

[2]The radiation data is from the Insolation Data Manual, Connie L. Knapp, Thomas J. Stoffel, and Stephen D. Whittaker, Solar Energy Research Institute, Golden, CO, 1980. The weather station reported is the New Orleans International Airport.

ANCHORAGE, ALASKA

Location: 61°N, 149°W
Elevation: Near Sea Level

Anchorage is located on Cook Inlet off the Gulf of Alaska along Alaska's southern edge. The average temperature is 2°C (35°F), the average relative humidity is 71%, and the average annual precipitation is 39 cm (15 in). The highest and lowest temperatures recorded (1951-1980) were 29°C (85°F) in June of 1969 and -37°C (-34°F) in January of 1975, respectively.[1]

Month	Average Temperature[1] Max °C	Max °F	Min °C	Min °F	Mean °C	Mean °F	R.H.[1] %	Total Precip.[1] (cm)	(in)	Avg. Daily Radiation[2] (MJ/m^2)	(BTU/ft^2)
Jan.	-7	20	-14	6	-11	13	71	2.0	0.8	1.4	122
Feb.	-4	26	-12	10	- 8	18	71	2.4	0.9	3.8	334
Mar.	0	32	- 9	16	- 5	24	67	1.8	0.7	8.6	759
Apr.	6	43	- 2	28	2	35	65	1.7	0.7	14.2	1248
May	12	54	4	38	8	46	62	1.4	0.6	18.0	1583
Jun.	17	62	8	47	12	54	66	2.7	1.1	19.9	1751
Jul.	18	65	11	51	15	58	71	5.0	2.0	18.1	1598
Aug.	17	63	10	49	13	56	75	5.4	2.1	13.5	1189
Sep.	13	55	5	41	9	48	76	6.2	2.4	9.0	791
Oct.	5	41	- 2	28	1	35	75	4.4	1.7	5.0	437
Nov.	- 2	28	- 9	15	- 6	22	77	2.8	1.1	2.0	175
Dec.	- 6	20	-14	7	-10	14	75	2.8	1.1	0.7	64
Totals								38.6	15.2		
Averages	6	42	- 2	28	2	35	71			9.5	838

[1]Temperature, humidity, and precipitation data is from p. 27 of Climates of the States, Vol. 1, National Oceanic and Atmospheric Administration, 3rd ed., 1985, Gale Research Company, Detroit, MI (DSET Library). The weather station reported is the Anchorage International Airport (61° 10'N, 150° 01'W, elevation 35 m [114 ft]). The averages and extremes for temperature, precipitation, and humidity are based on the period 1951-1980. Humidity is recorded at 0200, 0800 1400, and 2000 hours. The average daily humidity is the mean of these four values.

[2]The radiation data is from p. 13 of the Insolation Data Manual, Connie L. Knapp, Thomas J. Stoffel, and Stephen D. Whittaker, Solar Energy Research Institute, Golden CO, 1980. The weather station reported is Homer, Alaska (59° 38'N, 151° 30'W, elevation 22 m [72 feet]), 160 km (100 mi) southwest of Anchorage.

FAIRBANKS, ALASKA

Location: 65°N, 147°W
Elevation: 133 m (436 ft)

Fairbanks is located in central Alaska about 200 km (125 mi) south of the Arctic Circle. The average temperature is -3°C (26°F), the average relative humidity is 63%, and the average annual precipitation is 26 cm (10 in). The highest and lowest temperatures recorded (1951-1980) were 36°C (96°F) in June of 1969 and -52°C (-62°F) in December of 1961, respectively.[1]

Month	Average Temperature[1] Max °C	Max °F	Min °C	Min °F	Mean °C	Mean °F	R.H.[1] %	Total Precip.[1] (cm)	(in)	Avg. Daily Radiation (MJ/m^2)	(BTU/ft^2)
Jan.	-20	- 4	-30	-22	-25	-13	66	1.3	0.5	0.3	30
Feb.	-14	7	-26	-15	-20	- 4	63	1.1	0.4	2.5	221
Mar.	- 6	22	-20	- 5	-13	9	59	1.0	0.4	7.7	674
Apr.	5	41	- 7	20	- 1	30	55	0.7	0.3	13.5	1194
May	15	59	3	37	9	48	48	1.4	0.6	18.2	1604
Jun.	21	70	9	49	15	59	55	3.4	1.3	19.9	1752
Jul.	22	71	11	52	16	62	64	4.5	1.8	17.5	1543
Aug.	19	67	8	47	14	57	67	4.7	1.9	12.7	1118
Sep.	12	54	2	35	7	45	68	2.8	1.1	8.1	709
Oct.	0	33	- 8	18	- 4	25	72	1.9	0.7	3.3	293
Nov.	-11	12	-20	- 5	-16	4	71	1.7	0.7	0.8	74
Dec.	-19	- 2	-28	-18	-23	-10	67	1.9	0.7	0.0	3
Totals								26.4	10.4		
Averages	2	36	- 9	16	- 3	26	63			8.7	768

[1]Temperature, humidity and precipitation data is from p. 31 of Climates of the States, Vol. 1, National Oceanic and Atmospheric Administration, 3rd ed., 1985, Gale Research Company, Detroit, MI (DSET Library). The weather station reported is the Fairbanks International Airport (64° 49'N, 147° 52' W, elevation 133 m [436 ft]). The averages and extremes for temperature, precipitation and humidity are based on the period 1951-1980. Humidity is recorded at 0200, 0800, 1400, and 2000 hours. The average daily humidity is the mean of these four values.

[2]The radiation data is from p. 11 of the Insolation Date Manual, Connie L. Knapp, Thomas J. Stoffel, and Stephen D. Whittaker, Solar Energy Research Institute, Golden, CO, 1980. The weather station reported is the Fairbanks International Airport.

(THIS PAGE LEFT BLANK)

APPENDIX C

ARIZONA ENVIRONMENTAL CONDITIONS

(THIS PAGE LEFT BLANK)

DSET
LABORATORIES, INC.

Box 1850
Black Canyon Stage I
Phoenix, Arizona 85029

Telephone: 602-465-7356
TWX: 910-950-4681 DSET PHX

THE WEATHER AT NEW RIVER, ARIZONA — NOVEMBER 1987

DATE	TEMPERATURE (degrees C) HIGH	LOW	MEAN	HUMIDITY (%) HIGH	LOW	MEAN	SOLAR RADIANT EXPOSURE (MJ/m2) TOTAL 45	U.G. 45	TOTAL 34	UV 34	TOTAL 5	TOTAL TRACK	TOTAL EMMAQUA	UV EMMAQUA	WET TIME (hr)	RAIN (cm)	AVG. WIND (km/hr)	SKY COND.
1	20	14	17	92	76	86	9.7	8.3	6.6	0.44	4.8	10.4	0	0.00	12.6	1.4	7.1	BKN
2	21	14	17	92	67	81	13.6	11.7	12.0	0.62	10.0	16.4	50	1.33	5.4	0.0	6.4	BKN
3	25	14	19	87	42	69	24.5	20.9	23.1	0.92	13.6	32.4	192	5.13	0.0	0.0	7.4	CLR
4	29	14	22	76	19	45	22.6	19.3	21.6	0.82	13.7	27.7	145	3.88	0.6	0.0	10.5	CLR
5	22	12	16	92	56	84	9.3	8.0	8.6	0.42	4.1	8.8	41	1.09	12.9	0.6	7.0	BKN
6	22	11	15	92	48	79	16.3	15.6	17.1	0.71	15.7	20.7	89	2.35	3.9	0.0	6.6	SCT
7	21	10	15	91	53	75	24.1	20.6	22.4	0.83	13.9	30.1	169	4.45	0.0	0.0	7.7	CLR
8	25	11	18	87	25	58	25.6	21.9	23.8	0.86	14.6	32.6	196	5.20	0.0	0.0	11.3	CLR
9	25	14	19	58	16	34	25.3	21.7	23.7	0.85	14.6	31.7	192	5.04	0.0	0.0	10.5	CLR
10	26	13	20	43	14	25	24.3	20.7	22.6	0.82	14.1	30.6	174	4.53	0.0	0.0	9.2	CLR
11	25	12	18	44	20	35	25.3	21.7	23.8	0.83	14.3	32.3	196	5.09	0.0	0.0	10.3	CLR
12	26	13	18	42	14	30	26.0	22.2	24.4	0.83	14.5	33.1	206	5.38	0.0	0.0	10.9	CLR
13	23	10	16	51	24	39	16.1	13.8	15.6	0.56	10.9	19.7	66	1.78	0.0	0.0	7.4	SCT
14	19	10	14	81	40	57	13.5	11.5	13.0	0.52	7.1	15.5	53	1.34	1.1	0.0	8.1	BKN
15	17	6	11	65	20	39	25.8	22.0	24.2	0.81	13.7	32.6	200	5.10	0.0	0.0	9.4	CLR
16	18	6	11	60	21	40	24.9	21.3	23.4	0.78	13.6	31.4	197	4.99	0.0	0.0	8.0	CLR
17	19	7	11	51	21	41	13.2	11.3	12.7	0.49	9.1	15.5	48	1.22	0.0	0.0	7.3	BKN
18	22	11	15	43	14	22	26.4	22.6	24.6	0.79	14.2	33.5	70	1.76	0.0	0.0	18.3	CLR
19	26	14	19	24	12	16	26.4	22.6	24.6	0.79	14.0	33.6	142	3.55	0.0	0.0	15.1	CLR
20	27	13	18	24	12	16	26.4	22.5	24.4	0.80	13.9	33.3	210	5.16	0.0	0.0	12.6	CLR
21	22	9	15	41	15	24	24.9	21.3	23.3	0.76	13.3	31.2	196	4.87	0.0	0.0	7.9	CLR
22	22	8	14	40	21	34	24.4	20.9	22.6	0.75	12.9	30.7	204	5.07	0.0	0.0	8.5	CLR
23	22	9	14	45	19	35	9.4	8.1	9.0	0.33	6.0	10.9	41	1.00	0.0	0.0	6.7	BKN
24	23	9	14	49	17	35	24.9	21.2	23.2	0.73	13.0	31.2	181	4.43	0.0	0.0	11.0	CLR
25	18	5	11	56	18	36	24.2	20.7	22.5	0.70	12.8	30.8	204	4.98	0.0	0.0	10.5	CLR
26	18	6	10	43	20	35	24.8	21.2	23.0	0.72	12.8	30.8	0	0.00	0.0	0.0	10.0	CLR
27	20	7	12	43	18	31	25.1	21.5	23.3	0.74	12.9	31.7	219	5.31	0.0	0.0	11.4	CLR
28	20	8	13	35	17	27	26.1	22.3	19.0	0.67	11.9	27.0	150	3.63	0.0	0.0	11.2	CLR
29	17	3	10	49	27	38	22.6	19.4	21.0	0.66	12.0	27.9	174	4.18	0.0	0.0	7.0	CLR
30	18	5	11	50	23	39	21.9	18.7	20.5	0.66	11.6	26.4	171	4.08	0.0	0.0	8.5	CLR
TOTAL							649.6	555.5	600.0	21.17	363.6	798.5	4180	105.85	36.5	2.0		
AVG.	22	10	15	58	27	43	21.7	18.5	20.0	0.71	12.1	26.6	139	3.53			9.5	
YEAR TO DATE TOTALS							7303.1	6250.5	7602.7	333.84	7011.0	10583.2	57881	1642.09	239.8	17.1		

Global total measurements recorded using Eppley PSP Pyranometers. Part A
Global UV measurements recorded using Eppley TUVR ((383 nm).
EMMAQUA total measurements computed using direct-normal measurements from Eppley NIP Pyrheliometer.
EMMAQUA UV measurements computed using DSET ultraviolet sky model.
To convert from MJ/m2 to langleys, divide MJ/m2 by 0.04184.
— Not available.

DSET
LABORATORIES, INC.

Box 1850
Black Canyon Stage I
Phoenix, Arizona 85029

Telephone: 602-465-7356
TWX: 910-950-4681 DSET PHX

THE WEATHER AT NEW RIVER, ARIZONA — DECEMBER 1987

DATE	TEMPERATURE (degrees C) HIGH	LOW	MEAN	HUMIDITY (%) HIGH	LOW	MEAN	SOLAR RADIANT EXPOSURE (MJ/m2) TOTAL 45	U.V. TOTAL 45	TOTAL 34	UV 34	TOTAL 5	TOTAL TRACK	TOTAL EMMAQUA	UV EMMAQUA	WET TIME (hr)	RAIN (cm)	AVG. WIND (km/hr	SKY CONDITION
1	18	9	12	44	25	38	22.7	19.4	21.2	0.68	12.0	27.6	191	4.53	0.0	0.0	7.1	CLR
2	21	11	15	41	20	32	22.0	18.8	20.6	0.67	11.9	27.4	161	3.78	0.0	0.0	8.4	CLR
3	25	10	16	45	19	35	23.4	20.0	21.6	0.71	12.0	28.8	198	4.60	0.0	0.0	10.0	CLR
4	15	8	11	98	61	80	9.4	8.0	5.4	0.36	6.7	10.7	43	1.00	15.0	0.0	12.2	BKN
5	19	9	13	93	51	75	14.9	12.7	13.9	0.49	5.7	17.8	54	1.24	6.9	0.2	6.9	SCT
6	20	7	13	89	43	70	23.5	20.1	21.6	0.69	10.3	29.4	204	4.64	0.0	0.0	7.7	CLR
7	18	7	13	84	46	68	23.4	20.0	21.6	0.67	11.4	29.2	198	4.50	0.0	0.0	8.0	CLR
8	20	8	12	74	19	44	18.7	16.0	17.5	0.57	10.1	22.4	129	2.91	0.0	0.0	9.5	SCT
9	19	7	12	52	26	42	21.9	18.7	20.3	0.67	11.3	26.6	179	4.00	0.0	0.0	8.3	CLR
10	23	10	15	62	28	43	23.8	20.3	21.9	0.69	11.6	29.9	180	4.00	0.0	0.0	6.6	CLR
11	26	8	15	67	28	49	23.2	19.9	21.3	0.69	11.4	28.9	204	4.53	0.0	0.0	6.9	CLR
12	18	4	12	58	20	34	24.4	20.9	22.4	0.69	11.9	28.9	209	4.56	0.0	0.0	13.2	CLR
13	5	0	3	87	31	60	6.1	5.2	5.6	0.30	6.1	7.5	0	0.00	0.2	0.2	9.7	OVC
14	11	-1	4	84	38	63	19.5	16.7	18.2	0.61	10.2	23.8	148	3.21	0.0	0.0	6.2	SCT
15	14	4	8	49	23	36	21.0	17.9	19.6	0.63	10.9	25.3	158	3.38	0.0	0.0	8.4	SCT
16	16	7	10	46	25	37	6.1	5.2	6.3	0.29	6.0	6.3	0	0.00	0.0	0.0	9.3	OVC
17	12	5	9	92	67	85	1.0	0.8	0.8	0.06	1.0	1.5	0	0.00	16.9	0.2	10.7	OVC
18	15	6	9	92	67	85	8.7	7.5	9.4	0.40	7.9	10.2	0	0.00	3.3	0.2	6.5	BKN
19	11	6	8	94	86	91	2.3	2.0	2.5	0.17	0.2	2.6	0	0.00	9.1	0.0	4.2	OVC
20	17	4	9	93	45	75	21.9	18.7	21.3	0.67	11.2	28.4	195	4.07	7.6	0.0	8.3	CLR
21	19	5	10	80	31	61	24.2	20.7	22.2	0.68	11.7	29.6	217	4.51	0.0	0.0	8.9	CLR
22	19	5	11	83	34	57	24.1	20.6	22.1	0.68	5.6	30.0	216	4.48	0.0	0.0	7.2	CLR
23	20	8	11	72	19	43	19.3	16.5	18.0	0.57	6.6	23.0	119	2.46	0.0	0.0	6.2	CLR
24	15	6	9	89	41	70	10.4	8.9	10.0	0.40	6.7	11.9	0	0.00	0.0	0.0	7.7	SCT
25	17	4	10	91	47	77	7.9	6.8	7.9	0.35	5.9	8.0	0	0.00	0.0	0.0	7.5	OVC
26	16	6	10	55	24	35	14.4	12.3	13.7	0.46	8.1	17.3	63	1.29	0.0	0.0	5.6	SCT
27	19	8	11	44	24	37	24.4	20.8	22.4	0.69	11.2	30.2	202	4.12	0.0	0.0	8.3	CLR
28	18	7	11	57	33	45	18.9	16.2	17.5	0.58	9.7	23.6	71	1.45	0.0	0.0	6.8	SCT
29	19	37	11	59	19	37	24.6	21.1	22.6	0.67	11.9	30.3	213	4.34	0.0	0.0	9.2	CLR
30	13	0	6	88	31	58	19.9	17.0	18.7	0.61	10.8	23.8	148	3.01	0.0	0.0	7.9	SCT
31	14	25	8	65	20	34	14.0	11.9	13.2	0.45	8.7	16.7	17	0.34	0.0	0.0	14.9	BKN
TOTAL							540.0	461.5	501.4	16.77	275.7	657.5	3717	80.95	58.8	0.2		
AVG.	17	8	11	72	35	55	17.4	14.9	16.2	0.54	8.9	21.2	120	2.61			8.4	
YEAR TO DATE TOTALS							7843.1	6712.1	8184.1	350.61	7287.7	11240.8	61598	1723.94	298.6	17.3		

Global total measurements recorded using Eppley PSP Pyranometers. Part A
Global UV measurements recorded using Eppley TUVR ((383 nm).
EMMAQUA total measurements computed using direct-normal measurements from Eppley NIP Pyrheliometer.
EMMAQUA UV measurements computed using DSET ultraviolet sky model.
To convert from MJ/m2 to langleys, divide MJ/m2 by 0.04184.
— Not available.

DSET
LABORATORIES, INC.

Box 1850
Black Canyon Stage I
Phoenix, Arizona 85029

Telephone: 602-465-7356
TWX: 910-950-4681 DSET PHX

THE WEATHER AT NEW RIVER, ARIZONA — JANUARY 1988

DATE	TEMPERATURE (degrees C) HIGH	LOW	MEAN	HUMIDITY (%) HIGH	LOW	MEAN	SOLAR RADIANT EXPOSURE (MJ/m2) TOTAL 45	U.V. 45	TOTAL 34	UV 34	TOTAL 5	TOTAL TRACK	TOTAL EMMAQUA	UV EMMAQUA	WET TIME (hr)	RAIN (cm)	AVG. WIND (km/hr)	SKY COND.
1	15	7	10	23	16	20	19.2	16.4	16.8	0.59	10.5	22.2	61	1.24	0.0	0.0	20.1	SCT
2	16	5	9	57	20	31	19.2	16.4	17.9	0.59	10.4	20.4	115	2.44	0.0	0.0	11.4	SCT
3	16	3	10	58	32	46	16.4	14.1	15.5	0.53	9.1	19.5	121	2.47	0.0	0.0	7.4	SCT
4	21	10	14	47	19	38	11.3	9.6	10.9	0.44	7.9	11.9	18	0.37	0.0	0.0	7.4	SCT
5	15	9	12	93	44	67	2.7	2.3	3.3	0.20	4.1	2.7	0	0.00	5.9	0.0	5.6	OVC
6	15	5	9	93	66	85	17.9	15.3	16.4	0.55	9.9	20.6	116	2.37	16.3	0.0	5.1	CLR
7	16	5	9	92	43	74	18.3	15.6	17.3	0.58	7.7	21.4	117	2.38	8.2	0.0	7.1	CLR
8	16	3	9	86	48	73	20.4	17.5	18.9	0.61	10.5	24.1	151	3.08	0.1	0.0	6.5	SCT
9	16	6	10	85	34	62	23.8	20.3	21.9	0.69	11.7	27.1	192	3.94	0.0	0.0	7.8	CLR
10	20	6	12	75	34	55	22.1	18.9	20.7	0.67	11.9	26.5	167	3.42	0.0	0.0	7.9	CLR
11	18	7	12	74	41	55	10.3	8.8	10.0	0.41	7.9	10.7	0	0.00	0.0	0.0	6.5	BKN
12	20	6	13	71	17	37	24.3	20.8	22.4	0.71	12.5	26.4	205	4.23	0.0	0.0	13.0	CLR
13	21	9	13	48	16	27	19.7	16.8	18.7	0.62	11.3	23.8	134	2.77	0.0	0.0	12.0	SCT
14	23	10	14	41	13	23	25.3	21.6	23.5	0.73	12.8	24.0	168	3.48	0.0	0.0	13.6	CLR
15	18	8	12	89	24	34	6.5	5.7	6.6	0.31	6.0	6.5	0	0.00	1.4	0.1	8.1	OVC
16	16	8	10	93	60	82	12.0	10.2	14.9	0.55	8.4	16.5	0	0.00	9.8	0.1	5.9	BKN
17	14	6	9	94	60	80	2.4	2.1	2.7	0.15	1.3	1.9	0	0.00	7.3	0.2	9.1	OVC
18	8	7		93	63	83	6.3	5.4	5.3	0.28	4.1	4.5	0	0.00	13.2	0.0	14.1	OVC
19	10	-		77	40	54	21.3	18.2	20.8	0.70	10.7	23.8	118	2.49	0.0	0.0	9.6	CLR
20	11	1	5	62	20	39	19.9	17.0	17.2	0.68	8.7	23.5	171	3.60	0.0	0.0	12.6	CLR
21	12	0	6	65	26	45	25.0	21.4	22.9	0.78	13.0	29.5	200	4.22	0.0	0.0	9.6	CLR
22	15	6	10	37	18	25	25.8	22.0	24.4	0.79	13.9	32.5	205	4.36	0.0	0.0	14.0	CLR
23	15	3	8	68	23	40	23.0	19.7	22.7	0.76	13.4	26.7	187	3.98	0.0	0.0	7.6	CLR
24	18	2	11	77	16	32	25.1	21.5	24.6	0.79	13.9	33.1	203	4.34	0.0	0.0	12.6	CLR
25	21	6	12	55	15	27	25.5	21.8	24.8	0.80	14.3	33.1	186	3.97	0.0	0.0	15.2	CLR
26	24	9	16	36	14	24	24.4	20.8	23.9	0.80	14.1	27.7	207	4.44	0.0	0.0	12.4	CLR
27	24	14	17	25	14	21	15.2	13.0	15.8	0.62	11.5	17.5	25	0.54	0.0	0.0	12.1	BKN
28	26	13	17	39	14	24	18.8	16.1	18.7	0.70	12.0	23.1	134	2.90	0.0	0.0	9.9	SCT
29	22	11	15	68	21	40	22.6	19.3	22.1	0.77	13.7	27.6	182	3.97	0.0	0.0	7.0	CLR
30	19	8	13	67	34	53	24.4	20.9	23.7	0.79	14.3	27.8	192	4.21	0.0	0.0	7.6	CLR
31	18	5	11	68	34	53	18.6	15.9	18.3	0.51	12.2	23.1	73	1.60	0.0	0.0	7.5	SCT
TOTAL							567.7	485.4	544.8	18.70	323.7	659.8	3648	76.81	62.2	0.4		
AVG.	17	6	11	66	30	47	18.3	15.7	17.6	0.60	10.4	21.3	118	2.48			9.9	
YEAR TO DATE TOTALS							567.7	485.4	544.8	18.70	323.7	659.8	3648	76.81	62.2	0.4		

Global total measurements recorded using Eppley PSP Pyranometers.
Global UV measurements recorded using Eppley TUVR (<383 nm).
EMMAQUA total measurements computed using direct-normal measurements from Eppley NIP Pyrheliometer.
EMMAQUA UV measurements computed using DSET ultraviolet sky model.
To convert from MJ/m2 to langleys, divide MJ/m2 by 0.04184.
— Not available.

Part P

DSET
LABORATORIES, INC.

Box 1850
Black Canyon Stage I
Phoenix, Arizona 85029

Telephone: 602-465-7356
TWX: 910-950-4681 DSET PHX

THE WEATHER AT NEW RIVER, ARIZONA — FEBRUARY 1988

DATE	TEMPERATURE (degrees C) HIGH	LOW	MEAN	HUMIDITY (%) HIGH	LOW	MEAN	SOLAR RADIANT EXPOSURE (MJ/m2) TOTAL 45	U.V. 45	TOTAL 34	UV 34	TOTAL 5	TOTAL TRACK	TOTAL EMMAQUA	UV EMMAQUA	WET TIME (hr)	RAIN (cm)	AVG. WIND (km/hr)	SKY COND.
1	15	8	11	59	42	53	2.7	2.3	3.3	0.19	4.0	3.1	0	0.00	23.9	0.0	5.4	OVC
2	17	10	12	92	52	72	3.1	2.6	4.6	0.25	6.6	3.9	0	0.00	13.7	0.7	6.9	OVC
3	17	8	12	92	55	80	20.9	17.8	20.7	0.77	10.6	24.0	156	3.47	12.6	0.5	7.1	CLR
4	16	11	13	55	40	45	5.5	4.7	6.3	0.33	3.8	5.9	0	0.00	0.0	0.0	15.3	OVC
5	20	10	14	43	18	31	26.4	22.6	25.1	0.65	14.9	32.0	104	2.36	0.0	0.0	16.3	CLR
6	20	4	12	72	21	40	26.6	22.7	25.4	0.90	15.7	34.3	222	5.02	0.0	0.0	9.4	CLR
7	19	6	12	72	40	56	26.5	22.7	25.3	0.89	15.8	34.3	218	4.94	0.0	0.0	7.7	CLR
8	21	11	16	64	31	46	26.2	22.4	24.7	0.89	15.7	31.4	224	5.10	0.0	0.0	7.9	CLR
9	25	12	17	54	16	34	26.7	22.8	25.3	0.89	16.1	32.0	225	5.16	0.0	0.0	10.7	CLR
10	24	9	16	49	15	32	26.3	22.4	25.1	0.91	15.4	32.7	214	4.95	0.0	0.0	10.3	CLR
11	26	12	17	30	13	21	27.4	23.5	26.1	0.92	16.6	33.9	107	2.49	0.0	0.0	15.4	CLR
12	27	11	18	40	12	21	27.4	23.5	26.4	0.93	16.8	32.4	228	5.36	0.0	0.0	14.1	CLR
13	22	9	15	49	20	30	26.8	22.9	25.6	0.91	16.7	33.5	217	5.11	0.0	0.0	5.4	CLR
14	23	9	10	48	19	30	26.6	22.7	25.5	0.90	16.8	33.9	200	4.74	0.0	0.0	12.5	CLR
15	22	8	13	47	18	29	26.6	22.7	25.5	0.92	16.8	33.6	208	4.94	0.0	0.0	10.3	CLR
16	21	7	14	46	16	29	26.2	22.4	25.0	0.90	16.8	29.2	201	4.81	0.0	0.0	9.9	CLR
17	19	9	13	28	16	21	26.7	22.9	25.4	0.93	17.2	31.7	212	5.07	0.0	0.0	16.5	CLR
18	15	4	10	34	19	23	11.6	9.9	11.8	0.53	10.3	13.4	36	0.88	0.0	0.0	10.2	SCT
19	21	8	13	36	15	24	27.3	23.4	26.0	0.97	17.9	27.0	106	2.60	0.0	0.0	15.9	CLR
20	22	8	14	38	15	21	27.7	23.7	26.8	0.99	18.4	36.4	239	5.85	0.0	0.0	10.0	CLR
21	25	9	16	39	13	24	24.6	21.0	24.0	0.93	16.9	30.7	184	4.53	0.0	0.0	10.4	CLR
22	23	7	15	43	17	28	27.4	23.4	26.3	0.99	18.3	34.7	228	5.62	0.0	0.0	6.0	CLR
23	25	9	16	41	15	30	23.9	20.5	23.3	0.89	16.8	28.6	155	3.84	0.0	0.0	9.9	CLR
24	27	11	18	34	12	22	25.5	21.8	24.7	0.98	17.7	30.0	197	4.89	0.0	0.0	9.8	CLR
25	28	17	22	26	12	19	20.5	17.5	20.3	0.84	15.6	24.5	115	2.88	0.0	0.0	9.9	SCT
26	27	13	19	89	24	41	8.5	7.3	8.4	0.47	3.1	7.2	0	0.00	19.0	0.2	10.0	OVC
27	26	13	19	87	28	58	19.4	16.6	15.6	0.82	8.7	14.9	0	0.00	23.9	0.0	9.7	SCT
28	28	12	19	70	14	44	26.5	22.7	26.0	1.04	17.5	35.1	214	5.50	0.0	0.0	6.1	CLR
29	25	11	18	54	20	36	26.8	22.9	25.9	1.05	19.0	31.8	211	5.41	0.0	0.0	9.6	CLR
TOTAL							648.3	554.3	623.8	23.58	416.5	776.1	4421	105.52	93.1	1.4		
AVG.	22	10	15	53	22	36	22.4	19.1	21.5	0.81	14.4	26.8	152	3.64			10.8	
YEAR TO DATE TOTALS							1216.0	1039.7	1168.6	42.28	740.2	1435.9	8069	182.33	155.3	1.8		

Global total measurements recorded using Eppley PSP Pyranometers. Part A
Global UV measurements recorded using Eppley TUVR (303 nm).
EMMAQUA total measurements computed using direct-normal measurements from Eppley NIP Pyrheliometer.
EMMAQUA UV measurements computed using DSET ultraviolet sky model.
To convert from MJ/m2 to langleys, divide MJ/m2 by 0.04184.
--- Not available.

DSET
LABORATORIES, INC.

Box 1850
Black Canyon Stage I
Phoenix, Arizona 85029

Telephone: 602-465-7356
TWX: 910-950-4681 DSET PHX

THE WEATHER AT NEW RIVER, ARIZONA — MARCH 1988

DATE	TEMPERATURE (degrees C) HIGH	LOW	MEAN	HUMIDITY (%) HIGH	LOW	MEAN	SOLAR RADIANT EXPOSURE (MJ/m2) TOTAL 45	U.V. 45	TOTAL 34	UV 34	TOTAL 5	TOTAL TRACK	TOTAL EMMAQUA	UV EMMAQUA	WET TIME (hr)	RAIN (cm)	AVG. WIND (km/hr)	SKY COND.
1	22	7	13	47	18	29	21.8	18.6	21.6	0.90	16.5	26.9	156	4.00	0.0	0.0	7.6	SCT
2	19	9	13	91	43	71	14.7	12.5	14.4	0.69	15.3	9.9	0	0.00	14.4	0.5	7.5	BKN
3	19	6	11	92	56	82	17.6	15.1	16.9	0.76	12.9	8.4	91	2.35	9.2	0.1	7.4	BKN
4	22	8	14	91	40	68	25.2	22.4	21.2	0.99	17.4	22.7	179	4.67	18.7	0.0	7.9	CLR
5	25	9	17	79	25	53	26.5	22.6	26.3	1.06	18.3	34.6	230	6.06	0.0	0.0	8.1	CLR
6	25	11	18	60	18	41	26.8	22.9	26.6	1.07	19.8	35.1	238	6.29	0.0	0.0	9.8	CLR
7	26	9	17	63	15	34	25.8	22.1	25.7	1.05	19.8	32.8	214	5.64	0.0	0.0	13.0	CLR
8	23	10	15	19	13	16	28.9	24.7	28.4	1.12	21.8	35.3	196	5.18	0.0	0.0	16.9	CLR
9	24	8	16	21	13	16	28.0	23.9	27.8	1.09	21.4	35.7	253	6.74	0.0	0.0	9.7	CLR
10	19	7	14	20	15	16	29.0	24.8	28.7	1.14	22.1	37.2	265	7.06	0.0	0.0	14.1	CLR
11	17	2	10	29	15	20	28.5	24.4	28.4	1.15	22.2	36.9	264	7.10	0.0	0.0	8.6	CLR
12	18	3	11	35	15	21	28.4	24.3	27.3	1.14	22.3	39.9	266	7.16	0.0	0.0	9.7	CLR
13	21	5	13	21	14	17	29.0	24.8	29.1	1.15	22.7	40.8	268	7.24	0.0	0.0	12.0	CLR
14	22	5	14	22	14	17	28.9	24.7	28.8	1.11	22.9	37.9	268	7.29	0.0	0.0	12.8	CLR
15	22	5	14	22	13	17	28.3	24.2	28.3	1.12	22.7	36.8	258	7.03	0.0	0.0	12.4	CLR
16	20	5	14	38	14	20	28.6	24.5	28.7	1.15	23.1	37.4	263	7.21	0.0	0.0	11.8	CLR
17	23	7	15	23	13	17	28.3	24.2	28.4	1.14	23.0	36.9	260	7.15	0.0	0.0	11.3	CLR
18	24	9	16	19	13	16	28.2	24.1	28.4	1.15	23.3	38.6	255	7.05	0.0	0.0	12.2	CLR
19	29	12	19	17	11	14	28.9	24.7	29.3	1.19	23.9	40.7	268	7.39	0.0	0.0	12.3	CLR
20	31	13	21	17	10	14	28.7	24.5	29.2	1.17	23.9	41.0	266	7.35	0.0	0.0	10.5	CLR
21	30	13	21	17	11	14	24.6	21.0	25.2	1.03	21.2	33.8	187	5.21	0.0	0.0	10.1	SCT
22	28	10	19	18	11	15	26.7	22.8	27.2	1.11	22.7	33.0	221	6.17	0.0	0.0	8.7	CLR
23	30	13	21	18	11	14	26.3	22.5	27.0	1.11	22.9	34.3	220	6.15	0.0	0.0	9.7	CLR
24	32	15	23	18	10	13	27.6	23.6	28.2	1.17	23.7	36.1	252	7.07	0.0	0.0	11.6	CLR
25	35	18	25	15	9	12	27.9	23.8	28.5	2.00	24.3	38.1	260	7.33	0.0	0.0	14.4	CLR
26	37	21	27	14	8	12	27.7	23.7	28.5	1.21	24.4	40.5	265	7.50	0.0	0.0	13.3	CLR
27	33	17	25	16	9	12	27.6	23.6	28.4	1.20	24.4	39.6	263	7.47	0.0	0.0	12.7	CLR
28	28	10	20	18	11	14	28.2	24.1	28.9	1.20	26.5	39.2	120	3.41	0.0	0.0	16.9	CLR
29	25	8	15	18	12	16	28.5	24.4	29.4	1.22	25.6	40.6	182	5.17	0.0	0.0	12.8	CLR
30	24	7	16	19	13	16	25.3	21.6	26.2	1.10	23.4	34.6	180	5.13	0.0	0.0	14.0	CLR
31	21	7	13	21	14	17	21.2	18.1	22.2	0.99	20.3	27.2	120	3.42	0.0	0.0	10.3	SCT
TOTAL							822.7	703.2	823.2	34.68	674.7	1062.5	6728	163.99	42.3	0.6		
AVG.	25	9	17	33	16	24	26.5	22.7	26.6	1.12	21.8	34.3	217	5.94			11.3	
YEAR TO DATE TOTALS							2838.7	1742.9	1991.8	76.96	1414.9	2498.4	14797	366.32	197.6	2.4		

Global total measurements recorded using Eppley PSP Pyranometers. Part A
Global UV measurements recorded using Eppley TUVR ((383 nm).
EMMAQUA total measurements computed using direct-normal measurements from Eppley NIP Pyrheliometer.
EMMAQUA UV measurements computed using DSET ultraviolet sky model.
To convert from MJ/m2 to langleys, divide MJ/m2 by 0.04184.
--- Not available.

DSET
LABORATORIES, INC.

Box 1850
Black Canyon Stage I
Phoenix, Arizona 85029

Telephone: 602-465-7356
TWX: 910-950-4681 DSET PHX

THE WEATHER AT NEW RIVER, ARIZONA — APRIL 1988

DATE	TEMPERATURE (degrees C) HIGH	LOW	MEAN	HUMIDITY (%) HIGH	LOW	MEAN	SOLAR RADIANT EXPOSURE (MJ/m2) TOTAL 45	U.V. 45	TOTAL 34	UV 34	TOTAL 5	TOTAL TRACK	TOTAL EPPLEY	UV EPPLEY	WET TIME (hr)	RAIN (cm)	AVG. WIND (km/hr)	SKY COND.
1	24	7	15	29	13	18	27.3	23.4	28.4	1.22	24.8	37.4	249	7.13	0.0	0.0	9.4	CLR
2	27	8	18	21	12	16	27.2	23.3	28.4	1.22	31.8	40.3	247	7.06	0.0	0.0	6.4	CLR
3	29	12	20	18	11	14	26.9	23.0	28.1	1.22	25.2	36.7	243	6.99	0.0	0.0	9.6	CLR
4	29	11	21	18	11	14	27.0	23.1	28.2	1.23	25.3	36.0	246	7.06	0.0	0.0	8.9	CLR
5	33	14	24	17	9	13	27.3	23.3	28.5	1.24	26.0	33.6	241	6.96	0.0	0.0	10.7	CLR
6	36	20	27	14	8	12	27.3	23.3	28.6	1.24	26.1	39.5	255	7.40	0.0	0.0	11.7	CLR
7	34	17	26	15	9	12	26.1	22.3	27.4	1.23	25.3	37.6	239	6.97	0.0	0.0	9.1	CLR
8	33	16	25	19	10	13	26.5	22.6	27.8	1.22	25.8	39.0	241	7.07	0.0	0.0	9.4	CLR
9	33	18	24	15	9	12	27.5	23.5	29.1	1.27	27.4	25.7	149	4.36	0.0	0.0	16.0	CLR
10	34	17	24	15	9	13	27.6	23.6	29.1	1.26	32.8	40.6	197	5.78	0.0	0.0	15.5	CLR
11	34	17	25	15	9	12	25.7	22.0	27.2	1.18	25.2	36.0	188	5.51	0.0	0.0	11.0	CLR
12	35	16	26	15	9	12	22.3	19.0	23.8	1.05	23.0	30.5	118	3.47	0.0	0.0	9.4	SCT
13	31	19	23	47	11	21	14.1	12.0	15.1	0.76	15.5	17.4	1	0.04	1.0	0.0	12.6	OVC
14	27	16	21	72	23	43	20.1	17.2	21.5	1.03	20.6	27.2	71	2.10	0.8	0.0	9.6	SCT
15	21	10	16	91	36	63	4.9	4.2	2.8	0.23	6.6	4.6	0	0.00	10.7	1.0	9.5	OVC
16	16	9	11	98	61	83	6.3	5.4	4.9	0.58	4.2	4.2	0	0.00	9.7	0.1	9.9	BKN
17	15	9	11	91	75	88	4.6	3.9	4.7	0.25	5.2	3.7	0	0.00	15.3	0.5	8.2	OVC
18	23	11	17	91	41	68	19.4	16.6	20.8	1.07	17.0	18.2	114	3.38	6.2	0.0	5.9	SCT
19	27	12	19	79	28	52	23.9	20.4	25.6	1.20	25.4	34.6	199	5.91	0.0	0.0	8.9	CLR
20	26	12	20	77	18	39	20.8	17.8	22.5	1.09	22.6	28.5	98	2.92	0.0	0.0	12.3	SCT
21	18	9	13	92	39	75	8.2	7.1	8.5	0.49	8.3	9.2	0	0.00	12.9	1.7	10.6	OVC
22	18	7	12	92	48	77	13.6	11.7	12.9	0.80	9.2	14.7	0	0.00	10.3	1.0	7.6	BKN
23	22	10	16	86	23	54	22.9	19.5	24.1	1.14	11.0	30.5	134	3.99	0.1	0.0	10.3	SCT
24	23	8	16	85	23	48	25.5	21.8	27.6	1.29	21.7	38.0	233	6.93	0.7	0.0	8.5	CLR
25	28	11	20	64	12	35	25.7	21.9	28.1	1.26	28.4	42.3	259	7.71	0.0	0.0	9.0	CLR
26	32	14	23	41	10	22	25.4	21.7	27.7	1.23	28.3	40.3	253	7.54	0.0	0.0	10.2	CLR
27	33	16	25	34	9	19	25.1	21.5	27.4	1.23	27.8	37.9	234	6.98	0.0	0.0	9.9	CLR
28	29	17	23	38	12	18	21.3	18.2	23.0	1.10	23.6	28.0	110	3.30	0.5	0.0	11.7	SCT
29	30	14	22	48	13	26	25.0	21.4	27.4	1.22	28.5	36.6	242	7.17	0.0	0.0	7.5	CLR
30	31	15	23	39	11	21	24.2	20.7	26.6	1.21	27.2	37.0	220	6.54	0.0	0.0	14.2	CLR
TOTAL							649.7	555.4	685.8	31.76	649.8	889.8	4781	140.29	68.2	4.3		
AVG.	28	13	20	49	20	34	21.7	18.5	22.9	1.06	21.7	29.7	159	4.68			10.2	
YEAR TO DATE TOTALS							2688.4	2298.3	2677.6	108.72	2064.7	3388.2	19578	506.61	224.4	6.7		

Global total measurements recorded using Eppley PSP Pyranometers. Part 2

Global UV measurements recorded using Eppley TUVR (((383 nm).

EPPLEY total measurements computed using direct-normal measurements from Eppley NIP Pyrheliometer.

EPPLEY UV measurements computed using DSET ultraviolet sky model.

To convert from MJ/m2 to langleys, divide MJ/m2 by 0.04184.

— Not available.

DSET
LABORATORIES, INC.

Box 1850
Black Canyon Stage I
Phoenix, Arizona 85029

Telephone: 602-465-7356
TWX: 910-950-4681 DSET PHX

THE WEATHER AT NEW RIVER, ARIZONA — MAY 1988

DATE	TEMPERATURE (degrees C) HIGH	LOW	MEAN	HUMIDITY (%) HIGH	LOW	MEAN	SOLAR RADIANT EXPOSURE (MJ/m2) TOTAL 45	U.V. 45	TOTAL 34	UV 34	TOTAL 5	TOTAL TRACK	TOTAL EMMAQUA	UV EMMAQUA	WET TIME (hr)	RAIN (cm)	AVG. WIND (km/hr)	SKY COND.
1	28	10	15	20	14	17	21.7	18.5	23.9	1.15	25.3	35.4	181	5.40	0.0	0.0	17.2	SCT
2	25	10	17	21	12	16	25.7	22.0	28.4	1.19	30.0	41.4	266	7.94	0.0	0.0	9.7	CLR
3	30	12	21	21	10	15	25.2	21.5	27.8	1.18	29.5	40.5	264	7.88	0.0	0.0	8.8	CLR
4	32	15	24	19	10	13	25.2	21.5	27.9	1.31	29.6	41.2	187	5.60	0.0	0.0	9.8	CLR
5	29	14	22	18	11	14	22.9	19.6	25.1	1.20	27.4	33.5	192	5.75	0.0	0.0	17.3	SCT
6	20	7	14	26	14	18	23.2	19.8	25.6	1.21	27.5	37.6	159	4.75	0.0	0.0	9.2	CLR
7	23	8	16	29	14	19	24.9	21.3	27.7	1.30	25.6	41.0	246	7.35	0.0	0.0	11.2	CLR
8	26	9	18	47	14	26	24.5	20.9	27.3	1.32	29.4	40.1	253	7.60	0.0	0.0	7.5	CLR
9	32	13	23	33	10	18	24.4	20.9	27.2	1.31	29.4	42.3	252	7.57	0.0	0.0	9.3	CLR
10	37	16	26	20	8	13	24.2	20.7	27.1	1.29	29.4	35.9	253	7.63	0.0	0.0	10.9	CLR
11	39	25	31	13	7	10	24.5	20.9	27.4	1.31	30.1	39.9	259	7.80	0.0	0.0	12.5	CLR
12	40	25	31	13	7	10	23.8	20.3	26.6	1.28	29.1	39.1	238	7.20	0.0	0.0	10.4	CLR
13	39	22	31	15	7	11	23.9	20.5	26.7	1.24	29.3	39.5	238	7.20	0.0	0.0	12.1	CLR
14	38	21	30	15	7	11	23.6	20.2	26.6	1.25	29.1	41.4	228	6.90	0.0	0.0	10.6	CLR
15	39	21	30	15	7	11	23.3	20.0	26.2	1.24	28.7	40.7	223	6.77	0.0	0.0	8.8	CLR
16	38	22	29	17	8	12	14.7	12.6	16.5	0.84	18.8	25.2	33	1.02	0.0	0.0	8.0	SCT
17	33	20	27	34	10	16	15.9	13.6	17.4	0.89	19.3	22.8	12	0.37	0.0	0.0	9.9	SCT
18	31	17	25	31	10	17	23.5	20.1	26.6	1.34	29.8	35.5	241	7.33	0.0	0.0	7.3	CLR
19	34	18	27	28	9	16	23.6	20.2	26.7	1.34	29.7	41.8	253	7.70	0.0	0.0	9.7	CLR
20	35	20	27	14	9	12	24.1	20.6	27.4	1.36	30.9	42.0	264	8.07	0.0	0.0	12.6	CLR
21	37	20	29	14	8	11	24.0	20.5	27.4	1.34	31.0	45.1	268	8.20	0.0	0.0	11.0	CLR
22	39	21	30	14	7	11	23.8	20.4	27.0	1.32	30.3	42.8	249	7.63	0.0	0.0	9.7	CLR
23	39	21	30	14	7	10	22.8	19.5	25.8	1.25	29.4	40.0	221	6.90	0.0	0.0	9.3	CLR
24	38	19	29	15	7	11	23.0	19.6	26.0	1.28	29.5	37.9	238	7.34	0.0	0.0	7.5	CLR
25	39	20	30	16	7	11	23.0	19.7	26.1	1.29	29.8	39.0	277	8.59	0.0	0.0	8.8	CLR
26	39	20	30	16	7	11	23.6	20.2	26.7	1.22	30.3	39.7	261	8.15	0.0	0.0	10.8	CLR
27	39	19	30	15	6	10	23.6	20.2	26.7	1.32	30.5	37.4	231	7.21	0.0	0.0	10.8	CLR
28	39	20	30	15	5	10	22.8	20.4	27.0	1.38	30.6	43.6	287	8.99	0.0	0.0	8.7	CLR
29	32	17	25	27	14	17	18.3	15.6	20.6	1.07	26.1	32.2	120	3.74	0.0	0.0	18.2	SCT
30	39	20	29	17	8	12	23.8	20.3	26.8	1.33	30.9	27.0	248	7.77	0.0	0.0	9.9	CLR
31	39	20	30	15	6	11	23.8	20.3	27.1	1.38	30.1	37.1	249	7.84	0.0	0.0	9.1	CLR
TOTAL							716.2	612.4	803.3	38.73	886.4	1178.6	6891	210.10	0.0	0.0		
AVG.	34	18	26	20	9	14	23.1	19.8	25.9	1.25	28.6	38.0	222	6.78			10.5	
YEAR TO DATE TOTALS							3404.6	2910.7	3480.9	147.45	2951.1	4566.8	26469	716.71	224.4	6.7		

Global total measurements recorded using Eppley PSP Pyranometers. Part A

Global UV measurements recorded using Eppley TUVR (<383 nm).

EMMAQUA total measurements computed using direct-normal measurements from Eppley NIP Pyrheliometer.

EMMAQUA UV measurements computed using DSET ultraviolet sky model.

To convert from MJ/m2 to langleys, divide MJ/m2 by 0.04184.

--- Not available.

DSET
LABORATORIES, INC

Box 1850
Black Canyon Stage I
Phoenix, Arizona 85029

Telephone: 602-465-7356
TWX: 910-950-4681 DSET PHX

THE WEATHER AT NEW RIVER, ARIZONA — JUNE 1988

DATE	TEMPERATURE (degrees C) HIGH	LOW	MEAN	HUMIDITY (%) HIGH	LOW	MEAN	SOLAR RADIANT EXPOSURE (MJ/m2) TOTAL 45	U.G. 45	TOTAL 34	UV 34	TOTAL 5	TOTAL TRACK	TOTAL EMPIRICAL	UV EMPIRICAL	WET TIME (hr)	RAIN (cm)	AVG. WIND (km/hr)	SKY COND.
1	34	16	26	17	9	12	22.4	19.1	25.1	1.28	28.8	36.9	160	5.04	0.0	0.0	8.9	CLR
2	39	20	31	15	7	10	22.7	19.4	26.1	1.32	30.3	40.4	252	7.96	0.0	0.0	10.0	CLR
3	41	26	35	12	7	9	22.7	19.4	26.2	1.32	30.5	40.0	266	8.45	0.0	0.0	9.1	CLR
4	42	22	32	14	7	10	22.5	19.3	26.1	1.29	30.4	43.1	253	8.05	0.0	0.0	9.2	CLR
5	37	21	30	14	8	11	23.7	20.3	26.9	1.35	31.3	44.6	264	8.39	0.0	0.0	14.4	CLR
6	34	17	27	16	9	12	23.1	19.7	26.8	1.37	31.6	42.0	268	8.60	0.0	0.0	12.6	CLR
7	34	16	26	16	9	12	23.4	20.0	27.2	1.38	32.1	46.2	267	8.58	0.0	0.0	10.9	CLR
8	35	17	27	16	9	12	23.1	19.7	26.6	1.37	31.8	46.1	279	9.00	0.0	0.0	8.1	CLR
9	38	20	30	14	8	11	23.1	19.8	26.9	1.29	31.7	45.3	276	8.96	0.0	0.0	5.7	CLR
10	39	22	31	13	7	10	21.7	18.6	25.0	1.19	29.3	40.6	206	6.73	0.0	0.0	9.7	CLR
11	37	20	29	14	8	11	23.1	19.8	28.6	1.30	31.7	43.3	268	8.77	0.0	0.0	10.0	CLR
12	34	20	28	14	9	11	22.8	19.5	26.3	1.33	31.2	43.5	267	8.79	0.0	0.0	9.4	CLR
13	37	19	29	15	8	11	22.5	19.3	26.1	1.29	30.9	41.8	262	8.64	0.0	0.0	8.3	CLR
14	39	21	31	14	7	10	22.6	19.3	26.2	1.06	30.6	41.6	255	8.46	0.0	0.0	8.6	CLR
15	41	23	33	13	7	10	22.2	19.0	25.7	0.98	29.5	41.6	238	7.94	0.0	0.0	6.3	CLR
16	43	28	35	12	6	9	21.7	18.6	25.2	1.25	29.2	38.7	230	7.69	0.0	0.0	13.2	CLR
17	41	28	38	14	7	9	22.2	19.0	25.8	0.81	30.2	42.0	239	8.02	0.5	0.0	11.2	CLR
18	37	28	31	37	10	17	9.3	8.0	10.5	0.62	12.5	15.0	0	0.00	1.1	0.0	12.5	BKN
19	40	23	33	77	9	27	21.7	18.5	22.4	0.97	27.1	37.6	213	7.20	2.2	0.1	8.7	CLR
20	41	26	34	22	8	13	20.2	17.3	23.2	0.45	25.7	30.9	194	6.57	0.0	0.0	7.9	SCT
21	42	26	35	19	6	10	20.9	17.9	22.6	1.16	28.8	34.3	197	6.68	0.0	0.0	10.7	BKN
22	45	27	37	15	5	9	21.8	18.6	25.3	1.20	29.6	39.3	244	8.24	0.0	0.0	6.0	CLR
23	45	29	37	12	5	8	21.7	18.6	25.2	1.19	29.5	38.7	232	7.85	0.0	0.0	11.3	CLR
24	42	29	35	11	7	9	15.2	13.0	17.3	0.90	20.1	25.3	41	1.39	0.0	0.0	8.2	SCT
25	40	26	34	14	7	10	22.3	19.1	25.7	1.33	28.9	40.8	244	8.25	0.0	0.0	10.6	CLR
26	40	24	33	20	8	12	21.9	18.7	25.4	1.32	29.8	42.3	258	8.72	0.0	0.0	8.0	CLR
27	42	27	34	18	7	12	20.1	17.2	23.1	1.14	21.8	33.2	183	6.17	0.0	0.0	10.2	CLR
28	33	27	29	51	17	34	10.5	9.0	11.8	0.68	14.5	17.6	60	2.04	2.0	0.0	11.6	OVC
29	39	26	31	41	10	28	19.7	16.8	22.2	1.13	23.7	29.8	160	5.38	0.2	0.0	15.9	SCT
30	42	23	32	83	8	27	21.5	18.4	24.7	1.14	24.2	35.8	227	7.66	2.6	0.5	12.5	CLR
TOTAL							632.3	540.9	726.2	34.41	837.7	1138.3	6503	214.24	8.6	0.6		
AVG.	39	23	32	22	8	13	21.1	18.0	24.2	1.15	27.9	37.9	217	7.14			10.3	
YEAR TO DATE TOTALS							4036.9	3451.6	4207.1	181.86	3788.8	5705.1	32972	930.95	233.8	7.3		

Global total measurements recorded using Eppley PSP Pyranometers. Part A

Global UV measurements recorded using Eppley TUVR (<383 nm).

EMPIRICAL total measurements computed using direct-normal measurements from Eppley NIP Pyrheliometer.

EMPIRICAL UV measurements computed using DSET ultraviolet sky mode..

To convert from MJ/m2 to langleys, divide MJ/m2 by 0.04184.

— Not available.

DSET
LABORATORIES, INC.

Box 1850
Black Canyon Stage I
Phoenix, Arizona 85029

Telephone: 602-465-7356
TWX: 910-950-4681 DSET PHX

THE WEATHER AT NEW RIVER, ARIZONA — JULY 1988

DATE	TEMPERATURE (degrees C) HIGH	LOW	MEAN	HUMIDITY (%) HIGH	LOW	MEAN	SOLAR RADIANT EXPOSURE (MJ/m2) TOTAL 45	U.V. 45	TOTAL 34	UV 34	TOTAL 5	TOTAL TRACK	TOTAL EMMAQUA	UV EMMAQUA	WET TIME (hr)	RAIN (cm)	AVG. WIND (km/hr)	SKY COND.
1	41	25	33	54	6	24	20.5	17.6	23.4	1.14	26.8	32.9	176	5.92	0.0	0.0	9.3	SCT
2	42	26	34	32	7	18	20.9	17.9	23.8	1.16	27.0	31.9	195	6.56	0.0	0.0	11.6	SCT
3	41	26	34	35	7	17	22.0	18.8	25.3	1.23	29.7	39.8	244	8.21	0.0	0.0	11.5	CLR
4	41	24	34	33	7	13	22.0	18.8	24.7	1.22	29.7	36.3	222	7.47	0.0	0.0	8.9	CLR
5	41	27	34	16	8	11	21.5	18.4	24.5	1.21	28.0	35.9	239	8.02	0.0	0.0	9.0	CLR
6	42	25	35	18	7	11	22.1	18.9	25.4	1.23	29.3	37.2	250	8.37	0.0	0.0	10.2	CLR
7	42	33	38	18	11	13	21.7	18.6	25.2	1.19	29.7	38.9	230	7.69	0.0	0.0	9.9	CLR
8	44	29	35	36	8	20	15.2	13.0	19.1	1.10	24.0	29.3	154	5.10	0.1	0.0	10.7	SCT
9	43	27	34	40	8	20	15.8	16.8	19.6	1.09	23.3	31.5	182	6.09	0.0	0.0	9.2	SCT
10	39	25	31	44	13	24	15.4	13.2	18.0	0.98	21.9	28.1	161	5.36	0.3	0.0	8.8	SCT
11	37	24	31	58	16	32	21.8	18.7	26.0	1.26	28.8	38.7	237	7.82	0.0	0.0	8.3	CLR
12	40	24	33	36	7	17	22.6	19.3	27.1	1.26	29.5	39.9	265	8.71	0.0	0.0	8.3	CLR
13	43	25	34	14	6	9	23.0	19.7	25.4	1.20	29.2	37.0	219	7.18	0.0	0.0	10.0	CLR
14	43	26	35	13	6	9	22.4	19.1	25.4	1.23	29.0	38.6	250	8.19	0.0	0.0	10.0	CLR
15	43	25	35	14	6	9	22.4	19.2	25.7	1.24	29.6	40.1	249	8.13	0.0	0.0	9.4	CLR
16	45	26	36	13	5	9	22.7	19.4	23.6	1.25	29.2	38.8	251	8.15	0.0	0.0	10.8	CLR
17	41	28	35	35	8	12	16.2	13.8	18.0	0.97	23.0	24.5	0	0.00	0.0	0.0	10.0	OVC
18	37	27	32	58	18	35	17.6	15.1	19.6	1.02	24.4	25.4	92	2.97	0.0	0.0	12.7	BKN
19	39	25	32	63	11	37	22.1	18.9	24.8	1.25	28.5	38.4	229	7.37	0.3	0.0	10.3	CLR
20	41	12	29	84	13	46	18.0	15.4	18.5	0.92	23.2	25.3	104	3.34	2.4	1.4	9.4	SCT
21	41	26	33	61	12	36	21.6	18.5	24.1	1.20	27.5	32.6	201	6.37	0.0	0.2	7.9	BKN
22	42	27	34	59	9	26	21.3	18.2	24.0	1.15	26.3	33.3	212	6.70	0.0	0.0	9.3	CLR
23	43	26	35	31	7	17	22.7	19.4	25.7	1.19	28.7	38.1	237	7.50	0.0	0.0	10.1	CLR
24	44	28	35	41	8	21	21.2	18.1	23.8	1.12	26.0	32.3	199	6.25	0.2	0.0	9.1	CLR
25	43	28	35	39	12	18	17.9	15.3	20.0	0.97	21.6	25.1	82	2.56	0.0	0.0	10.3	SCT
26	40	26	34	39	14	26	22.4	19.2	25.1	1.21	27.5	34.8	218	6.78	0.0	0.0	9.1	CLR
27	40	27	32	42	16	31	21.5	18.4	23.8	1.17	25.9	31.8	186	5.75	0.0	0.0	11.8	CLR
28	38	26	32	43	20	33	18.5	15.8	20.4	1.01	21.8	25.0	94	2.89	0.0	0.0	9.7	CLR
29	40	14	30	86	19	43	20.1	17.2	20.9	1.05	25.1	26.8	135	4.13	5.0	1.5	10.2	SCT
30	34	23	28	83	41	62	16.3	14.0	18.8	1.09	22.0	24.1	0	0.00	1.3	0.0	7.7	BKN
31	34	25	28	78	42	63	15.3	13.1	17.7	1.06	19.0	20.9	0	0.00	2.1	0.2	6.9	OVC
TOTAL							624.7	537.8	707.4	35.37	815.2	1013.3	5513	179.58	11.7	3.3		
AVG.	41	25	33	42	12	25	20.2	17.3	22.8	1.14	26.3	32.7	178	5.79			9.7	
YEAR TO DATE TOTALS							4661.6	3989.4	4914.5	217.23	4684.0	6718.4	38485	1110.53	244.7	10.6		

Global total measurements recorded using Eppley PSP Pyranometers. Part A

Global UV measurements recorded using Eppley TUVR ((383 nm).

EMMAQUA total measurements computed using direct-normal measurements from Eppley NIP Pyrheliometer.

EMMAQUA UV measurements computed using DSET ultraviolet sky model.

To convert from MJ/m2 to langleys, divide MJ/m2 by 0.04184.

--- Not available.

THE WEATHER AT NEW RIVER, ARIZONA — AUGUST 1988

DATE	TEMPERATURE (degrees C) HIGH	LOW	MEAN	HUMIDITY (%) HIGH	LOW	MEAN	SOLAR RADIANT EXPOSURE (MJ/m2) TOTAL 45	U.V. 45	TOTAL 34	UV 34	TOTAL 5	TOTAL TRACK	TOTAL EMMAQUA	UV EMMAQUA	WET TIME (hr)	RAIN (cm)	AVG. WIND (km/hr)	SKY COND.
1	38	23	29	75	32	50	16.3	13.9	17.9	0.92	18.5	21.9	48	1.46	1.6	0.1	8.1	SCT
2	37	25	31	74	32	50	20.0	17.1	21.0	1.12	23.6	29.3	139	4.20	0.0	0.0	7.9	SCT
3	39	26	33	57	21	34	22.2	19.0	24.7	1.22	26.5	36.0	217	6.52	0.0	0.0	7.4	CLR
4	36	23	29	84	32	50	13.5	11.5	14.2	0.77	14.5	18.5	0	0.00	3.4	0.1	10.6	OVC
5	37	24	31	81	32	52	18.9	16.2	20.6	1.05	20.7	24.6	69	2.07	0.0	0.0	7.4	SCT
6	39	26	33	61	14	35	21.6	18.5	23.9	1.15	25.4	34.2	109	3.21	0.0	0.0	10.6	SCT
7	38	24	32	56	10	28	22.1	18.9	24.9	1.17	25.9	33.6	252	7.43	0.0	0.0	9.8	CLR
8	40	23	32	28	9	16	22.9	19.6	25.2	1.19	26.3	34.3	254	7.46	0.0	0.0	7.8	CLR
9	41	24	33	22	8	13	24.1	20.6	26.8	1.25	28.1	40.0	265	7.72	0.0	0.0	9.1	CLR
10	41	25	33	18	8	12	23.9	20.5	26.5	1.23	27.7	38.7	264	7.64	0.0	0.0	9.0	CLR
11	40	26	34	28	10	17	23.8	20.3	26.2	1.23	27.0	38.2	243	7.00	0.0	0.0	10.2	CLR
12	39	25	32	44	11	24	24.0	20.6	26.5	1.24	27.4	37.7	258	7.38	0.0	0.0	11.1	CLR
13	41	23	33	28	7	14	24.8	21.2	27.4	1.24	29.4	39.0	276	7.86	0.0	0.0	8.8	CLR
14	43	26	34	34	6	15	23.0	19.7	25.3	1.15	26.0	34.9	226	6.40	0.5	0.0	12.9	CLR
15	40	25	33	49	8	26	23.4	20.0	25.5	1.20	25.9	36.6	216	6.06	0.0	0.0	9.3	CLR
16	40	25	33	42	11	25	23.9	20.5	26.2	1.23	26.6	38.2	249	6.99	0.0	0.0	9.0	CLR
17	42	27	35	24	11	18	23.3	19.9	25.5	1.20	25.5	35.4	237	6.62	0.0	0.0	9.9	CLR
18	41	28	33	37	16	24	20.5	17.5	22.4	1.07	22.4	29.7	189	5.24	0.0	0.0	10.2	SCT
19	40	24	32	81	20	40	23.6	20.2	25.7	1.20	23.0	35.9	234	6.45	3.4	0.2	8.8	SCT
20	36	23	28	87	39	65	8.4	7.2	9.4	0.54	10.5	12.6	0	0.00	5.5	0.3	8.6	BKN
21	30	21	25	89	65	82	8.8	7.5	8.9	0.62	11.7	13.0	0	0.00	16.8	3.6	4.7	OVC
22	36	23	29	67	43	55	23.0	19.6	24.2	1.14	25.1	33.4	240	6.55	6.9	0.0	7.0	CLR
23	39	25	31	84	36	63	21.2	18.1	23.1	1.11	22.5	29.9	192	5.22	0.1	0.0	7.2	CLR
24	35	25	32	80	30	54	24.2	20.7	26.1	1.22	24.5	38.1	239	6.46	0.0	0.0	7.3	CLR
25	39	28	32	68	33	52	21.4	18.3	23.1	1.09	22.4	29.5	187	5.03	0.0	0.0	8.8	CLR
26	39	26	31	67	32	53	18.9	16.2	20.4	0.97	18.8	26.0	160	4.29	1.1	0.1	9.1	SCT
27	34	18	26	91	48	70	12.6	10.8	13.5	0.67	10.5	15.5	0	0.00	4.3	1.3	11.8	OVC
28	35	22	29	76	35	56	20.2	17.3	21.5	1.03	19.6	22.4	164	4.37	0.0	0.0	8.2	SCT
29	35	21	28	89	39	64	14.4	12.3	15.4	0.77	16.5	15.9	43	1.14	7.6	0.9	13.7	OVC
30	35	22	27	66	40	66	21.3	18.2	22.4	1.09	20.6	26.5	153	4.08	2.3	0.1	11.2	SCT
31	37	23	29	73	33	53	21.6	18.4	22.9	1.12	21.4	28.9	187	4.98	0.0	0.0	11.6	CLR
TOTAL							631.8	548.3	687.3	33.21	694.8	928.4	5310	149.83	53.5	6.7		
AVG.	38	24	31	61	25	42	20.4	17.4	22.2	1.07	22.4	29.9	171	4.83			9.3	
YEAR TO DATE TOTALS							5293.4	4529.7	5601.8	250.44	5298.8	7646.8	43795	1260.36	298.2	17.3		

Global total measurements recorded using Eppley PSP Pyranometers. Part A

Global UV measurements recorded using Eppley TUVR (383 nm).

EMMAQUA total measurements computed using direct-normal measurements from Eppley NIP Pyrheliometer.

EMMAQUA UV measurements computed using DSET ultraviolet sky model.

To convert from MJ/m2 to langleys, divide MJ/m2 by 0.04184.

--- Not available.

THE WEATHER AT NEW RIVER, ARIZONA — SEPTEMBER 1988

DATE	TEMPERATURE (degrees C) HIGH	LOW	MEAN	HUMIDITY (%) HIGH	LOW	MEAN	SOLAR RADIANT EXPOSURE (MJ/m2) TOTAL 45	U.G. 45	TOTAL 34	UV 34	TOTAL 5	TOTAL TRACK	TOTAL EMMAQUA	UV EMMAQUA	WET TIME (hr)	RAIN (cm)	AVG. WIND (km/hr)	SK CON
1	39	25	30	63	27	45	22.8	19.5	24.3	1.12	22.7	33.8	169	4.50	0.1	0.0	11.6	SC
2	38	25	32	67	20	39	24.4	20.8	25.8	1.16	23.7	35.4	196	5.22	0.0	0.0	11.1	CL
3	39	25	31	45	9	26	22.2	18.8	23.4	0.95	21.6	29.2	152	4.05	0.0	0.0	11.3	SC
4	37	24	31	37	11	23	24.8	21.2	25.9	1.13	23.3	34.9	199	5.30	0.0	0.0	11.7	SC
5	36	23	29	35	10	20	24.6	21.1	25.7	1.18	23.2	33.4	210	5.59	0.0	0.0	9.0	CL
6	39	21	30	34	8	19	25.3	21.6	26.3	1.23	24.3	35.2	243	6.49	0.0	0.0	8.1	CL
7	38	22	30	32	10	19	24.8	21.2	26.0	1.07	23.1	35.4	214	5.73	0.0	0.0	8.3	CL
8	39	23	30	34	11	23	24.6	21.1	25.8	1.09	21.2	35.4	219	5.89	0.0	0.0	7.8	CL
9	40	24	31	34	10	21	24.7	21.1	25.8	1.12	22.7	34.5	229	6.14	0.0	0.0	8.4	CL
10	39	26	32	31	12	20	21.9	18.7	22.8	1.00	19.6	30.5	98	2.63	0.0	0.0	9.3	SC
11	37	23	29	48	15	28	19.2	16.4	20.3	0.92	15.1	25.8	72	1.94	0.2	0.0	10.0	SC
12	34	23	27	48	12	26	25.0	21.4	25.9	1.12	17.5	34.1	213	5.74	0.0	0.0	11.5	CL
13	35	20	27	17	10	13	26.0	22.2	27.0	1.13	23.1	35.6	222	5.97	0.0	0.0	12.6	CL
14	35	20	26	18	9	14	26.3	22.5	27.2	1.13	23.2	35.8	240	6.45	0.0	0.0	10.6	CL
15	37	21	29	19	9	14	26.5	22.6	27.3	1.14	23.3	35.9	242	6.53	0.0	0.0	10.9	CL
TOTAL							363.1	310.2	379.5	16.49	327.6	504.9	2918	78.17	0.3	0.0		
AVG.	37	23	30	37	12	23	24.2	20.7	25.3	1.10	21.8	33.7	195	5.21			10.1	
YEAR TO DATE TOTALS							5855.5	4839.9	5981.3	266.93	5626.4	8151.7	46713	1338.53	299.5	17.3		

Global total measurements recorded using Eppley PSP Pyranometers.

Global UV measurements recorded using Eppley TUVR ((383 nm).

EMMAQUA total measurements computed using direct-normal measurements from Eppley NIP Pyrheliometer.

EMMAQUA UV measurements computed using DSET Ultraviolet sky model.

To convert from MJ/m2 to langleys, divide MJ/m2 by 0.04184.

— Not available.

Part

(THIS PAGE LEFT BLANK)

APPENDIX D

155MM PROPELLING CHARGE CONTAINER MATERIAL PERFORMANCE MODELS

(THIS PAGE LEFT BLANK)

Table 1-A
Performance Prediction Model
155mm Propelling Charge Container
Outdoor Exposure

Ea	4633.1	cal/mole
To	50	Deg. C
dP/duv	-0.00627	
Po	4.55	W/g

Ultraviolet Radiation (MJ/m2)	Degrees C Container Temperature 20	Degrees C Container Temperature 30	Degrees C Container Temperature 40	Degrees C Container Temperature 60
		Calculated Values		
0	4.5500	4.5500	4.5500	4.5500
100	4.2514	4.1613	4.0525	3.7706
200	3.9527	3.7726	3.5551	2.9912
300	3.6541	3.3839	3.0576	2.2119
400	3.3555	2.9953	2.5602	1.4325
500	3.0569	2.6066	2.0627	0.6531
600	2.7582	2.2179	1.5653	
700	2.4596	1.8292	1.0678	
800	2.1610	1.4405	0.5704	
900	1.8624	1.0518	0.0729	
1000	1.5637	0.6632		
1100	1.2651	0.2745		
1200	0.9665			
1300	0.6678			
1400	0.3692			
1500	0.0706			

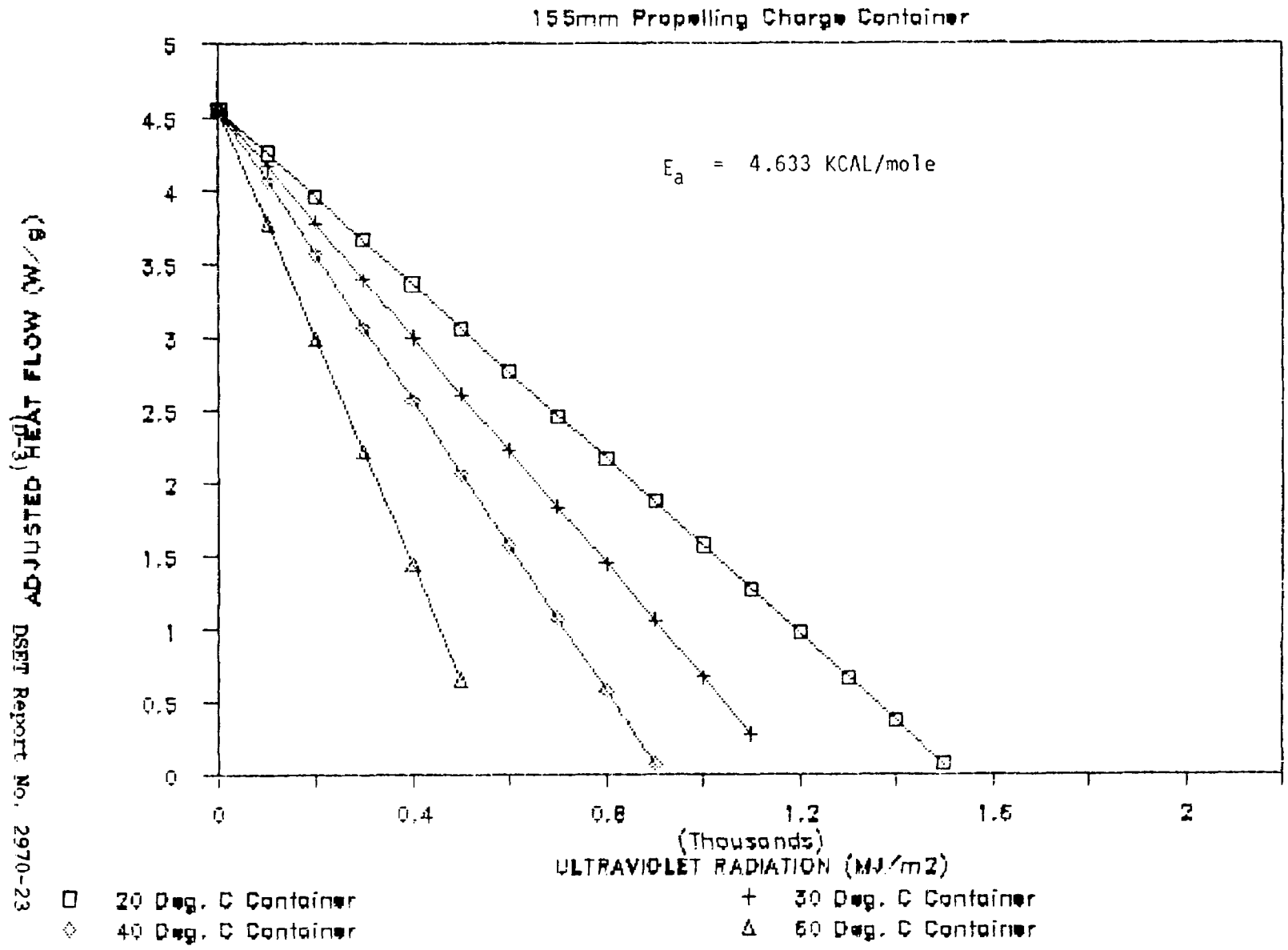

Figure 1-D: 155mm Propelling Charge Container Outdoor Ultraviolet Model - Measured Activation Energy

Table 2-D

Performance Prediction Model
155mm Propelling Charge Container
Outdoor Exposure

Ea	7000	cal/mole
To	50	Deg. C
dP/duv	-0.00627	
Po	4.55	W/g

Ultraviolet Radiation (MJ/m2)	Degrees C Container Temperature 20	Degrees C Container Temperature 30	Degrees C Container Temperature 40	Degrees C Container Temperature 60
		Calculated Values		
0	4.5500	4.5500	4.5500	4.5500
100	4.3456	4.2456	4.1080	3.6790
200	4.1411	3.9411	3.6660	2.8080
300	3.9367	3.6367	3.2241	1.9370
400	3.7323	3.3322	2.7821	1.0660
500	3.5278	3.0278	2.3401	0.1950
600	3.3234	2.7233	1.8981	
700	3.1189	2.4189	1.4562	
800	2.9145	2.1145	1.0142	
900	2.7101	1.8100	0.5722	
1000	2.5056	1.5056	0.1302	
1100	2.3012	1.2011		
1200	2.0968	0.8967		
1300	1.8923	0.5923		
1400	1.6879	0.2878		
1500	1.4834			
1600	1.2790			
1700	1.0746			
1800	0.8701			
1900	0.6657			
2000	0.4613			
2100	0.2568			
2200	0.0524			

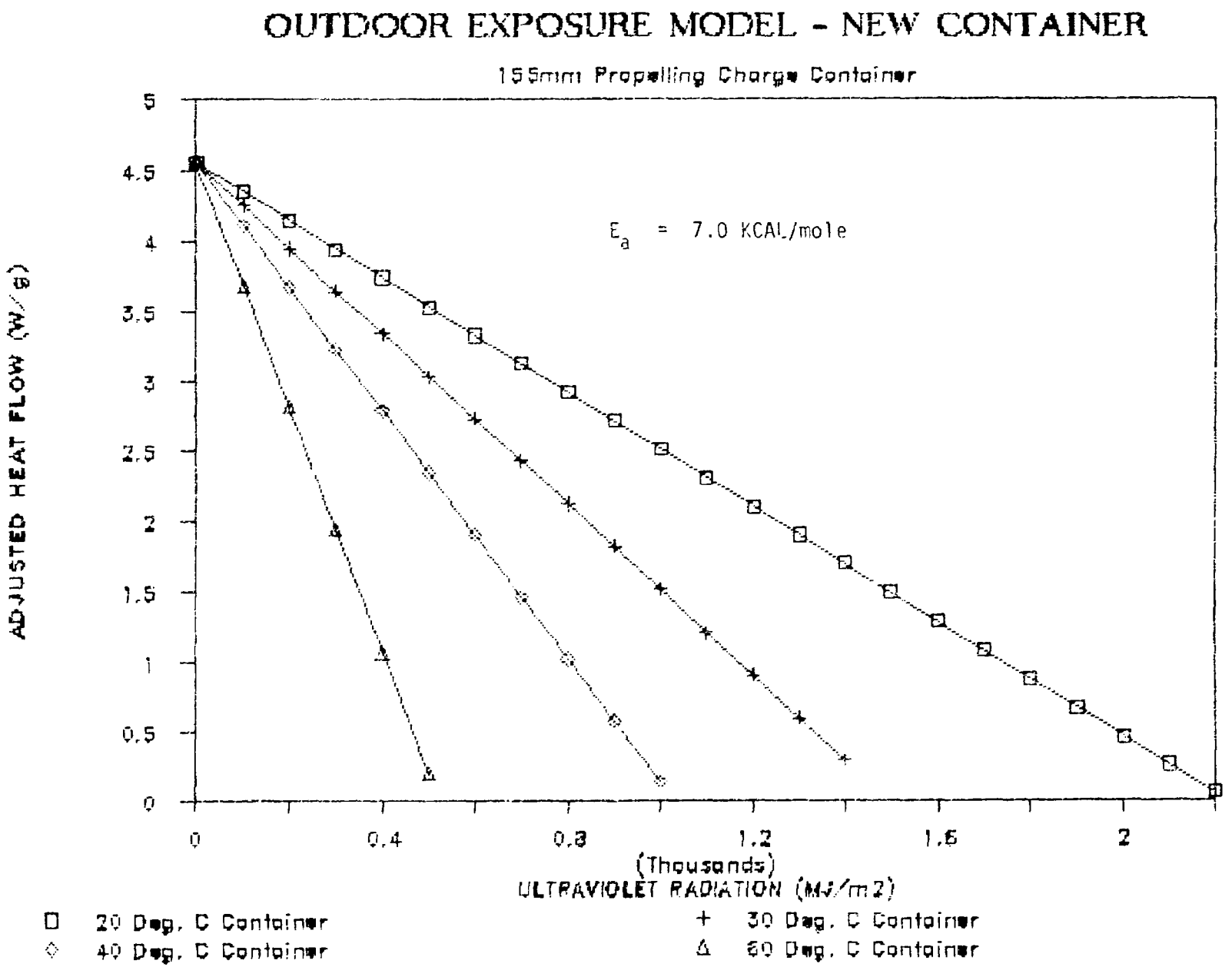

Figure 2-D: 155mm Propelling Charge Container Outdoor Ultraviolet Model - Published Activation Energy

Table 3-D
Performance Prediction Model
155mm Propelling Charge Container
Outdoor Exposure

Ea	9500	cal/mole
To	50	Deg. C
dP/duv	-0.00627	
Po	4.55	W/g

Ultraviolet Radiation (MJ/m2)	Degrees C Container Temperature 20	Degrees C Container Temperature 30	Degrees C Container Temperature 40	Degrees C Container Temperature 60
		Calculated Values		
0	4.5500	4.5500	4.5500	4.5500
100	4.4130	4.3148	4.1599	3.5705
200	4.2760	4.0796	3.7698	2.5910
300	4.1390	3.8444	3.3797	1.6115
400	4.0020	3.6092	2.9897	0.6321
500	3.8650	3.3740	2.5996	
600	3.7280	3.1388	2.2095	
700	3.5910	2.9036	1.8194	
800	3.4540	2.6684	1.4293	
900	3.3170	2.4332	1.0392	
1000	3.1800	2.1980	0.6492	
1100	3.0429	1.9627	0.2591	
1200	2.9059	1.7275		
1300	2.7689	1.4923		
1400	2.6319	1.2571		
1500	2.4949	1.0219		
1600	2.3579	0.7867		
1700	2.2209	0.5515		
1800	2.0839	0.3163		
1900	1.9469	0.0811		
2000	1.8099			
2100	1.6729			
2200	1.5359			

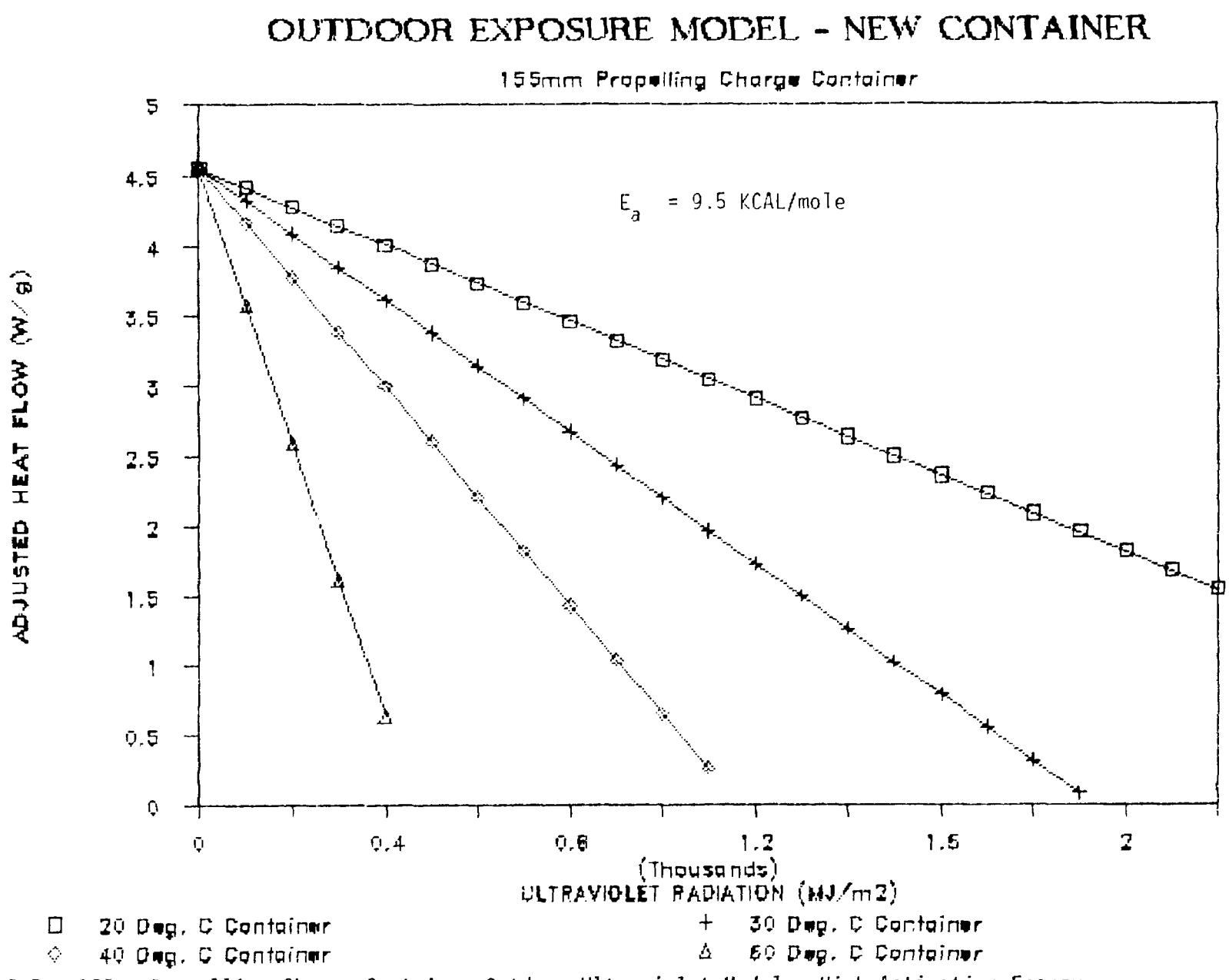

Figure 3-D: 155mm Propelling Charge Container Outdoor Ultraviolet Model - High Activation Energy

Table 4-D

Performance Prediction Model
155mm Propelling Charge Container
Outdoor Exposure

Ea	4633.1	cal/mole
To	50	Deg. C
dP/duv	-0.000803	
Po	4.55	W/g

Time at Temperature (hrs.)	Degrees C Container Temperature 20	Degrees C Container Temperature 30	Degrees C Container Temperature 40	Degrees C Container Temperature 60
		Calculated Values		
0	4.5500	4.5500	4.5500	4.5500
100	4.5213	4.5126	4.5022	4.4750
200	4.4926	4.4752	4.4543	4.4001
300	4.4638	4.4379	4.4065	4.3251
400	4.4351	4.4005	4.3586	4.2502
500	4.4064	4.3631	4.3108	4.1752
600	4.3777	4.3257	4.2630	4.1003
700	4.3490	4.2883	4.2151	4.0253
800	4.3202	4.2510	4.1673	3.9504
900	4.2915	4.2136	4.1194	3.8754
1000	4.2628	4.1762	4.0716	3.8005
2000	3.9756	3.8024	3.5932	3.0509
3000	3.6884	3.4286	3.1148	2.3014
4000	3.4012	3.0548	2.6364	1.5518
5000	3.1140	2.6810	2.1580	0.8023
6000	2.8268	2.3072	1.6795	
7000	2.5396	1.9334	1.2011	
8000	2.2524	1.5596	0.7227	
9000	1.9652	1.1857	0.2443	
10000	1.6780	0.8119		

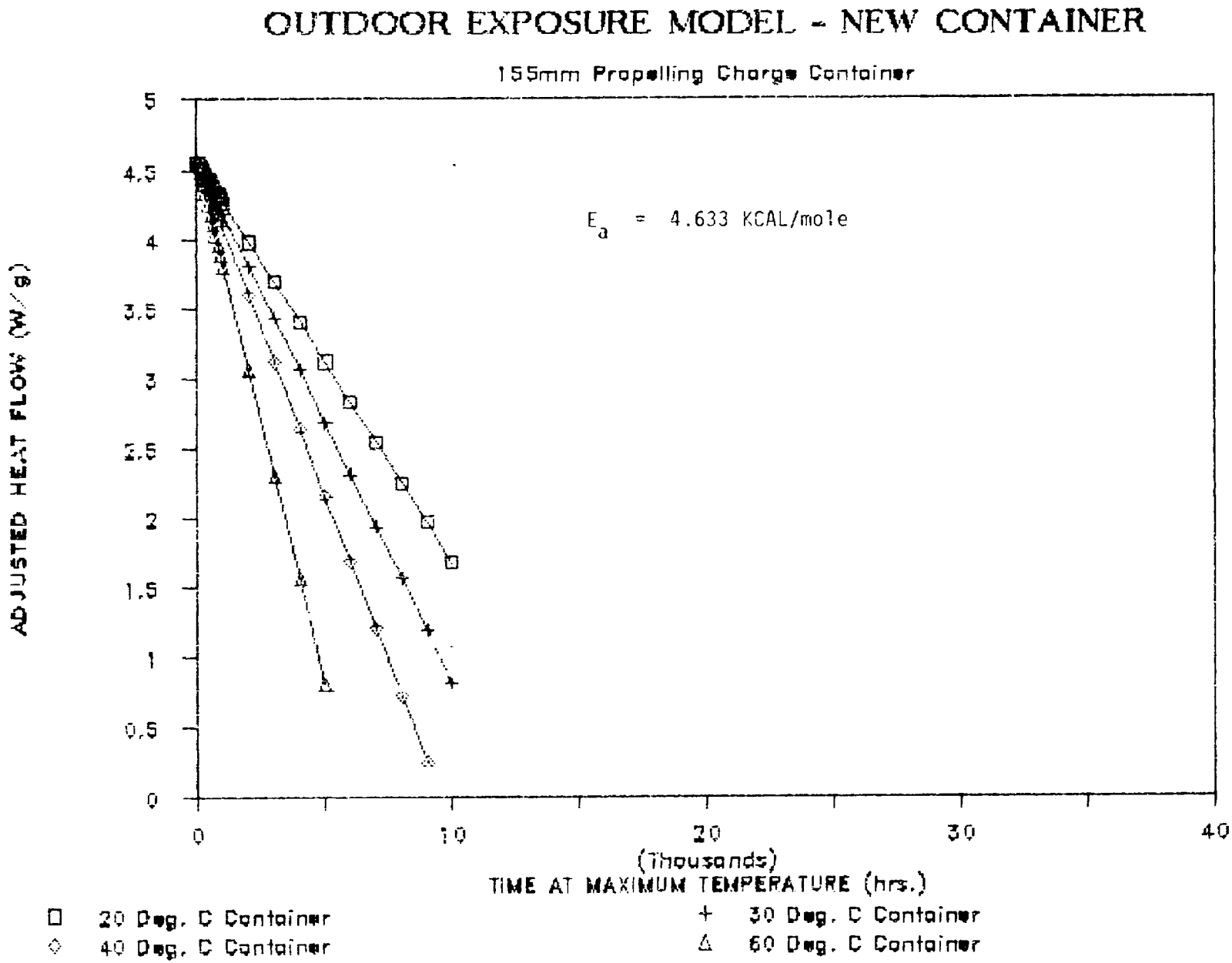

Figure 4-D: 155mm Propelling Charge Container Outdoor Ultraviolet/Temperature Model - Measured Activation Energy

Table 5-D

Performance Prediction Model
155mm Propelling Charge Container
Outdoor Exposure

Ea	7000	cal/mole
To	50	Deg. C
dP/duv	-0.000603	
Po	4.55	W/g

Time at Temperature (hrs.)	Degrees C Container Temperature 20	Degrees C Container Temperature 30	Degrees C Container Temperature 40	Degrees C Container Temperature 60
		Calculated Values		
0	4.5500	4.5500	4.5500	4.5500
100	4.5303	4.5207	4.5075	4.4662
200	4.5107	4.4914	4.4650	4.3825
300	4.4910	4.4622	4.4225	4.2987
400	4.4714	4.4329	4.3800	4.2149
500	4.4517	4.4036	4.3375	4.1312
600	4.4320	4.3743	4.2950	4.0474
700	4.4124	4.3450	4.2525	3.9636
800	4.3927	4.3158	4.2100	3.8799
900	4.3730	4.2865	4.1674	3.7961
1000	4.3534	4.2572	4.1249	3.7123
2000	4.1568	3.9644	3.6999	2.8747
3000	3.9602	3.6716	3.2748	2.0370
4000	3.7636	3.3788	2.8498	1.1994
5000	3.5669	3.0861	2.4247	0.3617
6000	3.3703	2.7933	1.9997	
7000	3.1737	2.5005	1.5746	
8000	2.9771	2.2077	1.1495	
9000	2.7805	1.9149	0.7245	
10000	2.5839	1.6221	0.2994	
20000	0.6178			

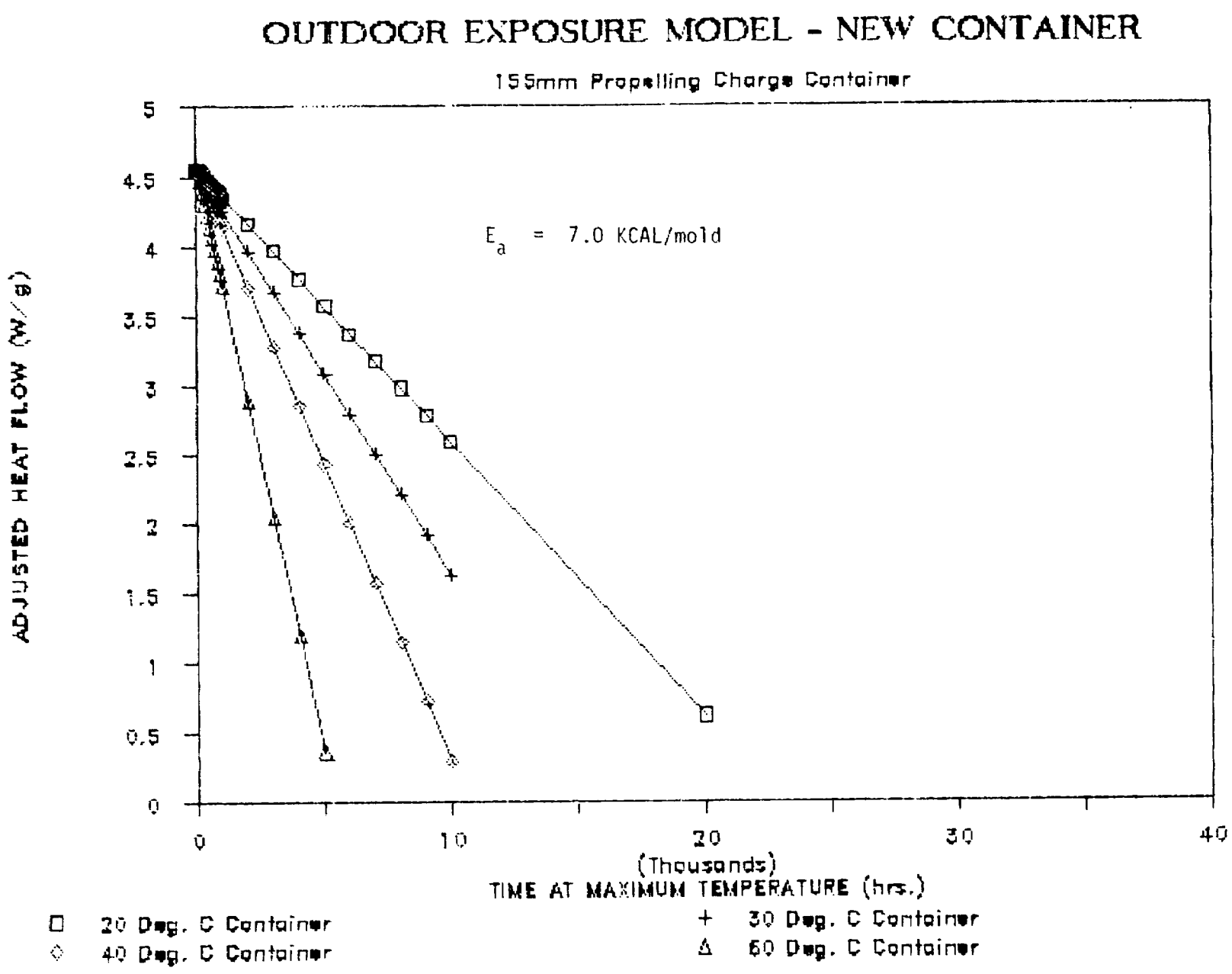

Figure 5-D: 155mm Propelling Charge Container Outdoor Ultraviolet/Temperature Model - Published Activation Energy

Table 6-D

Performance Prediction Model
155mm Propelling Charge Container
Outdoor Exposure

Ea	9500	cal/mole
To	50	Deg. C
dP/duv	-0.000603	
Po	4.55	W/g

Time at Temperature (hrs.)	Degrees C Container Temperature 20	Degrees C Container Temperature 30	Degrees C Container Temperature 40	Degrees C Container Temperature 60
		Calculated Values		
0	4.5500	4.5500	4.5500	4.5500
100	4.5368	4.5274	4.5125	4.4558
200	4.5236	4.5048	4.4750	4.3616
300	4.5105	4.4821	4.4375	4.2674
400	4.4973	4.4595	4.3999	4.1732
500	4.4841	4.4369	4.3624	4.0790
600	4.4709	4.4143	4.3249	3.9848
700	4.4578	4.3917	4.2874	3.8906
800	4.4446	4.3690	4.2499	3.7964
900	4.4314	4.3464	4.2124	3.7022
1000	4.4182	4.3238	4.1748	3.6080
2000	4.2865	4.0976	3.7997	2.6660
3000	4.1547	3.8714	3.4245	1.7240
4000	4.0230	3.6452	3.0494	0.7820
5000	3.8912	3.4190	2.6742	
6000	3.7594	3.1928	2.2991	
7000	3.6277	2.9666	1.9239	
8000	3.4959	2.7404	1.5488	
9000	3.3642	2.5142	1.1736	
10000	3.2324	2.2880	0.7985	
20000	1.9148			

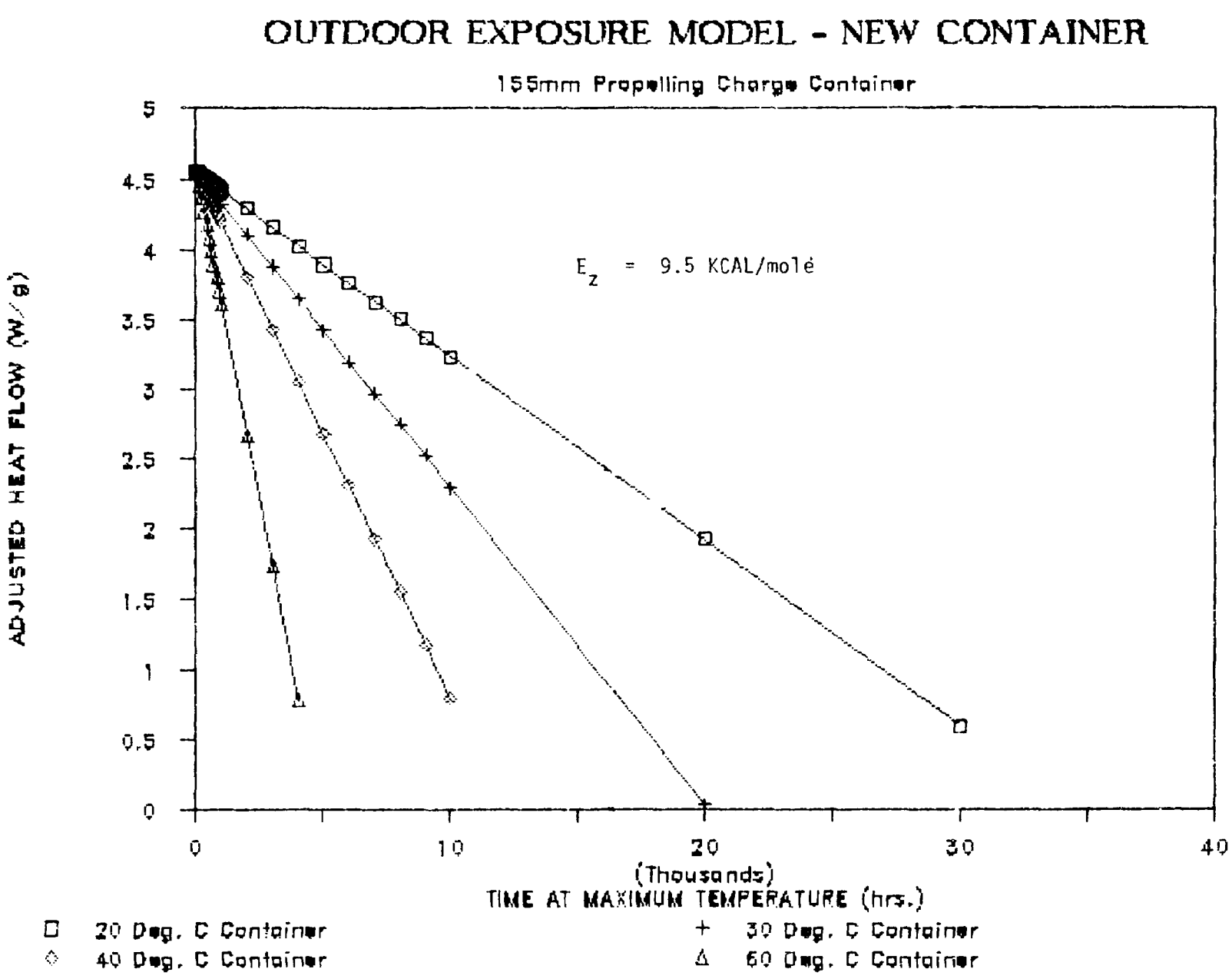

Figure 6-D: 155mm Propelling Charge Container Outdoor Ultraviolet/Temperature Model - High Activation Energy

Table 7-D

Performance Prediction Model
155mm Propelling Charge Container
Humid Indoor Storage

Ea	12000	cal/mole
To	60	Deg. C
dP/duv	-0.00013	
Po	4.55	W/g

Time at Temperature (hrs.)	Degrees C Container Temperature 0	Degrees C Container Temperature 10	Degrees C Container Temperature 20	Degrees C Container Temperature 30
		Calculated Values		
0	4.5500	4.5500	4.5500	4.5500
100	4.5498	4.5495	4.5489	4.5479
200	4.5495	4.5490	4.5478	4.5457
300	4.5493	4.5484	4.5467	4.5436
400	4.5490	4.5479	4.5457	4.5414
500	4.5488	4.5474	4.5446	4.5393
600	4.5486	4.5469	4.5435	4.5371
700	4.5483	4.5463	4.5424	4.5350
800	4.5481	4.5458	4.5413	4.5328
900	4.5479	4.5453	4.5402	4.5307
1000	4.5476	4.5448	4.5392	4.5286
2000	4.5452	4.5396	4.5283	4.5071
3000	4.5429	4.5343	4.5175	4.4857
4000	4.5405	4.5291	4.5067	4.4642
5000	4.5381	4.5239	4.4958	4.4428
6000	4.5357	4.5187	4.4850	4.4213
7000	4.5333	4.5135	4.4741	4.3999
8000	4.5310	4.5083	4.4633	4.3784
9000	4.5286	4.5030	4.4525	4.3570
10000	4.5262	4.4978	4.4416	4.3355
20000	4.5024	4.4457	4.3333	4.1211
30000	4.4786	4.3935	4.2249	3.9066
40000	4.4548	4.3413	4.1166	3.6921
50000	4.4309	4.2891	4.0082	3.4777
60000	4.4071	4.2370	3.8998	3.2632
70000	4.3833	4.1848	3.7915	3.0488
80000	4.3595	4.1326	3.6831	2.8343
90000	4.3357	4.0804	3.5747	2.6198
100000	4.3119	4.0283	3.4664	2.4054
200000	4.0738	3.5065	2.3828	0.2607
300000	3.8357	2.9848	1.2991	

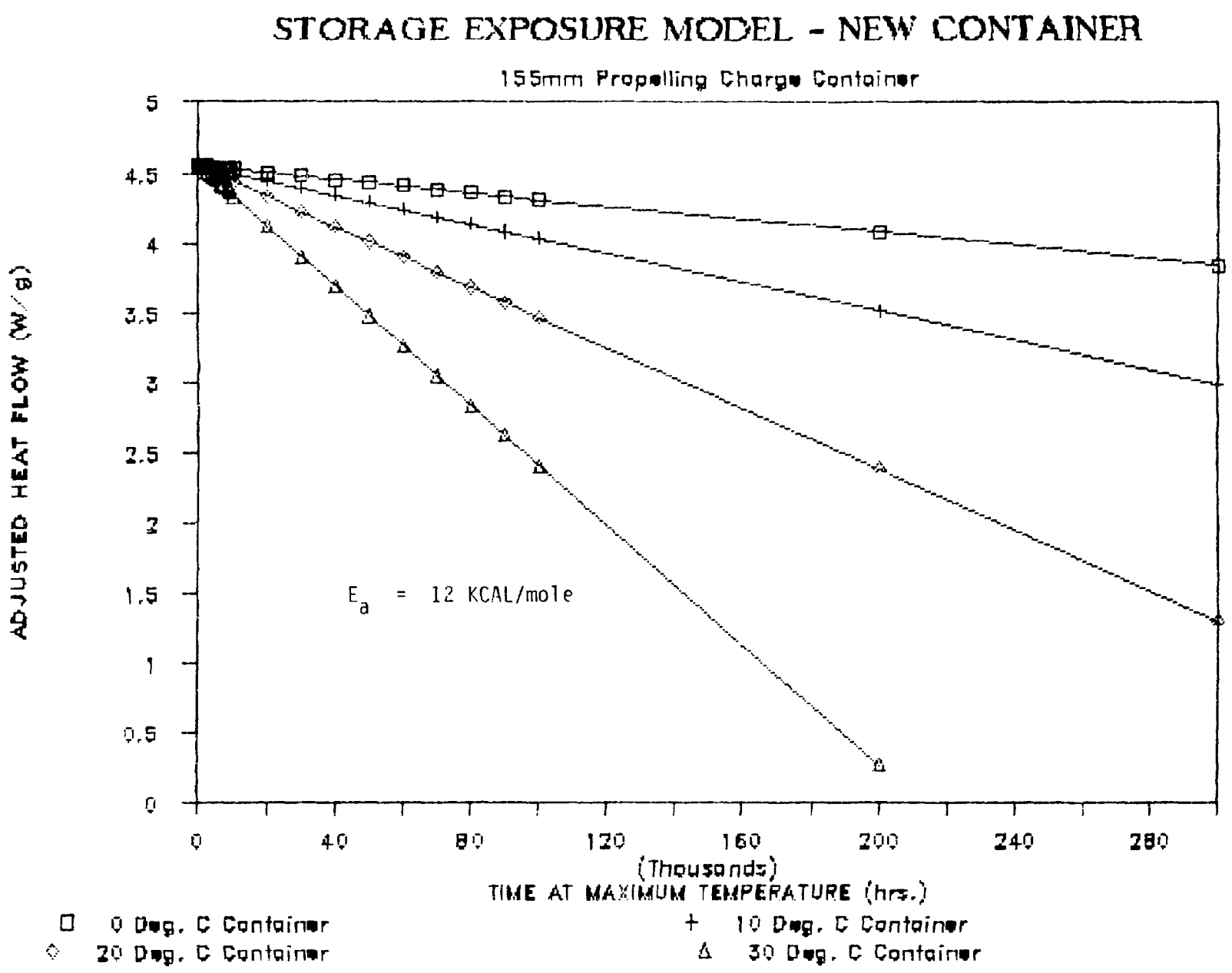

Figure 7-D: 155mm Propelling Charge Container Humid Indoor Storage Model - Low Activation Energy

Table 8-D

Performance Prediction Model
155mm Propelling Charge Container
Humid Indoor Storage

Ea	26000	cal/mole
To	60	Deg. C
dP/duv	-0.00013	
Po	4.55	W/g

Time at Temperature (hrs.)	Degrees C Container Temperature 0	Degrees C Container Temperature 10	Degrees C Container Temperature 20	Degrees C Container Temperature 30
		Calculated Values		
0	4.5500	4.5500	4.5500	4.5500
100	4.5500	.5500	4.5499	4.5497
200	4.5500	4.5500	4.5499	4.5495
300	4.5500	4.5500	4.5498	4.5492
400	4.5500	4.5500	4.5498	4.5490
500	4.5500	4.5499	4.5497	4.5487
600	4.5500	4.5499	4.5496	4.5484
700	4.5500	4.5499	4.5496	4.5482
800	4.5500	4.5499	4.5495	4.5479
900	4.5500	4.5499	4.5495	4.5476
1000	4.5500	4.5499	4.5494	4.5474
2000	4.5500	4.5498	4.5488	4.5448
3000	4.5499	4.5496	4.5482	4.5421
4000	4.5499	4.5495	4.5476	4.5395
5000	4.5499	4.5494	4.5470	4.5369
6000	4.5499	4.5493	4.5464	4.5343
7000	4.5498	4.5491	4.5458	4.5317
8000	4.5498	4.5490	4.5452	4.5290
9000	4.5498	4.5489	4.5446	4.5264
10000	4.5498	4.5488	4.5440	4.5238
20000	4.5496	4.5475	4.5381	4.4976
30000	4.5493	4.5463	4.5321	4.4714
40000	4.5491	4.5451	4.5261	4.4452
50000	4.5489	4.5439	4.5202	4.4190
60000	4.5487	4.5426	4.5142	4.3928
70000	4.5484	4.5414	4.5082	4.3666
80000	4.5482	4.5402	4.5022	4.3404
90000	4.5480	4.5390	4.4963	4.3142
100000	4.5478	4.5377	4.4903	4.2880
200000	4.5455	4.5255	4.4306	4.0260
300000	4.5433	4.5132	4.3709	3.7639

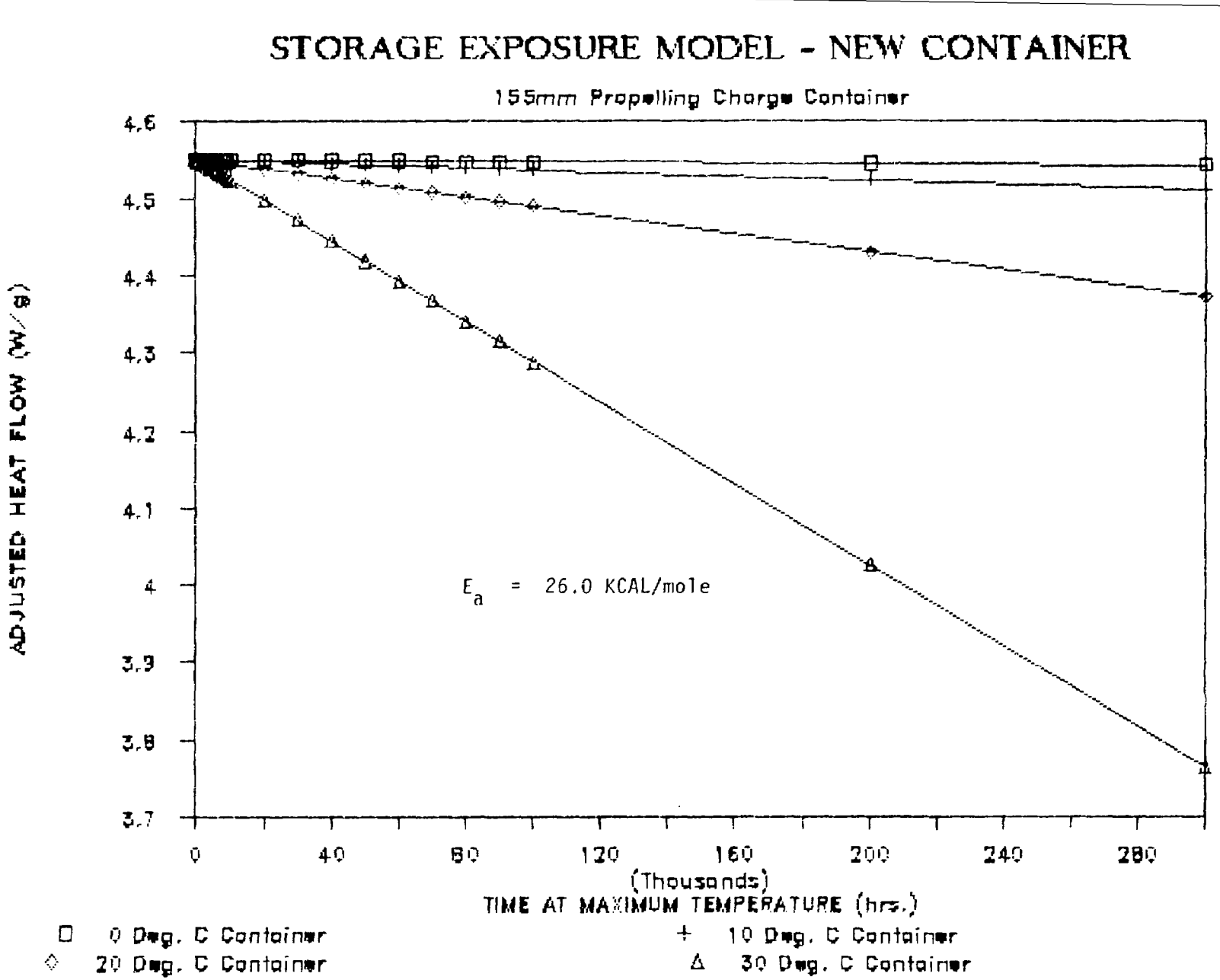

Figure 8-D: 155mm Propelling Charge Container Humid Indoor Storage Model - Published Activation Energy

Table 9-D

Performance Prediction Model
155mm Propelling Charge Container
Dry Indoor Storage

Ea	12000	cal/mole
To	71	Deg. C
dP/duv	-0.000036	
Po	4.55	W/g

Time at Temperature (hrs.)	Degrees C Container Temperature 0	Degrees C Container Temperature 10	Degrees C Container Temperature 20	Degrees C Container Temperature 30
		Calculated Values		
0	4.5500	4.5500	4.5500	4.5500
100	4.5500	4.5499	4.5498	4.5497
200	4.5499	4.5498	4.5497	4.5493
300	4.5499	4.5498	4.5495	4.5490
400	4.5499	4.5497	4.5493	4.5487
500	4.5498	4.5496	4.5492	4.5483
600	4.5498	4.5495	4.5490	4.5480
700	4.5497	4.5494	4.5488	4.5477
800	4.5497	4.5494	4.5487	4.5473
900	4.5497	4.5493	4.5485	4.5470
1000	4.5496	4.5492	4.5483	4.5467
2000	4.5493	4.5484	4.5466	4.5434
3000	4.5489	4.5476	4.5450	4.5400
4000	4.5485	4.5468	4.5433	4.5367
5000	4.5482	4.5460	4.5416	4.5334
6000	4.5478	4.5452	4.5399	4.5301
7000	4.5474	4.5443	4.5383	4.5268
8000	4.5471	4.5435	4.5366	4.5235
9000	4.5467	4.5427	4.5349	4.5201
10000	4.5463	4.5419	4.5332	4.5168
20000	4.5426	4.5339	4.5165	4.4836
30000	4.5389	4.5258	4.4997	4.4504
40000	4.5353	4.5177	4.4829	4.4173
50000	4.5316	4.5096	4.4662	4.3841
60000	4.5279	4.5016	4.4494	4.3509
70000	4.5242	4.4935	4.4326	4.3177
80000	4.5205	4.4854	4.4159	4.2845
90000	4.5168	4.4773	4.3991	4.2513
100000	4.5132	4.4693	4.3823	4.2181
200000	4.4763	4.3885	4.2146	3.8863
300000	4.4395	4.3078	4.0470	3.5544

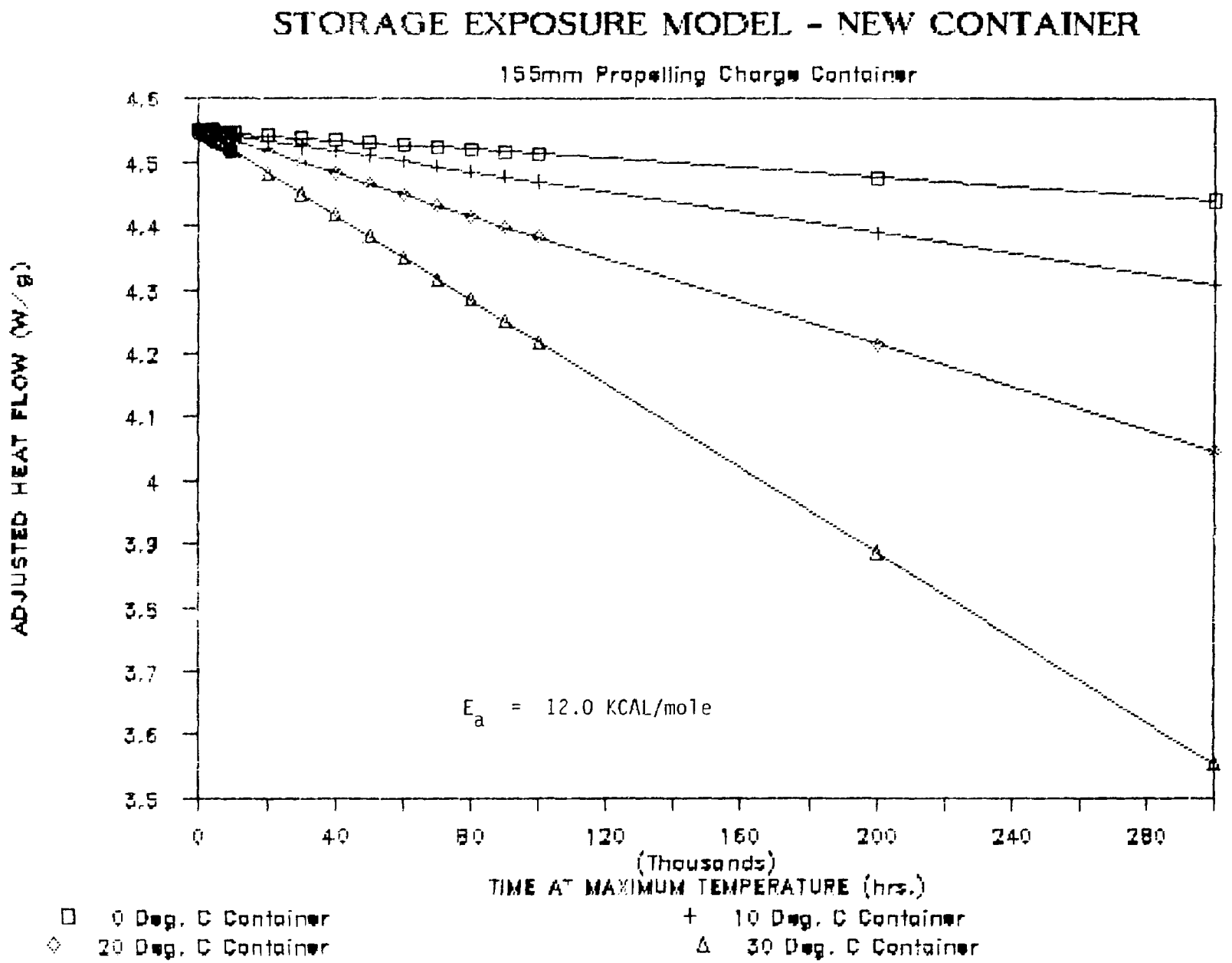

Figure 9-D: 155mm Propelling Charge Container Dry Indoor Storage Model - Low Activation Energy

Table 10-D

Performance Prediction Model
155mm Propelling Charge Container
Dry Indoor Storage

Ea	26000	cal/mole
To	71	Deg. C
dP/duv	-0.000036	
Po	4.55	W/g

Time at Temperature (hrs.)	Degrees C Container Temperature 0	Degrees C Container Temperature 10	Degrees C Container Temperature 20	Degrees C Container Temperature 30
		Calculated Values		
0	4.5500	4.5500	4.5500	4.5500
100	4.5500	4.5500	4.5500	4.5500
200	4.5500	4.5500	4.5500	4.5500
300	4.5500	4.5500	4.5500	4.5499
400	4.5500	4.5500	4.5500	4.5499
500	4.5500	4.5500	4.5500	4.5499
600	4.5500	4.5500	4.5500	4.5499
700	4.5500	4.5500	4.5500	4.5499
800	4.5500	4.5500	4.5500	4.5498
900	4.5500	4.5500	4.5500	4.5498
1000	4.5500	4.5500	4.5500	4.5498
2000	4.5500	4.5500	4.5499	4.5496
3000	4.5500	4.5500	4.5499	4.5494
4000	4.5500	4.5500	4.5498	4.5492
5000	4.5500	4.5500	4.5498	4.5490
6000	4.5500	4.5499	4.5497	4.5488
7000	4.5500	4.5499	4.5497	4.5486
8000	4.5500	4.5499	4.5496	4.5484
9000	4.5500	4.5499	4.5496	4.5481
10000	4.5500	4.5499	4.5495	4.5479
20000	4.5500	4.5498	4.5491	4.5459
30000	4.5499	4.5497	4.5486	4.5438
40000	4.5499	4.5496	4.5481	4.5418
50000	4.5499	4.5495	4.5477	4.5397
60000	4.5499	4.5494	4.5472	4.5377
70000	4.5499	4.5493	4.5467	4.5356
80000	4.5499	4.5492	4.5463	4.5336
90000	4.5498	4.5491	4.5458	4.5315
100000	4.5498	4.5490	4.5453	4.5294
200000	4.5496	4.5481	4.5406	4.5089
300000	4.5495	4.5471	4.5359	4.4883

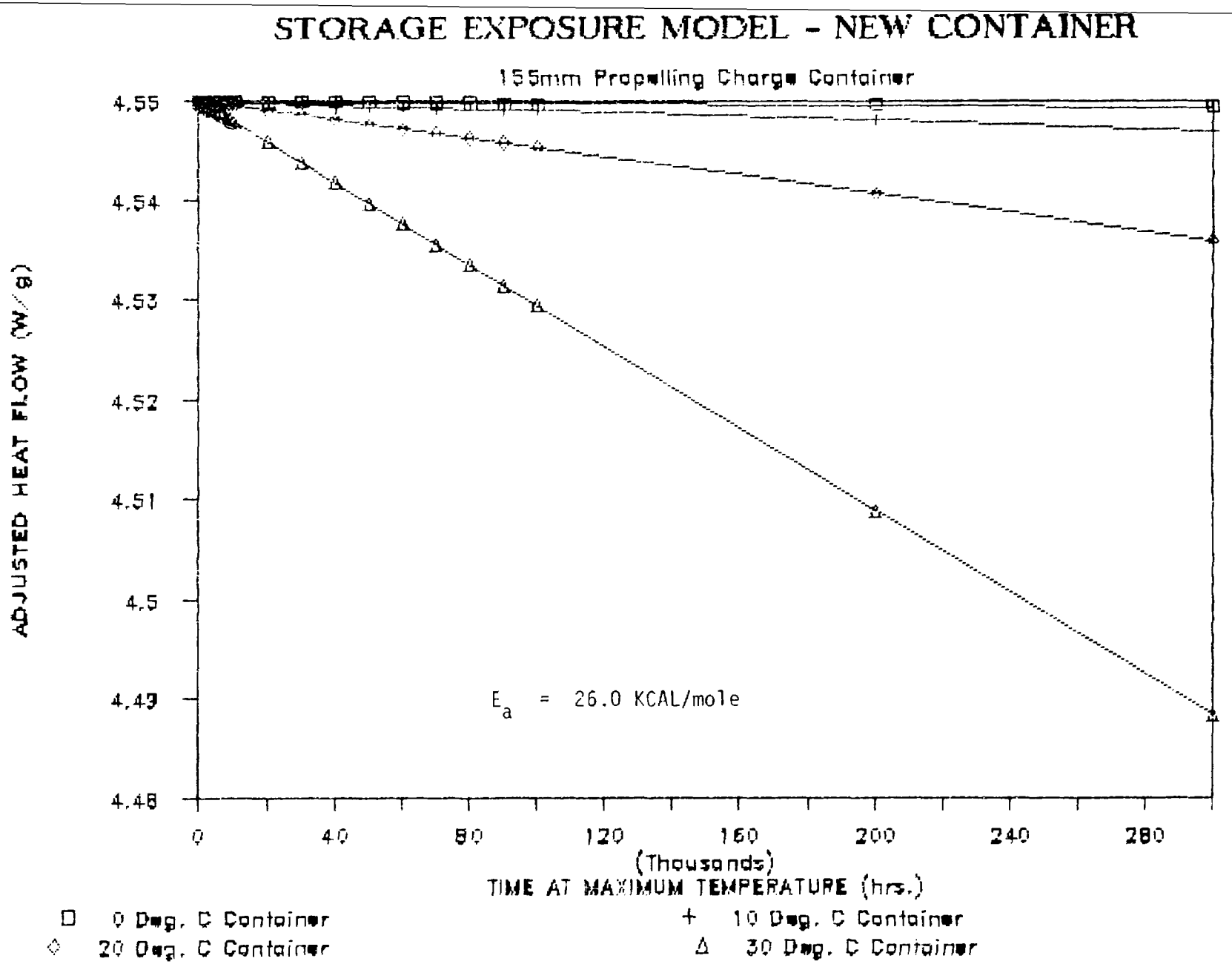

Figure 10-D: 155mm Propelling Charge Container Dry Indoor Storage Model - Published Activation Energy

DISTRIBUTION

Commander
Armament Research, Development and Engineering Center
U.S. Army Armament, Munitions and Chemical Command
ATTN: SMCAR-AEP(D)
Carl Morrison
Packaging Division
Building 455
Picatinny Arsenal, NJ 07806-5000

Commander
Armament Research, Development and Engineering Center
U.S. Army Armament, Munitions and Chemical Command
ATTN: SMCAR-IMI-I (Bldg 59)
SMCAR-AMSMC-QAR-R(D)
SMCAR-AMSMC-GCL(D)
Picatinny Arsenal, NJ 07806-5000

Administrator
Defense Technical Information Center
ATTN: Accessions Division (12)
Cameron Station
Alexandria, VA 22304-6145

Director
U.S. Army Materiel Systems Analysis Activity
ATTN: AMXSY-MP
Aberdeen Proving Ground, MD 21005-5066

Commander
Chemical Research, Development and Engineering Center
U.S. Army Armament, Munitions and Chemical Command
ATTN: SMCCR-MSI
Aberdeen Proving Ground, MD 21010-5423

Commander
Chemical Research, Development and Engineering Center
U.S. Army Armament, Munitions and Chemical Command
ATTN: SMCCR-RSP-A
Aberdeen Proving Ground, MD 21010-5423

Director
Ballistic Research Laboratory
ATTN: AMXBR-OD-ST
Aberdeen Proving Ground, MD 21005-5066

Chief
Benet Weapons Laboratory, CCAC
Armament Research, Development and Engineering Center
U.S. Army Armament, Munitions and Chemical Command
ATTN: SMCAR-CCB-TL
Watervliet, NY 12189-5000

Commander
U.S. Army Armament, Munitions and Chemical Command
ATTN: SMCAR-ESP-L
Rock Island, IL 61299-6000

Director
U.S. Army TRADOC Systems Analysis Activity
ATTN: ATAA-SL
White Sands Missile Range, NM 88002

Mr. J.E. Brzuskiewicz
R/NBD Division (2)
DSET LABORATORIES, INC.
Box 1850 Black Canyon Stage I
Phoenix, AZ 85027